Epigenetic based therapeutic strategies in breast cancer

Niaz Mahmood
Division of Experimental Medicine
Department of Medicine
McGill University, Montreal
Quebec, Canada
August 2020

A thesis submitted to McGill University in partial fulfillment of the requirements of the degree of Doctor of Philosophy

TABLE OF CONTENTS

LIST OF TABLES

Chapter One

LIST OF FIGURES

Chapter One

Chapter Two

Chapter Three

Chapter Four

Chapter Five

ABSTRACT

DNA methylation abnormalities have been strongly implicated in the coordinated targeting of various cancer-related signaling pathways involved in the development, progression, and metastasis of breast and other common cancers. Integrative transcriptome and epigenome-wide association studies have further revealed that the methylation abnormalities can be in both directions, i.e., hypermethylation and hypomethylation-mediated gene expression changes occur in cancer. The dynamic nature of the cancer epigenome makes it a suitable anti-cancer target. However, the currently approved epigenetic-based therapies mainly focus on targeting DNA hypermethylation, and there are still no approved agents to reverse abnormal DNA hypomethylation. Therefore, in the first part of this thesis, we have tested the therapeutic plausibility of targeting DNA hypomethylation using a naturally occurring methylating agent S-adenosylmethionine (SAM) and found a significant reduction in breast cancer growth, invasion, and metastasis *in vitro* and *in vivo.* Transcriptome analyses revealed that the SAM-mediated anti-cancer effects are due to changes in the molecular signatures related to several key oncogenic and prometastatic signaling pathways. Next, we tested the hypothesis of concurrent targeting of both hyper- and hypomethylation mediated abnormalities by treatment with FDA-approved demethylating agent decitabine and SAM *in vivo* and found an enhanced anti-cancer effect in the combination-treated group compared to either of the monotherapy arms. Integrative transcriptome and methylome analyses of breast tumor cells following a combination of SAM and decitabine treatment revealed significant downregulation of clinically relevant metastatic genes compared to vehicle-treated

controls. Since decitabine is a highly toxic chemotherapeutic agent and can only be used for cancer patients, we next assessed the plausibility of using SAM with other approved nutraceutical agents that can be used in a chemopreventive setting. Emerging evidence suggests that Vitamin D can increase the expression of tumor suppressor genes via demethylation of the promoters, which provided the rationale for its concurrent use with SAM to target hyper- and hypomethylation of DNA. We found that the combination treatment with SAM and Vitamin D prohormone significantly delayed mammary tumor emergence, decreased tumor growth and lung metastasis in transgenic MMTV-PyMT animals, and reduced breast cancer cell colonization to the bone in PyMT-R221A intratibial model. Finally, towards developing targeted epigenetic therapies, a combination of pharmacologic and gene knockout-based molecular genetics approaches was employed to assess the role of DNA methylation reader Mbd2, a downstream molecular target of SAM, during breast tumor progression. Our results show that depletion of *Mbd2* significantly reduced tumor volumes and metastasis in the MMTV-PyMT model by impairing the oncogenic PI3K/Akt/NF-κB signaling pathway. Collectively, these studies have provided compelling evidence for the anti-cancer effects of SAM alone and in combination settings and identified *Mbd2* as a key gene for targeted epigenetic therapies that will potentially lead to the initiation of clinical trials with SAM and Mbd2 inhibitors in cancer patients.

RÉSUMÉ

Les anomalies de la méthylation de l'ADN ont été fortement impliquées dans le ciblage coordonné de diverses voies de signalisation liées au cancer impliquées dans le développement, la progression et les métastases du sein et d'autres cancers courants. Des études intégratives de transcriptome et d'association à l'échelle de l'épigénome ont en outre révélé que les anomalies de méthylation peuvent être dans les deux directions, c'est-à-dire que des changements d'expression génique induits par l'hyperméthylation et l'hypométhylation se produisent dans le cancer. La nature dynamique de l'épigénome du cancer en fait une cible anticancéreuse appropriée. Cependant, les thérapies à base épigénétique actuellement approuvées se concentrent principalement sur le ciblage de l'hyperméthylation de l'ADN, et il n'y a toujours pas d'agents approuvés pour inverser l'hypométhylation anormale de l'ADN. Par conséquent, dans la première partie de cette thèse, nous avons testé la plausibilité thérapeutique du ciblage de l'hypométhylation de l'ADN à l'aide d'un agent de méthylation naturel S-adénosylméthionine (SAM) et avons trouvé une réduction significative de la croissance, de l'invasion et des métastases du cancer du sein in vitro et in vivo. Les analyses de transcriptome ont révélé que les effets anticancéreux médiés par SAM sont dus à des changements dans les signatures moléculaires liées à plusieurs voies de signalisation oncogéniques et prométastatiques clés. Ensuite, nous avons testé l'hypothèse d'un ciblage simultané des anomalies médiées par l'hyper et l'hypométhylation par un traitement avec un agent déméthylant approuvé par la FDA decitabine et SAM in vivo et avons trouvé un effet anticancéreux synergique dans le groupe traité en association par rapport à l’un ou l’autre des bras en monothérapie. Les

analyses intégratives du transcriptome et du méthylome des cellules tumorales du sein après une combinaison de SAM et de traitement à la décitabine ont révélé une régulation négative significative des gènes métastatiques cliniquement pertinents par rapport aux témoins traités avec le véhicule. Étant donné que la décitabine est un agent chimiothérapeutique hautement toxique et ne peut être utilisée que pour les patients cancéreux, nous avons ensuite évalué la plausibilité de l'utilisation de la SAM avec d'autres agents nutraceutiques approuvés pouvant être utilisés dans un cadre chimiopréventif. De nouvelles preuves suggèrent que la vitamine D peut augmenter l'expression des gènes suppresseurs de tumeur via la déméthylation des promoteurs, ce qui a fourni la justification de son utilisation simultanée avec SAM pour cibler l'hyper- et l'hypométhylation de l'ADN. Nos résultats ont démontré que le traitement combinatoire de la SAM et de la prohormone de vitamine D retardait significativement l'émergence de la tumeur mammaire, diminuait la croissance tumorale et les métastases pulmonaires chez les animaux transgéniques MMTV-PyMT et réduisait la colonisation des cellules cancéreuses du sein à l'os dans le modèle intratibial PyMT-R221A. Enfin, pour développer des thérapies épigénétiques ciblées, une combinaison d'approches de génétique moléculaire pharmacologiques et génétiques basées sur le knockout a été utilisée pour évaluer le rôle du lecteur de méthylation de l'ADN Mbd2, une cible moléculaire en aval de la SAM, au cours de la progression de la tumeur du sein. Nos résultats montrent que l'épuisement de Mbd2 réduit significativement les volumes tumoraux et les métastases dans MMTV-PyMT en altérant la voie de signalisation médiée par l'axe oncogénique PI3K / Akt / NF-κB. Collectivement, ces études ont fourni des preuves convaincantes des effets anticancéreux de la SAM seule

et en association et ont identifié Mbd2 comme un gène clé pour des thérapies épigénétiques ciblées qui mèneront potentiellement au lancement d'essais cliniques avec des inhibiteurs de la SAM et du Mbd2 chez les patients cancéreux.

ACKNOWLEDGMENTS

There is an African adage that says, '*It takes a village to raise a child*'. I feel that doing a Ph.D. is no different as there are so many people who helped me, and I am utterly grateful for the support that was given to me throughout my journey as a Ph.D. student at McGill University.

First of all, I would like to express my heartiest gratitude and sincere thanks to my supervisor Dr. Shafaat A Rabbani for giving me the opportunity to do my Ph.D. in his laboratory and for his unparalleled support and guidance throughout the process. He has always given me the freedom to express myself scientifically by letting me design my own experiments and provided me with the necessary advice whenever it was required. His enthusiasm for science and positive attitude towards life has been very inspiring and has greatly made my Ph.D. experience more exciting and rewarding.

I am also thankful to our collaborator Dr. Moshe Szyf for sharing his exciting new ideas, expertise, and knowledge in epigenetics, which greatly helped me to advance my research.

Thank you to all the members of my thesis advisory committee: Dr. Hugh P.J. Bennett, Dr. Andrew Bateman, Dr. Elena Torban and Dr. G.H. Hendy for their valuable time, advice and support throughout my Ph.D.

I am really thankful to our laboratory manager, Ani Arakelian, for patiently training me all the experimental techniques related to murine models as well as several *in vitro* techniques. She has always helped me in all the technically difficult situations I faced

during my Ph.D. Thanks to my lab mate Ali Mehdi for all the fun time in and out of the laboratory.

Special thanks to Loan Nguyen-Yamamoto for translating my abstract into French, and Aimee-Lee, Takeshi, and Laetitia for their friendship.

I would also like to thank all the members of Dr. Goltzman and Dr. Kremer's lab for their help whenever it was needed. Thanks to David and Farida from Dr. Szyf's lab for helping with DNA methylation data analysis and guiding me during pyrosequencing, Pat Hales for the administrative support, and the RI-MUHC histopathology and immunophenotyping platforms for their help with immunohistochemistry and Flow cytometry.

I want to acknowledge the Division of Experimental Medicine, the McGill Faculty of Medicine, the Research Institute of the McGill University Health Centre, and Fonds de recherche du Québec-Santé (FRQS) for their financial support during my Ph.D.

Finally, I would like to thank my family and friends outside the lab for their unconditional love, constant support, and encouragement during this five-year-long journey that kept me moving forward.

DEDICATION

This thesis is dedicated to my parents (Mahmudul Hoque and Syeda Jesmin Banu) and siblings (Nusrat Afroz and Nafis Mahmud). Thank you for always believing in me during my ups and downs. You all are my biggest motivation.

PREFACE

This thesis is presented in a manuscript-based format in accordance with the thesis preparation guidelines from the Faculty of Graduate Studies, McGill University. The entire thesis was written by me (Niaz Mahmood) and revised by my supervisor Dr. Shafaat A Rabbani.

The thesis includes three original research articles that are published (Chapters 2,3, and 4) and one research article prepared for publication and to be submitted soon (Chapter 5). Each of these chapters (Chapters 2,3,4, and 5) have their own abstract, introduction, materials and methods, results, discussion, references, and supplementary sections. The references for the published research articles presented in chapters 2,3, and 4 were consistent with the format of the journals where they are published. A separate preface section is added at the beginning of each of these chapters to provide the rationale and context of the study as well as to connect the chapters logically. The manuscripts related to chapters 2,3, and 4 were published in Oncotarget, Bone Research, and Journal of cellular and molecular medicine, respectively.

A general introduction and literature review are provided in Chapter 1, which contains excerpts and figures from two review articles and one book chapter that the author has published as the first author during his Ph.D. tenure. To be consistent in the referencing style between the three excerpts used in Chapter 1, a uniform referencing style was used for the 'Introduction and Literature review' section.

A general discussion with future directions is provided in Chapter 6. The references for Chapters 1 and 6 can be found together after the end of Chapter 6. The copyright permissions are attached to the end of the thesis as Appendices.

Published manuscripts included in this thesis

- **Mahmood, N.** and Rabbani, S.A. (2017) DNA methylation and breast cancer: mechanistic and therapeutic applications. Trends in Cancer Res, 12: 1-18. [Review] *(Chapter 1 contains excerpts of this review)*
- **Mahmood,N.**, Cheishvili,D., Arakelian,A., Tanvir,I., Khan,H.A., Pépin, A.S., Szyf,M. and Rabbani, S.A. (2018) Methyl Donor S-adenosylmethionine (SAM) supplementation Attenuates Breast Cancer Growth, Invasion, and Metastasis in vivo; therapeutic and chemopreventive applications. Oncotarget 9:5169-5183. *(Chapter 2 of this thesis)*
- **Mahmood,N.** and Rabbani, S.A. (2019) DNA methylation readers and breast cancer: mechanistic and therapeutic applications. Front Oncol. 9: 489. [Review] *(Chapter 1 contains excerpts of this review)*
- **Mahmood,N.** and Rabbani, S.A. (2019) Targeting DNA Hypomethylation in Malignancy by Epigenetic Therapies. Adv Exp Med Biol. 1164:179-196. [Book Chapter] *(Chapter 1 contains excerpts of this book chapter)*
- **Mahmood,N.,** Arakelian,A., Cheishvili,D., Szyf,M. and Rabbani, S.A. (2020) S-adenosyl methionine in combination with Decitabine shows enhanced anti-cancer effects in repressing breast cancer growth and metastasis. J Cell Mol Med. 00:1-16 *(Chapter 3 of this thesis)*
- **Mahmood,N.**, Arakelian,A., Muller, W.J., Szyf,M. and Rabbani, S.A. (2020) An enhanced chemopreventive effect of methyl donor S-adenosylmethionine in combination with 25-hydroxyvitamin D in blocking mammary tumor growth and metastasis. Bone Res. 8:28 *(Chapter 4 of this thesis)*

Manuscript in preparation and included in this thesis

- **Mahmood,N.**, Arakelian,A., Szyf,M. and Rabbani, S.A. Methyl-CpG binding domain protein 2 plays a causal role in breast cancer growth and metastasis. (*Chapter 5 of this thesis*)

The candidate also contributed to the following studies that were not included in this thesis.

- **Mahmood,N.**, Mihalcioiu,C., and Rabbani, S.A. (2018) Multi-faceted role of the urokinase plasminogen activator (uPA) and its receptor (uPAR); diagnostic, prognostic, and therapeutic applications. Front Oncol. 12; 8:24.
- Cheishvili,D, Parashar,S., **Mahmood,N.**, Arakelian,A., Kremer,R., Goltzman, D., Szyf,M. and Rabbani, S.A. (2018) Identification of an Epigenetic Signature of Osteoporosis in Postmenopausal Women. J Bone Min Res. 11: 1980-1989.
- Parashar,S., Cheishvili,D, **Mahmood,N.**, Arakelian,A., Tanvir,I., Khan,H.A., Kremer,R., Mihalcioiu,C., Szyf,M. and Rabbani, S.A. (2018) DNA methylation signatures of breast cancer in peripheral T-cells. BMC Cancer 18:574.
- **Mahmood,N.**, Arakelian,A., Tanvir,I., Khan,H.A., Mazar, A.P.. and Rabbani, S.A. (2020) uPAR antibody (huATN-658) and Zometa reduce breast cancer growth and skeletal lesions. Bone Res. 8:18.
- Mehdi, A., Attias, M., **Mahmood, N.**, Arakelian A, Mihalcioiu, C., Piccirillo, C.A. Szyf,M. and Rabbani, S.A. (2020) Enhanced anti-cancer effect of a combination of SAM and immune checkpoint inhibitor (ICPi) in a syngeneic mouse model of advanced melanoma. Front Oncol. 10:1361.

CONTRIBUTION OF AUTHORS

Chapter 1

The 'Introduction and Literature Review' contains excerpts from the following two review articles and one book chapter :

1. **Mahmood, N.** and Rabbani, S.A. (2017) DNA methylation and breast cancer: mechanistic and therapeutic applications. Trends in Cancer Res, 12: 1-18. [Review]
2. **Mahmood,N.** and Rabbani, S.A. (2019) DNA methylation readers and breast cancer: mechanistic and therapeutic applications. Front Oncol. 9: 489. [Review]
3. **Mahmood,N.** and Rabbani, S.A. (2019) Targeting DNA Hypomethylation in Malignancy by Epigenetic Therapies. Adv Exp Med Biol. 1164:179-196. [Book Chapter]

All of three documents were written by Niaz Mahmood and revised by Dr. Shafaat A Rabbani. The copyright permissions are attached in the Appendices.

Chapter 2

This Chapter contains the following published manuscript :

> **Mahmood,N.**, Cheishvili,D., Arakelian,A., Tanvir,I., Khan,H.A., Pépin, A.S., Szyf,M. and Rabbani, S.A. (2018) Methyl Donor S-adenosylmethionine (SAM) supplementation Attenuates Breast Cancer Growth, Invasion, and Metastasis in vivo; therapeutic and chemopreventive applications. Oncotarget 9:5169-5183.

Niaz Mahmood did all the *in vitro* studies, wrote this article with Drs. Shafaat A Rabbani and Moshe Szyf. The *in vivo* experiments in Figure 2 was done by Ani Arakelian. Drs. Imrana Tanvir and Haseeb Ahmed Khan performed the immunohistochemistry in Figure 4. The initial gene list of the microarray data was generated by the Canadian Centre for Computational Genomics for pay-for-service, and Niaz Mahmood performed the gene set

enrichment and other downstream analyses. David Cheishvili and Anne-Sophie Pépin advised in pyrosequencing and qPCR but the experiments were performed by Niaz Mahmood. The behavior experiments were done by Niaz Mahmood and Ani Arakelian.

Chapter 3

This Chapter contains the following published manuscript :

> **Mahmood,N.,** Arakelian,A., Cheishvili,D., Szyf,M. and Rabbani, S.A. (2020) S-adenosyl methionine in combination with Decitabine shows enhanced anti-cancer effects in repressing breast cancer growth and metastasis. J Cell Mol Med. 00:1-16

Niaz Mahmood carried out all the *in vitro* studies. Ani Arakelian and Niaz Mahmood carried out the *in vivo* studies. The sequencing facility provided the initial gene list from RNA-Sequencing. Niaz Mahmood made the volcano plots, Venn diagrams, carried out all the downstream pathways and database analyses, and all relevant experimental procedures described in the manuscript. Davis Cheishvili analyzed the methylation data. Immunohistochemistry was done at the RI-MUHC histopathology platform. Niaz Mahmood wrote the manuscript along with Drs. Shafaat A Rabbani and Moshe Szyf.

Chapter 4

This Chapter contains the following published manuscript :

> **Mahmood,N.**, Arakelian,A., Muller, W.J., Szyf,M. and Rabbani, S.A. (2020) An enhanced chemopreventive effect of methyl donor S-adenosylmethionine in combination with 25-hydroxyvitamin D in blocking mammary tumor growth and metastasis. Bone Res. 8:28

Niaz Mahmood carried out all the *in vitro* studies. Ani Arakelian and Niaz Mahmood carried out the *in vivo* studies in Figures 2 and 3. Niaz Mahmood analyzed the RNA-Sequencing data and carried out all relevant experimental procedures described in the manuscript. Immunohistochemistry was done at the RI-MUHC histopathology platform. Niaz Mahmood wrote the manuscript along with Drs. Shafaat A Rabbani and Moshe Szyf.

Chapter 5

This Chapter contains the following manuscript in preparation for submission:

> **Mahmood,N.**, Arakelian,A., Szyf,M. and Rabbani, S.A. Methyl-CpG binding domain protein 2 plays a causal role in breast cancer growth and metastasis.

Niaz Mahmood carried out all the *in vivo* and *in vitro* studies. Ani Arakelian helped with initial genotyping and during mammary fat pad injections related to Figure 5D. The sequencing facility provided the initial gene list from RNA-Sequencing, but all other downstream analyses were carried out by Niaz Mahmood. Immunohistochemistry was done at the RI-MUHC histopathology platform. Niaz Mahmood analyzed the proteomics data and carried out all relevant experimental procedures described in the manuscript. Niaz Mahmood wrote the manuscript along with Drs. Shafaat A Rabbani and Moshe Szyf.

CONTRIBUTION TO ORIGINAL KNOWLEDGE

1. It has been shown for the first time that SAM-treatment via gavage causes a dose-dependent decrease in primary tumor volumes and metastases to different organs (lung, liver, and spleen) in highly aggressive triple-negative MDA-MB-231 xenograft model of breast cancer.

2. SAM-treatment via gavage significantly delays mammary tumor emergence in transgenic MMTV-PyMT animals compared to the vehicle-treated control arm.

3. SAM also reduces mammary tumor volumes and lung metastases in transgenic MMTV-PyMT animals belonging to the luminal B subtype of breast cancer.

4. Skeleton is one of the major sites where breast cancer cells migrate in clinical settings. This study has shown that SAM-treatment reduces tumor incidence and tumor growth within the bone in a well-established intratibial model of breast cancer.

5. This is the first study demonstrating the transcriptome-wide changes in gene-expression signatures of triple-negative and luminal B breast cancer cells upon SAM-treatment. Furthermore, pathway enrichment analyses of the differentially expressed genes following SAM-treatment revealed the downregulation of molecular signatures related to cancer metastasis, EMT, and angiogenesis.

6. SAM-treatment does not downregulate the expression of known tumor suppressor genes. Several tumor suppressor genes like *CST6*, *TFPI2*, *PAI-2* were upregulated upon SAM-treatment.

7. Concurrent treatment of SAM and FDA-approved demethylating agent decitabine shows an enhanced anti-cancer effect in reducing tumor growth and metastasis compared to the monotherapy arms *in vivo.*

8. Integrative analyses of MDA-MB-231 transcriptome and methylome following combination of SAM and decitabine treatment revealed significant downregulation of clinically relevant metastatic genes compared to vehicle-treated controls.

9. Combined treatment of SAM and 25-hydroxyvitamin D shows an enhanced anti-cancer effect compared to monotherapy arms when tested on a panel of breast cancer cells *in vitro.*

10. The SAM+25-hydroxyvitamin D combination delays mammary tumor emergence, showed an enhanced chemopreventive effect in reducing tumor volume and metastasis compared to the monotherapy treatments in transgenic MMTV-PyMT animals.

11. In comparison with the control and monotherapy arms, SAM and 25-hydroxyvitamin D combination treatment significantly reduces breast cancer cell colonization to the bone in an intratibial model.

12. The SAM+25-hydroxyvitamin D combination causes an upregulation of several key genes from interferon signaling pathways that are otherwise repressed during bone metastasis.

13. The SAM+25-hydroxyvitamin D combination causes a downregulation of several key genes from the HIF-1 signaling pathway.

14. Generation of transgenic MMTV-PyMT mice with homozygous and heterozygous deletion of the *Mbd2* gene using a crossbreeding strategy.

15. *Mbd2* knockout shows a gene-dose dependent decrease in primary tumor burden in MMTV-PyMT mice.

16. The MMTV-PyMT mice with homozygous depletion of *Mbd2* survive significantly longer than wild and heterozygous knockouts. Moreover, the homozygous knockouts show a significant reduction in lung metastasis.

17. *Mbd2* depletion affects the ability of the PyMT oncoprotein to stimulate the oncogenic PI3K/Akt/NF-κB axis and thereby interferes with the transcription of crucial prometastatic genes like *Plau/uPA, Mmp2, Mmp9,* and others.

18. Transcriptome and proteome analyses revealed the role of Mbd2 protein in modulating several key molecular determinants of epithelial-mesenchymal transition (EMT) in transgenic MMTV-PyMT model.

19. Mbd2 regulates the oncogenic Pvt1-Myc axis.

20. A small-molecule inhibitor of the Mbd2 pathway (KCC-07) significantly represses breast tumor cell proliferation *in vitro* and *in vivo*.

LIST OF ABBREVIATIONS

$1,25(OH)_2D$	1,25-dihydroxyvitamin D
25(OH)D	25-hydroxyvitamin D
5-azaC	5-azacytidine
5-azadC	5-aza-2′deoxycytidine
AGRN	Agrin
ATP	Adenosine triphosphate
BCL-2	B-cell lymphoma 2
CADM1	Cell Adhesion Molecule 1
CpG	Cytosine-phosphate-guanine
CDH2	Cadherin 2
CDI	Coefficient of drug interaction
CSC	Cancer stem cell
CXCR4	C-X-C motif chemokine receptor 4
DEGs	Differentially expressed genes
DNMT	DNA methyltransferase
DUSP1	Dual specificity protein phosphatase 1
ECM	Extracellular matrix
EMT	Epithelial-mesenchymal transition
ER	Estrogen receptor
EWAS	Epigenome-wide association studies
FABP7	Fatty acid binding protein 7
FADS2	Fatty acid desaturase 2
FDA	Food and Drug Administration
FDR	False discovery rate
gDNA	Genomic DNA
GFP	Green fluorescent protein
GSTP1	Glutathione S-Transferase Pi 1
HAS2	Hyaluronan Synthase 2
HAS3	Hyaluronan Synthase 3
HBEC	Human breast epithelial cells
HDAC	Histone deacetylase
HIF-1	Hypoxia-inducible factor 1
IKK	IκB kinase
KEGG	Kyoto Encyclopedia of Genes and Genomes
KLF4	Kruppel-like factor 4

lncRNA	Long non-coding RNAs
MBPs	Methyl-binding proteins
MCL-1	Myeloid cell leukemia 1
MMP	Matrix metalloproteinase
MMTV-PyMT	Mouse mammary tumor virus-polyoma middle T oncoprotein
MUC1	Mucin 1
NEAT1	Nuclear Enriched Abundant Transcript 1
NF-κB	Nuclear factor kappa B
OPN	Osteopontin
PAI-2	Plasminogen activator inhibitor 2
PI3K	Phosphoinositide 3-kinase
PID	Pathway Interaction Database
PPI	Protein-protein interaction
PVT1	Plasmacytoma variant translocation 1
SAH	S-adenosylhomocysteine
SAM	S-adenosylmethionine
SOX4	SRY-Box Transcription Factor 4
SPP1	Secreted phosphoprotein 1
STAT	Signal transducer and activator of transcription
TET	Ten-eleven translocation
TFPI2	Tissue factor pathway inhibitor 2
TFs	Transcription factors
TGF-β	Transforming growth factor beta
TNBC	Triple-negative breast cancer
TNC	Tenascin C
uPA	Urokinase plasminogen activator
uPAR	Urokinase plasminogen activator receptor
URA	Upstream regulator analysis
VDR	Vitamin D receptor
VEGF	Vascular endothelial growth factor
XIST	X-inactive specific transcript

Chapter One: Introduction and literature review

Epigenetics and cancer

The identity of a cell is determined by its genetic makeup along with the epigenetic marks which dictate how the genetic information will eventually be read and interpreted (Klutstein et al., 2016). In tumor cells, these genetic and epigenetic codes are often altered in such a way that the information within the genome is read in a completely different manner than the normal cells so as to develop and promote various characteristics associated with cancer. Some of the most common forms of genetic alterations seen in cancer include mutation, amplification, and deletion within the genome while changes in DNA methylation, histone modifications, and microRNAs constitute the three main types of epigenetic alterations found in the cancer genome (Figure 1).

Despite its first identification in the early 1980s (Feinberg and Vogelstein, 1983a), the epigenetics of human cancer has greatly been over-shadowed by human cancer genetics. With the passage of time, as our understanding of the epigenetic mechanisms and their role in regulating gene expression patterns during the development and progression of cancer became clear, the idea of targeting the epigenome as an anti-cancer strategy became apparent. In this regard, targeting the epigenome gained a great deal of attention over the last two decades. A plethora of epigenetic drugs (Epi-drugs) has been shown to be effective as anti-cancer agents in preclinical and clinical settings with a number of them being already approved for treatment of several types of liquid tumors

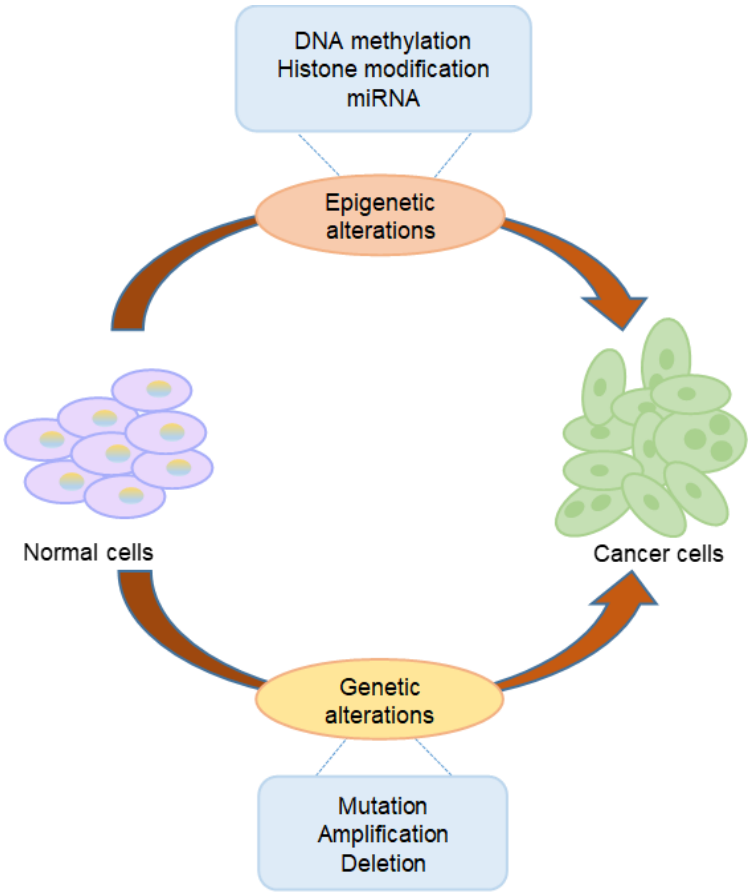

Figure 1: Common genetic and epigenetic aberrations in cancer.

Genetic alterations including mutation, amplification, and deletion within the genome as well as epigenetic alterations in DNA methylation, histone modifications and microRNAs change the identity of the cells and a normal cell can become cancerous during the process. Adapted from Mahmood and Rabbani, Trends in Cancer Research (Mahmood and Rabbani, 2017).

(Ganesan, 2016). Notwithstanding the fact that all three types of epigenetic alterations are important, this chapter, however, is mainly focused on various aspects of DNA methylation abnormalities seen in cancer and how they are targeted by some of the well-known anti-cancer agents to treat solid tumors like breast cancer.

DNA methylation

DNA methylation is a type of covalent modification in which methyl (-CH_3) groups are added to specific nucleotides of the genomic DNA (gDNA). In living systems, this reaction is catalyzed by DNA methyltransferase (DNMT) enzymes where universal methyl group donor S-adenosylmethionine (SAM) acts as a cofactor (Jeltsch, 2002; Zhang and Zheng, 2015). The presence of DNA methylation was first reported by Rollin Hotchkiss in 1948 shortly after the famous trio of Avery–MacLeod–McCarty identified DNA as the genetic material (Avery et al., 1944; Hotchkiss, 1948). However, it was during the late 1970s to early 1980s, almost three decades after its initial discovery, several groups reported that DNA methylation is involved in cell differentiation and gene regulation (Compere and Palmiter, 1981; Holliday and Pugh, 1975). Since then, a plethora of studies on its role in gene regulation followed and at present DNA methylation is regarded as one of the major mechanisms of gene regulation.

DNA methylation is evolutionarily primitive

Although DNA methylation is a widespread modification found in bacteria, plants, and mammalian species, there is a high degree of phylogenetic variability in the patterns of methylation across species (Bird, 2002). In prokaryotes, methylation can take place on adenine and cytosine residues of the DNA and play roles in processes like the initiation of DNA replication, DNA repair, cell cycle-coupled transcription and protection against foreign DNA (Sánchez-Romero et al., 2015). In mammals, methylation predominantly occurs on the carbon present at the 5th position of cytosine residues (5-mC) within the

cytosine-phosphate-guanine (CpG) dinucleotides (Suzuki and Bird, 2008). In plant and fungal genomes, methylation commonly occurs at the CpH and CpHpH ('H' stands for bases other than 'G') regions (Suzuki and Bird, 2008). In eukaryotes, DNA methylation plays a role during development, silencing of retroviral elements, maintenance of genome integrity, imprinting, lyonization/X-inactivation and gene expression regulation (Jeltsch, 2002; Moore et al., 2013). Recent evidence suggests that the genome of the nematode worm *Caenorhabditis elegans, which was previously* considered to be devoid of methylation, is actually methylated on the exocyclic -NH_2 groups at the 6th position of the purine ring in adenines (6-mA) (Greer et al., 2015). Taken together, this suggests that DNA methylation is indeed an evolutionarily ancient regulatory mechanism (Soojin, 2012).

DNA methylation writers, readers, and erasers: Role in gene regulation

In mammals, there is a specific distribution pattern of the CpG islands in the context of the whole genome where a higher propensity of CpG rich regions are found near the promoters of up to 70 % of the genes (Gardiner-Garden and Frommer, 1987; Saxonov et al., 2006). Non-CpG methylation is almost rare in mammals and is mainly found in the embryonic stem cells (Lister et al., 2009). Methylation at the CpG islands has been causally linked to transcription regulation, where the promoters of transcriptionally repressed genes are CpG methylated and the promoters of transcriptionally activated genes are unmethylated at the CpG islands (Figure 2) (Berger, 2016).

There are three major DNMTs that catalyze the transfer of -CH_3 groups in humans which include DNMT1, DNMT3a and DNMT3b (Bestor, 2000; Li et al., 1992; Okano et

al., 1999; Okano et al., 1998). S-adenosylmethionine (SAM) acts as the -CH_3 group donor for all three enzymes (Zhang and Zheng, 2015). DNMT1 is called 'maintenance methyltransferase' due to its preference for hemimethylated (newly synthesized) DNA *in vitro* and it mainly plays role in the methylation of the newly synthesized strand of DNA during cell division (Hermann et al., 2004). On the other hand, DNMT3a and DNMT3b are able to transfer the methyl moiety to both unmethylated and methylated DNA at an equal rate and are therefore called '*de novo* methyltransferases' (Okano et al., 1998).

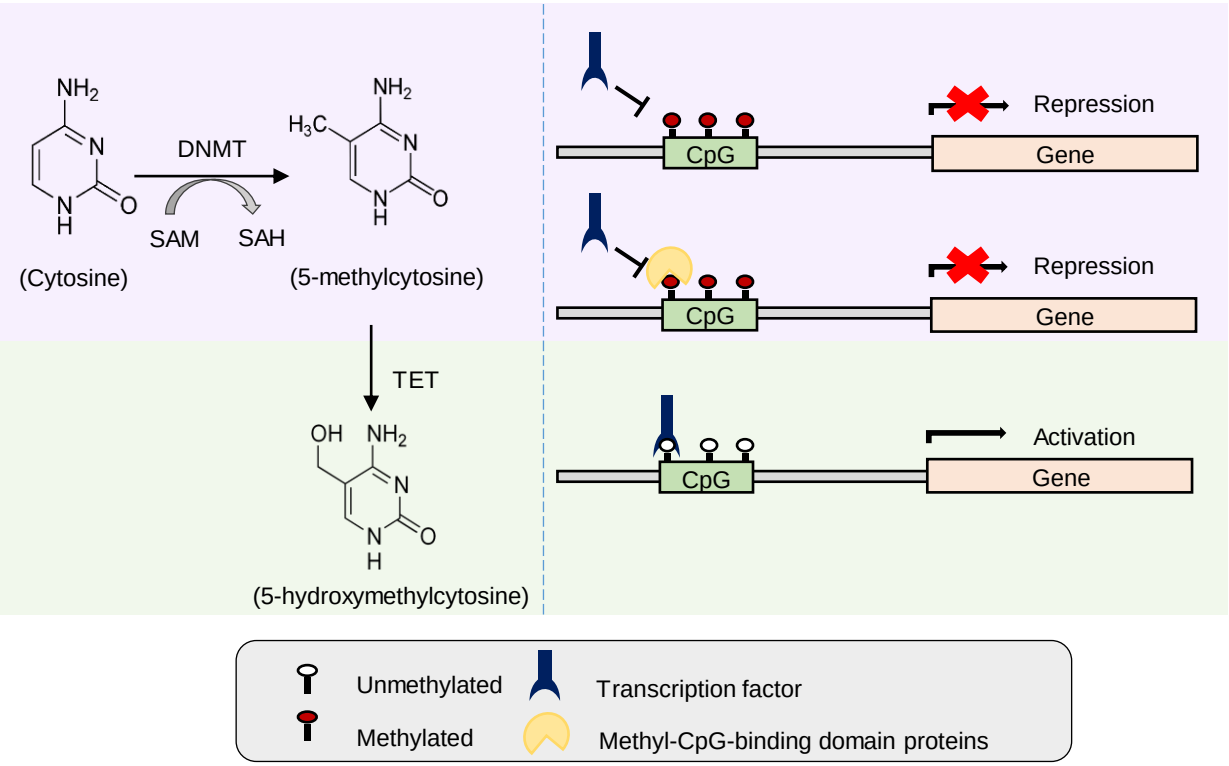

Figure 2: DNA methylation and its role in gene expression.

The chemical reaction in the left panel shows the process of methylation and demethylation of cytosine residues. At the molecular level, when cytosine is converted to 5-methylcytosine (5mC) by DNA methyltransferase (DNMT) two things may happen: (i) it may directly inhibit transcription factors (TFs) binding to the CpG islands to repress transcription, or (ii) it may attract the binding of a methyl CpG-binding protein to methylated CpG islands which recruits other repressive proteins at the site to prevent the access of TFs and thereby suppress transcription. When the methylation mark is removed by TET family of proteins, demethylation takes place. This likely allows the TFs to bind to the CpG sequences and cause activation of gene expression. Here, TET, Ten-eleven translocation (TET) family of proteins; SAM, S-adenosylmethionine; and SAH, S-adenosylhomocysteine. Adapted from Mahmood and Rabbani, Trends in Cancer Research (Mahmood and Rabbani, 2017).

The DNMTs are called ‘writers’ of methylation as they are the ones that copy the -CH_3 group on the cytosine residues of a CpG dinucleotide. In general, methylation at the CpG island may either directly interfere with the binding of transcription factors at the regulatory site to cause gene repression (Tate and Bird, 1993), or attract the binding of structural proteins called methyl-binding proteins (MBPs) which subsequently recruits different types of histone deacetylase (HDAC) complexes and chromatin remodeling factors that causes chromatin compaction and ultimately leading to transcriptional repression (Figure 2) (Nan et al., 1998). These proteins can sense or read the methylation at the CpG site and therefore they are known as the ‘readers’ of methylation. The first reported proteins with methyl binding activities in mammals were methyl-CpG binding protein 1 (MeCP1) and MeCP2 (Lewis et al., 1992; Meehan et al., 1989). However, later studies have demonstrated that MeCP1 is, in fact, a complex containing multiple proteins involved in chromatin remodeling (Feng et al., 2002; Feng and Zhang, 2001; Ng et al., 1999). Therefore, MeCP2 is regarded as the first ever single MBP to be identified (Meehan et al., 1989). At the structural level, MeCP2 contains a MBD domain comprising 70-85 amino acids that can recognize and bind to methylated CpGs (Nan et al., 1993). The MBD domain was later used to identify other proteins with methyl-binding potentials (Hendrich and Bird, 1998). At present, there are 11 known proteins with MBD domains which are classified as the family of “MBD-containing proteins”. More than a decade after the discovery of MeCP2, a second family of MBPs were identified that recognizes the methylated DNA using the Zinc finger motifs. Hence, they are called the ‘Methyl-CpG binding zinc fingers’ (Prokhortchouk et al., 2001). This particular family has

seen the most rapid expansion over the last few years, and, at present, there are at least 8 members in this family (Hudson and Buck-Koehntop, 2018). The third family of MBPs was identified based on their ability to bind methylated DNA using the Set and RING-associated (SRA) domain and hence called the 'SRA domain-containing proteins'. A schematic classification of the three main families of MBPs is shown in Figure 3.

There are some enzymes like Ten-eleven translocation (TET) methylcytosine dioxygenase family, activation-induced cytidine deaminase (AID) and thymine DNA glycosylase (TDG) that have been shown to be involved in passive and active demethylation of DNA (Cheishvili et al., 2015; Cortázar et al., 2011; Cortellino et al., 2011; Kohli and Zhang, 2013; Tahiliani et al., 2009). Since these enzymes can remove the $-CH_3$ group from the cytosine residues of a CpG dinucleotide, they are called the 'erasers' of methylation. When the $-CH_3$ groups are removed, it likely allows the transcription factors to bind to the CpG island and cause activation of gene expression (Figure 2) (Mariani et al., 2013).

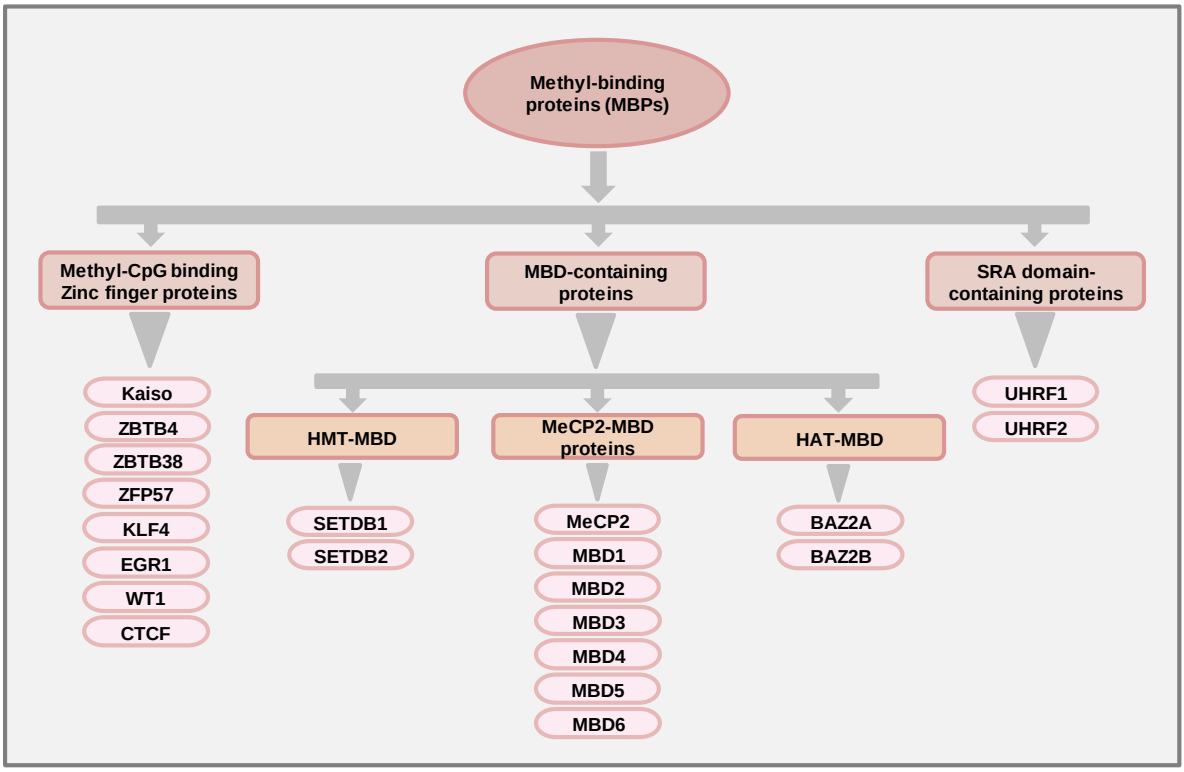

Figure 3: Classification of methyl-binding proteins (MBPs).

The proteins with methyl-CpG binding abilities are broadly classified into three families based on the functional domains used for binding to methylated DNA. The 'MBD-containing proteins' were the first group of MBPs to be identified and are further classified into three subfamilies (MeCP2-MBD, HMT-MBD, and HAT-MBD) based on the presence of functional domains other than MBD. The members of the HMT-MBD and HAT-MBD subfamilies have protein methyltransferase and acetylase activities respectively. The 'Methyl-CpG binding Zinc finger proteins' have at least 8 members (Kaiso, ZBTB4, ZBTB38, ZFP57, KLF4, EGR1, WT1, CTCF) that can bind to methylated region using the Zinc finger motifs while the third family of MBPs consisting of UHRF1 and UHRF2 proteins uses their Set and RING-associated (SRA) domain to bind methylated DNA. methyl-binding proteins (MBPs). From Mahmood and Rabbani, Frontiers in Oncology (Mahmood and Rabbani, 2019a)

Breast cancer heterogeneity: A challenge for therapeutic interventions

Breast cancer is a leading cause of mortality in women worldwide (DeSantis et al., 2016). Although a great deal of effort has been made over the years to understand the biology of breast cancer progression and metastasis, its etiology is still not fully understood. One of the main hurdles in breast cancer therapeutics is the high degree of heterogeneity of the breast tumors. For better prognosis and therapeutic regimens, more specific characterization of the breast tumor is warranted. Hence the idea of using specific biomarkers to classify different subtypes of breast cancer came to being (Weigel and Dowsett, 2010). The most commonly used breast cancer biomarkers are estrogen receptor (ER), progesterone receptor (PR) and epidermal growth factor 2 (HER2) which are routinely determined by immunohistochemistry (IHC) (Cornejo et al., 2014). In addition, expression of cell proliferation marker Ki-67 is combined with ER, PR and HER2 scores to form a better prognostic test called the 'IHC4' (Cuzick et al., 2011). These tests have been proven to be more effective for the prognosis of hormone receptor-positive breast cancers that express either ER, PR or both. Patients belonging to this group have a better prognosis in clinical settings, and hormone therapy drugs like tamoxifen and aromatase inhibitors showed considerable effectiveness in these patients. A relatively more aggressive subtype of breast cancer is the one that is hormone receptor negative but HER2 positive, for which targeted therapy using Herceptin showed a promising therapeutic response in patients. However, the most aggressive form of breast cancer does not express any of the known hormone receptor markers, and we are yet to identify any potential biomarker for these patients who are more commonly classified as the triple negative breast

cancer subtype. Chemotherapy is still the standard-of-care therapy for these patients, even though combination therapy with immunotherapy is showing promising therapeutic efficacy for TNBC patients. In addition to the protein biomarkers, assays using mRNA-based biomarkers have been developed and used for breast cancer subtyping (Cronin et al., 2007; Filipits et al., 2011; Toussaint et al., 2009).

Since DNA methylation regulates many gene expression programs, it has a profound impact on the prognosis of breast cancer which is dependent on molecular subtypes (Gyorffy et al., 2016). A specific pattern of methylation has been correlated with different subtypes of breast cancer (Kamalakaran et al., 2011; Stefansson et al., 2015). Notably, a higher frequency of DNA methylation is observed in luminal vs. non-luminal subtypes (Kamalakaran et al., 2011; Stefansson et al., 2015). These studies suggest that DNA methylation is crucial in the development and progression of distinct breast cancer subtypes (Gyorffy et al., 2016), and as such, the development of DNA methylation-based biomarkers is gaining interest in the recent years.

Aberrant DNA methylation in cancer

Accumulating evidence indicate that promoters of genes implicated in critical signaling pathways (for example, cell cycle, apoptosis, DNA repair, cell invasion etc.) are aberrantly methylated in breast cancer. This abnormal gene expression, in turn, dictates the gradual progression of breast cancer cells from less aggressive hormone-responsive phenotype into the more aggressive hormone-independent phenotype (Ferguson et al., 1995). With the advent of high-throughput technologies, there has been an exponential increase in studies

related to cancer epigenetics and as a result hundreds of abnormally methylated genes have been identified (Huang et al., 2011). Both hypermethylation of tumor suppressor genes and hypomethylation of oncogenes and prometastatic genes are seen in breast and other common cancers (Szyf et al., 2004). A selected list of some of the important genes frequently hyper or hypomethylated in breast cancer is shown in Table 1.

Table 1: Selected list of genes with aberrant methylation in breast cancer

Biological Function	**List of Genes**	**Methylation Status**		**Reference**
		Hyper	**Hypo**	
Invasion, metastasis (positive modulators)	*BCSG1, CDH3, NAT1, uPA*	-	+	(Gupta et al., 2003; Kim et al., 2008; Pakneshan et al., 2004a; Pakneshan et al., 2004b; Paredes et al., 2005)
Invasion, metastasis (negative modulators)	*CDH1, CDH13, CST6, SYK, TIMP3*	+	-	(Esteller et al., 2001; Rivenbark et al., 2006; Toyooka et al., 2001; Yuan et al., 2001)
DNA repair	*ATM, BRCA1, MGMT, MLH1*	+	-	(Esteller et al., 2000; Lotsari et al., 2012; Tserga et al., 2012; Vo et al., 2004)
Cell cycle	*AK5, CCND2, CDH1, FOXA2, RAD9, SFN (14-3-3 σ; HME1)*	+	-	(Cheng et al., 2005; Fackler et al., 2003; Miyamoto et al., 2005; Parrella et al., 2004)
Apoptosis	*APC, BCL-2, DAPK, DCC, HIC1, HOXA5, TMS1, TWIST*	+	-	(Conway et al., 2000; Esteller et al., 2001; Fackler et al., 2003; Fujii et al., 1998; Jin et al., 2001; Miyamoto et al., 2005; Raman et al., 2000; Stone et al., 2013)
Cell homeostasis, detoxification	*GSTP1, HOXD11*	+	-	(Lin and Nelson, 2003; Miyamoto et al., 2005)
Angiogenesis inhibitors	*SFRP5, THBS1*	+	-	(Li et al., 1999; Suzuki et al., 2008)
Hormone & receptor mediated signaling	*ER, HIN-1, PR, RAR-β2, RASSF1A,*	+	-	(Dammann et al., 2003; Dammann et al., 2001; Fackler et al., 2003; Lapidus et al., 1996; Ottaviano et al., 1994; Widschwendter et al., 2000)

DNA hypomethylation and cancer

DNA hypomethylation refers to the loss of CpG methylation at a specific site on the DNA that is otherwise methylated in a normal state (Peinado, 2011). In the context of the whole genome, the term DNA hypomethylation is used to describe a decrease in the percentage of methylated cytosines compared to the unmethylated ones (Peinado, 2011). There are two types of DNA hypomethylation abnormalities seen in cancer: (i) global hypomethylation, (ii) site-specific focal hypomethylation.

Loss of methylation of DNA was the first described epigenetic abnormality in cancer that was reported by two different laboratories in 1983. Feinberg and Vogelstein showed hypomethylation of specific regions on the genome of cancer cells (Feinberg and Vogelstein, 1983a, b). They used DNA from normal and cancer cells that were digested by methylation-sensitive restriction enzymes for Southern blotting and found a significant decrease in methylation in case of the cancer cells compared to their normal counterpart (Feinberg and Vogelstein, 1983a). Around the same time, by high-performance liquid chromatography (HPLC), the Ehrlich lab showed that the overall level of DNA methylation was considerably decreased in various types of cancer compared to normal tissues (Gama-Sosa et al., 1983). They also showed that the level of CpG methylation was significantly lower in the metastatic neoplasms compared to primary tumors suggesting the possible association between loss of methylation and tumor metastasis.

Even though DNA hypomethylation was identified before any other epigenetic alterations, it remained the least explored for decades and was often overshadowed by DNA hypermethylation. One of the reasons behind the preference of targeting

hypermethylation over hypomethylation of DNA has been a previous bias during the design of an experiment which focused on the sites that are normally unmethylated but becomes methylated in cancer (Feinberg and Tycko, 2004). In that case, there is no chance to observe any decrease in methylation because the sites are already unmethylated. However, with the advancements in high-throughput technologies, it has become apparent that hypomethylation is also a major player in cancer (Adorján et al., 2002; Iacobuzio-Donahue et al., 2003; Stefanska et al., 2011).

Factors contributing to DNA hypomethylation

DNA methylation is a tightly regulated process, and loss of methylation may be contributed by different factors. Some of the most prominent ones are described in the following section.

Methyl group metabolism and dietary insufficiency

The major component that may act as a limiting factor for methylation of DNA is the universal methyl group donor S-adenosylmethionine (SAM) (Hoffmann and Schulz, 2005). The availability of SAM is dependent on dietary methionine as well as recycled methionine obtained from one-carbon metabolism (Hoffmann and Schulz, 2005). It has been known for decades that dietary deficiencies of the methyl group donor may have implication in the development of cancer (Giovannucci, 2004). Prolonged dietary methyl deficiency in rats have shown to induce global hypomethylation which ultimately contributed to the initiation of hepatocarcinogenesis (Pogribny et al., 2006). The recycling

of methionine to produce SAM also requires several vitamins like B_6, B_{12}, and folic acid and it is important to maintain the level of these vitamins to avoid any abnormal alteration in DNA methylation (James et al., 2003). Imbalance in any one of these Vitamins may cause SAM deficiency. Several polymorphisms found within the genes (methylenetetrahydrofolate reductase, *MTHFR*; methionine synthase, *MTR*; methionine synthase reductase, *MTRR* and cystathionine β-synthase, CBS) encoding enzymes involved in the recycling of methionine also showed association with increased risk of cancer (Kim, 2000). Moreover, the rapidly proliferating cancer cells need more methionine to keep up with the needs of the cells which gets exhausted as cancer progresses (Hoffman, 1984). As a result, there is a decrease in the level of SAM which might cause hypomethylation in the cancer genome.

Alteration in DNA methylation writers and erasers

Even though DNA methylation is a stable epigenetic modification, however, the process can be reversible. There are specific enzymes that can mediate the addition and removal of the methyl groups. The DNMT enzymes are involved in the addition and maintenance of methyl group and as such known as the 'writers' of methylation (Mahmood and Rabbani, 2017). There are three major DNMTs found in mammalian organisms: DNMT1, DNMT3A, and DNMT3B (Smith and Meissner, 2013). In recent years, several enzymes have been identified that can directly or indirectly cause demethylation of DNA, and hence they are called the 'erasers' of methylation (Cheishvili et al., 2015; Cortázar et al., 2011; Cortellino et al., 2011; Kohli and Zhang, 2013; Tahiliani et al., 2009). Changes

in the level and activity of the DNA methylation writers and erasers also contribute to the induction of DNA hypomethylation. *In vitro* studies have demonstrated that loss of a single or combination of DNMTs can cause hypomethylation as well as chromosomal instability (Karpf and Matsui, 2005). Similarly, the *Dnmt*-deficient mice showed global hypomethylation which increased the incidence of oncogenesis *in vivo* (Gaudet et al., 2003; Yamada et al., 2005). Alteration in the activity of the DNMT enzymes has also been shown to cause hypomethylation of the repetitive sequences in mice (Eden et al., 2003; Li, 2002). Such loss of methylation of the repetitive elements may have detrimental consequences which is discussed in the next section of the chapter. In patients with instability-facial anomalies (ICF) syndrome, mutations in *DNMT3B* gene alter the enzymatic activity of its encoded protein which in turn cause hypomethylation at satellite repeats on chromosomes 1, 9 and 16, ultimately leading to chromosomal rearrangements (Ehrlich, 2003; Xie et al., 2006). Increased expression of methyl-CpG-binding domain protein 2 (MBD2), which also possess DNA demethylation/eraser activity (Bhattacharya et al., 1999), showed correlation with DNA hypomethylation (Liu et al., 2011; Sheng et al., 2013).

Contribution of other epigenetic factors and modifiers

Since there is crosstalk between DNA methylation and other epigenetic mechanisms like chromatin remodeling and histone modification, the roles of these factors in mediating DNA hypomethylation cannot be overruled. Loss of histone 4 monoacetylation at lysine 16 (H4K16ac) and trimethylation of histone 4 at lysine 20 (H4K20me3) showed association with the hypomethylation at the repetitive sequences

of DNA (Fraga et al., 2005). Histone modifications may also have an indirect effect on DNA hypomethylation through the alteration of chromatin architecture (Wilson et al., 2007). It has been shown that loss of methylation at H3K9, a modification which is typically associated with heterochromatin establishment and maintenance (Bannister and Kouzarides, 2005), caused genomic instability (Peters et al., 2001). Such disruption of chromatin architecture may have implications in changing the methylation pattern of the DNA.

External insults

DNA hypomethylation can be mediated by different environmental stressors like exposure to exogenous chemicals and radiation as well as pathogen infection. Koturbash *et al*. have shown an association between radiation-induced DNA hypomethylation and cancer (Koturbash et al., 2005). They found that majority of the radiation-induced lesions in mice were repaired a month after the insult, but the level of DNA hypomethylation remained the same which was speculated to cause tumorigenesis through the induction of genomic instability. It has been demonstrated that exposure to carcinogens such as benzopyrene and arsenic can cause the induction of DNA hypomethylation (Chen et al., 2004; Sadikovic and Rodenhiser, 2006). Moreover, viral as well as bacterial infection may also induce hypomethylation of DNA (Goldberg et al., 2000; Macnab et al., 1988).

Impact of DNA hypomethylation

Some of the important consequences of DNA hypomethylation is summarized below.

Activation of repetitive elements

DNA hypomethylation may induce the activation of transposable elements (Jackson-Grusby et al., 2001) which may induce insertional mutagenesis (Wilson et al., 2007). Recent studies have demonstrated that promotor hypomethylation activates LINE1 expression in cancer (Tubio et al., 2014), which enables their subsequent retrotransposition. For example, somatic insertion of LINE1 element within the *APC* gene in one allele along with a point mutation in the other allele has been implicated in colorectal tumorigenesis through the two-hit pathway (Scott et al., 2016). Once activated, the repetitive elements can also facilitate the expression of other oncogenes and thereby promote tumorigenesis. For example, DNA hypomethylation-induced expression of the LINE-1 transcripts in chronic myeloid leukaemia (CML) showed association with the upregulation of the *c-MET* oncogene (Roman-Gomez et al., 2005).

Transcriptional activation of cancer-related genes

Pioneering studies have shown that the promoter of urokinase plasminogen activator (*PLAU,* also called *uPA*) is hypomethylated in cancer which is responsible for its increased gene expression in relatively more aggressive, hormone-insensitive breast cancer cell lines (Pakneshan et al., 2004b). This was one of the initial studies that provided the proof-of-concept that site-specific focal hypomethylation contributes to cancer progression and metastasis. Other cancer-related genes that showed hypomethylation-mediated activation of gene transcription include heparanase (*HPSE*), cadherin 3 (*CDH3*), breast cancer-specific gene 1 (*BCSG1*), S100 calcium binding protein P (*S100P*), *maspin* (also

known as *SERPINB5*), N-Acetyltransferase 1 (*NAT1*), pro-opiomelanocortin (*POMC*), related RAS viral oncogene homolog (*R-RAS*), claudin 4 (*CLDN4*), Ubiquitin C-Terminal Hydrolase L1 (*UCHL1*, also known as *PGP9.5*), mesothelin (*MSLN*), *Trefoil factor 2* (*TFF2*) (Ehrlich, 2009; Lee et al., 2006; Liu et al., 2005; Nishigaki et al., 2005; Ogishima et al., 2005; Paredes et al., 2005; Sato et al., 2004; Ye et al., 2005). Recent epigenome-wide association studies (EWAS) by our group have revealed the presence of hypomethylated sites at the promoters of several oncogenes and prometastatic genes (Parashar et al., 2015; Shukeir et al., 2015). We have also shown that treatment with the FDA-approved demethylating agent decitabine (5-Aza-2´-deoxycytidine) caused hypomethylation-induced expression of *PLAU* and several other prometastatic genes and transformed less aggressive breast cancer cells (MCF-7, ZR-75-1) into more aggressive ones (Ateeq et al., 2008). This further verified the notion that hypomethylation is involved in metastasis and careful considerations should be taken while using demethylating agents to treat cancer.

Genomic instability

Genomic instability is a common characteristic of cancer cells which includes structural variations in the genome like increased tendencies of base pair mutation, microsatellite instability, and variability in the structure and number of chromosome (chromosome instability) (Yao and Dai, 2014). In the late 1990s, Chen et al. have shown that murine embryonic stem cells devoid of *Dnmt1* gene predominantly increased the rates of deletion mutations which ultimately led to chromosomal instability (Chen et al., 1998).

This demonstrated the importance of DNA methylation in the maintenance of genomic stability in mammals. Later on, by generating a mouse model with hypomorphic *Dnmt1* allele that caused global hypomethylation, Gaudet *et al.* have shown that the mutant mice had increased susceptibility to develop T-cell lymphomas associated with increased chromosomal instability (Gaudet et al., 2003).

The first link between DNA hypomethylation and genomic instability in human was reported in human lymphoblastoid cell lines (Almeida et al., 1993). Further studies have demonstrated that demethylation of classical satellite 2 (Sat2) heterochromatic regions of chromosomes 1 and 16 caused non-clonal rearrangements in lymphoblastoid cells (Vilain et al., 2000). Since then many studies have demonstrated the association between hypomethylation and genome instability in human cancer. For example, in hepatocellular carcinoma (HCC), hypomethylation of Sat2 sequences showed association with chromosome 1 copy number gain (Wong et al., 2001). In urothelial cancer, hypomethylation of Sat2 and Sat3 repeats is associated with loss of heterozygosity (LOH) at chromosome 9 (Nakagawa et al., 2005). Cadieux *et al.* have shown that Sat2 hypomethylation in primary human glioblastomas caused alterations of copy number at the adjacent euchromatin regions (Cadieux et al., 2006). In prostate cancer, hypomethylation is associated with the alterations in chromosome 8 (Schulz et al., 2002).

DNA hypomethylation in diagnosis and prognosis of cancer

There is a growing interest in the identification of epigenetic signatures as biomarkers for the early diagnosis and prognosis of cancer. One of the advantages of this

strategy is that both DNA and its methylation signatures are quite stable, and they can also be extracted from the formalin-fixed, paraffin-embedded samples (Mahmood et al., 2018b). Therefore, the limitations related to sample quantity and quality for diagnosis can be mitigated.

Since there is focal hypomethylation of oncogenes in cancer, we and others have reasoned that these specific regions can be exploited as clinical biomarkers for diagnosis and prognosis of different stages of the disease. One of the classic examples in this regard is hypomethylation at the promoter of *PLAU*. Our group was the first to report that there is a reciprocal correlation between aggressiveness of breast cancer and the level of methylation at the *PLAU* promoter (Pakneshan et al., 2004b). We found that the percentage of methylation decreased with the advancement of breast cancer to a higher histological grade. This suggested that *PLAU* promoter hypomethylation can be used as a biomarker for early detection and aggressiveness of breast cancer (Pakneshan et al., 2004b). A similar pattern of *PLAU* promoter hypomethylation was also observed between benign prostate hyperplasia and prostate cancer where the methylation level decreased with the advancement of the disease (Pulukuri et al., 2007). Hypomethylation-mediated activation of *DDX43* (also known as *HAGE*) gene that encodes Cancer testis antigens (CTA) protein showed significant association with disease progression and poor patient outcome in CML patients (Roman-Gomez et al., 2007). Furthermore, *DDX43* promoter hypomethylation also correlated with poorer response to imatinib or interferon treatment in CML patients. This indicates that DNA hypomethylation can also be used for patient stratification before deciding a therapeutic intervention.

It has been demonstrated that hypomethylation of Sat2 repeats in the juxtacentromeric region showed strong association with ovarian cancer progression and mortality and therefore can be used as a marker of poor prognosis (Widschwendter et al., 2004). In urothelial carcinoma, Sat2 and Sat3 hypomethylation showed significant correlation with tumor grade and invasiveness of cancer (Nakagawa et al., 2005). Hypomethylation of LINE-1 showed association with better prognostic outcome in urothelial carcinoma patients (Neuhausen et al., 2006). Using the combined bisulfite restriction analysis (COBRA) PCR assay, Tangkijvanich et al. have shown that serum LINE-1 hypomethylation may serve as a prognostic factor for decreased overall survival in HCC (Tangkijvanich et al., 2007).

Another attractive method for early diagnosis of cancer that has been recently demonstrated by us and others is the use of DNA methylation signatures found in blood (Parashar et al., 2018; Zhang et al., 2018). During the progression of cancer, the DNA methylation profiles of the host immune cells are altered (Teschendorff et al., 2009). Taking advantage of this phenomena, we have identified and validated six hypomethylated CpG sites [cg27182070 (*RPA2*), cg19761014 (*LRRC37B2*), cg16624210 (*TPPP*), cg00481259 (*DECR2*), cg01252526 (*WDR9*), cg07271186 (TRY2P)] from the peripheral T-cells of breast cancer patients that can be used as an early detection biomarker (Parashar et al., 2018).

Hypermethylation in cancer:

Hypermethylation of hundreds of genes have been reported in case of breast cancer (Hinshelwood and Clark, 2008). Many of these hypermethylated genes are involved in important pathways like DNA damage repair, cell-cycle regulation, apoptosis, cell invasion and metastasis, angiogenesis and hormone signaling (Table 1-1).

Hypermethylation of estrogen receptor (ER) and progesterone receptor (PR) has been observed in breast cancer and has been proposed to be a mechanism for the development of ER-negative (ER-) breast tumor (Jovanovic et al., 2010; Weigel, 1993). Most of the breast carcinomas are ER positive (ER+) in the beginning and subsequently lose the ER to become more aggressive ER- breast cancer. Even though the link between *ER* (also called *ESR1*, estrogen receptor 1) promoter hypermethylation and subsequent decrease in ER expression is clear in the case of breast cancer cell lines (Ferguson et al., 1995), similar correlation is not always found in the clinical sample (Hori et al., 1999; Lapidus et al., 1996) Hori *et al.* found no association between promoter hypermethylation and expression of ER protein in human breast tumors (Hori et al., 1999). On the other hand, Lapidus *et al.* found correlation between promoter methylation and reduced expression of ER and PR in breast tumors (Gaudet et al., 2009; Lapidus et al., 1996). Another steroid receptor called retinoic acid beta 2 (*RAR-β2*) is hypermethylated in breast cancer (Widschwendter et al., 2000). Binding of RAR-β2 with retinoic acid may trigger anti-proliferative signals which can be skipped by the hypermethylation-mediated inactivation of the *RAR-β2* gene (Szyf et al., 2004). Hypermethylation has also been shown to inhibit

tumor suppressors like Ras association domain family 1 isoform A (*RASSF1A*) (Dammann et al., 2001).

Several genes involved in DNA repair mechanisms are hypermethylated in breast cancer. The loss of DNA repair genes results in genomic instability in the breast cancer genome. Methylation of the CpG islands at the promoter of *MGMT* gene is unique for the tumor tissues and is a predictor of overall survival in cancer (Esteller et al., 1999; Esteller and Herman, 2004). Tserga and colleagues found that aberrant methylation of the promoter of *MGMT* gene has an association with advanced breast tumor grade (Tserga et al., 2012). Spitzwieser *et al*. found more frequent *MGMT* promoter methylation in patients with breast tumor grade 3 compared to those having tumor grade 2 (Spitzwieser et al., 2015). *MLH1* promoter methylation results in the production of a non-functional protein which impairs the ability of the cells to repair the mismatches occurring during proliferation (Wajed et al., 2001). Interestingly, pharmacological reversal of methylation using 5-aza-2′deoxycytidine (5-azadC) has been shown to restore the expression of the protein as well as the DNA mismatch repair capacity of the cells in colorectal cancer (Herman et al., 1998). Other important DNA-repair genes that are hypermethylated in breast cancer include *BRCA1* (Esteller et al., 2001) and Ataxia Telangiectasia Mutated (*ATM*) gene (Vo et al., 2004).

One of the typical characteristics of tumor cells is to manipulate the cell cycle genes to aid rapid cell growth, proliferation as well to evade cell death. Inactivation of several critical cell cycle regulators and genes involved in apoptosis through hypermethylation is common for the breast cancer cells. In addition, hypermethylation is seen at the promoters

of several genes like *CDH1*, *CDH13*, *CST6*, *SYK* and *TIMP3* that directly or indirectly inhibit tumor cell invasion and metastasis (Esteller et al., 2001; Rivenbark et al., 2006; Toyooka et al., 2001; Yuan et al., 2001). Inactivation of these genes promotes invasion and metastasis of tumor cells.

Targeting abnormal DNA methylation as an anti-cancer strategy

In contrast to the genetic changes, DNA methylation changes are potentially reversible by either therapeutic strategies or dietary interventions (Szyf, 2009). This makes DNA methylation an excellent target for anti-cancer therapeutics (Szyf, 1994).

Targeting hypomethylation

It is obvious that DNA hypomethylation is a crucial player involved in upregulating the expression of many prometastatic genes as well as in the induction of genomic instability in cancer. Since DNA methylation-mediated changes are reversible (Ramchandani et al., 1999), targeting hypomethylation may serve as a suitable anti-cancer therapeutic strategy. Despite the identification of the role of DNA hypomethylation over three decades ago, there is still no approved agent targeting DNA hypomethylation. On the other hand, many drugs have been developed to target DNA hypermethylation and two of them are already approved by the FDA. This further emphasizes the fact how DNA hypomethylation remained neglected over the years. Our group has been exclusively focused on targeting DNA hypomethylation as an anti-cancer therapeutic strategy by using SAM. In the following section we will discuss on the effect of SAM-treatment in cancer.

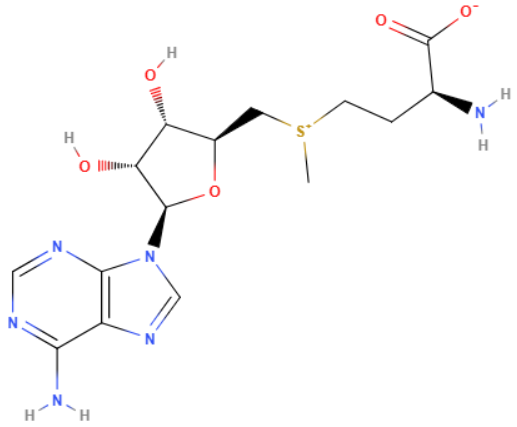

Figure 4: Chemical structure of S-adenosylmethionine ($C_{15}H_{23}N_6O_5S^+$).

The structure was generated using MolView (http://molview.org). From Mahmood and Rabbani, Adv Exp Med Biol. (Mahmood and Rabbani, 2019b)

S-Adenosylmethionine as a blocker of DNA hypomethylation in cancer

SAM is a naturally occurring sulfonium compound available in all living cells where it plays role in biochemical processes like transmethylation, transsulfuration, and aminopropylation (Bottiglieri, 2002). Italian biochemist Giulio Leonardo Cantoni initially discovered it in the early 1950s (Cantoni, 1951).

SAM has a unique chemical structure with a high energy sulfonium moiety attached to three carbon atoms that are susceptible to nucleophilic substitution (Lu, 2000) (Figure 4). This renders SAM the ability to donate methyl (-CH_3), adenosyl, and aminopropyl groups in different cellular processes. Because of its highly reactive nature, SAM can meditate cofactor functions in different biochemical reactions (Lu, 2000). In animals, a major portion of the SAM is used in transmethylation pathways where the methyl groups

are transferred to different acceptor molecules like DNA, RNA, proteins, and lipids (Lu and Mato, 2005; Roje, 2006). SAM also donates the aminopropyl groups to produce the polyamines required for cell growth via the aminopropylation pathway (Lu, 2000). By the transsulfuration pathway, SAM is converted to cysteine which then produces antioxidants like glutathione and taurine (Finkelstein, 1990). SAM also donates the adenosyl portion as well as the -NH_2 group for the synthesis of biotin (Delle Cave et al., 2017). Taken together, it is obvious that SAM plays a crucial role in the maintenance of cellular function and abnormalities in SAM metabolism may give rise to different pathological conditions (Lu, 2000). As such, SAM has been used to treat different diseases. It is approved as a nutraceutical agent for depression, fibromyalgia, osteoarthritis, as well as for diseases related to the liver (Bottiglieri, 2002). Our group was one of the pioneers to test whether DNA hypomethylation-mediated abnormalities of cancer can be reversed by using SAM (Pakneshan et al., 2004a). Since then the anti-cancer effect of SAM has been tested both *in vitro* and *in vivo* using rodent models in different cancer which is summarized in Table 2.

Table 2: Summary of anti-cancer effect of SAM *in vitro* and *in vivo*.

Cancer type	Effect of SAM-treatment	Reference
Breast	Decreased cell proliferation, invasion, migration, colony formation *in vitro*; Increased apoptosis; Combination of SAM with other known chemotherapeutic agents (decitabine, doxorubicin) showed a better anti-cancer effect than single-agent treatment *in vitro*; Reduced MDA-MB-231 xenograft tumor volume and metastasis *in vivo* upon daily supplementation by oral gavage	(Chik et al., 2013; Ilisso et al., 2015; Mahmood et al., 2018a)
Prostate	Decreased cell proliferation, invasion, migration, colony formation *in vitro*; Reduced skeletal lesion when SAM-treated PC-3 prostate cancer cells were injected into the tibia of immunocompromised mice	(Schmidt et al., 2016; Shukeir et al., 2006; Shukeir et al., 2015)
Liver	Decreased cell proliferation, invasion, colony formation *in vitro*	(Wang et al., 2017)
Lung	Combination of SAM with 5-fluorouracil (5-FU) significantly decreased cell proliferation by restoring the levels of DNMTs which are otherwise downregulated by 5-FU monotherapy *in vitro*	(Ham et al., 2013)
Gastric	Decreased cell proliferation, colony formation *in vitro*; Reduced SGC-7901 xenograft tumor volume *in vivo* upon administration of SAM through intraperitoneal injection	(Luo et al., 2010; Zhao et al., 2010)
Colorectal	Decreased cell proliferation, invasion, migration *in vitro*; Increased apoptosis; Reduction of inflammation-induced colon cancer *in vivo*; Inhibits the metastatic spread of colon cancer cells in the liver *in vivo*	(Hussain et al., 2013; Li et al., 2011; Tomasi et al., 2017)
Osteosarcoma	Decreased cell proliferation, invasion, migration, colony formation *in vitro*; Increased apoptosis; Reduced skeletal lesion and lung metastasis when SAM-treated LM-7 osteosarcoma cancer cells were injected in immunocompromised mice via intratibial and intravenous routes respectively	(Ilisso et al., 2016; Parashar et al., 2015)

Suppression of proliferation and enhancement of apoptosis by SAM-treatment

Uncontrolled cell growth along with suppression of apoptotic cell death is a major characteristic of cancer cells which has led to the development of several anti-cancer drugs targeting tumor cell proliferation. It has been shown that treatment with SAM can inhibit cell proliferation *in vitro* in different types of malignancies like breast cancer (Chik et al., 2013; Ilisso et al., 2015; Mahmood et al., 2018a), prostate cancer (Shukeir et al., 2015), liver cancer (Wang et al., 2017), colorectal cancer (Hussain et al., 2013), gastric cancer (Zhao et al., 2010), and osteosarcoma (Ilisso et al., 2016; Parashar et al., 2015). Our recent studies have demonstrated that daily administration of SAM by oral gavage caused a dose-dependent decrease in tumor volume in a xenograft model of breast cancer (Mahmood et al., 2018a). Similarly, SAM-treatment reduced tumor loads in animal models of gastric and colon cancer (Li et al., 2011; Zhao et al., 2010).

It is also known that rapidly proliferating cancer cells need compact polypeptides known as growth factors for cell proliferation. Therefore, these polypeptides are often targeted by many anti-cancer therapies. In prostate cancer and osteosarcoma cells, we have shown that SAM-treatment decreased the expression of genes encoding important growth factors like transforming growth factor β (*TGF-β*), vascular endothelial growth factor (*VEGF*), platelet-derived growth factor alpha (*PDGFA*) (Parashar et al., 2015; Shukeir et al., 2015). In addition, SAM-treatment attenuated key survival pathways mediated by ERK, β-Catenin and signal transducer and activator of transcription 3 (STAT3) in different cancer cells which also confirms the anti-proliferative effect of SAM (Ilisso et al., 2016; Li et al., 2011; Shukeir et al., 2015).

SAM-treatment increases both gene and protein expression of dual specificity phosphatase 1 (DUSP1) which is an inhibitor of ERK (Tomasi et al., 2010). In proliferating cancer cells, active ERK1/2 causes phosphorylation at the Ser296 residue of DUSP1 and thereby facilitates its proteasomal degradation via SKP2-CKS1 ubiquitin ligase (Calvisi et al., 2008a; Calvisi et al., 2008b). It has been suggested SAM-treatment protects DUSP1 from undergoing proteasomal degradation (Tomasi et al., 2010).

EWAS using Illumina methylation 450K array revealed that SAM-treatment caused hypermethylation at the promoter of *STAT3* gene which in turn caused a reduction of its gene expression (Shukeir et al., 2015). In gastric and colon cancer cell, SAM-treatment reversed the promoter hypomethylation state of proto-oncogenes *MYC* and *HRAS* which in turn decreased their gene expression (Luo et al., 2010).

In vitro experiments by us and others have suggested that SAM-treatment significantly increases the percentage of apoptotic cell death in different types of cancer and arrests the cancer cells at the G_2M phase of the cell cycle progression (Ilisso et al., 2016; Mahmood et al., 2018a; Parashar et al., 2015; Shukeir et al., 2015). At the molecular level, SAM treatment reduces the expression of anti-apoptotic protein BCl-2 and increases the expression of the pro-apoptotic Bcl-2-associated X (BAX) protein (Ilisso et al., 2016; Mahmood et al., 2018a). This might explain the increase in apoptosis upon SAM-treatment. In addition, SAM-treatment reduces the expression of cyclin D and E and increases the expression of p53, p21and p27 (Cave et al., 2018; Ilisso et al., 2016).

The anti-tumor effect of SAM can be partly explained from its unique biochemical structure. SAM can donate methyl groups via the transmethylation pathway which can

reduce the hypomethylation mediated genomic instability seen in cancer. It can produce antioxidants via the transsulfuration pathway which may prevent the development of cancer. However, SAM can also donate the aminopropyl groups for polyamine biosynthesis (Figure 4). Polyamines are involved in the promotion of proliferation in both preneoplastic and neoplastic cells (Frau et al., 2013). In rapidly proliferating cancer cells, the level of endogenous SAM goes down favoring polyamine synthesis (Feo et al., 1987). Feo *et al.* showed that exogenous administration of SAM inhibited the activity of a key enzyme of polyamine biosynthesis pathway known as ornithine decarboxylase (ODC), which in turn reduced in the development of nodules in a rat model of liver cancer (Feo et al., 1987). Therefore, an overall reduction in tumor volume is observed upon exogenous administration of SAM.

Attenuation of cancer cell invasion and metastasis upon SAM-treatment

Tumor associated metastasis is the most common cause of cancer-related mortality in humans (Mehlen and Puisieux, 2006). It is a multi-step process driven by different types of growth factors and proteases that can enable the tumor cells to break down the extracellular matrix (ECM) and migrate into different tissues via the lymphatic system and circulation (Barkan et al., 2010; Mehlen and Puisieux, 2006). The plasminogen activator (PA) system plays a central role in this process (Mahmood et al., 2018b). In cancer cells, hypomethylation-mediated upregulation of *PLAU* gene results in the increased production of uPA protein which binds to its receptor (uPAR) and thereby activates plasminogen to plasmin. Once activated, plasmin can initiate a cascade of proteolytic events to cause the

degradation of ECM components (Mahmood et al., 2018b). Our group was the first to show that epigenetic targeting of *PLAU* promotor hypomethylation through the use of methylating agent like SAM can reverse its transcriptional state (Pakneshan et al., 2004a). We found that SAM-treatment could downregulate *PLAU* and matrix metalloproteinase 2 (*MMP2*) expression and thereby reduced the invasiveness of the cancer cells as determined by the transwell Boyden chamber invasion assay (Pakneshan et al., 2004a; Shukeir et al., 2006). These effects were also confirmed by several other research groups working on different types of cancer (Hussain et al., 2013; Zhao et al., 2010). We have also shown that oral administration of SAM reduces the metastatic burden of orthotopically implanted MDA-MB-231 breast tumor cells in different peripheral tissues like lung, liver, and spleen of immunocompromised mice (Mahmood et al., 2018a). Microarray-based gene expression analysis of the MDA-MB-231 transcriptome revealed that treatment with SAM significantly reduced the expression of several prometastatic and epithelial-mesenchymal transition (EMT) pathway genes (Mahmood et al., 2018a). In another study, Tomasi *et al.* (2017) have shown that oral administration of SAM reduces the ability of the colon cancer cells to metastasize to the lung. They have further demonstrated that SAM-treatment increases the expression of microRNA-34a and b (miR-34a and miR-34b) which in turn downregulate the IL-6 signaling pathway and thereby decrease the metastatic potential of the cancer cells.

Transcriptome analysis of liver and prostate cancer cells upon SAM-treatment also showed downregulation of genes related to cell migration, metastasis, and angiogenesis (Schmidt et al., 2016; Wang et al., 2017). Consistent with these observations, methylome

analysis upon SAM-treatment showed hypermethylation at the promoters of several oncogenes and prometastatic genes (Parashar et al., 2015; Shukeir et al., 2015; Wang et al., 2017). In prostate cancer and osteosarcoma, we showed that inoculation of SAM-treated cells into the tibia of immunocompromised mice reduced skeletal lesion formation at the bone which is a major site of metastasis in many cancer (Parashar et al., 2015; Shukeir et al., 2015). Sahin *et al.* have shown that SAM-treatment inhibited endothelial cell proliferation which is suggestive of the anti-angiogenic effect of SAM (Şahin et al., 2011).

Combination of SAM with other anti-cancer agents

Since SAM shows little to no toxicity, several groups have tested the anti-cancer properties of SAM in combination settings with currently approved chemotherapeutic agents. Ilisso *et al.* (2015) investigated the effect of SAM in combination with Doxorubicin on different breast cancer cell lines. Doxorubicin is a classic chemotherapeutic agent used for patients with breast cancer. Even though it is highly effective as an anti-cancer agent, it also elicits several side effects including cardiomyopathy, alopecia, vomiting as well as resistance to therapy (Shapiro and Recht, 2001). The authors have reasoned that combination of SAM and doxorubicin will allow lowering the concentration of doxorubicin and thereby reduce doxorubicin associated side effects (Ilisso et al., 2015). They found a significantly synergistic anti-proliferative effect following combination therapy with doxorubicin and SAM in hormone-dependent breast cancer cells. This highly significant effect on cancer cells following combination therapy was shown to be due to the increase in the percentage of apoptotic cells.

Using human A549 lung cancer cells, Ham *et al.* (2013) showed that the anti-cancer effect of another agent 5-fluorouracil (5-FU) is markedly enhanced when used in combination with SAM. They have shown that single-agent treatment with 5-FU reduced the expression of DNMTs which is restored upon combination treatment with SAM.

It has been recently demonstrated that SAM in combination with autophagy inhibitor Chloroquine (CLC) show better anti-proliferative effect through the induction of apoptotic cell death (Cave et al., 2018). The authors have further shown that the combination treatment synergistically inhibited the phosphorylation of AKT/mTOR kinases which are major survival pathways of the cancer cells.

SAM has also been used in combination with other epigenetic drugs. Previous studies by our group have demonstrated that the FDA-approved DNA methylation inhibitor decitabine undesirably activates the expression of several prometastatic genes [*PLAU*, heparanase (*HPSE*), synuclein-γ (*SNCG*), and C-X-C motif chemokine receptor 4 (*CXCR4*)] along with the activation of tumor suppressor gene like Ras association domain family member 1 (*RASSF1*) and proapoptotic gene *BAX* (Ateeq et al., 2008). We found that inoculation of decitabine treated MCF7 breast cancer cells into the fat pad of immunocompromised mice showed significantly reduced tumor burden compared to the control group of mice implanted with untreated cells which is consistent with the known tumor suppressive effect of decitabine. However, when the tumors were analyzed after the sacrifice of the animals on week 6, a significant induction of several prometastatic factors like PLAU, Heparanase, and CXCR4 was observed in the decitabine treated group. So, we concluded that decitabine treatment increased the invasiveness of less aggressive MCF7

breast cancer cells. This might be a reason why these drugs are not as effective in solid tumors compared to the liquid tumors for which they are approved. SAM, on the other hand, reduces the expression of several prometastatic genes (Pakneshan et al., 2004a). Since the cancer cells are heterogeneous, the pattern of DNA methylation abnormalities may be different between the cells within the tumor microenvironment. As such, targeting both hypermethylation (by decitabine) and hypomethylation (by SAM) has been tested as a proof-of-concept, and it was found that the combination treatment synergistically reduces proliferative and invasive capacities of several breast cancer cell lines (Chik et al., 2013). It was shown that the combination of SAM and decitabine could inhibit the expression of prometastatic genes like *PLAU* and *MMP2* which are otherwise induced by single agent treatment by decitabine. Moreover, SAM did not hinder the expression of tumor suppressor genes (*CDKN2AIP* and *p21*) which are normally induced upon decitabine treatment. This implies that SAM affects tumor suppressor genes and prometastatic genes differently. However, the study was limited to a few genes only and whether a similar effect can be recapitulated *in vivo* using mouse models of breast cancer remained unknown. Nevertheless, the study has opened the door for a novel combinatorial approach using two epigenetic agents that can target various elements of the DNA methylation-mediated abnormalities seen in cancer. A summary of SAM-mediated reversal of cancer-related events is shown in Figure 5.

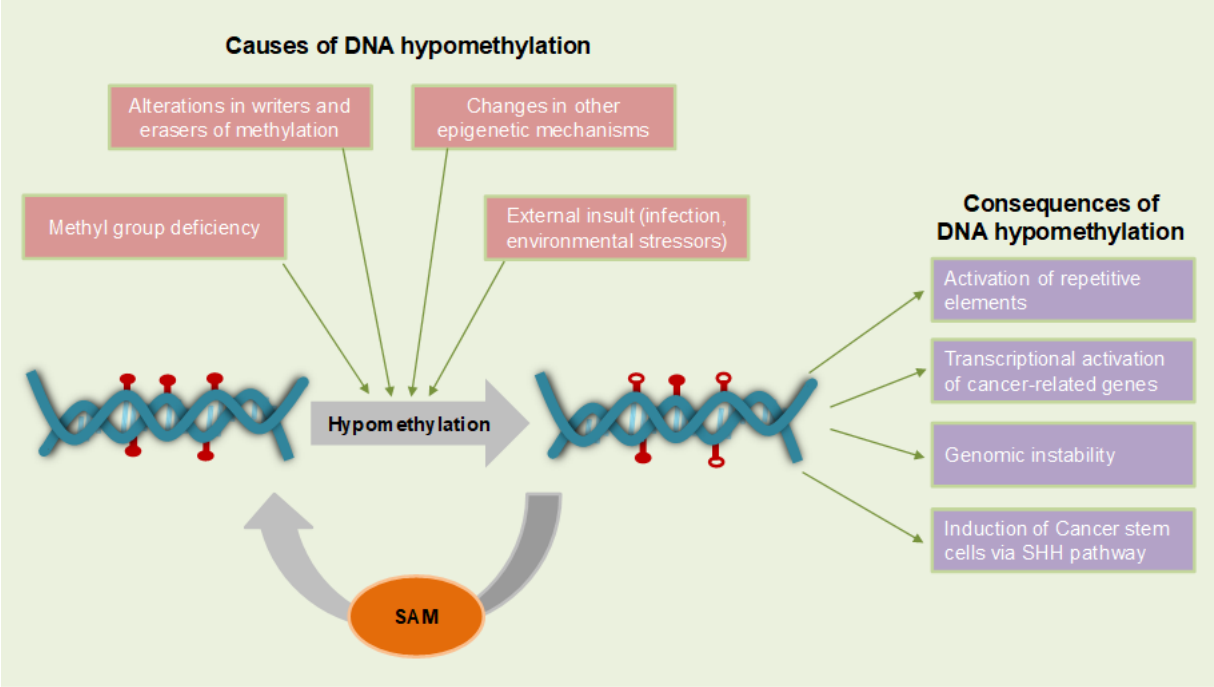

Figure 5: Causes and consequences of DNA hypomethylation and reversal of the hypomethylated state by methylating agent like SAM.

From Mahmood and Rabbani, Adv Exp Med Biol. (Mahmood and Rabbani, 2019b)

Targeting hypermethylation

The main focus of attention for the past two decades has been on the activation of tumor suppressor genes by blocking DNA hypermethylation using DNMT inhibitors. Over the years, many DNMT inhibitors have been developed and Table 3 contains a list of DNMT inhibitors that have been used in many preclinical and clinical studies. Two cytidine analogs 5-azacytidine (Vidaza®) and 5-aza-2′deoxycytidine (Decitabine, Dacogen®) have been approved by the Food and Drug Administration (FDA) and European Medicines Agency (EMA). This chapter will explain these two hypomethylating agents in detail. In addition, the role Vitamin D as a demethylating agent will also be discussed.

Table 3: List of DNMT inhibitors used in cancer

Class of inhibitors	Compound
Nucleoside analogs	5-azacytidine (Vidaza®) 5-aza-2′deoxycytidine (decitabine, Dacogen®) Zebularine (dZTP) Guadecitabine (*SGI-110*) 5-fluoro-2′-deoxycytidine (FdCyd, NSC-48006) 5-azacytidine-5'-elaidate (CP-4200) 2'-Deoxy-N4-[2-(4-nitrophenyl) ethoxycarbonyl]-5-azacytidine (*NPEOC-DAC*) Fazarabine (Arabinofuranosyl-5-azacytosine) 5,6-Dihydro-5-azacytidine (DHAC; NSC 264880)
Non-nucleoside analogs	RG108 Procaine Procainamide Epigallocatechin-3-Gallate (EGCG) Hydralazine Psammaplin A Mitozantrone *Mithramycin* A (Plicamycin)
SiRNA	MG98 (antisense oligonucleotide against *DNMT1*)

5-azacytidine and 5-aza-2′deoxycytidine

5-azacytidine (5-azaC), an analog of cytidine nucleoside, and its deoxy derivative 5-aza-2′deoxycytidine (5-azadC) are both hypomethylating agents that are currently approved for treating several specific forms of myelodysplastic syndromes (MDS), acute myeloid leukemia (AML), and chronic myelomonocytic leukemia (CMML) (Figure 6) (Derissen et al., 2013) These two compounds were first synthesized in Czechoslovakia by Sorm *et al.* in 1964 for use as cytostatic agents (Šorm et al., 1964). The initial clinical trials to examine their role as anti-cancer agents for liquid cancers started as early as 1967 in

Europe followed by 1970 in the United States of America (VON HOFF et al., 1976) (Figure 6).

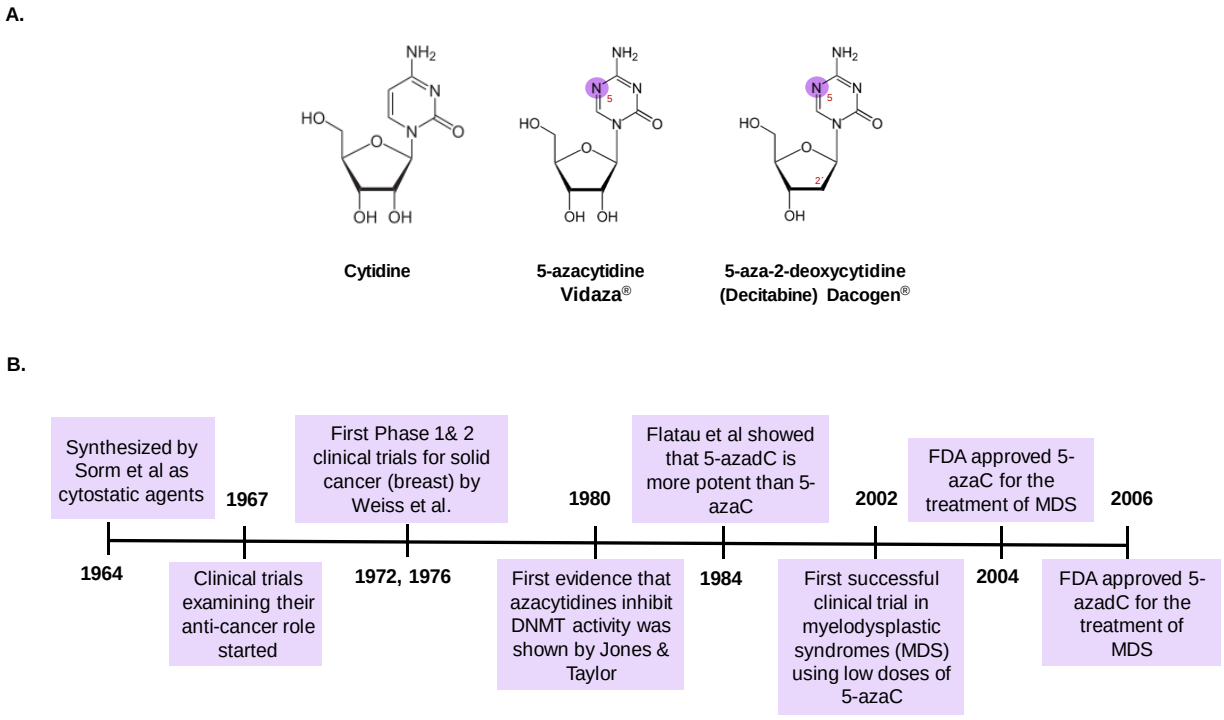

Figure 6: Approved DNMT inhibitors 5-azaC and 5-azadC.

A. Chemical structures of cytidine nucleoside, its analogs 5-azacytidine (5-azaC) and 5-aza-2′deoxycytidine (5-azadC). **B.** A timeline from the discovery until the approval of two well-known azacytidines (5-azaC and 5-azadC). Adapted from Mahmood and Rabbani, Trends in Cancer Research (Mahmood and Rabbani, 2017).

During the 1970s it was demonstrated that both of these drugs could be incorporated into the DNA and only 5-azaC can incorporate itself into the RNA and causes disruption of RNA and subsequent blockade of protein synthesis (Li et al., 1970; Veselý and Čihák, 1978). Later on, it was demonstrated that the deoxy derivative 5-azadC is more cytotoxic as well as more potent than 5-azaC (Flatau et al., 1984; Momparler et al., 1984).

The first clinical trials that used 5-azaC as monotherapy for phase I and II studies in solid tumors commenced during the 1970s (Weiss et al., 1976; Weiss et al., 1972). A phase II clinical trial by Weiss *et al.* demonstrated an anti-cancer effect of 5-azaC in 17% and 21% patients having breast cancer and malignant lymphomas respectively when they were given a dose of 1.6 mg/kg of the drug daily for ten days (Weiss et al., 1976). There was a minimal effect of 5-azaC on solid tumors (Weiss et al., 1976). Moreover, 5-azaC induced toxic effects like leucopenia, thrombocytopenia, sepsis, and cerebral hemorrhage in patients (Weiss et al., 1972). These studies demonstrated that these drugs should not be used as a monotherapy in solid tumors (Cheishvili et al., 2015). It should be noted that the dose at which these drugs were used in these studies was too high. So, the therapeutic window was smaller.

In a landmark study published in 1980, Jones and Taylor demonstrated that 5-azaC can inhibit DNMT activity (Jones and Taylor, 1980). This study also demonstrated the first link between DNA methylation and cellular differentiation and thereby opened the avenue for targeting DNMTs for cancer treatment. They found that prolonged exposure to lower concentrations of the drug led to optimal DNA demethylation and inhibited cell differentiation. On the other hand, at higher concentrations the DNMT inhibitors decreased

DNA demethylation as well as differentiation (Jones and Taylor, 1980, 1981). Taken together, these observations renewed the interest in 5-azaC and 5-azadC as anti-cancer therapeutic agents and provided a basis for designing the subsequent clinical trials. The first successful clinical trial of 5-azaC used a low dose (75 mg/m^2) of the drug in patients with myelodysplastic syndromes (MDS) where prolonged administration for a period of 7 days repeated every 28 days showed better response over the best available supportive care (Silverman et al., 2002). This led to the FDA approval of using 5-azaC for the treatment of patients having MDS in 2004. Similarly, a low dose of 5-azadC (15 mg/m^2) given every 8 hours for 3-5 days was effective in MDS patients (Kantarjian et al., 2007; Lübbert et al., 2011). In 2006, 5-azadC (decitabine) was also got the FDA approval for the treatment of patients with MDS. Currently, many clinical trials are going on using these drugs to treat solid tumors.

Mechanism of action of 5-azacytidine and 5-aza-2′deoxycytidine

Two major mechanisms of anti-cancer activity of 5-azaC and 5-azadC have been shown so far. These include (i) demethylation of DNA upon the inhibition of DNMT enzyme which enables the activation of tumor suppressor genes and (ii) cellular cytotoxicity due to the incorporation into DNA (both 5-azaC and 5-azadC) and RNA (5-azaC only) leading to the initiation of DNA damage response (Stresemann and Lyko, 2008).

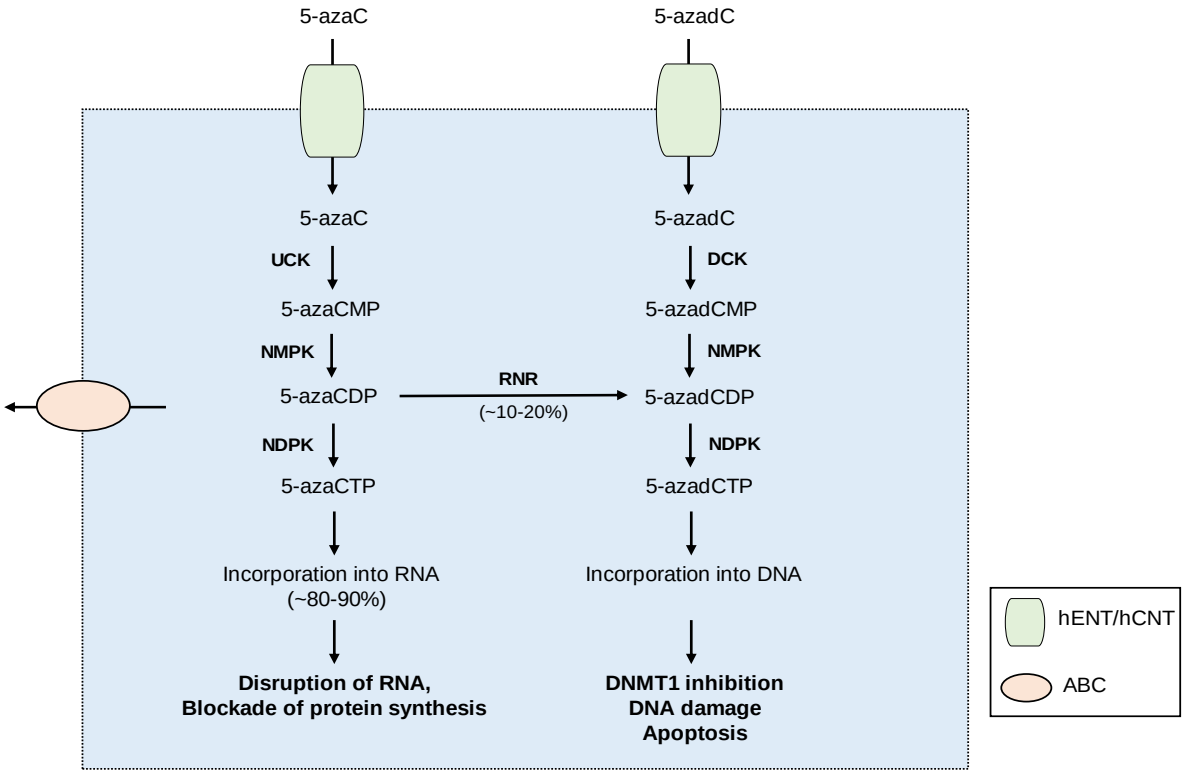

Figure 7: Cellular uptake, metabolism, and mechanism of action of 5-azaC and 5-azadC.

Upon cellular uptake by human equilibrative (hENT) and concentrative nucleoside transporters (hCNT) these drugs are activated through a three-step phosphorylation process. The first step is catalyzed by uridine-cytidine kinase (UCK) and deoxycytidine kinase (DCK) for 5-azaC and 5-azadC respectively. The second step is catalyzed by nucleoside monophosphate kinase (NMPK) for both of these drugs and then a small portion (~10-20%) of 5-azaCDP is converted into 5-azadCDP by the action of ribonucleotide reductase (RNR). The third step is catalyzed by nucleoside diphosphate kinase (NDPK) where 5-azaCTP incorporates into RNA and 5-azadCTP incorporates into the DNA, and they can subsequently mediate their demethylation and cytotoxic effects depending on the dose of the drugs being administered. ABC transporters play a role in the excretion of these drugs out of the cells. Adapted from Mahmood and Rabbani, Trends in Cancer Research (Mahmood and Rabbani, 2017).

Both 5-azaC and 5-azadC are prodrugs and upon cellular uptake by human equilibrative (hENT, SLC29A family) and concentrative nucleoside transporters (hCNT, SLCA28 family), they are activated through three consecutive ATP-dependent phosphorylation steps to achieve their active forms that can be subsequently incorporated into the DNA and RNA (Figure 7) (Rius et al., 2009; Stresemann and Lyko, 2008). The first phosphorylation step to transform the drugs to a monophosphorylated form is catalyzed by uridine-cytidine kinase (UCK) for 5-azaC and deoxycytidine kinase (DCK) for 5-azadC (Li et al., 1970; Stresemann and Lyko, 2008).

The enzymes catalyzing the second and third phosphorylation steps are same for both the drugs. Nucleoside monophosphate kinase (NMPK) and nucleoside diphosphate kinase (NDPK) catalyzes the incorporation of the second and third phosphate groups respectively to yield active forms of the drugs (5-aza-CTP and 5-aza-dCTP) (Stresemann and Lyko, 2008). Afterward, 5-aza-dCTP is incorporated into the newly synthesized strand of DNA during replication to inhibit DNMT enzyme and cause subsequent DNA damage and apoptosis. However, in the case of 5-azaC, 80–90 % are incorporated into the RNA in the form of 5-aza-CTP to cause inhibition of RNA and protein synthesis. Therefore, only 10–20 % is available for incorporation into the DNA after the conversion from 5-aza-CDP to 5-aza-dCDP by ribonucleotide reductase (RNR) enzyme (Figure 7) (Stresemann and Lyko, 2008). ATP-binding cassette transporters (ABC family) play a role in transporting both these drugs out of the cells.

Effects of 5-azaC and 5-azadC on breast cancer

As mentioned earlier, both 5-azaC and 5-azadC have been approved for specific types of liquid tumors in the early 2000s. At present, the focus of attention is towards the possibility of using them in solid tumors.

We and others have shown that 5-azaC and 5-azadC can reduce breast cancer growth *in vitro* and *in vivo* (Ateeq et al., 2008; Thakur et al., 2012). Treatment with 5-azadC was able to transform the less invasive breast cancer cell lines like MCF-7 and ZR-75-1 into more invasive cells both *in vitro* and *in vivo* (Ateeq et al., 2008). We found that inoculation of MCF-7 cells pretreated with 5-azadC showed significantly reduced tumor growth in mice compared to the control mice inoculated with vehicle-treated MCF-7 cells (Ateeq et al., 2008). However, pharmacological inhibition of methylation by 5-azadC also induced the expression of previously quiescent prometastatic (*uPA, HEPARANASE, CXCR4* and *SNCG*) genes involved in tumor cell invasion and metastasis (Ateeq et al., 2008). A similar increase in invasiveness and metastasis has also been demonstrated in other types of cancers (Habets et al., 1990; Olsson and Forchhammer, 1984; Sato et al., 2003). So careful considerations should be given prior to the use of these drugs for the treatment of cancer.

5-azaC and 5-azadC in combination with other agents

Both 5-azaC and 5-azadC showed a modest therapeutic effect in solid tumors compared to liquid tumors. However, these drugs can reduce solid tumor growth (Ateeq et al., 2008). Hence, combinations of the DNMT inhibitors with other types of therapeutic

agents are now in various phases of clinical trials for breast and other types of solid tumors (source: www.clinicaltrial.gov). A phase II clinical trial of 5-azaC (Vidaza) in combination with a chemotherapeutic agent called Nab-paclitaxel (Abraxane) is ongoing for breast cancer patients. Other types of therapeutic strategies like 5-azadC (decitabine) in combination with Anti-PD-1 antibody, neoadjuvant therapy using pembrolizumab and 5-azadC (decitabine) before surgery followed by standard chemotherapy are currently in the initial phases of clinical trials with breast cancer patients.

More recently, the combination of DNMT inhibitors with other types of epigenetic drugs like the histone deacetylase (HDAC) inhibitors have gained much interest. It has been demonstrated that a crosstalk exists between DNA methylation and histone acetylation in terms of gene expression (Cervoni and Szyf, 2001). Therefore, the effect of 5-azaC and 5-azadC in combination with different types of HDAC inhibitors has been tested in several studies (Cameron et al., 1999; Elangovan et al., 2013). Cameron *et al*. first demonstrated the synergistic anti-cancer effect of a combination of DNMT and HDAC inhibitors (Cameron et al., 1999). Elangovan *et al.* have shown that sodium butyrate (an inhibitor of HDAC) in combination with 5-azadC inhibits tumorigenesis in a mouse model of breast cancer (Elangovan et al., 2013).

Vitamin D as demethylating agent

The steroid hormone Vitamin D was classically used to prevent and treat rickets (DeLuca, 1988). However, it is now well-established that Vitamin D also plays an important role during several pathological conditions, including cancer (Holick, 1995). At

the molecular level, Vitamin D functions by regulating gene expression programs, mainly through the association with its receptor [Vitamin D receptor (VDR)] (Deeb et al., 2007; Kongsbak et al., 2013). To exert the genomic effects, VDR first forms a dimer with retinoid X receptor (RXR). Then the VDR-RXR dimer binds to VDR responsive elements near the promoters of target genes and modulates their expression in a context-dependent manner (Kimmel-Jehan et al., 1999). However, it should be noted that Vitamin D can also function via non-genomic pathways by stimulating calcium influx and subsequent induction of phosphorylation cascades (Civitelli et al., 1990).

The primary links between Vitamin D and the epigenome were established through the studies related to histone modification. The VDR-RXR dimer can interact with histone acetyltransferases to cause activation of gene expression (Karlic and Varga, 2011). However, emerging evidence suggests that Vitamin D is also associated with other types of epigenetic modifications like DNA methylation (Tapp et al., 2013; Zhu et al., 2013). It has been shown that the biologically active 1,25-dihydroxyvitamin D [1,25$(OH)_2$D] can cause demethylation of DNA and thereby change gene expression patterns (Doig et al., 2013; Fetahu et al., 2014). For example, higher dietary intake of Vitamin D showed association with hypomethylation of *WNT5A* and dickkopf1 (*DKK1*) genes in Canadian patients with colorectal cancer (Rawson et al., 2012). These results show concordance with previous studies where administration of either Vitamin D or its analogue EB1089 caused activation of the Wnt antagonist *DKK1* and thereby showed potent anti-tumor effects against colorectal cancer cells *in vitro* and *in vivo* (Aguilera et al., 2007). An inverse correlation was also observed between the Vitamin D level and methylation at the promoter

of the adenomatous polyposis coli (*APC*) tumor suppressor gene (Tapp et al., 2013). In addition, the treatment of highly aggressive triple-negative MDA-MB-231 cells with Vitamin D caused demethylation at the promoter of *CDH1* gene encoding the epithelial cell marker E-cadherin (Lopes et al., 2012). Therefore, Vitamin D also plays a vital role in modulating cancer progression by repressing the epithelial to mesenchymal transition through DNA demethylation. In other studies, Vanoirbeek *et al.* have shown that Vitamin D treatment caused a demethylation-mediated activation of the adaptor molecule PDZ-LIM domain-containing protein 2 (*PDLIM2*) which is involved in the attachment of components of the cytoskeleton, and thereby reduced breast cancer cell migration and invasion (Vanoirbeek et al., 2014).

Taken together, these studies suggest that the anti-proliferative effects of Vitamin D and its metabolites may, in part, be exerted through DNA demethylation. Currently, there is a paucity of the studies deducing the exact mechanism by which Vitamin D regulates DNA methylation. However, from an anti-cancer therapeutic perspective, the use of Vitamin D as a single agent therapy or in combination with other agents to reverse the DNA hypermethylation mediated abnormalities is attractive because of the lower toxicity of vitamin D compared to the currently approved DNMT inhibitors. Moreover, Vitamin D is available as an over the counter nutraceutical agent that can be used for chemoprevention against cancer.

Targeting DNA methylation readers

As mentioned above, DNA methylation takes place when methyl groups are added to the appropriate bases on the genome by the action of 'writer' molecules known as DNA methyltransferases. How these methylation marks are read and interpreted into different functionalities represents one of the main mechanisms through which the genes are switched 'ON' or 'OFF' and typically involves different types of 'reader' proteins that can recognize and bind to the methylated regions. A tightly balanced regulation exists between the 'writers' and 'readers' in order to mediate normal cellular functions. However, alterations in normal methylation pattern is a typical hallmark of cancer which alters the way methylation marks are written, read and interpreted in different disease states. This unique characteristic of DNA methylation 'readers' has identified them as attractive therapeutic targets. Even though several 'reader' proteins have been shown association with cancer, this chapter will be mainly focused on MBD2 which was previously shown to be a target of SAM (Pakneshan et al., 2004a). The summary of the current state of knowledge on targeting DNA methylation readers will also be provided.

Role of MBD2 in normal physiology and cancer

The *MBD2* is a multiexon gene located on chromosome 18 of both human and mouse genomes. The encoded protein (MBD2) from this locus shows more than 70% amino acid sequence similarity with another protein called MBD3 (Hendrich and Bird, 1998). In addition, a high level of gene-sequence homology exists between human and mouse *MBD2* and *MBD3* genes which is suggestive a gene duplication event during the

course of evolution (Hendrich and Tweedie, 2003). Initial studies proposed that MBD2 functions as a transcriptional repressor by recruiting co-repressors like the NuRD (Nucleosome Remodeling Deacetylase) complex to the methylated sites (Ng et al., 1999).

MBD2 protein has three main isoforms due to the use of alternative translational start site and alternative splicing: MBD2a, MBD2b, and MBD2c (also called MBD2t) (Hendrich et al., 1999; Hendrich and Bird, 1998). The presence of different domains that give the different MBD2 isoforms the ability to interact with different binding partners and thereby carry out different functions (Figure 8A). However, all three isoforms have the MBD domain to bind to methylated CpG. MBD2a is the canonical isoform and contains an N-terminal glycine-arginine (GR) repeat that can undergo post-translational modification, followed by the MBD domain, the TRD domain, and lastly the coiled-coil (CC) domain at the c-terminal region that has the ability to mediate protein-protein interactions (Du et al., 2015; Gnanapragasam et al., 2011) (Figure 8B).

The MBD2b uses an alternative start site during translation, and the only difference from MBD2a is the absence of the N-terminal GR repeat. The presence of the MBD and TRD domain in both of these isoforms helps them to bind different corepressor complexes to mediate transcriptional repression (Boeke et al., 2000). The third isoform MBD2c is devoid of the TRD and CC domains due to the inclusion of an alternative exon 3 that produces a truncated protein (Hendrich and Bird, 1998). The MBD2c may function differently than the other isoforms. For example, in human pluripotent stem cells (hPSC), MBD2a interacts with NuRD to promote cell differentiation while MBD2c mediates the reprogramming to pluripotency (Lu et al., 2014).

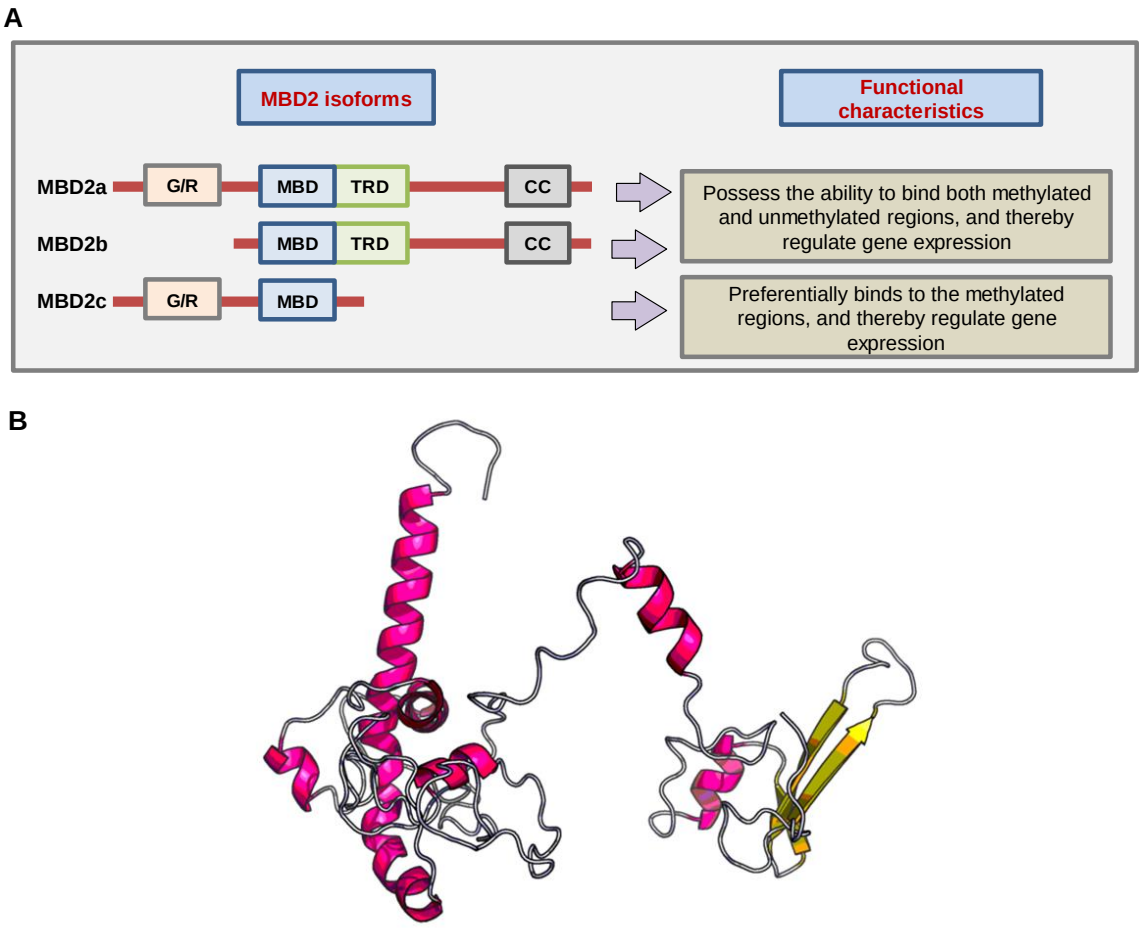

Figure 8: Characteristic domain architecture and function of different MBD2 isoforms.

A. MBD2a is the canonical isoform containing four domains while MBD2a lacks the N-terminal G/R-repeat due to the use of alternative start site during translation. On the other hand, the MBD2c isoform is formed due to the inclusion of an alternative third exon which produces a premature stop codon, and as a result, the MBD2c lacks the TRD and CC domains. From Mahmood and Rabbani, Frontiers in Oncology (Mahmood and Rabbani, 2019a). **B.** Molecular modelling of the Mbd2 (cannonical Mbd2a isoform) was predicted by the RaptorX online server (http://raptorx.uchicago.edu/).

It has been shown that MBD2 can also bind to unmethylated DNA to cause changes in gene expression (Baubec et al., 2013). However, the TRD-domain deficient MBD2c

isoform cannot bind to unmethylated DNA which suggests that MBD2 binding to the unmethylated regions of the DNA is dependent on the interaction between TRD domain and NuRD complex (Baubec et al., 2013). More recent evidence suggests that the MBD2 protein can also mediate the activation of gene expression (Angrisano et al., 2006; Wang et al., 2013; Weaver et al., 2014). MBD2 has been proposed to function as a demethylase enzyme that can remove or 'erase' the DNA methylation marks (Bhattacharya et al., 1999). However, this finding has been contested by several others (Boeke et al., 2000; Zhang et al., 1999). The *Mbd2* knockout mice (*Mbd2*$^{-/-}$) are viable and do not show any abnormalities during embryonic development even though the female *Mbd2*$^{-/-}$ mice have been reported to show some abnormalities related to maternal behavior (Hendrich et al., 2001).

MBD2 plays an important role in cancer by silencing key tumor suppressor genes in prostate cancer (Pulukuri and Rao, 2006), colon cancer (Magdinier and Wolffe, 2001), and liver cancer (Bakker et al., 2002). On the other hand, in several cancer-types, MBD2 has been shown to mediate transcriptional repression of human telomerase reverse transcriptase (*hTERT*) which is suggestive of a tumor suppressive function of MBD2 (Chatagnon et al., 2008). In breast cancer, Müller *et al.* could not detect any discernable difference in *MBD2* expression (Müller et al., 2003), while Billard *et al.* detected a statistically significant upregulation of *MBD2* in the mammary tumor (Billard et al., 2002).

Stable knockdown of the *MBD2* gene suppressed the proliferation of several breast cancer cell lines *in vitro* and decreased tumor volume *in vivo* (Mian et al., 2011). Furthermore, it was demonstrated that tumor suppressor genes like *DAPK1* and *KLK10* are de-repressed upon depletion of MBD2 in breast cancer cells. Interestingly, MBD2 has been

also shown to function in the maintenance and spread of DNA methylation at specific regulatory regions of prostate cancer cells (Stirzaker et al., 2017). Moreover, knockout of *Mbd2* gene mice protected against tumorigenesis when crossed with $Apc^{Min/+}$ mice (a rodent model for colorectal cancer) (Sansom et al., 2003). The loss of MBD2 function causes downregulation of the Wnt signaling pathway which plays a major role in the development of colorectal cancer (Phesse et al., 2008; Sansom et al., 2003). However, later studies have found that depletion of several other epigenetic and chromatin binding factors like Kaiso, DNMTs, and Brg1 also downregulated the Wnt signaling pathway and thereby protected from tumorigenesis (Cai et al., 2014; Holik et al., 2014; Prokhortchouk et al., 2006). This suggests that the downregulation of Wnt signaling is not MBD2-specific, and it is instead a result of a general perturbation of chromatin remodeling complex (Wood and Zhou, 2016).

Emerging evidence supports that MBD2 plays a role in immunity partly because of its tissue localization pattern. Among the various members of the MeCP2-MBD family, MBD2 shows the highest expression in spleen which is a major site for both adaptive and innate immune responses (Wood et al., 2016; Wood and Zhou, 2016). Wang *et al.* demonstrated that MBD2 regulates the expression of Foxp3 which is the master regulator of regulatory T cells (Tregs) (Wang et al., 2013). They have shown that MBD2 binds to the Treg-specific demethylation region (TSDR) located upstream of the *Foxp3* gene and thereby facilitates TET2-mediated demethylation to induce *Foxp3* expression. Furthermore, knockout of *Mbd2* gene reduced the number of Tregs and impaired the immunosuppressive function meditated by the Tregs. Interestingly, the $Mbd2^{-/-}$ mice did

not develop autoimmunity which makes it an attractive target in pathological conditions like cancer where the Tregs have been suggested as potential targets for immunotherapy (Shitara and Nishikawa, 2018).

Current state of knowledge on targeted Epi-therapies

Even though the field is still at its infancy, several studies have shown promising effects in terms of developing anti-cancer therapeutic strategies against the MBPs. A summary of the currently described anti-cancer strategies targeting different known MBPs is shown in Figure 9.

It has been demonstrated that treatment of prostate cancer cells with green tea polyphenols (GTPs) reversed the DNA hypermethylation-mediated silencing of the known tumor suppressor gene glutathione-*S*-transferase pi (*GSTP1*) through the downregulation of DNMT1, MeCP2 and several other MBD proteins (Pandey et al., 2010). The authors have shown that GTP treatment causes demethylation at the promoter of *GSTP1*. Furthermore, chromatin immunoprecipitation (ChIP) assays revealed that GTP treatment also reduced the association of the transcriptional repressor MBD2 with Sp1 binding site that leads to the increased transcriptional activation of the *GSTP1* gene. In other studies, it has been shown that natural compounds like curcumin, resveratrol, guggulsterone, EGCG, withaferin A, and genistein can also cause the reversal of epigenetic state in cancer cells through the reduction of DNMT1, HDAC1, and MeCP2 protein expression (Mirza et al., 2013).

Interestingly, polyphenols obtained from natural products have also been shown to decrease cancer cell proliferation through the downregulation of UHRF1 predominantly via the p53 and p73-dependent signaling pathways (Arima et al., 2004; Sharif et al., 2012; Sharif et al., 2010). *Limoniastrum guyonianum* aqueous gall extract (G extract), as well as luteolin, independently inhibited proliferation of cervical cancer HeLa cells by arresting the cells in G2/M phase and induced apoptosis through the inhibition of UHRF1 along with the upregulation of p16 tumor suppressor (Krifa et al., 2013). In a mouse model of colon cancer, red wine polyphenols (RWPs) inhibited tumor growth, metastasis, angiogenesis, and increased apoptosis through the downregulation of UHRF1 and other proliferation markers like ki67, cyclin D1 (Walter et al., 2010). The UHRF1 expression has also been shown to be downregulated in mechanisms independent of the p53 and p73 signaling pathways. For example, in chronic lymphocytic leukemia patients, polyphenols from Bilberry extract (Antho 50) decreased UHRF1 expression and increased apoptosis via targeting the Bcl-2/Bad pathway (Alhosin et al., 2015).

The expression of *MBD2* gene was downregulated when the cancer cells were treated with the naturally occurring methyl group donor SAM that shows anti-proliferative and anti-metastatic effects (Pakneshan et al., 2004a; Shukeir et al., 2006). This approach is particularly attractive because SAM is non-toxic to cancer cells and has been shown to cause downregulation of several other oncogenes and prometastatic genes without changing the expression of the known tumor suppressor genes *in vitro* and *in vivo* (Mahmood et al., 2018a). Moreover, antisense oligonucleotides against *MBD2* gene decreased tumorigenesis in human lung and colorectal cancer cells both *in vitro* and *in vivo*

(Campbell et al., 2004). In human promyelocytic leukemia cells, an amonafide analog named B1 [chemical name: *N*-(2-(dimethylamino) ethyl)-2-aminothiazonaphthalimide] has been demonstrated to cause relief from the MBD2-mediated repression of 14-3-3σ tumor suppressor gene (Liang et al., 2010). Moreover, KCC07, a brain-permeable small molecule inhibitor of the MBD2 pathway, have been demonstrated to suppress medulloblastoma *in vivo* through the activation of BAI1/p53 axis (Zhu et al., 2018).

Cancer immunotherapies have shown great promise as therapeutic strategies in patients. There are several forms of immunotherapies that include the use of checkpoint inhibitors, monoclonal antibody therapies, and vaccine immunotherapies against the tumor-associated antigens (TAAs) (Tsuboi et al., 2019). With the advancements of cancer immunology, several TAAs have been identified, and one of them is a WT1 product (Gao et al., 2000; Ohminami et al., 2000). Indeed, immunotherapies against the WT1 antigen showed promising outcomes in clinical trials on patients with several solid and hematological cancers (Ohno et al., 2012; Oji et al., 2018; Oka et al., 2017; Tsuboi et al., 2019).

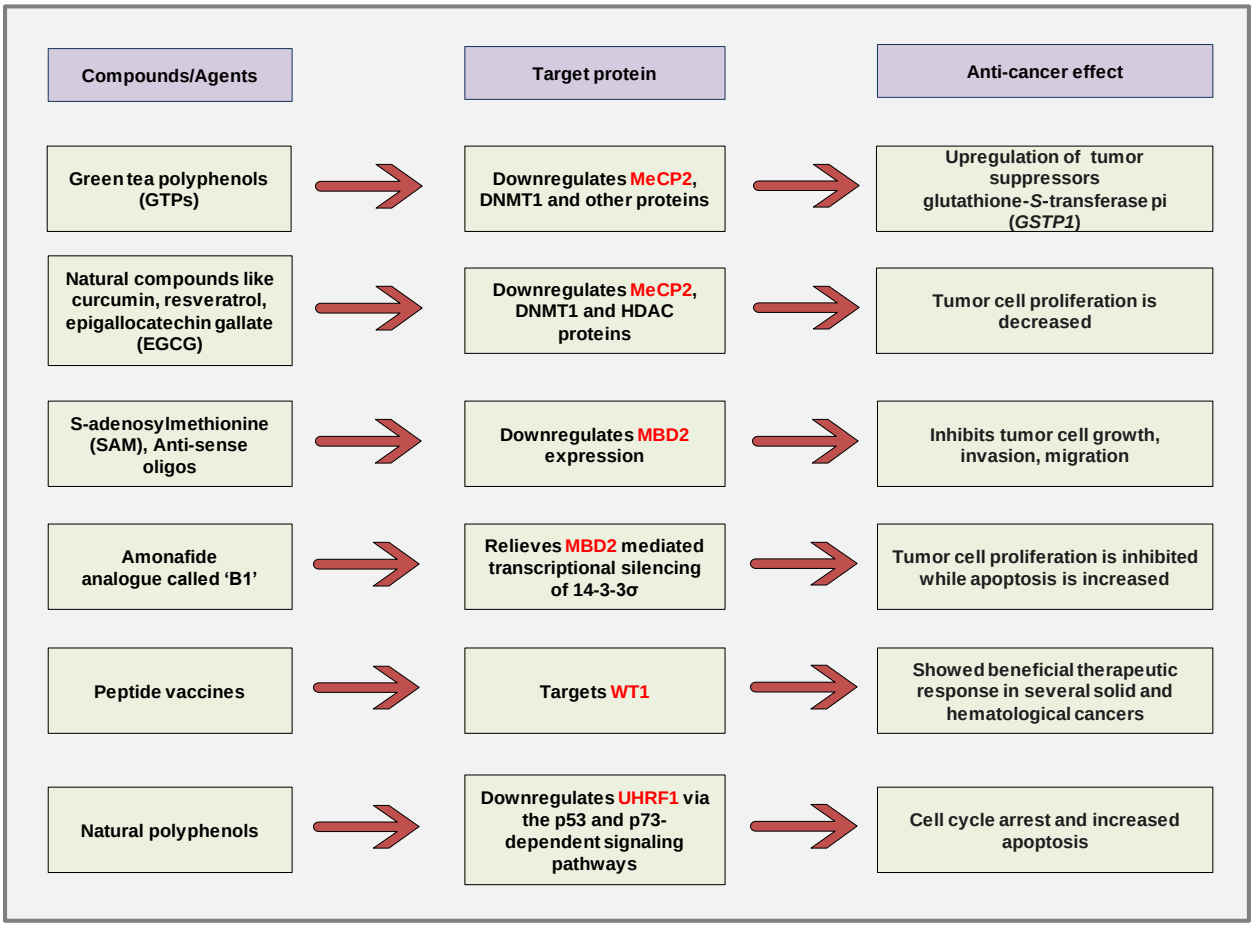

Figure 9: Schematic representation of the currently described anti-cancer strategies against different MBPs.

Polyphenols obtained from natural compounds can downregulate the aberrantly expressed MeCP2, UHRF1 in cancer cells via differential regulation of cancer-related signaling pathways. The naturally occurring physiologic compound S-adenosylmethionine as well as anti-sense oligonucleotides can downregulate the elevated expression of *MBD2* gene and cause inhibition of tumor growth, invasion, and metastasis. Immunotherapy against WT1 antigen has shown promising effects in clinical trials for several malignancies. From Mahmood and Rabbani, Frontiers in Oncology (Mahmood and Rabbani, 2019a)

Rationale of the project

Abnormal DNA methylation is an archetypal hallmark of cancer. Both hypermethylation-mediated inactivation of tumor suppressor genes and hypomethylation-mediated activation of prometastatic genes are common attributes of cancer cells, which make the methylome an attractive anti-cancer drug target. In contrast to genetic changes, DNA methylation-mediated epigenetic abnormalities are reversible by either dietary interventions or therapeutic strategies, and a plethora of epigenetic drugs (Epi-drugs) primarily targeting DNA hypermethylation have been shown to be effective in preclinical and clinical settings. However, the currently approved DNA hypermethylation inhibitors, even though useful against tumor growth, can also promote the activation of prometastatic genes, which leads to increased metastasis. Moreover, these drugs are highly toxic with short half-lives. Therefore, it stands to reason that targeting DNA hypomethylation by using methylating agents that can downregulate the prometastatic genes will serve as a suitable therapeutic strategy to block tumor metastasis. Previous studies at our lab have shown that treatment of various cancer cell lines (breast, prostate, osteosarcoma) with a naturally occurring methyl group donor S-adenosyl methionine (SAM) could block tumor growth, invasiveness and metastatic spread. At the molecular level, treatment with SAM causes DNA hypermethylation at the promoters of several known pro-metastatic genes as well as oncogenic DNA methylation readers like *MBD2*; and thereby inhibit their expression. However, these studies were done either *in vitro* or using pretreated cancer cells implanted into immunocompromised animals. Therefore, the *in vivo* anti-cancer therapeutic potential of SAM has never been tested before. In this study, we hypothesized

that SAM could serve as an effective anti-cancer agent as a monotherapy or in combination with other epigenetic agents like decitabine. Additionally, SAM could act as a chemo-preventive agent alone and in combination with other known agents like vitamin D in immunocompetent systems. We also hypothesize that depletion of *MBD2*, which is also a downstream target of SAM, could inhibit tumor growth and metastasis in a mouse model of spontaneous breast cancer.

Objectives of the project

1. To test the effect of SAM treatment on breast cancer growth and metastasis in a xenograft model and deduce the global gene expression networks altered by SAM.
2. To test the combinatorial effect of the demethylation inhibitor (SAM) along with a methylation inhibitor (decitabine) on breast cancer growth and metastasis *in vitro* and *in vivo.*
3. To test the chemopreventive effect of SAM in combination with Vitamin D prohormone [25(OH)D3] on breast cancer growth, lung metastasis, and colonization to the bone using well established transgenic and syngeneic models of breast cancer.
4. To deduce the functional role of Methyl-CpG Binding Domain Protein 2 (Mbd2), a downstream effector of SAM, in tumor growth and metastasis of transgenic MMTV-PyMT animals and identify the molecular signaling pathways affected by the depletion of *Mbd2.*

Chapter Two: Methyl Donor S-adenosylmethionine (SAM) supplementation Attenuates Breast Cancer Growth, Invasion, and Metastasis *in vivo*; therapeutic and chemopreventive applications

Preface

The global methyl group donor S-adenosylmethionine has been previously shown to suppress cell proliferation and invasion of different types of cancer cells *in vitro.* Moreover, tumor volumes of xenograft animals implanted with *ex vivo* SAM-treated cancer cells were significantly reduced compared to control groups implanted with untreated or SAH-treated cells. The question that remained unanswered was whether oral administration of methylating agents like SAM would be efficacious and safe in preclinical settings to translate to breast cancer patients in clinical settings. This is the first study that tested the anti-cancer therapeutic potential of SAM against xenografted breast tumors. Previous studies have shown that SAM-treatment downregulated the expression of several known prometastatic genes like *Plau, Mmp2*. Therefore, to gain insights into the global transcriptomic changes, Affymetrix gene expression microarray profiling was done on the vehicle (control) and SAM-treated MDA-MB-231 cells. Herein, an author-generated version of the manuscript is presented with permission from the publisher. The manuscript related to this study was published in the 'Oncotarget' in 2018:

> "**Mahmood,N.**, Cheishvili,D., et al. (2018) Methyl Donor S-adenosylmethionine (SAM) supplementation Attenuates Breast Cancer Growth, Invasion, and Metastasis in vivo; therapeutic and chemopreventive applications. Oncotarget 9:5169-5183."

 In addition, email consent was obtained from the Editor which can be found in the Appendices.

Abstract

DNA hypomethylation coordinately targets various signaling pathways involved in tumor growth and metastasis. At present, there are no approved therapeutic modalities that target hypomethylation. In this regard, we examined the therapeutic plausibility of using universal methyl group donor S-adenosylmethionine (SAM) to block breast cancer development, growth, and metastasis through a series of studies *in vitro* using two different human breast cancer cell lines (MDA-MB-231 and Hs578T) and *in vivo* using an MDA-MB-231 xenograft model of breast cancer. We found that SAM treatment caused a significant dose-dependent decrease in cell proliferation, invasion, migration, anchorage-independent growth and increased apoptosis *in vitro*. These results were recapitulated *in vivo* where oral administration of SAM reduced tumor volume and metastasis in green fluorescent protein (GFP)-tagged MDA-MB-231 xenograft model. Gene expression analyses validated the ability of SAM to decrease the expression of several key genes implicated in cancer progression and metastasis in both cell lines and breast tumor xenografts. SAM was found to be bioavailable in the serum of experimental animals as determined by enzyme-linked immunosorbent assay and no notable adverse side effects were seen including any change in animal behavior. The results of this study provide compelling evidence to evaluate the therapeutic potential of methylating agents like SAM in patients with breast cancer to reduce cancer-associated morbidity and mortality.

Introduction

Despite the advancements being made in our understanding of the biology, diagnosis, prevention, and treatment of cancer, metastasis remains the dominant cause of breast cancer-associated morbidity and mortality [1]. The 10-year survival rate for stage I/II breast cancer patients, whose cancer is localized within the breast tissue, is around 88% [2]. However, the 10-year survival rate for Stage III and IV cancer patients with metastatic spread of breast tumors is 40% and less than 10% respectively [2]. Hence, there is an urgent need for the development of novel and less toxic therapeutic strategies that can be useful to block both tumor growth and metastatic spread of cancer cells.

Tumor metastasis occurs when the cancer cells are dislodged from the primary site due to their ability to degrade the component of the extracellular matrix, invade into the blood vessels through intravasation, survive in the circulation, extravasate from the blood vessels, and finally start to proliferate as new tumors at a distant organ [3]. The highly organized multi-step process of metastasis is regulated and driven by networks of growth factors, cytokines, adhesion molecules, and proteolytic enzymes [4]. We and others have shown that several key molecules implicated in the metastatic cascade are epigenetically regulated through DNA hypomethylation [5-7]. For example, a positive correlation between promoter hypomethylation and subsequent increase in the expression of protease-encoding urokinase plasminogen activator (*PLAU*) gene has been observed with the progression of breast and prostate cancer [8, 9]. Some other cancer-related genes that are induced by DNA hypomethylation include *heparanase (HPSE)* [10], *synuclein-γ* (*SNCG*) [11], pro-opiomelanocortin (*POMC)* [12], cadherin 3 (*CDH3*) [13], related RAS viral

oncogene homolog (*R-RAS*) [14], *maspin* (also called *SERPINB5*) [15], and S100 calcium binding protein P (*S100P*) [15]. Moreover, pharmacological inhibition of methylation of non-invasive breast cancer cell lines (MCF-7, ZR-75-1) by using 5-Aza-2´-deoxycytidine increased the expression of prometastatic genes like *PLAU*, *HPSE*, C-X-C motif chemokine receptor 4 (*CXCR4*), and *SNCG*, and thereby transformed them into more invasive cells [16]. Therefore, it stands to reason that the use of inhibitors targeting hypomethylation to downregulate genes of the metastatic cascade may serve as a suitable anti-cancer therapeutic strategy.

The universal methyl donor SAM (also known as AdoMet) could be used in this regard as an inhibitor of demethylation/hypomethylation. SAM is a naturally occurring physiologic molecule found ubiquitously in all living cells, and functions in transmethylation, transsulfuration, and aminopropylation pathways [17]. SAM is second only to adenosine triphosphate (ATP) in terms of playing a versatile role in different types of physiological processes [18]. Currently, it is used as a preventive agent for mood disorders, fibromyalgia, and joint pain. Even though the chemical structure of SAM was first described in the 1950s by Cantoni [19], its potential use as an anti-cancer therapeutic agent has only emerged over the last two decades [20]. SAM-treatment has been found to be effective in repressing the invasiveness as well as proliferative capabilities of different types of cancer cell lines [21, 22]. We have previously shown that the anti-metastatic activity of SAM is likely due to downregulation of pro-metastatic genes like *PLAU* and matrix metalloproteinase 2 (*MMP2)* [6, 23]. SAM has been shown to inhibit angiogenesis [24], and reduce inflammation-induced colon cancer [25]. Taken together, these studies

provided a strong rationale towards the possible use of SAM in cancer prevention and treatment. However, the anti-cancer effects of SAM have never been examined in a therapeutic setting for hormone-dependent malignancies like breast cancer.

In the present study, we have investigated whether blocking demethylation and promoting methylation by SAM-treatment alone could exhibit anti-tumor effects using well-established *in vitro* and *in vivo* models of breast cancer. Results from this study show that SAM-treatment causes a significant reduction in tumorigenesis and metastatic spread of breast cancer cells which can be attributed in part to the ability of SAM to impact methylation and downregulation of the expression of several important genes implicated in the metastatic cascade.

Results

SAM-treatment suppresses cell proliferation, migration, invasion, anchorage-independent growth and potentiates apoptosis in vitro

Uncontrolled expansion of tumor cells through deregulated cell proliferation marks one of the critical events underlying the complexity and idiopathy of cancer cells [26]. Targeting cell proliferation has been one of the main focuses in cancer therapeutics. We, therefore, first examined the effect of SAM on the growth characteristics of two highly invasive human breast cancer cell lines MDA-MB-231 and Hs578T using our well-established experimental protocol (Fig. 1A). Our results showed that treatment with different doses of SAM (100 μM and 200 μM) caused a significant dose-dependent reduction in tumor cell proliferation compared to vehicle-treated control cells, which

demonstrates the anti-proliferative effect of SAM on breast cancer cells (Fig. 1B). To determine whether SAM-treatment causes any adverse effect on the viability of normal non-tumorigenic cells *in vitro*, we treated normal human breast epithelial cells (HBEC) with the highest dose of SAM (200 μM) used in this study. Results from these studies showed that SAM-treatment did not cause any significant change in the percentage of viability in the treated cells compared to the control cells (Supplementary File 1, Fig. S1).

To determine the effect of SAM on cell migration, *in vitro* wound-healing capacity of control and SAM-treated (100 and 200 μM) MDA-MB-231 and Hs578T cells were assessed over a period of 48 hours from the initial scratch on the culture plate. The area of the initial scratch was similar for all the experimental groups. However, with the passage of time, control and SAM-treated cells displayed different migratory profiles during wound healing in both the cell lines. SAM treatment caused a significant dose-dependent decrease in the migratory ability of both breast cancer cell lines as compared to vehicle-treated control cells; effects which were most pronounced at 48 hours after the initial scratch (Fig. 1C).

We next investigated whether SAM could suppress the invasiveness of MDA-MB-231 and Hs578T cells using Boyden chamber Matrigel invasion assay. Our *in vitro* data suggested that SAM-treatment caused a significant dose-dependent decrease in tumor cell invasion of both cell lines (Fig. 1D). The number of cells in both upper and lower part of Boyden chamber was counted which showed the presence of a similar number of tumor cells in both parts of the chamber suggesting that the anti-invasive effects of SAM are independent of its anti-proliferative effect.

We also evaluated the effect of SAM on anchorage-independent growth which is a hallmark of carcinogenesis *in vitro*. The ability of tumor cells to form colonies in soft agar allows for semi-quantitative evaluation of cellular transformation under different experimental conditions [27]. We observed a significant dose-dependent reduction of anchorage-independent growth by comparing the number of colonies formed by the control and SAM-treated (100 μM and 200 μM) cells from both cell lines (Fig. 1E).

Next, to determine the effect of SAM on programmed cell death, an annexin V/PI apoptosis assay was performed using flow cytometry. As shown in Fig. 1F, treatment with 200 μM of SAM caused a significant increase in the percentage of apoptotic cells in both cell lines as compared to the controls. To elucidate the potential mechanism of apoptosis, we determined the expression of anti-apoptotic Bcl-2 protein in control and experimental cells using Western blot analysis. These results a significant reduction in the expression of Bcl-2 in MDA-MB-231 cells treated with SAM as compared to the control cells (Supplementary File 1, Fig. S2). Results from these studies suggest that SAM mediates its apoptotic effects via the Bcl-2 signaling pathway. These results are in agreement with similar effects of SAM on other cancer cell types [28].

SAM-treatment reduces tumorigenesis and metastasis in MDA-MB-231 xenograft mice model

Next, we moved to the principal aim of this study i.e. to assess the therapeutic potential of SAM in a xenograft model of breast cancer. MDA-MB-231-GFP cells were inoculated into the fat pad of the fourth mammary gland of immunodeficient female CD-1

nude mice, and the animals were treated with either vehicle only or two different doses (40 and 80 mg/kg/day) of SAM via daily oral gavage. A schematic representation of the treatment strategy is shown in Fig. 2A. All the animals from vehicle-treated control, as well as the group receiving lower dose of SAM (40 mg/kg/day), developed primary tumors starting from week 5 which continued to grow until the sacrifice of animals at week 10 post tumor cell inoculation. In contrast 3 out of 10 animals treated with higher dose of SAM (80 mg/kg/day) did not grow any primary tumor during the ten weeks of this study (Fig. 2B). The treatment regimen using two different doses of SAM (40 and 80 mg/kg/day) via daily oral gavage showed a significant dose-dependent reduction in tumor volume as compared to the vehicle-treated control group (Fig. 2C, Supplementary File 1, Fig. 3). SAM-treatment also showed a significant reduction in the weight of extirpated tumor compared to the controls after the sacrifice of all animals at week 10 (Supplementary File 1, Fig. 4). We did not observe any significant difference in the overall body weight of control and SAM-treated animals throughout the study (Supplementary File 1, Fig. S5).

We then assessed the anti-metastatic potential of SAM treatment. Lung, liver, and spleen of control and experimental animals were collected after sacrifice, and the number GFP-positive metastatic foci were counted. Experimental animals treated with 80mg/kg/day of SAM via daily oral gavage showed a significant reduction in the number of GFP-positive metastatic foci in lung, liver, and spleen as compared to vehicle-only controls (Fig. 2D). However, the treatment with low dose of SAM (40mg/kg/day) didn't show anti-metastatic properties in all the organs (Fig. 2D). Hence, further analysis was performed on the high dose (80 mg/kg/day) of SAM receiving group.

SAM-treatment differentially regulates genes implicated in cancer progression and metastasis

We first evaluated the transcriptomic changes of MDA-MB-231 cells upon SAM-treatment. For that, we carried out microarray-based gene expression profiling (Affymetrix Human Gene 2.0 ST Array) using three independent sets of control and 200 μM SAM-treated RNA samples. We found that 476 microarray mRNAs were significantly altered in SAM-treated samples compared to controls (|fold change|>1.5 and P<0.01). A total of 231 microarray mRNAs were upregulated and 245 microarray mRNAs were downregulated in the SAM-treated samples when compared with control (Supplementary File 2). Hierarchical clustering of top 50 most significantly changed microarray mRNAs are shown in Fig. 3A.

Next, we analyzed the signaling pathways that were significantly altered upon SAM-treatment. The enriched pathway analysis of differentially regulated genes in breast cancer was performed using the Kyoto Encyclopedia of Genes and Genomes (KEGG) and Pathway Interaction Database (PID) databases. Our analysis showed that 14 pathways were significantly changed upon SAM-treatment (Fig. 3B). Interestingly, most of the pathways that were altered by SAM-treatment have strong implication in cancer progression and metastasis.

To gain further insight into the biological processes affected by the genes that are differentially expressed upon SAM-treatment, we used WebGestalt [29] (Supplementary File 1, Fig. S6). Our analysis showed that the top biological process identified to be

overrepresented by the genes upregulated by SAM-treatment functions in the negative regulation of endopeptidases (P=2.0 × 10^{-7}; FDR=1.59 × 10^{-3}). In contrary, the top hit for the genes downregulated by SAM is associated with positive regulation of cell-substrate adhesion (P=2.5 × 10^{-6}; FDR=3.2 × 10^{-2}). This further implies that SAM, through some unknown but surprisingly explicit mechanisms, plays a crucial role in regulating genes involved in tumor progression and metastasis.

Next, some of the genes identified through the expression array (*HAS2, Sox4, MUC1*) along with selected genes (*PLAU, SPARC, FABP7, HAS3*) implicated in cancer progression and metastasis were subjected to quantitative polymerase chain reaction (qPCR) analysis using the total RNA from control and 200 μM SAM-treated MDA-MB-231 cells. In experimental cells treated with SAM, a marked decrease in the expression of these genes was observed compared to vehicle-treated control cells (Fig. 3C).

Next, RNA of primary tumors from control and experimental animals treated with 80 mg/kg/day of SAM were subjected to qPCR analysis. Similar to the results seen in the MDA-MB-231 cells *in vitro*, SAM-treatment showed a marked reduction of all the genes in primary tumors (Fig. 3D). Gene set analysis revealed that in human breast cancer cell lines the expression of these seven genes (*MUC1, PLAU, FABP7, SPARC, HAS2, HAS3, SOX4*) are higher in basal-B subtype compared to other subtypes (Fig. 3E). More interestingly, Kaplan-Meier analysis found significantly positive correlation between the higher expression of these seven genes and poor distant-metastasis free survival in breast cancer patients (Fig. 3F). Collectively these results and data analysis shows that SAM can downregulate genes that have prognostic value for breast cancer metastasis.

SAM-treatment changes promoter methylation status and protein expression of prometastatic genes

We then focused on the promoter methylation of prometastatic genes that were downregulated by SAM treatment in the qPCR assay. Tumor DNA of experimental animals treated with SAM showed increased methylation of *SPARC* by pyrosequencing as compared to vehicle-treated control tumors (Fig. 4A). We have previously shown the SAM-mediated methylation changes at the promoter of *PLAU* in breast cancer [23]. We didn't observe any significant methylation changes in the other genes (*MUC1, FABP7, HAS2, HAS3, SOX4*) that showed downregulation in qPCR (data not shown). There might be several possibilities behind such observations. First, the differentially methylated site upon SAM-treatment might be located beyond the regions that were focused during pyrosequencing. Second, these genes are downstream of some other genes that are regulated by SAM, and the changes seen in qPCR are caused by indirect methylation effect of SAM. Third, SAM regulates these genes by a mechanism that is independent of DNA methylation such as histone methylation or other non-epigenetic mechanisms.

Next, we wanted to confirm the changes in protein expression in MDA-MB-231 tumors upon SAM-treatment through immunohistochemical analysis. As shown by the representative image of control and SAM-treated tumors probed with antibodies for MUC1, SPARC, and FABP7 in Fig. 4B, a significantly reduced staining of these proteins was observed in SAM-treated tumors compared to the control tumors. The SAM-mediated protein level changes of PLAU have been previously shown by our group [6, 23]. We were

unable to determine the change in the expression of SOX4, HAS2, and HAS3 proteins due to lack of well-characterized antibodies with a higher specificity of staining pattern.

SAM is bioavailable in the serum of experimental animal with no adverse behavioral and physiological changes

Lack of bioavailability often hinders the therapeutic potential of anti-cancer agents. To be efficacious, the therapeutic molecule needs to be available in the blood for a reasonable amount of time so that it can be absorbed and then circulated to the target organ(s). Towards these goals, serum from control and experimental animals were analyzed for the presence of SAM using an enzyme-linked immunosorbent assay (ELISA). We found that the average basal level of SAM in the control animals was 10.43 ± 0.57 μM which increased to 34.22 ± 1.45 μM in the treatment group receiving 80 mg/kg/day of SAM (Fig. 5A). We also performed a relative analysis of the SAM levels in the serum of control and experimental animals treated with exogenous SAM by LC-MS/MS and observed a similar increase in the levels of SAM in experimental group of animals (data not shown). This confirms that SAM is bioavailable in the animals after administration through oral gavage suggesting that it might also be orally available in humans.

Even though SAM is widely used as a supplement for depression, some transient adverse behavioral effects were previously reported in human clinical trials [30]. To assess whether SAM treatment causes any behavioral change at the efficacious dose of this study i.e. 80 mg/kg/day, we next conducted two different behavioral tests on control and SAM-treated mice. First, a novel object recognition test measuring the cognitive function of mice

was performed. We didn't observe any difference between the control and experimental group of animals in the quest for exploration for the novel object (Fig. 5B).

Next, we performed the open field test. This test is used to evaluate any potential anxiolytic or anxiogenic effect of a therapeutic agent by measuring locomotion related anxiety levels of experimental animals placed inside an open field box. The open field test is based on the concept that the natural instinct of the mice is to stay in proximity to the protective wall rather than exposing themselves to danger in the open areas [31]. When control and SAM-treated mice were exposed to an open field apparatus, there was no significant difference in the frequency and time spent in the central region (Fig. 5C-D). Moreover, both control and SAM-treated mice moved around at almost similar speed (Fig. 5E), and there was also no significant difference in the total distance traveled within the central zone as well as the whole experimental arena (Fig. 5F-G). Taken together, these observations suggest that SAM does not cause any detrimental behavioral defects at the doses used in this study.

When serum from control and experimental animals were analyzed for different biochemical measurements (liver function test, kidney function test, major electrolytes/minerals), we didn't see any significant changes in the SAM-treated animals compared to control animals (Supplementary File 1, Table S1). This suggests that SAM is non-toxic at the highest dose (80 mg/kg/day) used in this study.

In summary, we have shown that SAM-treatment reduced proliferation, invasiveness of breast cancer cells and increased apoptosis *in vitro*, and reduced tumorigenesis and metastasis *in vivo* (Fig. 5H).

Discussion

A large body of evidence has shown that abnormal DNA methylation is associated with cancer development and progression [32, 33]. Both hypomethylation and hypermethylation are involved in cancer [34]. Despite that, the focus of attention for the past two decades has been on targeting hypermethylation by the administration of inhibitors of DNA methyltransferase enzyme (DNMTi). Two inhibitors, 5-Azacitidine (Vidaza®) and 5-aza-2'-deoxycytidine (Dacogen®), have already received FDA-approval for the treatment of several specific forms of myelodysplastic syndromes (MDS), acute myeloid leukemia (AML), and chronic myelomonocytic leukemia (CMML) and additional clinical trials are ongoing for several other cancers [20, 35]. However, the activity of DNMTi has been limited in the case of the solid tumors largely due to toxicity and lower stability of these drugs [36, 37]. In addition, these drugs also promote the invasiveness in cancer cells through hypomethylation-mediated upregulation of prometastatic genes [16].

Accumulating evidence support the fact that there are broad regions of hypomethylation in the cancer genome and that hypomethylation is prevalent at promoters [38, 39]. Epigenome-wide association studies (EWAS) in osteosarcoma, prostate, and liver cancer revealed that the promoters of a large number of genes involved in tumor growth and metastasis are hypomethylated [21, 22, 39]. These findings lead to the hypothesis that agents that induce hypermethylation at the promoters of metastatic genes would repress tumor metastasis.

Although the exact reason behind the increase in hypomethylation during the progression of the disease is still an enigma in the field of cancer epigenetics, Hoffmann

and Schulz suggested that this might be partly due to inadequate amounts of the methyl group donor SAM [40]. Treatment with SAM has been shown to trigger hypermethylation of several genes in cell culture experiments. To date, SAM is the only therapeutic agent that is known to cause hypermethylation of DNA and silencing of hypomethylated genes in cells. SAM is attractive as a therapeutic agent since it is an approved natural supplement and has a very good safety profile.

Although past studies provided evidence that SAM has antiproliferative and anti-metastatic effects *in vitro* against breast cancer cells and this was replicated in this study using two different basal-like breast cancer cell lines (MDA-MB-231 and Hs578T), the critical question that remained to be answered was whether SAM was effective as an oral therapeutic agent under conditions that could be replicated in breast cancer patients. In the current study, we tested whether *in vivo* supplementation of SAM would exhibit anti-proliferative and anti-metastatic effects in a xenograft model of breast cancer *in vivo*. Our study demonstrated that oral administration of SAM caused a significant dose-dependent reduction in mammary tumor volume and metastasis in our well-characterized xenograft model of breast cancer, which shows great promise in translating similar treatment strategies for breast cancer patients. It should be noted that our results demonstrate responses in basal-like breast cancer cells (MDA-MB-231) which are highly aggressive, and patients with such type of breast cancer have shorter survival rate compared to other types of breast cancer patients [42]. In addition, unlike other subtypes, there is still no known target for basal-like breast cancers which warrants continued efforts to develop effective therapeutic approaches for this group of patients. We hypothesize that if SAM

can show favorable outcome in the most aggressive form of breast cancer, it can be more easily translated into other subtypes as well. Since SAM is an accepted orally bioavailable nutritional supplement, it might be used in a preventative setting to prevent recurrence and metastasis post surgery.

Another aspect of the current study was to assess the underlying molecular changes pertaining to SAM-treatment both *in vitro* and *in vivo*. Towards achieving this goal, we first examined the changes in the expression of genes implicated in tumor metastasis by selecting a combination of genes already known to have a role in cancer along with those selected by a gene expression array on MDA-MB-231 cells. Our microarray-based transcriptome-wide analysis as well as qPCR validation showed that SAM-treatment caused downregulation of several genes implicated in cancer progression and metastasis (Fig. 3B & 3C). More importantly, the gene expression changes observed in the cell lines could be recapitulated in the xenograft tumors. When qPCR was performed using the same set of genes that were downregulated *in vitro*, they showed similar downregulation in tumor RNA extracted from SAM-treated animals as compared to vehicle-treated controls. Such reduction in the expression of these genes might be either due to a direct effect on promoter methylation upon SAM-treatment or an indirect effect in which SAM caused the methylation and silencing of critical activators or enhancers of transcription of these genes. Previously we have shown that SAM-treatment caused direct methylation in the promoter of *PLAU* [23]. In this study, we found a marked increase in methylation at the promoter of *SPARC* in the SAM-treated xenograft tumor DNA as compared to controls, suggesting direct promoter methylation effect of SAM on this promoter as well. However, we did not

observe any significant change in methylation in other genes (*MUC1, FABP7, SOX4, HAS2, HAS3*) that were tested through pyrosequencing. These genes might be regulated indirectly by DNA methylation of other genes which are required for their activation. Alternatively, SAM might suppress these genes by other epigenetic mechanisms such as histone methylation or non-epigenetic mechanisms. Further experiments are required to address this question. We also validated the SAM-mediated downregulation of three proteins (MUC1, SPARC, FABP7) by immunohistochemistry.

To confirm the bioavailability of SAM, we performed an ELISA-based assay and found a significant increase in the level of SAM in experimental animals compared to non-treated controls. SAM was bioavailable at the dose used in this study and caused changes in the expression levels of genes present in the mammary tissue to reduce or inhibit cancer cell growth and metastasis.

A major concern with the use of hypermethylating agent is the possible silencing of tumor suppressor genes through hypermethylation of promoter and other regulatory regions. Such methylation could override the beneficial effect of SAM. When we checked the expression of some of the well-known tumor-suppressor genes in the MDA-MB-231 tumor, there was no significant difference between control and SAM-treated groups (Supplementary File 1, Fig. S7). This also complements our previous genome-wide analyses in prostate cancer and osteosarcoma cell lines where the methylation effect of SAM was limited to cancer-promoting genes for yet unknown reasons [21, 22]. More interestingly, database search using the panel of seven genes (*MUC1, PLAU, FABP7, SPARC, HAS2, HAS3, SOX4*) downregulated by SAM revealed that these genes are highly

expressed in basal B-type breast cancer cell lines and higher expression of these genes significantly decreases the probabilities of distant metastasis-free survival in breast cancer patients [43].

It has been previously suggested that SAM shows selective cytotoxicity for cancer cells and not for normal cells [44]. SAM-treatment did not have any significant effect on the viability of normal human breast epithelial cells at the highest dose used in this study (Supplementary File 1, Fig. S1). This further verifies that SAM is not cytotoxic to the normal breast epithelial cells. We also performed extensive biochemical analysis of the blood samples collected from SAM-treated animals and observed no significant changes in any of the parameters tested as compared to controls (Supplementary File 1, Table S1). In addition, our study demonstrated that SAM-treatment also didn't cause any adverse behavioral changes as shown by novel object test and open field test.

The main question that pertains to numerous other pharmacological agents as well is how does a general methylating agent such as SAM target only a subset of genes and has an effective anticancer effect with very little adverse effect on normal tissue. We have recently investigated this question at the genomic level in normal and liver cancer cell lines by analyzing the transcriptome and methylome of normal and cancerous cells treated with SAM (Wang et al., Oncotarget, in press). It appears that the matrix of the transcriptome and methylome that SAM acts upon in normal and cancer cells is very different and that the outcome of this interaction between a general agent and an exquisite transcription and methylation landscape appears to be different. SAM does not methylate DNA on its own, DNMTs do. The consequence of an elevation in SAM levels is dependent on the pre-

existing distribution of DNMTs. Similarly, inspection of the vast literature on DNA methylation inhibitor 5azaC shows that demethylation results in different transcription and cell fate consequences, for example myogenesis and induction of muscle-specific genes in fibroblasts and globin genes in erythroleukemia cells. The most plausible explanation is that modulation of DNMT activity is restricted by the distribution of DNMTs and factors that regulate the accessibility of DNMTs across the genome and these define the specific outcome of modulation of DNMTs by either methyl donors or DNMT inhibitors.

This study examined the involvement of DNA methylation in mediating SAM cellular effects and provided evidence for silencing of several prometastatic genes as a plausible mechanism for SAM action on metastatic breast cancer. But it is most probable that the alteration of DNA methylation is just one of several mechanisms through which SAM exerts its effects. SAM is a pleiotropic molecule, and acts as a methyl group donor to other biological substrates like RNAs, proteins, lipids and small molecules [47]. Therefore, it is likely that SAM exerts its anti-cancer effect through biochemical pathways in addition to DNA methylation. It is possible that SAM-treatment alters the methylation status of histone proteins which in turn interfere with the chromatin architecture to make the promoters of the cancer-promoting genes inaccessible for transcription factor binding. The pleiotropic effect is evident by the changes seen in multiple cellular processes like tumor cell proliferation, invasion, and apoptosis upon SAM-treatment. Further detailed studies are required to explore these mechanisms to extend our understanding of how SAM exerts these effects.

To our knowledge, this is the first direct evidence for the potential therapeutic effect of SAM in a well-recognized model of breast cancer. Results from these studies provide compelling evidence to evaluate the therapeutic as well as a chemopreventive potential of epigenetic-based agents such as SAM alone and in the combination setting for patients with several common cancers including breast cancer.

Materials and Methods

Cell culture and treatments

The cell lines were obtained from the American Type Culture Collection (ATCC; Manassas, Virginia). The MDA-MB-231(*ATCC*® HTB- 26™) human breast cancer cells were maintained in Dulbecco's modified Eagle's medium (DMEM) supplemented with 10% fetal bovine serum (FBS), 2 mM L-glutamine and 100 units/ml penicillin-streptomycin sulfate at 37°C and 5% CO_2. For Hs578T (*ATCC*® *HTB-126*™) cells, DMEM containing 10% FBS, 1.25 mg/mL insulin, 2 mM L-glutamine and 100 units/ml penicillin-streptomycin sulfate was used. These cell lines were routinely examined based on their viability, cellular morphology, growth patterns and microbial presence by microscopic observation. The cell lines were authenticated by the Genetic Analysis Facility, The Hospital for Sick Children, Toronto. The human breast epithelial cells (HBEC) were purchased from Celprogen (Cat# 36056-01) and were maintained in commercially available human breast epithelial cell culture serum free media (Celprogen, Cat# M36056-01).

Cells were treated with SAM (New England Biolabs, Mississauga, Ontario, Canada; Catalog # B9003S) by directly adding it to regular growth medium under sterile conditions following the treatment plan shown in Fig. 1A. Different doses of SAM ranging between 25–500 μM were previously tested by our group for *in vitro* efficacy in different cancer cell lines [5, 6, 21, 22]. In this study, the effect of 100 and 200 μM doses of SAM were evaluated.

Cell proliferation, migration, invasion and anchorage-independent growth assay

These assays were done according to our previous studies [21, 22]. Details are available in the 'Supplementary Methods'.

Apoptosis assay

For apoptotic assays, 1×10^6 cells from control and SAM-treated groups were stained using 'Dead Cell Apoptosis Kit' (TheremoFisher, Cat# V13242, Eugene, Oregon, USA) according to the manufacturer's instructions. The apoptotic cells were detected using recombinant annexin V conjugated to green fluorescent FITC dye, and dead cells were detected using propidium iodide (PI). Stained cells were then analyzed using a BD FACSCanto II flow cytometer (BD Biosciences, San Jose, California, USA). For data acquisition and analysis of apoptotic events, BD FACSDiva™ (BD Biosciences) and FlowJo software (FlowJo LLC, Ashland, OR, USA) were used, respectively.

Study approval and in vivo xenograft model

All the *in vivo* procedures carried out during this study were done in compliance with a protocol approved by the McGill University Facility Animal Care Committee. Female CD-1® Nude mice aged between 4-6 weeks were obtained from Charles River, St-Constant, Quebec, Canada and maintained at the Animal Resource Division of the McGill University Health Center. This is a well-established mouse model used for the studies related to tumor xenografts [48-50]. Highly invasive MDA-MB-231 cells expressing green fluorescent protein (MDA-MB-231-GFP), which has the capacity to metastasize to different secondary organs [6], were used for inoculation into the immunodeficient mice. Briefly, mice were inoculated with $5x10^5$ MDA-MB-231-GFP cells with 20% Matrigel (BD Biosciences) into the fat pad of the fourth mammary gland. Three days post-inoculation; the animals were randomized into three different groups: phosphate buffer saline (PBS) as the vehicle-treated controls, a group receiving 40 mg/kg/day of SAM and another group receiving 80 mg/kg/day of SAM via oral gavage. We have used SAM from two sources (New England Biolabs, Mississauga, Ontario, Canada and Life Science Laboratories, Lakewood, NJ, USA) which showed similar anti-cancer effects in our *in vitro* studies (data not shown). However, since SAM from Life Science Laboratories is human grade, it was used for all *in vivo* studies since this product could be also used in future clinical trials in patients with breast cancer.

Tumor diameters were determined weekly using a Vernier caliper for a 10-week period after inoculation, and tumor volume was calculated using the following formula:

$V = (\text{length} \times \text{Width}^2)/2$. At the end of the study period, the animals were sacrificed, and different tissues were collected for further analysis.

For studying metastasis, the harvested lung, liver and spleen were cut into 1-mm thick slices, smeared on a glass slide, and placed under a fluorescent microscope for detecting the presence of GFP-expressing tumor foci. Randomly selected fields were counted for the presence of GFP-positive foci in each organ, and the average number of foci per group was graphed.

RNA extraction and quantitative real-time PCR (qPCR)

Total RNA from the cell lines and xenograft tumors was extracted using the RNeasy kit (Qiagen; Hilden, Germany, Cat# 71404) and AllPrep DNA/RNA Mini Kit (Qiagen; Cat# 80204) respectively following the manufacturer's protocol. The qPCR assay was performed following our previously described protocol [22]. The primers are listed in Supplementary Methods, Table 1. Gene expression changes between control and SAM-treated samples were carried out using the $2^{-\Delta\Delta C}$T method.

Gene expression microarrays

For gene expression array, 100 nanograms of total RNA from control and 200 μM SAM-treated MDA-MD-231 samples from three independent experiments was used. RNA quality and quantity were assessed using NanoDrop® ND-1000 spectrophotometer (Thermo Scientific, Wilmington, Delaware, USA) (260/280 >1.8 accepted) and Agilent 2100 Bioanalyzer (Waldbronn, Germany) (RIN 7 ≥ accepted). Gene expression profiling

was performed using Affymetrix Human Gene 2.0 ST Array (Santa Clara, California, USA) at the Génome Québec Innovation Centre (McGill University) following standard protocols.

Data from the biological replicates were then normalized using the Robust Multi-array Average (RMA) method implemented in the Bioconductor package *oligo* [51]. Differential gene expression analysis was performed using the Bioconductor package Limma with a threshold defined by P <0.01 and |fold change| >1.5. The data was submitted to Gene Expression Omnibus (GEO) under the accession number of GSE98275.

Determination of SAM levels in the serum by ELISA

To assess bioavailability, ELISA was done by using the serum from experimental mice collected within 1-hour post oral administration of SAM. Serum from control mice was also obtained for comparison. Then ELISA (myBioSource, San Diego, CA, USA, Cat# MBS169240) was performed according to the manufacturer's protocol. The level of SAM was extrapolated from the curves obtained from the manufacturer provided synthetic standards of SAM.

DNA extraction, Bisulfite conversion, and Pyrosequencing

Genomic DNA from the tumors was extracted using AllPrep DNA/RNA Mini Kit (Qiagen) and bisulfite conversion was conducted using the EZ DNA Methylation-Gold Kit (Zymo Research, Irvine, CA, USA; Cat#D5005). Selected regions from the bisulfite converted sequences were then amplified with Taq DNA polymerase (Thermo Fisher

Scientific, Lithuania, EU; Cat# EP0402) using biotinylated primers (listed in Supplementary Methods, Table S1). Then pyrosequencing was conducted on the biotinylated DNA strands using PyroMark Q24 instrument (Biotage, Qiagen). For post-run data analysis, PyroMark Q24 software (Qiagen) was used.

Western blot and immunohistochemistry

Details are available in the 'Supplementary Methods'.

Behavior test

To assess any potential behavior adversities induced by SAM-treatment novel object recognition test and open field tests were done. Details are available in the 'Supplementary Methods'.

Statistical analysis

The results are expressed as mean ± standard error of the mean (SEM). Depending on the experimental design, statistically significant differences between different quantitative measurements were carried out by two-tailed Student's *t*-test, one-way or two-way ANOVA. $*P < 0.05$, $**P < 0.01$, and $***P < 0.001$ were considered statistically significant. Gene set enrichment analysis (GSEA) was carried out by using ConsensusPathDB [52]. The association between the expression of the different cancer-related gene and distant metastasis-free survival was determined using Kmplotter

[43]. Gene expression-based outcome analysis of breast cancer was carried out by GOBO [53].

Acknowledgement

We thank Life Science Laboratories, Lakewood, NJ, USA for their kind gift of SAM. This work was supported by a grant from the Canadian Institutes for Health Research (MOP 130410) to S. A. R. and M. S. NM is the recipient of a studentship award from Research Institute, McGill University Health Centre.

Conflict of Interest

The authors have no conflict of interest to declare.

Reference

1. Rizwan A, Cheng M, Bhujwalla ZM, Krishnamachary B, Jiang L, Glunde K. Breast cancer cell adhesome and degradome interact to drive metastasis. NPJ Breast Cancer. 2015; 1: 15017.
2. Singletary SE, Connolly JL. Breast cancer staging: working with the sixth edition of the AJCC Cancer Staging Manual. CA: a cancer journal for clinicians. 2006; 56: 37-47.
3. Chambers A, Groom A, MacDonald I. Dissemination and Growth of Cancer Cells in Metastatic Sites. Nat Rev Cancer. 2002; 2: 563-572
4. Rabbani SA, Mazar AP. Evaluating distant metastases in breast cancer: from biology to outcomes. Cancer and Metastasis Reviews. 2007; 26: 663-74.
5. Shukeir N, Pakneshan P, Chen G, Szyf M, Rabbani SA. Alteration of the methylation status of tumor-promoting genes decreases prostate cancer cell invasiveness and tumorigenesis in vitro and in vivo. Cancer research. 2006; 66: 9202-10.
6. Pakneshan P, Szyf M, Farias-Eisner R, Rabbani SA. Reversal of the hypomethylation status of urokinase (uPA) promoter blocks breast cancer growth and metastasis. Journal of Biological Chemistry. 2004; 279: 31735-44.

7. Shteper PJ, Zcharia E, Ashhab Y, Peretz T, Vlodavsky I, Ben-Yehuda D. Role of promoter methylation in regulation of the mammalian heparanase gene. Oncogene. 2003; 22: 7737-49.
8. Pakneshan P, Têtu B, Rabbani SA. Demethylation of urokinase promoter as a prognostic marker in patients with breast carcinoma. Clinical Cancer Research. 2004; 10: 3035-41.
9. Pulukuri SMK, Estes N, Patel J, Rao JS. Demethylation-linked activation of urokinase plasminogen activator is involved in progression of prostate cancer. Cancer research. 2007; 67: 930-9.
10. Ogishima T, Shiina H, Breault JE, Tabatabai L, Bassett WW, Enokida H, Li L-C, Kawakami T, Urakami S, Ribeiro-Filho LA. Increased heparanase expression is caused by promoter hypomethylation and up-regulation of transcriptional factor early growth response-1 in human prostate cancer. Clinical Cancer Research. 2005; 11: 1028-36.
11. Liu H, Liu W, Wu Y, Zhou Y, Xue R, Luo C, Wang L, Zhao W, Jiang J-D, Liu J. Loss of epigenetic control of synuclein-γ gene as a molecular indicator of metastasis in a wide range of human cancers. Cancer research. 2005; 65: 7635-43.
12. Ye L, Li X, Kong X, Wang W, Bi Y, Hu L, Cui B, Li X, Ning G. Hypomethylation in the promoter region of POMC gene correlates with ectopic overexpression in thymic carcinoids. Journal of endocrinology. 2005; 185: 337-43.
13. Paredes J, Albergaria A, Oliveira JT, Jerónimo C, Milanezi F, Schmitt FC. P-cadherin overexpression is an indicator of clinical outcome in invasive breast carcinomas and is associated with CDH3 promoter hypomethylation. Clinical cancer research. 2005; 11: 5869-77.
14. Nishigaki M, Aoyagi K, Danjoh I, Fukaya M, Yanagihara K, Sakamoto H, Yoshida T, Sasaki H. Discovery of aberrant expression of R-RAS by cancer-linked DNA hypomethylation in gastric cancer using microarrays. Cancer research. 2005; 65: 2115-24.
15. Sato N, Fukushima N, Matsubayashi H, Goggins M. Identification of maspin and S100P as novel hypomethylation targets in pancreatic cancer using global gene expression profiling. Oncogene. 2004; 23: 1531-8.
16. Ateeq B, Unterberger A, Szyf M, Rabbani SA. Pharmacological inhibition of DNA methylation induces proinvasive and prometastatic genes in vitro and in vivo. Neoplasia. 2008; 10: 266-78.
17. Bottiglieri T. S-Adenosyl-L-methionine (SAMe): from the bench to the bedside—molecular basis of a pleiotrophic molecule. The American journal of clinical nutrition. 2002; 76: 1151S-7S.
18. Loenen W. (2006). S-adenosylmethionine: jack of all trades and master of everything? : Portland Press Limited).

19. Cantoni G. The nature of the active methyl donor formed enzymatically from l-methionine and adenosinetriphosphate1, 2. Journal of the American Chemical Society. 1952; 74: 2942-3.
20. Mahmood N, Rabbani SA. DNA methylation and breast cancer: Mechanistic and therapeutic applications. Trends in Cancer Research. 2017; 12.
21. Shukeir N, Stefanska B, Parashar S, Chik F, Arakelian A, Szyf M, Rabbani SA. Pharmacological methyl group donors block skeletal metastasis in vitro and in vivo. British journal of pharmacology. 2015; 172: 2769-81.
22. Parashar S, Cheishvili D, Arakelian A, Hussain Z, Tanvir I, Khan HA, Szyf M, Rabbani SA. S-adenosylmethionine blocks osteosarcoma cells proliferation and invasion in vitro and tumor metastasis in vivo: therapeutic and diagnostic clinical applications. Cancer medicine. 2015; 4: 732-44.
23. Chik F, Machnes Z, Szyf M. Synergistic anti-breast cancer effect of a combined treatment with the methyl donor S-adenosyl methionine and the DNA methylation inhibitor 5-aza-2′-deoxycytidine. Carcinogenesis. 2014; 35: 138-44.
24. Şahin M, Şahin E, Gümüşlü S, Erdoğan A, Gültekin M. Inhibition of angiogenesis by S-adenosylmethionine. Biochemical and biophysical research communications. 2011; 408: 145-8.
25. Li TW, Yang H, Peng H, Xia M, Mato JM, Lu SC. Effects of S-adenosylmethionine and methylthioadenosine on inflammation-induced colon cancer in mice. Carcinogenesis. 2011: bgr295.
26. Evan GI, Vousden KH. Proliferation, cell cycle and apoptosis in cancer. Nature. 2001; 411: 342-8.
27. Borowicz S, Van Scoyk M, Avasarala S, Rathinam MKK, Tauler J, Bikkavilli RK, Winn RA. The soft agar colony formation assay. JoVE (Journal of Visualized Experiments). 2014: e51998-e.
28. Lu SC, Mato JM. S-Adenosylmethionine in cell growth, apoptosis and liver cancer. Journal of gastroenterology and hepatology. 2008; 23.
29. Zhang B, Kirov S, Snoddy J. WebGestalt: an integrated system for exploring gene sets in various biological contexts. Nucleic acids research. 2005; 33: W741-W8.
30. Goren JL, Stoll AL, Damico KE, Sarmiento IA, Cohen BM. Bioavailability and lack of toxicity of S-adenosyl-L-methionine (SAMe) in humans. Pharmacotherapy. 2004; 24: 1501-7. doi: 10.1592/phco.24.16.1501.50943.
31. Christakis DA, Ramirez J, Ramirez JM. Overstimulation of newborn mice leads to behavioral differences and deficits in cognitive performance. Scientific reports. 2012; 2: 546.

32. Suzuki H, Toyota M, Caraway H, Gabrielson E, Ohmura T, Fujikane T, Nishikawa N, Sogabe Y, Nojima M, Sonoda T. Frequent epigenetic inactivation of Wnt antagonist genes in breast cancer. British journal of cancer. 2008; 98: 1147-56.
33. Dobrovic A, Simpfendorfer D. Methylation of the BRCA1 gene in sporadic breast cancer. Cancer Research. 1997; 57: 3347-50.
34. Chik F, Szyf M, Rabbani SA. (2011). Role of epigenetics in cancer initiation and progression. Human Cell Transformation: Springer), pp. 91-104.
35. Jones PA, Issa J-PJ, Baylin S. Targeting the cancer epigenome for therapy. Nature Reviews Genetics. 2016; 17: 630-41.
36. Stewart DJ, Issa J-P, Kurzrock R, Nunez MI, Jelinek J, Hong D, Oki Y, Guo Z, Gupta S, Wistuba II. Decitabine effect on tumor global DNA methylation and other parameters in a phase I trial in refractory solid tumors and lymphomas. Clinical Cancer Research. 2009; 15: 3881-8.
37. Weiss A, Stambaugh J, Mastrangelo M, Laucius J, Bellet R. Phase I study of 5-azacytidine (NSC-102816). Cancer chemotherapy reports. 1972; 56: 413-9. doi:
38. Ehrlich M. DNA hypomethylation in cancer cells. Epigenomics. 2009; 1: 239-59.
39. Stefanska B, Huang J, Bhattacharyya B, Suderman M, Hallett M, Han Z-G, Szyf M. Definition of the landscape of promoter DNA hypomethylation in liver cancer. Cancer research. 2011; 71: 5891-903.
40. Hoffmann MJ, Schulz WA. Causes and consequences of DNA hypomethylation in human cancer. Biochemistry and Cell Biology. 2005; 83: 296-321.
41. Fuso A, Nicolia V, Ricceri L, Cavallaro RA, Isopi E, Mangia F, Fiorenza MT, Scarpa S. S-adenosylmethionine reduces the progress of the Alzheimer-like features induced by B-vitamin deficiency in mice. Neurobiology of aging. 2012; 33: 1482. e1-. e16.
42. Perou CM, Sørlie T, Eisen MB, van de Rijn M, Jeffrey SS, Rees CA, Pollack JR, Ross DT, Johnsen H, Akslen LA. Molecular portraits of human breast tumours. Nature. 2000; 406: 747-52.
43. Győrffy B, Lanczky A, Eklund AC, Denkert C, Budczies J, Li Q, Szallasi Z. An online survival analysis tool to rapidly assess the effect of 22,277 genes on breast cancer prognosis using microarray data of 1,809 patients. Breast cancer research and treatment. 2010; 123: 725-31.
44. Luo J, Li Y-N, Wang F, Zhang W-M, Geng X. S-adenosylmethionine inhibits the growth of cancer cells by reversing the hypomethylation status of c-myc and H-ras in human gastric cancer and colon cancer. Int J Biol Sci. 2010; 6: 784-95.
45. Ansorena E, García-Trevijano ER, Martínez-Chantar ML, Huang ZZ, Chen L, Mato JM, Iraburu M, Lu SC, Avila MA. S-adenosylmethionine and methylthioadenosine are antiapoptotic in cultured rat hepatocytes but proapoptotic in human hepatoma cells. Hepatology. 2002; 35: 274-80.

46. Yang H, Sadda MR, Li M, Zeng Y, Chen L, Bae W, Ou X, Runnegar MT, Mato JM, Lu SC. S-adenosylmethionine and its metabolite induce apoptosis in HepG2 cells: Role of protein phosphatase 1 and Bcl-xS. Hepatology. 2004; 40: 221-31.
47. Chiang PK, Gordon RK, Tal J, Zeng G, Doctor B, Pardhasaradhi K, McCann PP. S-Adenosylmethionine and methylation. The FASEB Journal. 1996; 10: 471-80. doi:
48. Mason JM, Wei X, Fletcher GC, Kiarash R, Brokx R, Hodgson R, Beletskaya I, Bray MR, Mak TW. Functional characterization of CFI-402257, a potent and selective Mps1/TTK kinase inhibitor, for the treatment of cancer. Proceedings of the National Academy of Sciences. 2017: 201700234.
49. Bzyl J, Lederle W, Rix A, Grouls C, Tardy I, Pochon S, Siepmann M, Penzkofer T, Schneider M, Kiessling F. Molecular and functional ultrasound imaging in differently aggressive breast cancer xenografts using two novel ultrasound contrast agents (BR55 and BR38). European radiology. 2011; 21: 1988-95.
50. De Luca A, Sanna F, Sallese M, Ruggiero C, Grossi M, Sacchetta P, Rossi C, De Laurenzi V, Di Ilio C, Favaloro B. Methionine sulfoxide reductase A down-regulation in human breast cancer cells results in a more aggressive phenotype. Proceedings of the National Academy of Sciences. 2010; 107: 18628-33.
51. Carvalho BS, Irizarry RA. A framework for oligonucleotide microarray preprocessing. Bioinformatics. 2010; 26: 2363-7.
52. Kamburov A, Stelzl U, Lehrach H, Herwig R. The ConsensusPathDB interaction database: 2013 update. Nucleic acids research. 2013; 41: D793-D800.
53. Ringnér M, Fredlund E, Häkkinen J, Borg Å, Staaf J. GOBO: gene expression-based outcome for breast cancer online. PloS one. 2011; 6: e17911.

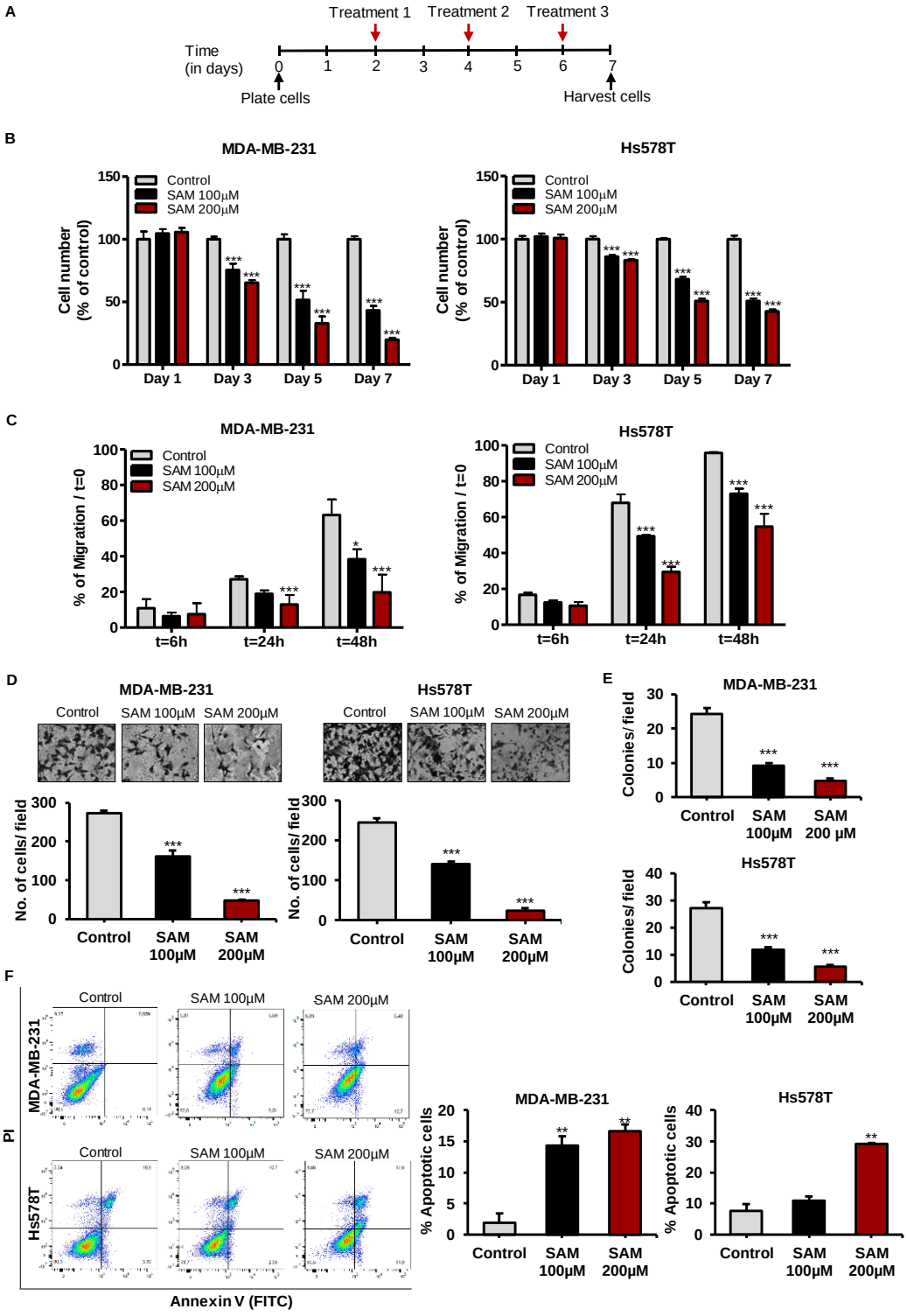

Figure 1: Effect of S-adenosylmethionine (SAM) on breast cancer cell proliferation, migration, invasion, anchorage-independent growth, and apoptosis *in vitro*.

A. Schematic diagram of the treatment strategy for all the *in vitro* experiments. Human breast cancer cells MDA-MB-231 and Hs578T were treated with SAM (100 and 200 μM) by directly adding it to regular growth medium every other day from day 2 until they were harvested. **B.** Human breast cancer cells MDA-MB-231 and Hs578T were plated in 6-well plates and treated with vehicle alone as control or SAM (100 and 200 μM). Cell growth rate in each group was determined on day 1, 3, 5, and 7 by Coulter counter as described in Methods. Results are shown as bar graphs of data obtained from three different experiments. **C**. Wound healing assay for determining the migration capacity of the cells was carried out by making a cross-like scratch on the plate when they reached 90% confluency. Control and SAM (100 and 200 μM) treated cells were grown in culture media containing 2% FBS and migrating cells were photographed and recorded at different time points, and percentage of wound healing with respect to initial scratch (T0) was calculated using the equation described in 'Supplementary Methods'. The results are represented as bar graphs obtained from three experiments. **D.** Boyden chamber Matrigel invasion assay was used to measure the invasiveness of control and SAM-treated (100 and 200 μM) MDA-MB-231 and Hs578T cells. The cells were placed in the upper chamber, and conditioned media used as 'chemoattractant' was added into the lower chamber. Following an incubation period of 18 hours, the invasion process was stopped and the invaded cells from control and 100 and 200 μM SAM-treated groups were fixed, stained and randomly selected fields were counted under the microscope and averaged. Representative image of one randomly selected field for each treatment for both cell lines along with the number of cells invaded per field are shown. **E.** After the usual treatment regimen, 5×10^3 cell from control and SAM-treated (100 μM and 200 μM) groups were plated onto soft agar for anchorage-independent growth assay. The culture media was replenished every other day for two weeks, and the number of colonies was counted. **F.** Apoptosis was determined by flow cytometry after staining the control and SAM-treated cells with Annexin V/propidium iodide. Representative contour plots of annexinV-FITC staining of apoptotic cells vs. PI staining for both control and SAM-treated (100 μM) cells are shown. The bar graphs on the right panels show the total percentages of apoptotic cells for different treatments. Results are presented as the mean ± SEM from control and SAM-treated experimental cells. Significant differences were determined using ANOVA followed by *post hoc* Bonferroni test and are represented by asterisks (*$P < 0.05$; ** $P < 0.01$, and ***$P < 0.001$).

A

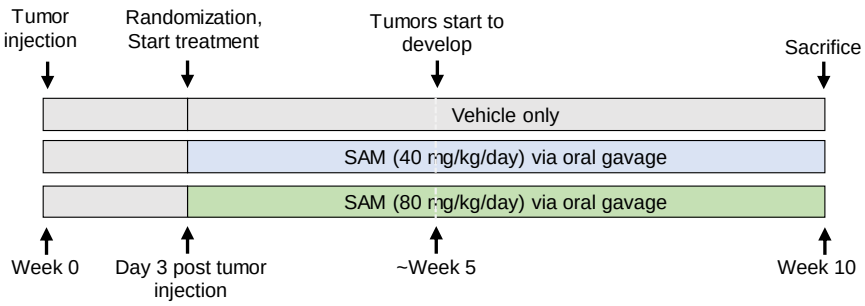

B

Treatments	Tumor incidence
Control	10 out of 10
SAM (40 mg/kg/day)	10 out of 10
SAM (80 mg/kg/day)	7 out of 10

C

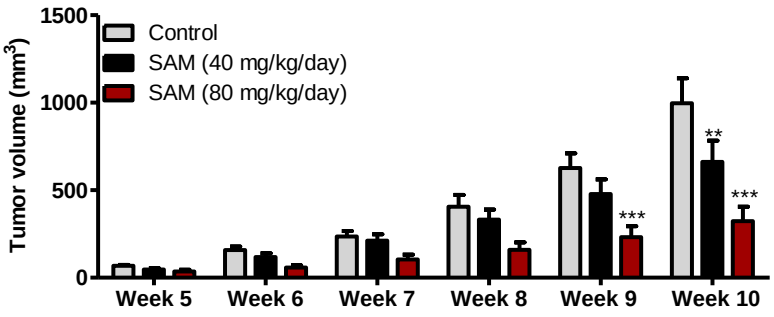

D

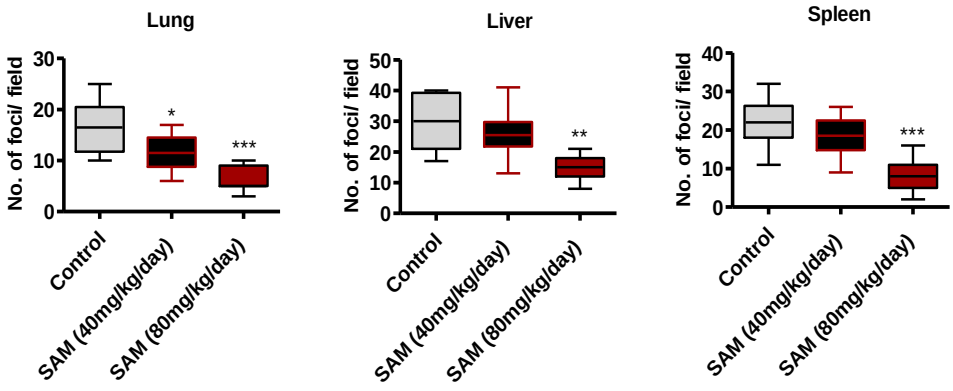

Figure 2: Effect of SAM on MDA-MB-231 tumor growth and metastasis.

A. Schematic representation of SAM-treatment in MDA-MB-231 tumor xenograft mice. Female CD1 mice inoculated with MDA-MD-231-GFP cells via orthotopic route were randomized, and treatment with SAM at different doses was started from day three post tumor cell inoculation. Animals were treated daily with vehicle alone or SAM (40 mg/kg/day or 80 mg/kg/day) via daily oral gavage. **B.** Tabular representation of the incidence of tumor in control and two experimental groups. **C.** Tumor volume was determined at weekly intervals from week 5 when the animals started to develop tumors. Treatment with SAM caused a significant dose-dependent decrease in tumor growth. Results are representative of mean ± SEM of tumor volumes obtained from at least seven animals per group. Significant differences were determined using ANOVA followed by *post hoc* Bonferroni test and are represented by asterisks. (**$P < 0.01$; *** $P < 0.001$). **D**. To evaluate the effect of SAM on tumor metastasis, control and SAM (40 and 80 mg/kg/day) treated animals were sacrificed at week 10 and different organs (lungs, liver, spleen) were collected. Organ slices of 1-mm thickness were mounted on a glass slide, and the GFP-positive foci were examined under the fluorescent microscope. Ten randomly selected slides were counted and averaged to determine the GFP-positive metastatic foci in each organ. Significant differences were determined using ANOVA followed by *post hoc* Bonferroni test and are represented by asterisks. (*$P < 0.05$; ** $P < 0.01$, and ***$P < 0.001$).

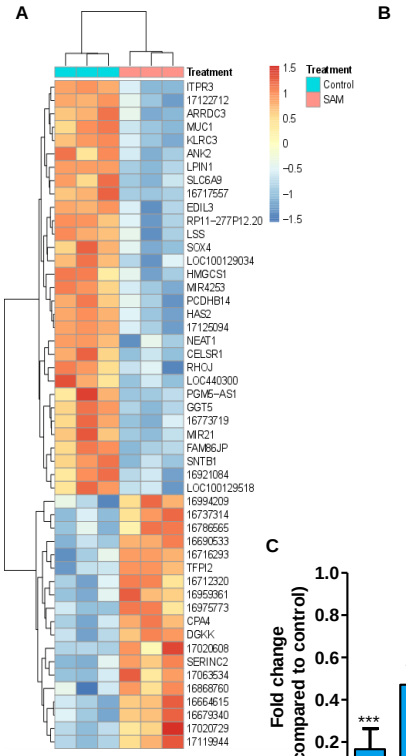

B

Enriched pathway (KEGG and PID)	p-value	q-value
ECM-receptor interaction	1.09E-06	2.29E-05
Alpha6 beta4 integrin-ligand interactions	5.32E-06	5.59E-05
Beta1 integrin cell surface interactions	5.37E-05	0.000375819
Arrhythmogenic right ventricular cardiomyopathy	0.00061726	0.00220724
Focal adhesion	0.00066266	0.00220724
uPA and uPAR-mediated signaling	0.00073575	0.00220724
Beta3 integrin cell surface interactions	0.00073575	0.00220724
Complement and coagulation cascades	0.00094288	0.002475073
a6b1 and a6b4 Integrin signaling	0.0011182	0.002609142
Small cell lung cancer	0.00138179	0.002739884
PI3K-Akt signaling pathway	0.00155152	0.002739884
Systemic lupus erythematosus	0.00165888	0.002739884
Alcoholism	0.00169612	0.002739884
Hematopoietic cell lineage	0.00224864	0.003372967

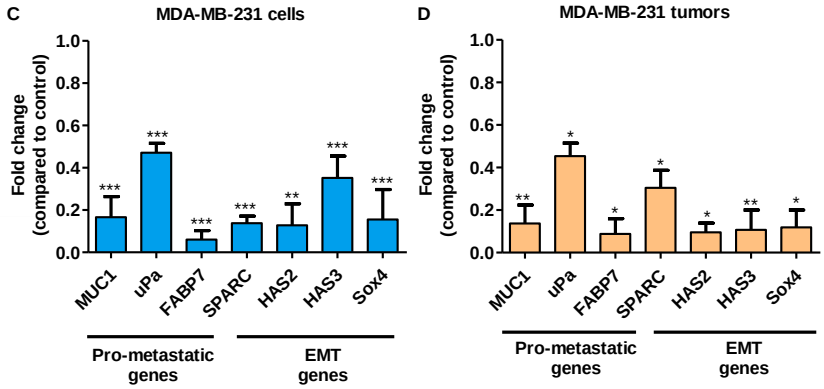

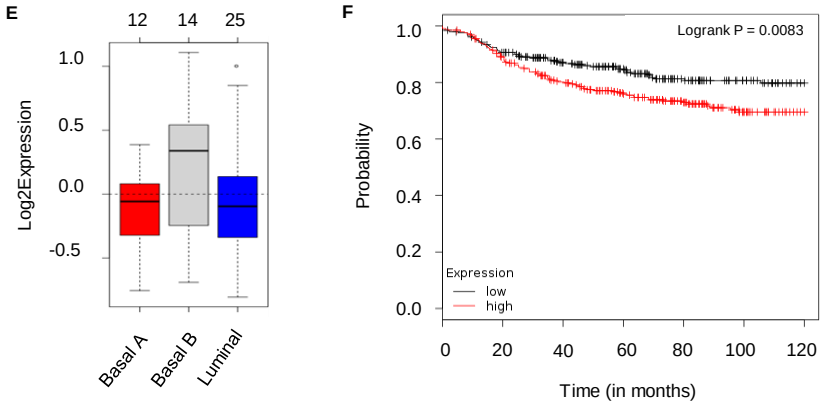

Figure 3: Gene expression analysis of MDA-MB-231 cells and tumors treated with SAM.

A. MDA-MB-231 cells from control and SAM-treated (200 µM) group were subjected to Affymetrix array and the heat map of the most differentially expressed genes are shown (n=3 in each group). **B.** Pathway analysis (from KEGG and PID database) of the genes

that are differentially expressed upon SAM-treatment. **C.** Selected genes differentially regulated by SAM were validated by quantitative real-time PCR (qPCR) in MDA-MB-231 cells. Results are shown as mean ± SEM of at least three independent experiments. (** $P < 0.01$, and ***$P < 0.001$). **D.** RNA obtained from the tumor of control and 80 mg/kg/day SAM-treated animals were subjected to qPCR for the same set of genes that showed downregulation by SAM *in vitro.* Results are shown as mean ± SEM of at least three independent animals per group. (*$P < 0.05$ and ** $P < 0.01$). **E.** Gene Set Analysis (GSA) representing the expression of these genes in human breast cancer cell lines. **F.** Kaplan-Meier plot of distance metastasis-free survival from a dataset of 664 breast cancer patients categorized according to the expression of the seven down-regulated genes in Fig. 3D.

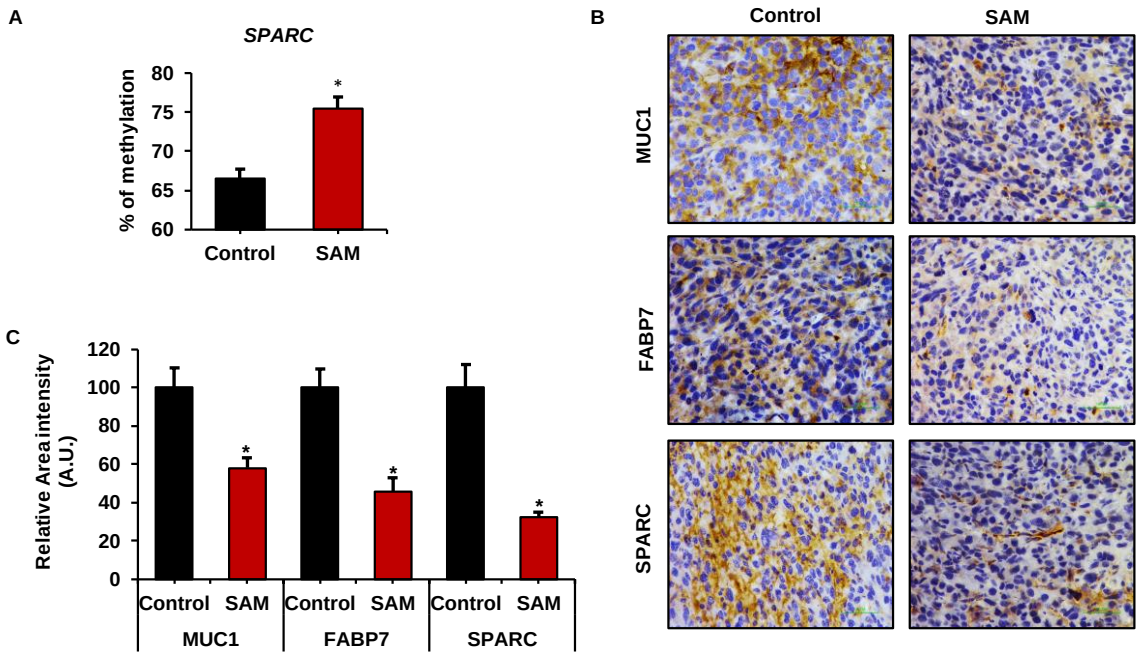

Figure 4: Effect of SAM-treatment on promoter methylation and protein expression of cancer-related genes.

A. Site-specific methylation analysis by pyrosequencing at the promoter of *SPARC* (location: chromosome 5: 151066730; corresponding to Illumina 450K ID: cg22116670). **B.** Immunohistochemistry of control and SAM-treated tumors using antibodies against MUC1, FABP7 and SPARC proteins. **C.** The stained areas were quantified using Fiji plugin (ImageJ). Results are shown as mean ± SEM (n=3). *$P < 0.05$.

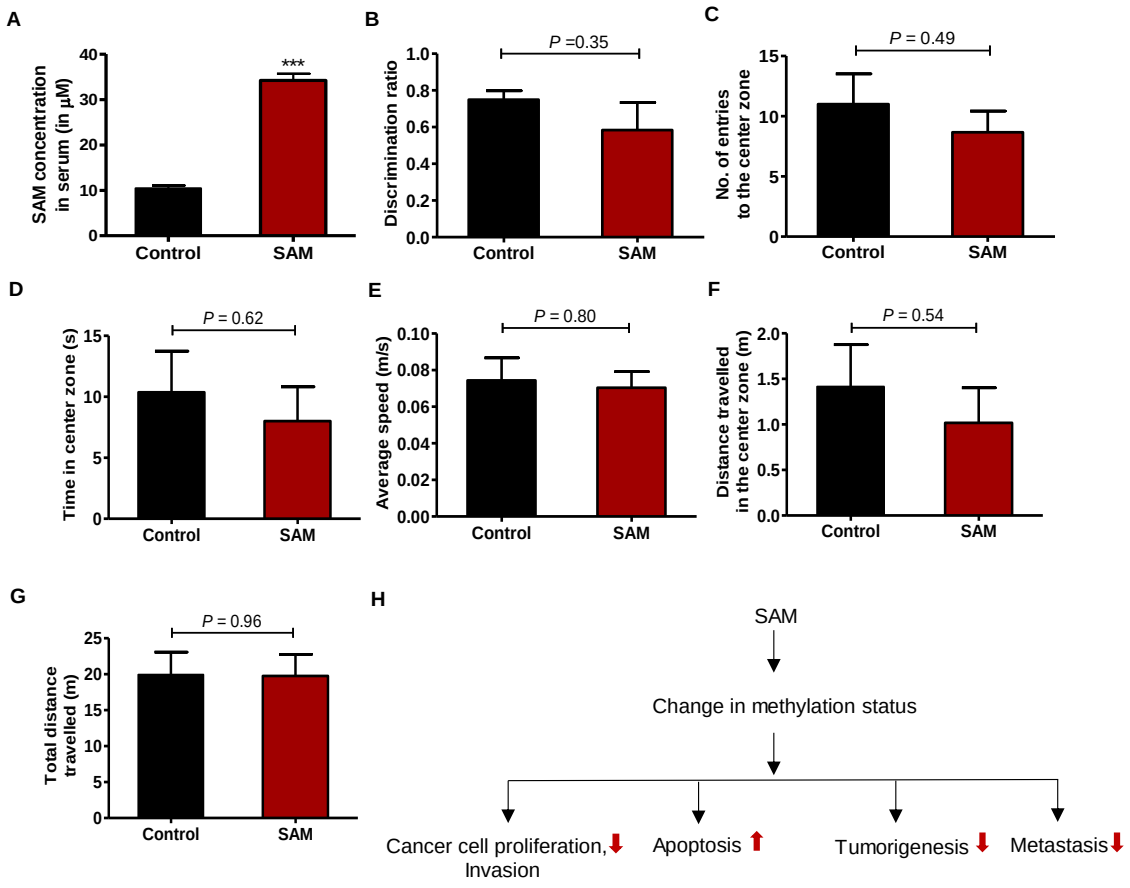

Figure 5: Assessment of bioavailability and animal behavior upon SAM-treatment.

A. The average level of SAM in control and the experimental group receiving 80 mg/kg/day of SAM as determined by the SAM ELISA. Results are obtained from the analysis of serum from four animals in each group. (***$P < 0.001$). **B.** Novel object recognition test of control and SAM-treated mice. Average Discrimination ratio (time spent with the novel object/ total time spent with both object). No significant differences in cognitive abilities are detected between control and SAM-treated groups. **C-G.** Different parameters determined by the open field test of control and SAM-treated mice also showed no significant difference between control and SAM-treated animals. Results are shown as mean ± SEM (n=3 for each group of CD-1 nude mice), and statistical analyses were done using student's *t*-test. **H.** A summary of biological processes shown to be affected by SAM as determined in this study includes cell proliferation, invasion, apoptosis *in vitro* and tumorigenesis and metastasis *in vivo*.

Supplementals for Chapter 2

Supplementary Methods

Cell proliferation and viability assay

For proliferation assay, MDA-MB-231 and Hs578T cells plated in each well of 6-well plates were treated with 100 and 200 μM SAM or vehicle every second day for six days (Fig 1A). The cells were trypsinized and counted at different time points starting from day 1 (no treatment) until the end of each treatment period (on day 7 from the initial plating) using a Coulter counter (Model ZF; Coulter Electronics, Hertfordshire, UK). For viability assay, cells were trypsinized, stained with 0.4% trypan blue (Sigma) and the viable cells were counted under a light microscope.

Cell migration / Wound healing assay

For *in vitro* wound healing analysis, MDA-MB-231 and Hs578T cells were treated with 100 and 200 μM SAM or vehicle following the treatment strategy mentioned in Fig 1A in the presence of regular cell culture media supplemented with 10% FBS in 10 cm Petri dishes. Afterward, the cells were trypsinized, and 500,000 cells were plated in each well of 6-well plates to form a monolayer and then wounded manually with a sterile 200 μL pipette tip in the center of each well forming a cross-like section of the wound. Cells were then washed twice with serum-free culture medium to get rid of the detached cells and debris. From this point, the cells were grown in the presence of culture media supplemented with 2% FBS and migrating cells were photographed at different time points (0, 6, 24, 48 hours after initial wounding) with an inverted bright field microscope under

the 4X objective. Analysis and quantification of the cell-free area were carried out using the Image Pro-Plus software (Media Cybernetics, Inc, Rockville, MD, USA). The measurements obtained from the software were calculated as percentage wound healing using the equation: % wound healing = [1 − (wound area at T_x h/wound area at T_0)], where T_x is the respective time point, and T_0 is the initial time immediately after the scratch.

Boyden chamber Matrigel invasion assay

The changes in the invasive capacity of control and SAM-treated samples of MDA-MB-231 and Hs578T breast cancer lines was tested using a two-compartment Boyden chamber invasion assay (Costar Transwell, Corning Corporation, Sigma-Aldrich, Oakville, Ontario, Canada). The 8-μm-pore polycarbonate filters provided by the manufacturer were first coated with basement membrane Matrigel (50 μg/filter). Briefly, 2.5×10^5 viable cells from different treatment groups were resuspended in 100 μL of serum-free culture media and added to the upper chambers of the Matrigel Boyden wells. 800 μL of conditioned media was added to the lower chamber as the chemoattractant. After an incubation period of 18 hours at 37°C with 5% CO_2, the invasion assay was stopped by moving the cells out of the incubator. The upper chamber was then washed with PBS to remove the non-invading cells from the top of the membrane. Then invading cells at the bottom of the membrane were fixed using 2% paraformaldehyde and 0.5% glutaraldehyde (Sigma-Aldrich) in 0.1 M phosphate buffer saline (PBS) with a pH of 7.4, at room temperature for 30 minutes. The membranes were then stained with 1.5% toluidine blue, washed with PBS,

mounted onto glass slides, and the number of invading cells from randomly selected fields were counted under a light microscope and averaged.

Colony formation assay

To determine the effect of SAM on anchorage-independent growth, a measure of cellular transformation *in vitro*, soft agar colony formation assay was performed as previously described [1]. Briefly, 5×10^3 MDA-MB-231 and HS578T cells from control SAM-treated groups were counted and seeded in triplicates onto 6-well Petri dishes (BD Falcon™) in the presence of 4 ml of complete culture medium containing 1.5% agar (Bioshop®; Catalog# AGR001) solution. The culture medium was replenished every second day and the colonies formed after 2 weeks were counted under a light microscope.

Western blot

Cell lysates from control and SAM-treated cells were prepared using radioimmunoprecipitation assay buffer (RIPA) containing a cocktail of protease and phosphatase inhibitors. Equal amounts of proteins were loaded and resolved on a 15% sodium dodecyl sulfate-polyacrylamide gel and then transferred to polyvinylidene difluoride (PVDF) membrane using standard protocols. After transfer, non-specific binding was blocked by using 5% milk in Tris-buffered saline (TBS). Mouse monoclonal Bcl-2 antibody (Santa Cruz Biotechnology, Cat# sc-7382) was used to detect the anti-apoptotic Bcl-2 protein, and anti-mouse β-tubulin (BD Pharmingen cat# 556321) was used a loading control. The anti-mouse secondary antibodies used in this study were purchased

from Bio-Rad, and the proteins were visualized by using an enhanced chemiluminescence detection kit (Amersham, GE Healthcare Life Sciences).

Immunohistochemistry

Immunohistochemistry was performed on paraffin-embedded sections, cleared with xylene. Heat-mediated antigen retrieval was carried out by Tris/EDTA pH 9.0 buffer, Envision™ FLEX Target Retrieval Solution (Dako, Denmark) at 1:50 dilution for SPARC, MUC1 and FABP7. Endogenous peroxidase activity was blocked by Envision FLEX Peroxidase-Blocking Reagent (Dako). Antibodies for SPARC, MUC1, and FABP7 (Abcam, Cambridge, UK) were used at 1:250, 1:100, and 1:200 dilutions respectively as primary antibodies. Horseradish Peroxidase (HRP)-conjugated secondary antibody was used. EnvisionTM FLEX DAB+ Chromogen (Dako) and EnvisionTM FLEX Substrate buffer (Dako) were applied. The slides were counterstained with hematoxylin (MERCK, NJ, USA). Sections were washed twice for 10 minutes in Tris buffered saline solution pH7.6 (EnvisionTM FLEX Wash Buffer, DAKO) at 1:20 dilution after every step during the procedure. Slides were mounted with DPX (MERCK). The stained areas from randomly selected fields were then quantified using ImageJ (Fiji plugin) (National Institutes of Health, USA).

Novel object recognition test

For the novel object recognition test to assess whether SAM-treatment has any adverse effect on memory, animals were allowed to explore two identical copies of the first

object in an open field enclosure for 10 minutes. By this time, the first object is now familiar to the mouse. Then there was a 60-minute break before the assessment of short-term memory began. During this period, the animals explored a familiar object (first object used during training) for eight minutes and a novel object (different shape) for 5 minutes and the time spent in exploration of the objects were recorded. Discrimination index (DI), a ratio of the time spent with the novel object in comparison with the familiar object, was determined and used for comparing between control and SAM-treated animals [2].

Open field test

The open field test to assess any potential increase in the anxiety levels upon SAM-treatment was conducted by placing mice from control and treatment group in an open field arena measuring 45 × 45 × 60 cm. The mice were tested individually for 5 minutes, their movement activity during this period was recorded using a camera and later analyzed by ANY-maze software. During the analysis stage, the open field arena was partitioned into nine squares having similar areas using the ANY-maze software. The square in the center was regarded as the central zone, and the surrounded areas were called the peripheral zone. Different parameters like the frequency and time spent in the center, total distance traveled within the central zone as well as the whole open field box along with their locomotion speed were calculated by ANY-maze, and the results were shown in bar graphs.

TABLE 1: Primers used in this study are listed below [Source: [3-7]]

Gene Name		**Sequences used for qPCR (5'→ 3')**
uPA	For	TTCGGAGGGCAGCACTGTGAAATA
	Rev	GCATGGTACGTTTGCTGAAGGACA
SPARC	For	TCACATTAGGCTGTTGGTTCAAA
	Rev	CGCTGACCACTTCCCAGAGA
FABP7	For	TGCTTGCTGAGGTGTAAAGGGTCT
	Rev	TGACTGTTGGTCAGCTTCCAGGTA
HAS3	For	GGTACCATCAGAAGTTCCTAGGCAGC
	Rev	GAGGAGAATGTTCCAGATGCG
SOX4	For	CCAAATCTTTTGGGGACTTTT
	Rev	CTGGCCCCTCAACTCCTC
MUC1	For	CTGCTCCTCACAGTGCTTACAGTTG
	Rev	TGAACCGGGGCTGTGGCTGG
NEAT1	For	CCAGTTTTCCGAGAACCAAA
	Rev	ATGCTGATCTGCTGCGTATG
HAS2	For	TTATGGGCAGCCAATGTA
	Rev	ACTTGCTCCAACGGGTCT
NEAT1	For	CCAGTTTTCCGAGAACCAAA
	Rev	ATGCTGATCTGCTGCGTATG
PTEN	For	TGTGCTGCCTGCAAGCTTCT
	Rev	GGTGGAACGGCTGACAGCTA
RASSF1	For	AGGTGAACTTGCAATGCGC
	Rev	ACCTCTGTGGCGACTTCATCT
GAPDH	For	TGCACCACCAACTGCTTA
	Rev	AGAGGCAGGGATGATGTTC
Gene Name		**Sequences used for Pyrosequencing (5'→ 3')**
SPARC	For	TTTTTGAGGTGGGTTGTTTTGATTAA
	Rev	Biotin/TACCCTCTAAACAAAAAAAAAACTATTCT
	Seq	ATTTGTTTAGGGGTTGTTG
FABP7	For	TAGGTATAAGGGTTGTAGTGTGAG
	Rev	Biotin/TATCCCTCTTTCCAAAAAACTATCACAA
	Seq	AAGAGGATTGGAGTTTTA
SOX4	For	AGGGATTAAGTGTTAGAGATTATGT
	Rev	Biotin/TTTCCCTAAAACAATTAATTCCAATTCAC
	Seq	AGATTATGTAGTTTTTTTGAGTTAT
MUC1	For	ATTTTTGGGTAGGGTATAAGGG
	Rev	Biotin/CAAAAACCCCAAATTCCAAACTAC
	Seq	GGTAGGGTATAAGGGTTTTA

HAS2	For	Biotin/GTTTGTAGGAGTTGGAAGTTTAGATTG
	Rev	CCACCCCTTCCCTTCTTTTTTTC
	Seq	ATAAAAAAAAAAACTAAAATAACC
HAS3	For	GTGAAAAAGAAGAGGAGGAATTGT
	Rev	Biotin/AAACCAAAACAACAAAACCTTCCTACT
	Seq	GGAATTGTTTTGGTTTTAAGA

Reference (for Supplementary Methods in Chapter 2):

1. Shukeir N, Stefanska B, Parashar S, Chik F, Arakelian A, Szyf M, Rabbani SA. Pharmacological methyl group donors block skeletal metastasis in vitro and in vivo. British journal of pharmacology. 2015; 172: 2769-81.
2. Ennaceur A, Delacour J. A new one-trial test for neurobiological studies of memory in rats. 1: Behavioral data. Behavioural brain research. 1988; 31: 47-59. doi:
3. Cheishvili D, Chik F, Li CC, Bhattacharya B, Suderman M, Arakelian A, Hallett M, Rabbani SA, Szyf M. Synergistic effects of combined DNA methyltransferase inhibition and MBD2 depletion on breast cancer cells; MBD2 depletion blocks 5-aza-2′-deoxycytidine-triggered invasiveness. Carcinogenesis. 2014; 35: 2436-46.
4. Tiwari N, Tiwari VK, Waldmeier L, Balwierz PJ, Arnold P, Pachkov M, Meyer-Schaller N, Schübeler D, van Nimwegen E, Christofori G. Sox4 is a master regulator of epithelial-mesenchymal transition by controlling Ezh2 expression and epigenetic reprogramming. Cancer cell. 2013; 23: 768-83.
5. Chaika NV, Gebregiworgis T, Lewallen ME, Purohit V, Radhakrishnan P, Liu X, Zhang B, Mehla K, Brown RB, Caffrey T. MUC1 mucin stabilizes and activates hypoxia-inducible factor 1 alpha to regulate metabolism in pancreatic cancer. Proceedings of the National Academy of Sciences. 2012; 109: 13787-92.
6. Eißmann M, Gutschner T, Hämmerle M, Günther S, Caudron-Herger M, Groß M, Schirmacher P, Rippe K, Braun T, Zörnig M. Loss of the abundant nuclear non-coding RNA MALAT1 is compatible with life and development. RNA biology. 2012; 9: 1076-87.
7. Liu J, Tu F, Yao W, Li X, Xie Z, Liu H, Li Q, Pan Z. Conserved miR-26b enhances ovarian granulosa cell apoptosis through HAS2-HA-CD44-Caspase-3 pathway by targeting HAS2. Scientific reports. 2016; 6.

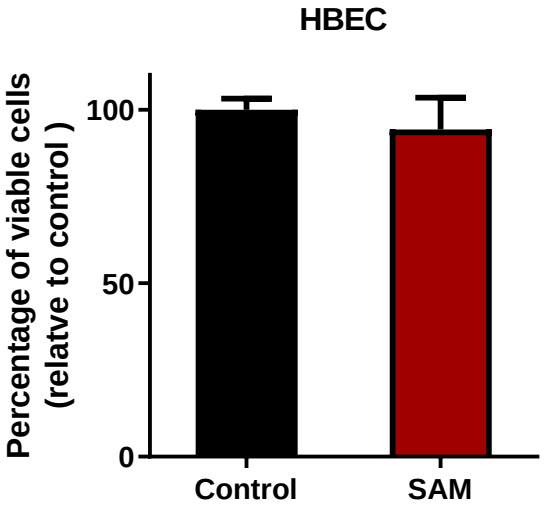

Supplementary Figure S1: Effect of SAM-treatment on the viability of human breast epithelial cells (HBEC). Briefly, HBEC were plated at the same density and treated with vehicle only control or 200 µM SAM every other day from day 2 until they were harvested on day 7. The cells were trypsinized, stained with trypan blue and the number of viable cells was counted under a light microscope daily throughout the 6-day treatments. Results from triplicate experiments are shown as a bar graph.

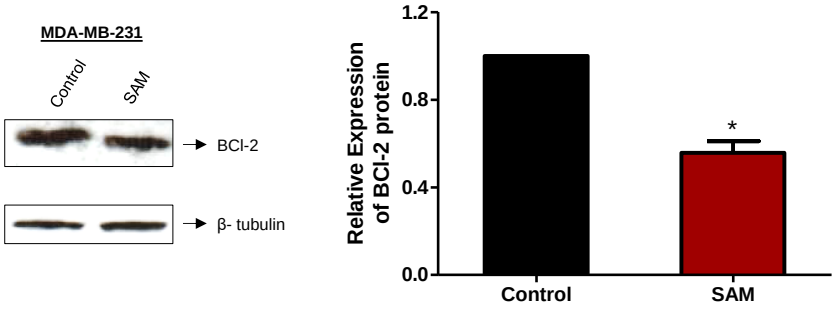

Supplementary Figure S2: Western blot from the whole cell lysates of control and 200 µM SAM-treated MDA-MB-231 cells. The membrane was probed with mouse monoclonal anti-BCl-2 (Santa Cruz Biotechnology, Cat#sc-7382) antibody. β- tubulin (BD Pharmingen, Cat#556321) was used as a loading control. The densitometric intensities of the bands were quantified by ImageJ (Fiji plugin) and plotted as bar graph in the right panel. Treatment with SAM caused a reduction in the expression of anti-apoptotic protein BCl-2 suggesting that SAM induces apoptosis by reducing the level of BCl-2. Results are shown as mean ± SEM of three independent experiments. (* $P < 0.05$).

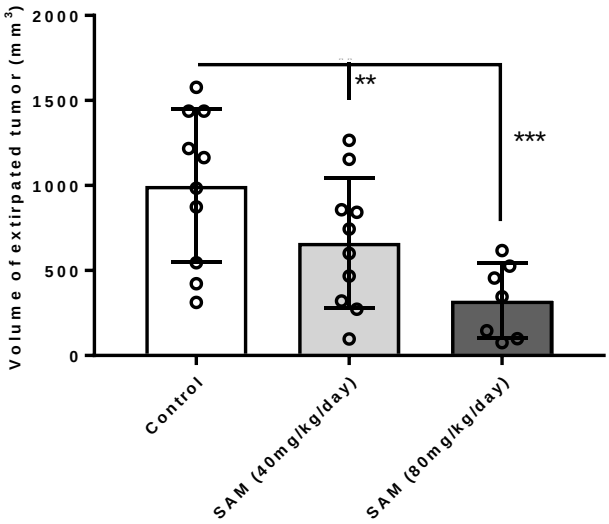

Supplementary Figure S3: The volume of the extracted mammary tumor measured after sacrificing the animal from different groups. Results are shown as mean ± SEM of at least seven animals in each group. Significant differences were determined using ANOVA followed by *post hoc* Bonferroni test and are represented by asterisks (** $P < 0.01$; *** $P < 0.001$)

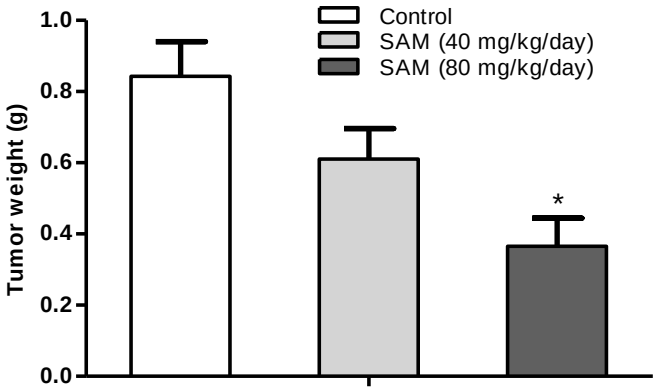

Supplementary Figure S4: Tumor weight after sacrifice. The weight of the extracted mammary tumor measured after sacrificing the animal from different groups on week 10. There is a dose-dependent reduction in tumor weight upon SAM-treatment. Results are shown as mean ± SEM of at least seven animals in each group. Significant differences are represented by asterisks (* $P < 0.05$)

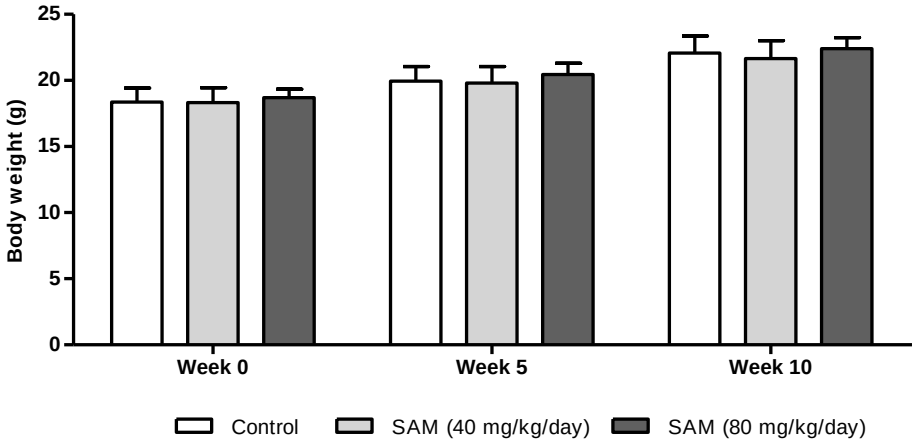

Supplementary Figure S5: Body weight of the xenograft mice. The total body weight of control and SAM-treated animals measured at different time points from the beginning of the study when the tumor cells were injected into the fourth mammary fad of the immunocompromised mice on week 0 until they were sacrificed on week 10. There was no significant difference in the weight of the animals.

A

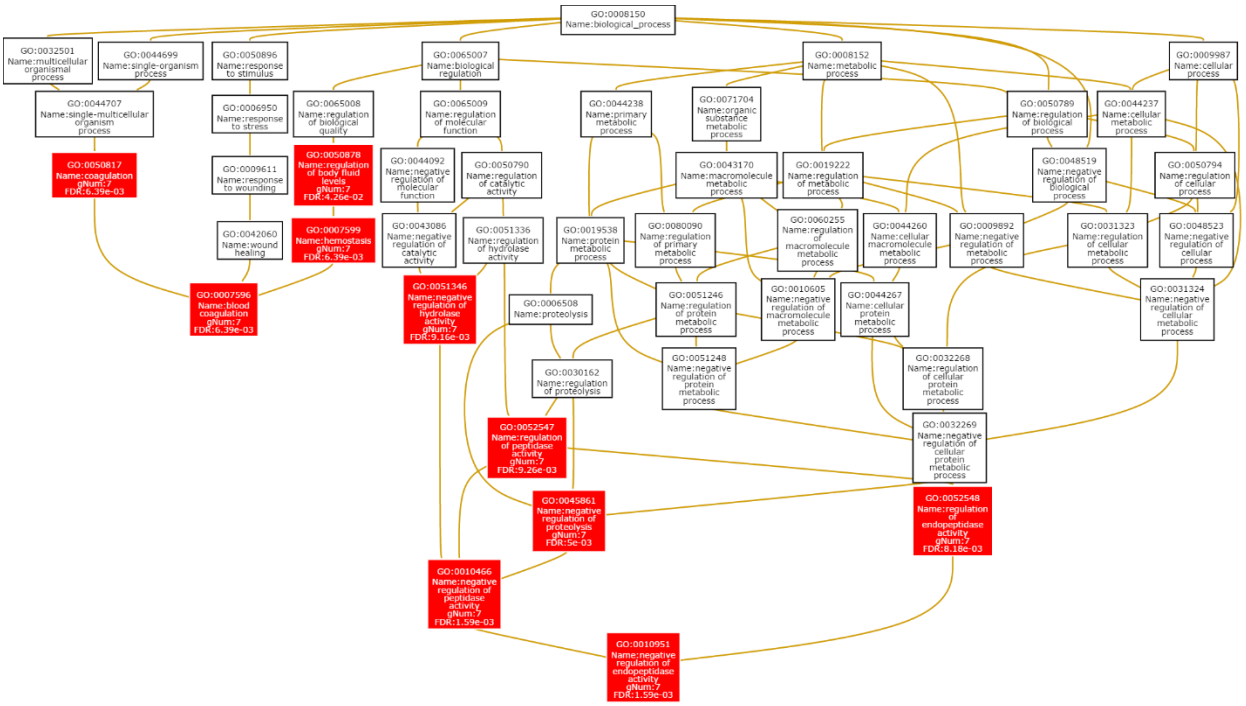

B

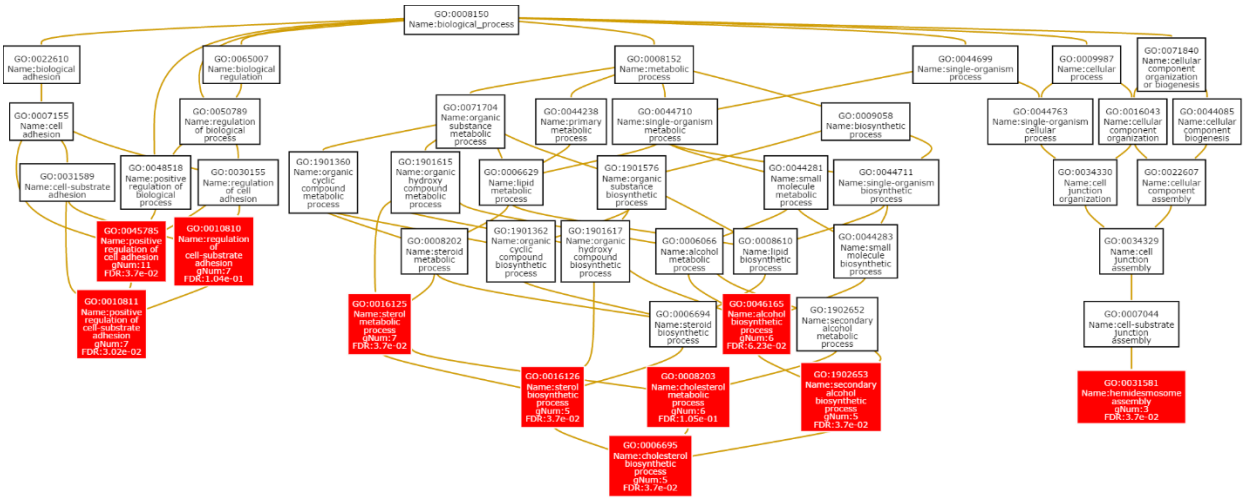

Supplementary Figure S6: Gene Ontology (GO) analysis of the top 10 biological processes enriched in the genes that upregulated (A) and downregulated (B) by SAM-treatment using WebGestalt.

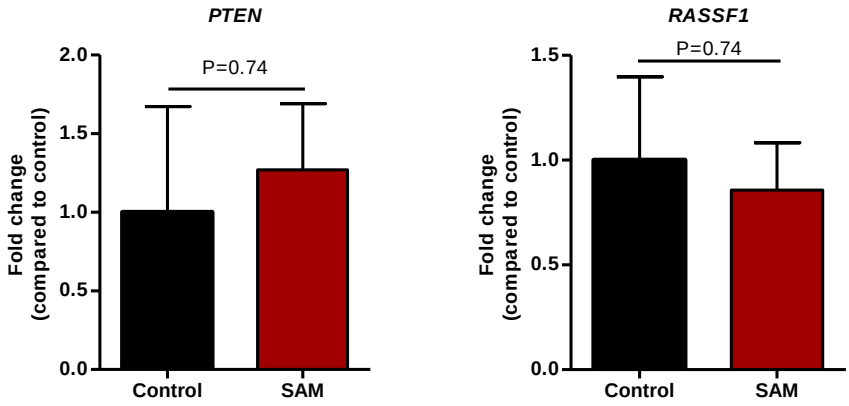

Supplementary Figure S7: Measurement of the gene expression of tumor suppressor genes. Briefly, qPCR for two well-known tumor suppressor genes (*PTEN*, *RASSF1*) from the RNA isolated from tumor samples showed no significant difference between control and high dose SAM (80 mg/kg/day). The results are shown are mean ± SEM from three different mice in each group.

Supplementary Table S1: SAM-treatment is non-toxic *in vivo* as shown by different parameters tested from the blood sample obtained from control and 80 mg/kg/day SAM-treated mice. The results are shown are mean±SEM from three different mice in each group.

Parameter	**Control mice**	**SAM-treated mice**	***P*-value**
Total protein (g/L)	38.67 ± 1.19	36.33 ± 0.54	0.22
Albumin (g/L)	19.33 ± 0.72	17.67 ± 0.27	0.15
Albumin/Globulin ratio	0.97 ± 0.03	0.93 ± 0.03	0.52
Glucose (mmol/L)	14.13 ± 0.94	15.10 ± 0.86	0.57
BUN Urea (mmol/L)	8.27 ± 0.50	10.67 ± 0.59	0.06
Creatinine (µmol/L)	9.33 ± 0.27	9.0 ± 0.82	0.77
Total Bilirubin (µmol/L)	4.0 ± 0.47	5.67 ± 0.27	0.07
ALT (U/L)	37.0 ± 1.69	38.33 ± 1.96	0.69
AST (U/L)	65.33 ± 12.95	65.33 ± 6.83	1.0
CK (U/L)	105.33 ± 47.65	74.0 ± 17.21	0.64
Sodium (mmol/L)	148.67 ± 0.72	145.33 ± 0.72	0.06
Potassium (mmol/L)	4.60 ± 0.24	4.50 ± 0.22	0.77
Chloride (mmol/L)	108.33 ± 1.19	106.67 ± 0.98	0.43
Calcium (mmol/L)	2.26 ± 0.05	2.35 ± 0.04	0.22
Magnesium (mmol/L)	1.04 ± 0.01	1.67 ± 0.04	0.08

BUN: Blood urea nitrogen; ALT: Alanine aminotransferase; AST: Aspartate aminotransferase; CK: Creatinine kinase

Supplementary Table 2

The differentially expressed genes from microarray datasets can be viewed by downloading the ‘Supplementary File 1’ from following link: https://www.oncotarget.com/index.php?journal=oncotarget&page=rt&op=suppFiles&path[]=23704&path[]=0

Chapter Three: S-adenosylmethionine in combination with Decitabine shows enhanced anti-cancer effects in repressing breast cancer growth and metastasis

Preface

Previous studies by our group have shown that treatment with demethylating agents indiscriminately demethylates at the gene regulatory regions. As a result, treatment with DNMT inhibitors induces the undesirable hypomethylation mediated activation of prometastatic genes in addition to the desirable activation of tumor suppressor genes. Since the universal methyl donor SAM can downregulate the expression of prometastatic genes without affecting the expression of tumor suppressors, we tested the hypothesize that concurrent targeting of abnormal hyper and hypomethylation in breast cancer by Decitabine (demethylating agent) and SAM (methylating agent) would provide a superior anti-cancer response compared to single-agent treatment with either of the drugs *in vivo.* In-depth analyses of the MDA-MB-231 methylome and transcriptome was performed to understand the gene expression changes upon the combination treatment. The manuscript related to this study was published in the 'Journal of Cellular and Molecular Medicine' in 2020:

> "**Mahmood,N**., Arakelian,A., Cheishvili,D., Szyf,M. and Rabbani, S.A. (2020) S-adenosyl methionine in combination with Decitabine shows enhanced anti-cancer effects in repressing breast cancer growth and metastasis. J Cell Mol Med. 00:1-16."

Herein, an author-generated version of the manuscript is presented. The article is published as open access under the terms of the Creative Commons Attribution License, which permits use, distribution and reproduction in any medium with proper citation. In addition, email consent was obtained from the Editor which can be found in the Appendices.

Abstract

Abnormal DNA methylation orchestrates many of the cancer-related gene expression irregularities such as the inactivation of tumor suppressor genes through hypermethylation as well as activation of prometastatic genes through hypomethylation. The fact that DNA methylation abnormalities can be chemically reversed positions the DNA methylation machinery as an attractive target for anti-cancer drug development. However, although *in vitro* studies suggested that targeting concordantly hypo- and hypermethylation is of benefit in suppressing both oncogenic and prometastatic functions of breast cancer cells, this has never been tested in a therapeutic setting *in vivo*. In this context, we investigated the combined therapeutic effects of an approved nutraceutical agent S-adenosylmethionine (SAM) and FDA-approved hypomethylating agent Decitabine using the MDA-MB-231 xenograft model of breast cancer and found a pronounced reduction in mammary tumor volume and lung metastasis compared to the animals in the control and monotherapy treatment arms. Immunohistochemical assessment of the primary breast tumors showed a significantly reduced expression of proliferation (Ki-67) and angiogenesis (CD31) markers following combination therapy as compared to the control group. Global transcriptome and methylome analyses have revealed that the combination therapy regulates genes from several key cancer-related pathways that are abnormally expressed in breast tumors. To our knowledge, this is the first preclinical study demonstrating the anti-cancer therapeutic potential of using a combination of methylating (SAM) and demethylating agent (Decitabine) *in vivo*. Results from this study provide a

molecularly founded rationale for clinically testing a combination of agents targeting the epigenome to reduce the morbidity and mortality from breast cancer.

Introduction

Abnormal DNA methylation is one of the earliest and most common hallmarks of cancer [1,2]. Since the addition or removal of the methyl group to the CpG islands is a dynamic and reversible process, it stands to reason that targeting the methylome may serve as an attractive anti-cancer strategy [3,4]. Research over the past thirty years has led to the development of different types of DNA methylation inhibitors, and two drugs [5-azacytidine (5AzaC, marketed as Vidaza) and 5-aza-2'-deoxycytidine (5AzadC, marketed as Decitabine/Decogen)] targeting the DNA methyltransferase (DNMT) enzymes are already approved by the Food and Drug Administration (FDA) for the treatment of several hematological malignancies [5-7]. Both 5AzaC and 5AzadC are cytosine analogs that can be incorporated into the DNA during replication where they function as suicide substrates for DNMT enzymes and trap them for subsequent proteasomal degradation, which ultimately leads to DNA demethylation at a genome-wide scale [8,9]. At the molecular level, DNMT inhibitors (DNMTi) cause demethylation at the promoters of tumor suppressor genes that are otherwise methylated in cancer and thereby derepress their normal gene expression [10]. More recently, it has been shown that DNMTi treatment also upregulates the expression of endogenous retroviral sequences (ERVs), which in turn activates viral defense response genes and thereby reduces the number of cancer-initiating cells [11]. These events reprogram the cancer cells to behave similarly to the virus-infected

cells to cause the induction of an anti-tumor immune response against them, by a process known as “viral mimicry” [10].

Even though DNMTis are approved for several hematological malignancies, they have only shown modest success in the case of solid tumors and generally induce toxic side effects like anemia, bleeding, and arthralgia [12]. In addition, primary and secondary resistance to these drugs has been reported in clinical settings [13], which warrants the development of a different rational approach to target the methylome in solid cancers.

Since 5AzaC and 5AzadC induce demethylation across the genome, it stands to reason that the effect will not be limited to tumor suppressor genes and that they will also induce genes that promote cancer; notably genes involved in metastasis that are activated by loss of methylation. This might result in adverse effects and limit the utility of these agents. Indeed it has been shown that DNMTi treatment also potentiates promotor demethylation-mediated activation of several known prometastatic genes [urokinase plasminogen activator (*PLAU*), C-X-C motif chemokine receptor 4 (*CXCR4*), heparanase (*HPSE*)] in less aggressive MCF-7 and ZR-75-1 breast cancer cells which facilitates their transformation to become more aggressive tumor cells [14]. Interestingly, the treatment of cancer cells with universal methyl donor S-adenosylmethionine (SAM) reverses these effects via hypermethylation of the promoters of the prometastatic genes [15]. SAM is an approved nutraceutical agent used for osteoarthritis, fibromyalgia, cholestasis, and depression [16,17], and results from long term clinical trials showed no behavioral or biochemical adversities upon administration of the agent except for the individuals with bipolar disorder [18,19]. Our recent studies using xenograft models of breast cancer have

demonstrated the anti-cancer properties of SAM when administered via an oral route without causing any detrimental biochemical or behavioral adversities [20]. Moreover, microarray-based methylation studies on different types of cancer cells have revealed that SAM treatment caused hypermethylation-mediated inactivation of prometastatic genes without repressing the expression of the known tumor suppressor genes [21,22].

Since DNA hypomethylation and hypermethylation are common characteristics of the cancer epigenome [17,23], we have previously hypothesized and tested that combined administration of methylating and demethylating agents could block breast cancer growth and invasion *in vitro* [24]. However, a critical question that remained unanswered was whether simultaneous targeting of DNA hypo- and hypermethylation using SAM and 5AzadC combination could show similar effects *in vivo* so that it could be further translated in clinical settings to breast cancer patients. Herein, we examined the anti-cancer therapeutic potential of the approved demethylating agent 5AzadC in combination with global methyl-group donor SAM in reducing tumor growth and metastasis using the MDA-MB-231 xenograft model of breast cancer.

Material and Methods

Cell culture and treatments

Human MDA-MB-231 (*ATCC*® HTB- 26™) and Hs578T *(ATCC*® *HTB-126*™) triple-negative breast cancer (TNBC) cell lines were maintained as described before [20]. Authentication of both of these cell lines was done by short tandem repeat (STR) profiling using GenePrint® 10 System (Promega, Madison, WI, USA). DNA obtained

from both cell lines showed a 100% match with the core alleles tested for authentication, which confirmed their identity. The mouse PyMT-R221A breast cancer cell line was kindly provided by Dr. Conor C. Lynch (H. Lee Moffitt Cancer Center and Research Institute, Tampa, FL, USA). These cells were initially extracted and cultured from the mammary tumors of transgenic MMTV-PyMT mice in FVB background that resembles the luminal B subtype [25]

The cells were treated with 200 μM human-grade SAM (a gift from Life Science Laboratories, Lakewood, NJ, USA), 1 μM 5AzadC (Sigma-Aldrich, St. Louis, MO, USA; Cat# A3656) or SAM+5AzadC through direct administration of the agents into the culture medium every other day for six days as previously described [24].

Cell proliferation and anchorage-independent growth assay

The cells were seeded onto 6-well cell culture grade plates (BD Falcon^{TM}) and treated with SAM, 5AzadC, SAM+5AzadC, or vehicle (as control) every second day for six days. The coefficient of drug interaction (CDI) was measured to determine whether the interaction between the two drugs is synergistic, additive, or antagonistic in different cell lines, as described before [26]. On the day after each of the three treatments (on days 1,3, and 5), the cells were trypsinized and counted using a Coulter counter (Model ZF; Coulter Electronics, Hertfordshire, UK). Following the usual treatment period, 5×10^3 cells were used for anchorage-independent growth assay as described before [20].

Apoptosis assay

Following the usual treatment period stated above, both floating and adherent cells from vehicle-treated control and different treatment groups were collected and subjected to Annexin V and propidium iodide staining using 'Dead Cell Apoptosis Kit' (Thermo Fisher, Eugene, Oregon, USA; Cat# V13242). As a positive control of apoptosis, the cells were treated with 20 µM cisplatin (Abcam, Cambridge, UK; Cat# ab141398). Upon staining, the subsequent steps related to flow cytometry was performed as described before [20]. The caspase-3 enzyme activity was measured using the caspase-3 assay kit (Abcam, Cambridge, UK; Cat# ab39401) following the supplier provided protocol. The cell lysates from control and different treatment groups were incubated with DEVD-*p*-NA substrate containing buffer for 3 hours, and absorbance at 405 nm was measured by using a Tecan Infinite® 200 PRO microplate reader.

In vivo xenograft model of breast cancer

For *in vivo* experimental purpose, 6-8 weeks old female immunocompromised NOD-SCID mice were purchased from Charles River Laboratories (St-Constant, QC, Canada) and housed at the Animal Resource Division (ARD) of the Research Institute of the McGill University Health Center (RI-MUHC) at a 12-hour light-dark cycle in sterile cages with *ad libitum* access to food and water. After one week of acclimation in the RI-MUHC ARD housing facility, animals were anesthetized, and $5x10^5$ viable MDA-MB-231 cells mixed with 20% Matrigel (BD Biosciences) were inoculated into the fourth mammary fat pad of NOD-SCID mice, as described by us previously [27]. Three days after tumor cell

inoculation, the animals were randomized and divided into four groups: vehicle [phosphate buffer saline (PBS)] treated controls, SAM (80 mg/kg/day) via oral gavage, 5AzadC (0.8 mg/kg/3 times per week for 3 weeks) by intraperitoneal (IP) injection, and combination of SAM+5AzadC. The doses used for the different agents were previously determined by us and others [20,28] and, therefore, the experimental protocol remained the same throughout the course of this study. Palpable tumors started to emerge from week 5 after inoculation, and the tumor volumes were measured at weekly intervals from week 6 until experimental endpoint on week 10 using the following formula: Volume= (length × $Width^2$)/2. Relative tumor growth inhibition was measured using the following formula: $100*(1-T_t/T_0)$, where T_t and T_0 stand to the mean tumor volumes for a treatment arm relative to the control arm [29].

RNA extraction and qPCR

Total RNA was isolated using the AllPrep DNA/RNA Mini Kit (Qiagen, Hilden, Germany; Cat# 80204) and converted to cDNA. Then a quantitative PCR (qPCR) assay was performed using an ABI StepOnePlus™ (Applied Biosystems) machine following a previously described protocol [21]. All primers used in this study are listed in Supplementary File 1, Table S1.

RNA-Seq and analysis pipeline

Total RNA extracted from control, SAM, 5AzadC, and SAM+5AzadC treated MDA-MB-231 cells were assessed by Agilent 2100 Bioanalyzer, and the samples that

passed the quality control were used for transcriptome sequencing (n=3/group). The supplier protocol for the NEBnext Ultra ii Stranded mRNA kit (New England Biolabs, Ipswich, MA, United States) was used for sample preparation, and an Illumina NextSeq 500 System was used for paired-end sequencing. Once the sequencing was done, the alignment of the raw reads to the hg19 reference sequence (for *Homo sapiens*) was done using STAR aligners [30]. Sequence assembly and differential gene expression analyses were done using the package Cufflinks [31]. Differentially expressed genes from each treatment group relative to control MDA-MB-231 cells were chosen using a false discovery rate (FDR) adjusted p-value of less than 0.2.

DNA isolation and MethylationEpic 850 K BeadChip microarray

DNA was extracted using the AllPrep DNA/RNA Mini Kit (Qiagen, Hilden, Germany; Cat# 80204) following the standard protocol. Biological duplicates from each group were bisulfite-converted, and epigenome-wide methylation patterns were assessed using Infinium Human MethylationEpic 850K BeadChip microarray (Illumina) following the manufacturer's protocols. The Illumina intensity data (IDAT) files from the microarray experiment were normalized with BMIQ [32] and processed using the ChAMP [33] package as described by us before [34]. The methylation levels were obtained as β values that ranged from zero to one ('0'= fully unmethylated probe and '1'=fully methylated probe). Probes with single nucleotide polymorphism (SNPs) were removed from the downstream analysis. For differential methylation analysis in each treatment group relative to controls, Bioconductor package Limma [35] was used where a methylation difference

(delta β value) greater than 0.05 [36] and $P < 0.05$ was considered statistically significant as previously described [37].

Western blot

Cell lysates were prepared using radioimmunoprecipitation assay (RIPA) buffer containing a mixture of protease and phosphatase inhibitors, and western blot was done as described by us previously [38].

Immunohistochemistry

The immunohistochemical assessment was performed on formalin-fixed tumor tissues by double staining each sample slide using antibodies against Ki-67 (Cat# M7240, Dako, Glostrup, Denmark) and CD31 (Cat# 760-4378, Roche, Basel, Switzerland) markers. The staining was done at the RI-MUHC Histopathology platform using a standardized protocol. Then photomicrographs of five randomly selected fields from each sample slides were taken. The Ki-67 positive cells were counted based on their distinct nuclear staining. The area of CD31 staining was quantified using ImageJ (Fiji plugin) (National Institutes of Health, Bethesda, MD, USA).

Statistical analysis

The results are expressed as the mean ± standard error of the mean (SEM). Statistical analyses were carried out by Student's *t*-test, ANOVA depending on the type of experimental data. $P \leq 0.05$ was considered as significant.

Results

Effect of SAM+5AzadC combination on TNBC cell lines in vitro

To examine the *in vitro* effect of combining SAM and 5azadC on the growth properties of cells, we first used two highly metastatic TNBC cell lines: MDA-MB-231 and Hs578T. Both SAM and 5AzadC were previously shown to reduce tumor cell proliferation [21,22,39]. As expected, either 200 μM SAM or 1 μM 5AzadC caused a significant reduction in cell growth compared to vehicle-treated controls (Figure 1A). However, combination therapy caused a more substantial reduction in growth than either of the monotherapies. A coefficient of drug interaction (CDI) test using cell proliferation data showed a moderately synergistic effect of the combination treatment in MDA-MB-231 (CDI=0.78) cells and an additive effect in Hs578T cells (CDI=1.1) *in vitro*.

Next, we evaluated whether the combination of SAM and 5AzadC could suppress the anchorage-independent growth, a cellular measure of malignant transformation. A significant decrease in the ability of the MDA-MB-231 and Hs578T cells to form colonies was observed upon single-agent treatment with either SAM or 5AzadC (Figure 1B). The suppression was significantly more pronounced when the cells were treated with the combination of SAM and 5AzadC in both cell lines (Figure 1B).

Next, we wanted to evaluate whether the combination treatment shows a similar anti-cancer effect in breast cancer cells belonging to a different subtype and species. For that, we used the PyMT-R221A murine luminal B breast cancer cell line. Our data showed a moderately synergistic effect of the combination (CDI=0.75) in decreasing PyMT-R221A cell proliferation (Supplementary File 1, Figure S1A). A significant reduction in

the ability of the PyMT-R221A cells to form colonies was also observed (Supplementary File 1, Figure S1B). Taken together, these observations suggest that the combination treatment inhibits the growth of a broad spectrum of breast cancer cells representing different subtypes and species.

We then examined the effect of the combination treatment on apoptotic cell death using a flow cytometry-based annexin V/PI assay. While all three treatment groups induced apoptosis, the SAM+5AzadC treated cells showed the highest percentage of apoptotic cell deaths (Figure 1C). We used the DNA-damaging agent cisplatin as a positive control for the induction of apoptosis. To further confirm these results, we measured the enzymatic activity of caspase-3, which functions as an executioner caspase to induce apoptosis [40]. A significant increase in caspase-3 activation was observed in the treated groups compared to the control MDA-MB-231 and Hs578T cells (Figure 1D). During these studies, we did not observe any noticeable change in the morphology of the cells.

Effect of SAM+5AzadC combination on MDA-MB-231 xenograft model of breast cancer

We then tested the anti-cancer therapeutic effect of SAM combined with 5AzadC *in vivo* using a human MDA-MB-231 xenograft model of TNBC, where 5×10^5 tumor cells were orthotopically implanted into the fourth inguinal mammary fat pads of 6-8-week-old female NOD-SCID mice. Three days post-injection of the tumor cells, the animals were randomized into four groups: PBS vehicle-treated controls, 80 mg/kg/day of SAM via oral gavage, 0.8 mg/kg of 5AzadC by IP injection, and combination [SAM (80

mg/kg/day)+5AzadC (0.8 mg/kg)], and treatment was carried out using the strategy depicted in Figure 2A. The 5AzadC treatment, for the monotherapy and combination groups, was carried out for three weeks to avoid potential adverse effects [12]. In contrast, all animals treated with SAM in the monotherapy and the combination setting received SAM daily via oral gavage from the start of treatment until the experimental endpoint was reached. Our results show that all animals in the control group developed tumors that continued to grow until the experimental endpoint at week 10 after tumor cell injection (Figure 2B; Supplementary File 1, Figure S2). On the other hand, 87.5% of the animals in either SAM or 5AzadC monotherapy treatment groups developed a tumor at the experimental endpoint while only 66.67% of the animals in the SAM+5AzadC combination treatment group developed a tumor (Supplementary File 1, Figure S1). Moreover, in comparison with the control animals, significant reductions in tumor volumes were observed in the treatment groups at experimental endpoint on week 10 (Figure 2B-C). To determine whether the anti-cancer therapeutic effects in the combination treatment is either additive, synergistic or antagonistic, we measured CDI and found that the combination treatment shows a moderately synergistic effect (CDI=0.86) in reducing the primary mammary tumor volumes in this model. We also measured tumor growth inhibition at experimental endpoint in each group relative to control animals and found 49.13% and 67.95% reduction in average tumor volume in SAM and 5AzadC treated animals, respectively. However, the reduction in tumor volume in the combination treatment group was 85.96% relative to the controls suggesting an enhanced anti-cancer activity of the combination treatment in reducing mammary tumor growth *in vivo.*

Since MDA-MB-231 cells orthotopically implanted into the mouse mammary fat pad metastasize to different target organs [20], we evaluated the effect of the different treatment regimens on lung metastasis using H&E staining of formalin-fixed lung tissue sections from the different treatment groups. Compared to the vehicle-treated control animals, a significant reduction in lung metastasis was observed in both SAM and 5AzadC monotherapy treated animals, which was further reduced in the SAM+5AzadC treated animals (Figure 2D), demonstrating a higher anti-cancer therapeutic effect of the combination treatment.

The aggressiveness of breast cancer correlates with proliferative capabilities as well as the vascularization of the tumor cells, which prompted us to determine the expression of Ki-67 (proliferation marker) and CD31 (angiogenesis marker) in formalin-fixed tumor tissues from control and the treatment groups using a double immunostaining strategy. Our data showed that animals from all three treatment groups had a significant reduction in the expression of proliferation and angiogenesis markers, an effect that was more pronounced in the SAM+5AzadC combination-treated group (Figure 2E). Taken together, these results complement the phenotypic effect seen by the reduced tumor volume and metastasis in response to the combination treatment.

Next, we checked whether the SAM+5AzadC combination treatment elicits any toxicities in the animals by measuring different biochemical parameters related to liver and kidney function as well as major electrolytes. Our data demonstrated that there were no statistically significant differences in any of the blood parameters tested between control

and the treatment arms (Supplementary File 1, Table S2), suggesting that the treatments are not overtly toxic.

Effect of SAM+5AzadC combination on the MDA-MB-231 transcriptome

To evaluate gene expression changes mediated by different treatments, we next performed a transcriptome analysis of the control and treated MDA-MB-231 cells by RNA-Sequencing (n=3/group). Our data revealed that, in comparison to the vehicle-treated control MDA-MB-231 cells, single-agent treatment with SAM and 5AzadC caused significant gene expression changes of 238 (141 downregulated, 97 upregulated) and 179 (104 downregulated, 75 upregulated) genes, respectively (Figure 3A, Supplementary File 2). Interestingly, these effects were more pronounced in the SAM+5AzadC combination-treated cells, where 801 (389 downregulated, 412 upregulated) genes were differentially expressed relative to the control (Figure 3A, Supplementary File 2). We then used Venn diagrams and circus plots to depict the numeric and functional common and exclusive transcriptomic footprints in the different treatment groups. Our analyses indicated that the combination therapy significantly changes the expression profiles of 556 genes (305 upregulated and 251 downregulated) that are not significantly affected by either of the monotherapy treatments using our study cut-offs (Figure 3B&C).

We then performed comparative pathway enrichment analyses between differentially expressed genes (DEGs) in SAM, 5AzadC, and SAM+5AzadC treated cells using the well-annotated Reactome and Kyoto Encyclopedia of Genes and Genomes

(KEGG) databases from Metascape [41] (Figure 3D). We found that the genes downregulated by the combination treatment are enriched in 'Laminin interactions', 'Extracellular matrix organization' pathways that are involved in migration, invasion, and metastatic spread while the genes upregulated upon the combination treatment are enriched in crucial cancer-related pathways like 'Interferon alpha-beta signaling', 'Jak-STAT signaling pathway' and others as shown by the heatmap in Figure 3D.

Validation of differentially expressed cancer-related genes affected by the combination treatment in MDA-MB-231

We next validated the differential expression of several prometastatic and tumor suppressor genes that are involved in various cancer-related signaling pathways in the treatment groups by quantitative polymerase chain reaction (qPCR) analysis (Figure 4A). There was a significant correlation between fold change in expression determined by RNA-Seq and by qPCR between combination treatment and control (Figure 4B).

Recent evidence suggests that suppression of MUC1, in turn, downregulates the anti-apoptotic MCL1 protein in breast cancer cells [42]. Interestingly, *MCL1* gene expression is reduced upon SAM+5AzadC, as shown by RNA-Seq (Supplementary File 2) and qPCR (Figure 4A). We then measured the levels of the anti-apoptotic proteins MCl-1 and BCl-2 and found that they were reduced in response to the combination treatment (Supplementary File 1, Figure S3A). Previous studies have demonstrated that increased MUC1 expression stabilized beta-catenin from degradation by Glycogen synthase kinase 3 beta (GSK3B) [43]. Therefore, we measured the expression of β-catenin, which is a

component of the pro-proliferative Wnt/β-catenin signaling pathway and found it to be downregulated upon SAM+5AzadC treatment (Supplementary File 1, Figure S3A). These results indicate that the combination treatment affects multiple components of pro-proliferative and anti-apoptotic pathways to elicit an anti-cancer response (Supplementary File 1, Figure S3B).

We next used publicly available cancer transcriptome dataset (as described by Solzak *et al.* [44]) to determine whether the genes targeted by the combination treatments (DEGs) are known to be differentially expressed in triple-negative breast cancer patients and therefore potentially important for the cancer state. Although the overlap between the genes which were upregulated by SAM+5AzadC but downregulated in patients was not significant as determined by a hypergeometric test (Figure 4C), there was a significant overlap of 71 genes which were downregulated by SAM+5AzadC treatment with the set of genes which were upregulated in breast cancer patients (hypergeometric test, $p<0.05$) (Figure 4D). These data point to a potential benefit of SAM+5AzadC treatment for highly aggressive TNBC patients. Pathway enrichment analysis of these genes revealed that they are involved in several cancer-related signaling pathways like the p53 downstream pathway, apoptosis, Beta1 integrin cell surface interactions, and PI3K signaling pathways (Figure 4D), suggesting the clinical relevance of the genes differentially regulated by SAM+5AzadC combination.

We then assessed whether the phenotypic changes related to metastasis and angiogenesis seen *in vivo* could be linked to the gene expression changes induced by the SAM+5AzadC combination treatment *in vitro*. We first overlapped the genes

downregulated by the combination treatment with the complete repertoire of metastatic genes obtained from the human cancer metastasis database [45] and found a significant overlap of 66 genes (hypergeometric test, $p<0.05$) (Supplementary File 1, Figure S4). We then compared the genes downregulated by the SAM+5AzadC combination with the list of genes involved in angiogenesis and found a statistically significant overlap of 19 genes (hypergeometric test, $p<0.05$) (Figure 4E). Some of the crucial genes in this overlap include *VEGFA, PDGFC, FN1* that were known to be involved in angiogenesis in different types of cancers. Taken together, these results suggest that the transcriptome-wide gene expression changes show congruence with the phenotypic changes mediated by the SAM+5AzadC combination.

Effect of the SAM+5AzadC combination on the upstream regulators of gene expression

To identify the potential upstream regulators that mediate the gene expression changes seen in RNA-Seq, an upstream regulator analysis (URA) was performed using ingenuity pathway analysis (IPA) tool [46]. This analysis can decipher the potential transcription regulators, growth factors, and any gene or chemical that has been shown to affect gene expression by experimental evidence. We mainly focused on the 'transcription regulators' that directly regulate gene expression. Our results show that a total of 16 (1 up, 15 down), 10 (6 up, 4 down), and 18 (7 up, 11 down) transcription regulators are predicted to be significantly affecting the DEGs enriched in SAM, 5AzadC, and SAM+5AzadC combination-treated groups, respectively (Figure 5A). The upstream transcription

regulators that were activated in SAM+5AzadC were TFAP2A, PIAS1, ZBTB48, TCF3, DACH1, SMARCA4, IRF6 which affect a diverse array of target genes that are graphically depicted in Supplementary File 1, Figure S5. For example, PIAS1 activation might repress *MCL-1* expression, whereas TFAP2A activation might downregulate *VEGFA*, *KLF4*, and several other genes, as seen in the RNA-Seq data. When we investigated the upstream transcription regulators that were inhibited upon SAM+5AzadC treatment, we found a significant change in some of the well-known cancer-related transcription factors like HIF1A, SOX4 (Figure 5A), whose downstream target genes are shown in Figure 5B. The genes targeted by the other upstream regulators inhibited by SAM+5AzadC treatment are presented in Supplementary File 1, Figure S6. We next focused on HIF1A and SOX4 mediated effects through the construction of mechanistic networks using the existing knowledge found in the IPA tool (Figure 5C). The mechanistic network analyses suggest that the inhibition of SOX4 possibly mediates HIF1A downregulation which, in turn, affects various downstream oncogenic factors, as shown in Figure 5C. These observations indicate that the SAM+5AzadC treatment alters the expression of crucial transcription factors that mediate the downstream changes in expression of a vast array of genes in the MDA-MB-231 transcriptome.

Effect of SAM+5AzadC combination on the MDA-MB-231 methylome

Since both SAM and 5AzadC modulate DNA methylation, we next used a genome-wide approach to delineate the changes in MDA-MB-231 methylome in response to treatment with either single-agent therapies or the combination using Illumina

MethylationEPIC arrays that cover more than 850k probes. In this study, we defined probes with >5% change in methylation in both directions in treatment compared to control groups as either hypermethylated or hypomethylated, respectively. As expected, we found that SAM monotherapy caused more hypermethylation while 5AzadC monotherapy caused more hypomethylation of CpG sites (Figure 6A). The combination treatment caused broader changes in the DNA methylation landscape than the monotherapy treatments by either SAM or 5AzadC; DNA methylation changes happened in both directions at different locations in the genome (Figure 6A). The combination-treatment caused more hypomethylation near the promoter regions (TSS1500, TSS200, and 5′UTR as defined in [47]) and slightly more hypermethylation in the IGRs.

Differential methylation at the promoter region of genes is believed to mediate tumorigenesis either via the downregulation of tumor-suppressor genes or upregulation of oncogenes. We then focused on the CpGs that are differentially regulated by the SAM+5AzadC combination treatment at or near promoter regions. Using a gene set enrichment analysis, we found that combination treatment causes significant methylation changes of genes involved in several crucial cancer-related pathways (Figure 6B). For example, we found that the genes whose promoters become hypomethylated upon combination treatment are enriched in pathways that are involved in ‘negative regulation of cell proliferation’ while the genes whose promoters are hypermethylated are engaged in ‘cell proliferation’ (Figure 6B). Taken together, these observations further validate that epigenetic therapies with SAM and 5AzadC alter DNA methylation of critical cancer-related pathways. It should also be noted that the methylation changes have context-

dependent roles in regulating gene expression, and not all the methylation changes will result in altered gene expression.

Integrated analyses of methylation and gene expression in the combination therapy group

To gain further molecular mechanistic insights to the set of genes regulated by the combination therapy, we determined whether the changes seen in DNA methylation were associated with changes in gene expression as determined by RNA-Seq. The integrated analyses of transcriptome and methylome showed that differential expression of 267 genes was associated with differential DNA methylation (Figure 7A). Further analysis revealed that these genes are enriched in cancer-related signaling pathways like focal adhesion, ECM-receptor interaction, apoptosis, PI3K-AKT signaling, and others as listed in Figure 7B. In addition, we found that 60 out of these 267 genes showed a significant overlap with the list of genes obtained from the human cancer metastasis database (hypergeometric test, $p<0.05$) (Supplementary File 1, Figure S7).

Next, from the list of 267 overlapping genes between expression and methylation, we focused on genes whose promoter was hypermethylated with downregulated gene expression and genes whose promoters were hypomethylated with upregulated gene expression. Through integrated analyses of gene expression and promoter methylation, we identified 45 genes that showed hypomethylation-mediated upregulation and 15 genes that showed hypermethylation-mediated downregulation upon SAM+5AzadC combination treatment (Supplementary File 1, Table S3). We then validated the expression of the several

genes from the list in Table S3 that showed hypomethylation-mediated activation (*TFPI2* and *GSTP1*) and hypermethylation-mediated inactivation (*FADS2*) upon combination treatment by qPCR (Figure 7C). Further analysis of the Cancer Genome Atlas (TCGA) database suggested that these genes show aberrant expression patterns in breast cancer patients in the opposite direction (Figure 7D).

Taken together, through a series of *in vitro* and *in vivo* studies, we demonstrated a higher anti-cancer effect of the SAM+5AzadC combination in comparison with monotherapies in well-established models of breast cancer and elucidated its potential molecular basis (Figure 7E).

Discussion

Epigenetic reprogramming in cancer involves a combination of demethylation-mediated activation of tumor-promoting and prometastatic gene networks and hypermethylation-mediated silencing of tumor suppressor gene networks. Currently, Vidaza and Decitabine are the only approved DNA methylation inhibitors used clinically to treat cancer patients. However, a long line of evidence has established in cell culture studies that loss of methylation can lead to the induction of genes that promote metastasis, the most morbid facet of cancer. Several studies showed that demethylating agents can enhance the invasiveness of breast cancer cells *in vitro* [14,39] and that the methyl donor SAM could inhibit invasiveness and bone metastasis *in vivo* [15,21]. One possible way to attenuate the adverse effects of DNA demethylation agents is to enhance methylation of tumor and metastasis promoting genes using the ubiquitous methyl donor SAM. This

suggestion is presumably counterintuitive however, since the addition of a methylation promoting agent such as SAM might cancel the activation effect of 5AzadC on tumor suppressor genes and thus both agents will nullify each other and eliminate the therapeutic effect. However, if SAM targets different gene pathways than 5AzadC, the combination could be synergistic. A rational approach to cancer therapy should involve a combinatorial approach targeting different nodal pathways of growth and metastasis concurrently. A previous *in vitro* study confirmed that a combination of SAM and 5AzadC would be efficacious and, more importantly, inhibit metastasis which is stimulated by 5AzadC [24]. Could this be translated into clinical practice? A first step should be demonstrating that a combination of SAM and 5AzadC will have more efficacious anticancer activity than monotherapies *in vivo* and second that this combination inhibits cancer metastasis *in vivo*.

In this study, we compared SAM+5AzadC combination therapy with monotherapies with either compound using a well-established *in vivo* model of breast cancer. Even though the combination treatment shows anti-cancer effects on breast cancer cells from different subtypes, we focused on TNBC due to the high rate of mortality in patients with this breast cancer subtype and a paucity of effective therapeutic strategies. Our data showed that the combination of SAM+5AzadC had a moderately synergistic anti-cancer effect on reducing primary tumor volumes of MDA-MB-231 xenografts without causing additional toxicity as measured by standard biochemical tests. Moreover, the metastatic spread of primary tumor cells from the breast to the lung tissue was robustly inhibited by combination therapy as compared to monotherapy with 5AzadC. These data support the conclusion that a combination of 5AzadC and SAM might be of utility in

treating breast cancer and potentially other cancers and warrant further clinical testing. Our results show that SAM does not nullify the effects of 5AzadC, but it rather enhances the antitumor effect.

To examine the molecular mechanism underlying enhanced anti-cancer potential of the combination therapy, and to test whether combination therapy interferes with the effect of DNA demethylation on the induction of tumor suppressor genes, we performed genome-wide methylome and transcriptome analyses following treatment with SAM, 5AzadC, and their combination. Results from these studies demonstrate that the two agents (SAM, 5AzadC) target a diverse array of genes acting in different functional pathways involved in cancer development and progression, explaining why SAM doesn't nullify the effects of 5AzadC. The combination therapy didn't block 5AzadC activation of tumor suppressor genes and didn't result in the silencing of other tumor suppressor genes. On the contrary, the combination treatment upregulated expression of several known tumor suppressor genes like *CST6*, *TFPI2*, *GSTP1* and several others.

The combination treatment showed enhanced anti-cancer effects in reducing the expression of genes related to metastasis compared to the monotherapy treatment. For example, the expression of *Sox4*, a master regulator of EMT [48], was significantly reduced in the combination group suggesting the possible modulation of the treatment through the pathway. We also found that the expression of the *MUC1* gene, which is overexpressed in breast cancer patients (Supplementary File 1, Figure S8), and encodes the widely used CA 15-3 (Cancer antigen 15-3) serum biomarker for breast cancer, was significantly reduced upon SAM+5AzadC combination treatment. MUC1 promotes cancer cell invasion and

epithelial to mesenchymal transition (EMT) through its interaction with beta-catenin [49], both of which are reduced upon treatment with SAM+5AzadC (Figure 4A; Supplementary File 1, Figure S2). The expression of *KLF4*, required for breast cancer stem cell (CSC) maintenance [50], was also significantly repressed upon combination treatment (Figure 4A). This prompted us to check if any other critical modulators of the pathways related to CSC were altered by the combination treatment and found that the expression of *SHH*, which is upregulated in human breast tumors (Supplementary File 1, Figure S9A), is downregulated by the combination treatment (Supplementary File 1, Figure S9B).

Only 27 DEGs (10 upregulated and 17 downregulated) were found to be commonly targeted by SAM, 5AzadC and SAM+5AzadC treated breast cancer cells in RNA-Seq. The combination-treated cells shared more DEGs with SAM monotherapy (185 common genes) treated cells than 5AzadC monotherapy (33 common genes) treated cells. Importantly the combination therapy targeted 556 genes that were not targeted by either agent on its own, and these genes involved in pathways related to cancer growth and metastasis (Supplementary File 1, Figure S10). Thus, the molecular footprint of the combination therapy is not just an additive combination of either monotherapy; it affects hundreds of genes that would not be affected by either monotherapy suggesting a synergism between these two epigenetic modulators. These data provide a molecular rationale for combining these agents in the clinical setting.

Most phase I clinical trials using DNMTis for the treatment of solid tumors have not been successful [51], possibly due to the relatively short half-life of the agent as well as susceptibility to deamination and subsequent inactivation [52,53]. Hence, combining

5AzadC with other anti-cancer agents was proposed in the case of solid cancers [52]. Our data provide a different mechanism to counteract the adverse effects of 5AzadC monotherapy by using a unique molecularly and preclinically validated combination warranting further clinical testing.

Data availability

All data analyzed or generated during this study are either available within the main article or attached as supplementary files.

Authors' contributions

SAR and MS conceived the study. NM and AA carried out all relevant experimental procedures described in the manuscript. DC analyzed the methylation data. NM wrote the manuscript along with SAR and MS. All authors listed thoroughly read the manuscript and approved the final version.

Conflict of interests

MS is the founder of HKG Epitherapeutics and Montreal EpiTerapia. DC is also engaged by HKG Epitherapeutics and Montreal EpiTerapia. All other authors declare no competing financial interests.

Ethics approval

All *in vivo* procedures were performed in compliance with the protocol assessed and approved by the McGill University Facility Animal Care Committee (FACC).

Acknowledgement

This work was supported by a grant from the Canadian Institutes for Health Research 'MOP 130410' to SAR. and MS and 'PJT-156225' to SAR. NM is the recipient of Fonds de la recherche en santé du Québec (FRQS) Doctoral fellowship from the Government of Quebec, Canada.

References

1. **Cheishvili D, Boureau L, Szyf M.** DNA demethylation and invasive cancer: implications for therapeutics. *British journal of pharmacology*. 2015; 172: 2705-15.
2. **Baylin SB, Jones PA.** A decade of exploring the cancer epigenome—biological and translational implications. *Nature Reviews Cancer*. 2011; 11: 726.
3. **Mahmood N, Rabbani SA.** DNA methylation and breast cancer: Mechanistic and therapeutic applications. *Trends Cancer Res*. 2017; 12: 1-18.
4. **Mahmood N, Rabbani SA.** DNA Methylation Readers and Cancer: Mechanistic and Therapeutic Applications. *Frontiers in Oncology*. 2019; 9.
5. **Kantarjian H, Issa JPJ, Rosenfeld CS, Bennett JM, Albitar M, DiPersio J, Klimek V, Slack J, De Castro C, Ravandi F.** Decitabine improves patient outcomes in myelodysplastic syndromes. *Cancer*. 2006; 106: 1794-803.
6. **Kantarjian HM, Thomas XG, Dmoszynska A, Wierzbowska A, Mazur G, Mayer J, Gau J-P, Chou W-C, Buckstein R, Cermak J.** Multicenter, randomized, open-label, phase III trial of decitabine versus patient choice, with physician advice, of either supportive care or low-dose cytarabine for the treatment of older patients with newly diagnosed acute myeloid leukemia. *Journal of clinical oncology*. 2012; 30: 2670.
7. **Fenaux P, Mufti GJ, Hellstrom-Lindberg E, Santini V, Finelli C, Giagounidis A, Schoch R, Gattermann N, Sanz G, List A.** Efficacy of azacitidine compared with that of conventional care regimens in the treatment of higher-risk myelodysplastic syndromes: a randomised, open-label, phase III study. *The lancet oncology*. 2009; 10: 223-32.
8. **Kelly TK, De Carvalho DD, Jones PA.** Epigenetic modifications as therapeutic targets. *Nature biotechnology*. 2010; 28: 1069-78.
9. **Christman JK.** 5-Azacytidine and 5-aza-2'-deoxycytidine as inhibitors of DNA methylation: mechanistic studies and their implications for cancer therapy. *Oncogene*. 2002; 21: 5483-95.
10. **Jones PA, Issa J-PJ, Baylin S.** Targeting the cancer epigenome for therapy. *Nature Reviews Genetics*. 2016; 17: 630-641.
11. **Roulois D, Loo Yau H, Singhania R, Wang Y, Danesh A, Shen SY, Han H, Liang G, Jones PA, Pugh TJ, O'Brien C, De Carvalho DD.** DNA-Demethylating Agents Target Colorectal Cancer Cells by Inducing Viral Mimicry by Endogenous Transcripts. *Cell*. 2015; 162: 961-73.
12. **Giri AK, Aittokallio T.** DNMT Inhibitors Increase Methylation in the Cancer Genome. *Frontiers in Pharmacology*. 2019; 10.
13. **Qin T, Castoro R, El Ahdab S, Jelinek J, Wang X, Si J, Shu J, He R, Zhang N, Chung W.** Mechanisms of resistance to decitabine in the myelodysplastic syndrome. *PloS one*. 2011; 6: e23372.
14. **Ateeq B, Unterberger A, Szyf M, Rabbani SA.** Pharmacological inhibition of DNA methylation induces proinvasive and prometastatic genes in vitro and in vivo. *Neoplasia (New York, NY)*. 2008; 10: 266-78.

15. **Pakneshan P, Szyf M, Farias-Eisner R, Rabbani SA.** Reversal of the hypomethylation status of urokinase (uPA) promoter blocks breast cancer growth and metastasis. *Journal of Biological Chemistry*. 2004; 279: 31735-44.
16. **Bottiglieri T.** S-Adenosyl-L-methionine (SAMe): from the bench to the bedside—molecular basis of a pleiotrophic molecule. *The American journal of clinical nutrition*. 2002; 76: 1151S-7S.
17. **Mahmood N, Rabbani SA.** Targeting DNA Hypomethylation in Malignancy by Epigenetic Therapies. *Adv Exp Med Biol*.2019; 1164: 179-196.
18. **Spillmann M, Fava M.** S-adenosylmethionine (ademetionine) in psychiatric disorders. *Cns Drugs*. 1996; 6: 416-25.
19. **Mischoulon D, Fava M.** Role of S-adenosyl-L-methionine in the treatment of depression: a review of the evidence. *Am J Clin Nutr*. 2002; 76: 1158s-61s.
20. **Mahmood N, Cheishvili D, Arakelian A, Tanvir I, Ahmed H, Khan A-SP, Szyf M, Rabbani SA.** Methyl donor S-adenosylmethionine (SAM) supplementation attenuates breast cancer growth, invasion, and metastasis in vivo; therapeutic and chemopreventive applications. *Oncotarget*. 2018; 9: 5169-83.
21. **Parashar S, Cheishvili D, Arakelian A, Hussain Z, Tanvir I, Khan HA, Szyf M, Rabbani SA.** S-adenosylmethionine blocks osteosarcoma cells proliferation and invasion in vitro and tumor metastasis in vivo: therapeutic and diagnostic clinical applications. *Cancer medicine*. 2015; 4: 732-44.
22. **Shukeir N, Stefanska B, Parashar S, Chik F, Arakelian A, Szyf M, Rabbani SA.** Pharmacological methyl group donors block skeletal metastasis in vitro and in vivo. *British journal of pharmacology*. 2015; 172: 2769-81.
23. **Stefanska B, Huang J, Bhattacharyya B, Suderman M, Hallett M, Han Z-G, Szyf M.** Definition of the landscape of promoter DNA hypomethylation in liver cancer. *Cancer research*. 2011; 71: 5891-903.
24. **Chik F, Machnes Z, Szyf M.** Synergistic anti-breast cancer effect of a combined treatment with the methyl donor S-adenosyl methionine and the DNA methylation inhibitor 5-aza-2′-deoxycytidine. *Carcinogenesis*. 2013; 35: 138-44.
25. **Martin MD, Carter KJ, Jean-Philippe SR, Chang M, Mobashery S, Thiolloy S, Lynch CC, Matrisian LM, Fingleton B.** Effect of ablation or inhibition of stromal matrix metalloproteinase-9 on lung metastasis in a breast cancer model is dependent on genetic background. *Cancer Res*. 2008; 68: 6251-9.
26. **Prichard MN, Shipman C, Jr.** A three-dimensional model to analyze drug-drug interactions. *Antiviral research*. 1990; 14: 181-205.
27. **Mahmood N, Arakelian A, Khan HA, Tanvir I, Mazar AP, Rabbani SA.** uPAR antibody (huATN-658) and Zometa reduce breast cancer growth and skeletal lesions. *Bone Research*. 2020; 8: 1-12.
28. **Chen MY, Liao WS, Lu Z, Bornmann WG, Hennessey V, Washington MN, Rosner GL, Yu Y, Ahmed AA, Bast RC, Jr.** Decitabine and suberoylanilide hydroxamic acid (SAHA) inhibit growth of ovarian cancer cell lines and xenografts while inducing expression of imprinted tumor suppressor genes, apoptosis, G2/M arrest, and autophagy. *Cancer*. 2011; 117: 4424-38.

29. **Ghosh S, Sharma G, Travers J, Kumar S, Choi J, Jun HT, Kehry M, Ramaswamy S, Jenkins D.** TSR-033, a Novel Therapeutic Antibody Targeting LAG-3, Enhances T-Cell Function and the Activity of PD-1 Blockade In Vitro and In Vivo. *Mol Cancer Ther*. 2019; 18: 632-41.
30. **Dobin A, Davis CA, Schlesinger F, Drenkow J, Zaleski C, Jha S, Batut P, Chaisson M, Gingeras TR.** STAR: ultrafast universal RNA-seq aligner. *Bioinformatics*. 2013; 29: 15-21.
31. **Trapnell C, Roberts A, Goff L, Pertea G, Kim D, Kelley DR, Pimentel H, Salzberg SL, Rinn JL, Pachter L.** Differential gene and transcript expression analysis of RNA-seq experiments with TopHat and Cufflinks. *Nature protocols*. 2012; 7: 562-78.
32. **Teschendorff AE, Marabita F, Lechner M, Bartlett T, Tegner J, Gomez-Cabrero D, Beck S.** A beta-mixture quantile normalization method for correcting probe design bias in Illumina Infinium 450 k DNA methylation data. *Bioinformatics*. 2013; 29: 189-96.
33. **Morris TJ, Butcher LM, Feber A, Teschendorff AE, Chakravarthy AR, Wojdacz TK, Beck S.** ChAMP: 450k Chip Analysis Methylation Pipeline. *Bioinformatics*. 2014; 30: 428-30.
34. **Parashar S, Cheishvili D, Mahmood N, Arakelian A, Tanvir I, Khan HA, Kremer R, Mihalcioiu C, Szyf M, Rabbani SA.** DNA methylation signatures of breast cancer in peripheral T-cells. *BMC Cancer*. 2018; 18: 574.
35. **Smyth GK.** Limma: linear models for microarray data. In: R. Gentleman VC, S. Dudoit, R. Irizarry, W. Huber editor. Bioinformatics and Computational Biology Solutions using R and Bioconductor. New York: Springer,, 2005. p. 397-420.
36. **Dayeh T, Volkov P, Salo S, Hall E, Nilsson E, Olsson AH, Kirkpatrick CL, Wollheim CB, Eliasson L, Ronn T, Bacos K, Ling C.** Genome-wide DNA methylation analysis of human pancreatic islets from type 2 diabetic and non-diabetic donors identifies candidate genes that influence insulin secretion. *PLoS Genet*. 2014; 10: e1004160.
37. **Lubecka K, Kurzava L, Flower K, Buvala H, Zhang H, Teegarden D, Camarillo I, Suderman M, Kuang S, Andrisani O, Flanagan JM, Stefanska B.** Stilbenoids remodel the DNA methylation patterns in breast cancer cells and inhibit oncogenic NOTCH signaling through epigenetic regulation of MAML2 transcriptional activity. *Carcinogenesis*. 2016; 37: 656-68.
38. **Rabbani SA, Ateeq B, Arakelian A, Valentino ML, Shaw DE, Dauffenbach LM, Kerfoot CA, Mazar AP.** An anti-urokinase plasminogen activator receptor antibody (ATN-658) blocks prostate cancer invasion, migration, growth, and experimental skeletal metastasis in vitro and in vivo. *Neoplasia*. 2010; 12: 778-88.
39. **Cheishvili D, Chik F, Li CC, Bhattacharya B, Suderman M, Arakelian A, Hallett M, Rabbani SA, Szyf M.** Synergistic effects of combined DNA methyltransferase inhibition and MBD2 depletion on breast cancer cells; MBD2 depletion blocks 5-aza-2′-deoxycytidine-triggered invasiveness. *Carcinogenesis*. 2014; 35: 2436-46.

40. **Walsh JG, Cullen SP, Sheridan C, Lüthi AU, Gerner C, Martin SJ.** Executioner caspase-3 and caspase-7 are functionally distinct proteases. *Proceedings of the National Academy of Sciences*. 2008; 105: 12815-9.
41. **Tripathi S, Pohl MO, Zhou Y, Rodriguez-Frandsen A, Wang G, Stein DA, Moulton HM, DeJesus P, Che J, Mulder LC.** Meta-and orthogonal integration of influenza "OMICs" data defines a role for UBR4 in virus budding. *Cell host & microbe*. 2015; 18: 723-35.
42. **Hiraki M, Suzuki Y, Alam M, Hinohara K, Hasegawa M, Jin C, Kharbanda S, Kufe D.** MUC1-C Stabilizes MCL-1 in the Oxidative Stress Response of Triple-Negative Breast Cancer Cells to BCL-2 Inhibitors. *Scientific Reports*. 2016; 6: 26643.
43. **Huang L, Chen D, Liu D, Yin L, Kharbanda S, Kufe D.** MUC1 Oncoprotein Blocks Glycogen Synthase Kinase 3β–Mediated Phosphorylation and Degradation of β-Catenin. *Cancer Research*. 2005; 65: 10413-22.
44. **Solzak JP, Atale RV, Hancock BA, Sinn AL, Pollok KE, Jones DR, Radovich M.** Dual PI3K and Wnt pathway inhibition is a synergistic combination against triple negative breast cancer. *NPJ breast cancer*. 2017; 3: 17.
45. **Zheng G, Ma Y, Zou Y, Yin A, Li W, Dong D.** HCMDB: the human cancer metastasis database. *Nucleic acids research*. 2018; 46: D950-D5.
46. **Kramer A, Green J, Pollard J, Jr., Tugendreich S.** Causal analysis approaches in Ingenuity Pathway Analysis. *Bioinformatics*. 2014; 30: 523-30.
47. **Gu Y, Zou YM, Lei D, Huang Y, Li W, Mo Z, Hu Y.** Promoter DNA methylation analysis reveals a novel diagnostic CpG-based biomarker and RAB25 hypermethylation in clear cell renel cell carcinoma. *Scientific Reports*. 2017; 7: 14200.
48. **Lourenço AR, Coffer PJ.** SOX4: joining the master regulators of epithelial-to-mesenchymal transition? *Trends in cancer*. 2017; 3: 571-82.
49. **Schroeder JA, Adriance MC, Thompson MC, Camenisch TD, Gendler SJ.** MUC1 alters beta-catenin-dependent tumor formation and promotes cellular invasion. *Oncogene*. 2003; 22: 1324-32.
50. **Yu F, Li J, Chen H, Fu J, Ray S, Huang S, Zheng H, Ai W.** Kruppel-like factor 4 (KLF4) is required for maintenance of breast cancer stem cells and for cell migration and invasion. *Oncogene*. 2011; 30: 2161-72.
51. **Aparicio A, Weber JS.** Review of the clinical experience with 5-azacytidine and 5-aza-2'-deoxycytidine in solid tumors. *Current opinion in investigational drugs (London, England : 2000)*. 2002; 3: 627-33.
52. **Ahuja N, Easwaran H, Baylin SB.** Harnessing the potential of epigenetic therapy to target solid tumors. *The Journal of Clinical Investigation*. 2014; 124: 56-63.
53. **Momparler RL, Rossi M, Bouchard J, Vaccaro C, Momparler LF, Bartolucci S.** Kinetic interaction of 5-AZA-2'-deoxycytidine-5'-monophosphate and its 5'-triphosphate with deoxycytidylate deaminase. *Molecular Pharmacology*. 1984; 25: 436-40.

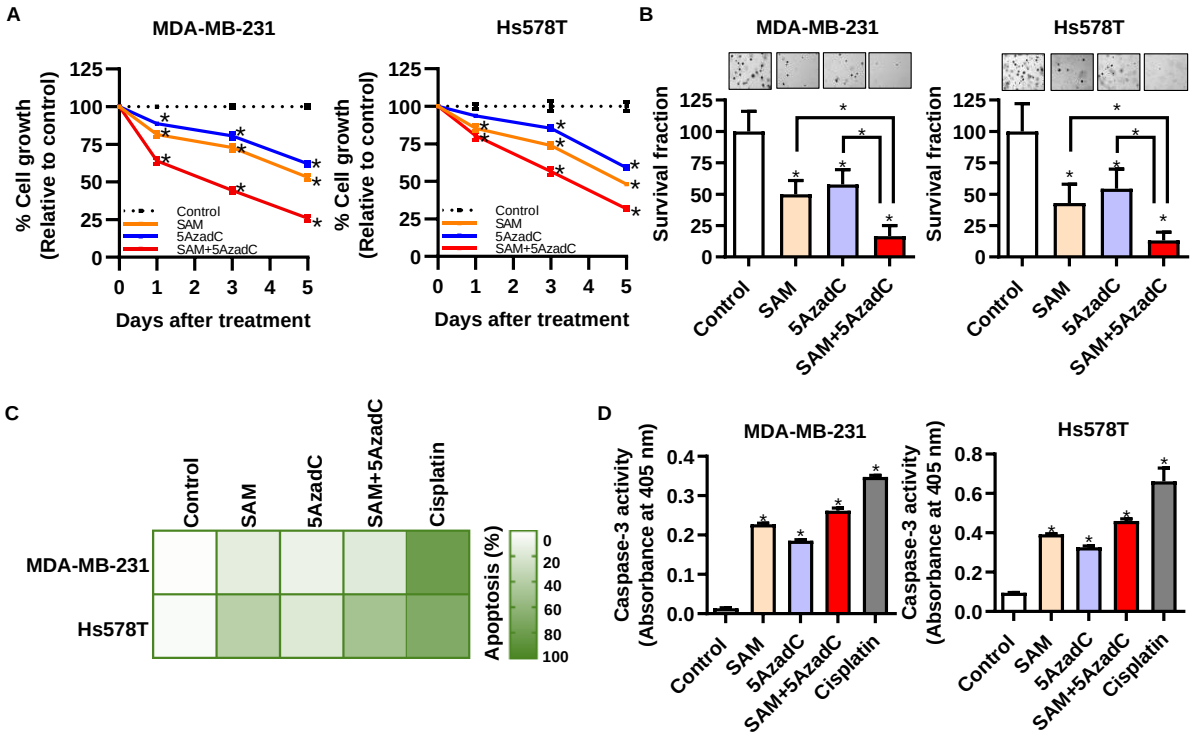

Figure 1: Effect of SAM, 5AzadC, and their combination on cell proliferation, colony formation, and apoptosis *in vitro*.

(A) MDA-MB-231 and Hs578T were treated with vehicle only (as control), SAM (200.0 µM), 5AzadC (1.0 µM) and SAM+5AzadC every second day for a period of six days, and the percentage change in cell proliferation relative to the control group at different time points is shown as line graphs. **(B)** The total number of colonies in each treatment group were directly counted under a light microscope and plotted as bar graphs. **(C)** Heatmap showing the average levels of apoptosis in control and different treatment groups. As a positive control for apoptosis, both cell lines were treated with 20 µM cisplatin. **(D)** Caspase-3 enzyme activity was measured from the cell lysates of control and different treatment groups. Results are represented as the mean ± SEM. Statistical analysis was done using ANOVA followed by *post hoc* Tukey's test, and significant differences are shown by asterisks (*$P < 0.05$).

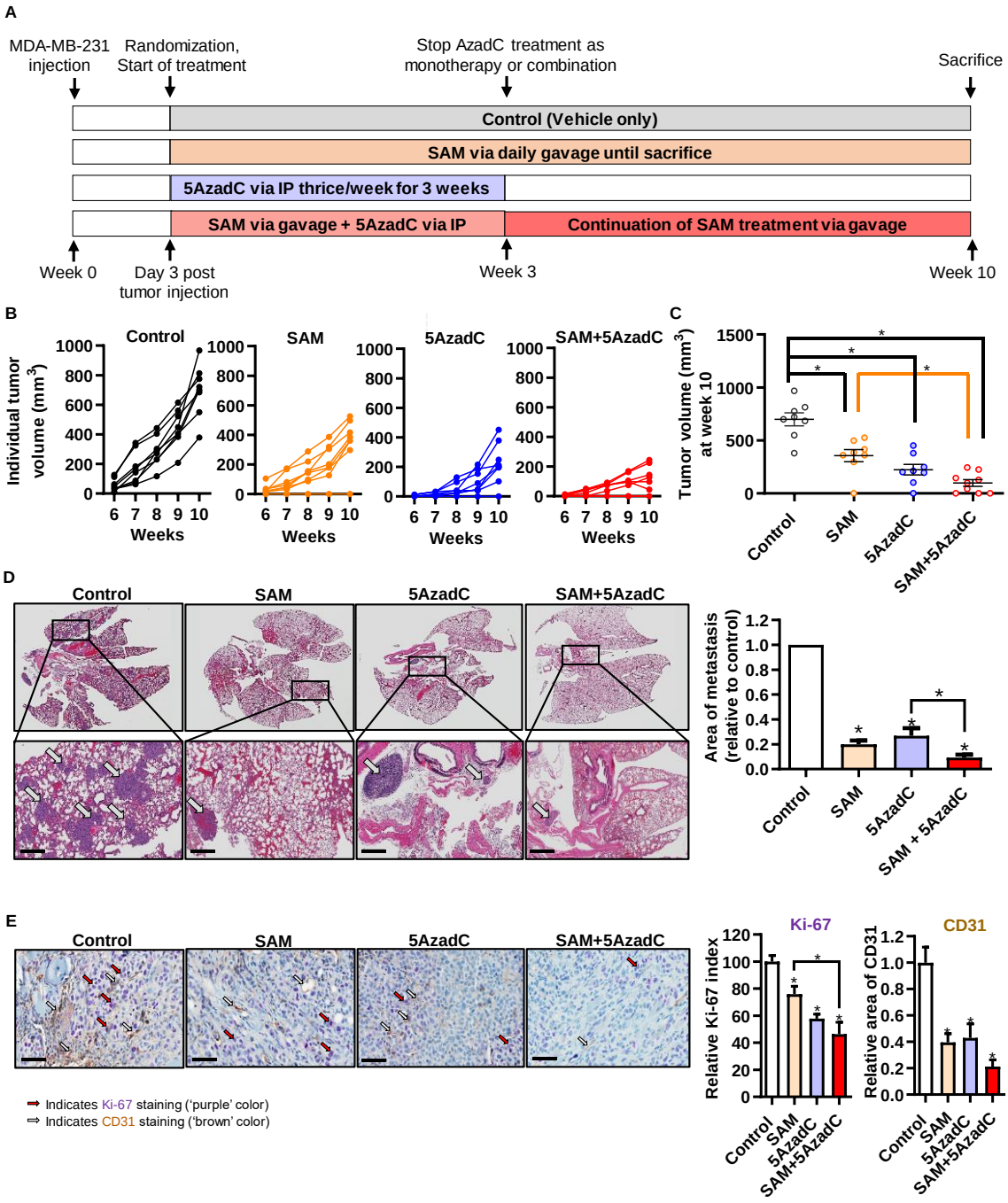

Figure 2: Effect of SAM, 5AzadC, and their combination on MDA-MB-231 xenograft tumor growth and lung metastasis.

(A) Schematic of the treatment protocol. (**B)** The tumor growth kinetics of individual animals from each group were plotted as line graphs. (**C)** The average tumor volume in

each group of animals at the time of experimental endpoint (10 weeks after the initial injection of tumor cells). Results are represented as the mean ± SEM of at least eight animals in each group. (*$P < 0.05$). **(D)** Representative photomicrographs of whole lung sections from each group (top panel). The bottom panel shows a higher magnification image from a region of micrometastases [scale bar size =500 μm]**.** The average areas of metastases were plotted as a bar graph (n=3 animals/group). **(E)** Formalin-fixed primary breast tumors were double immunostained with Ki-67 and CD31 antibodies (n=3 animals/group). The photomicrograph of five randomly selected fields from each sample was analyzed and represented as bar graphs. Results are shown as the mean ± SEM. Statistical analysis was done using ANOVA followed by *post hoc* Tukey's test, and significant differences are shown by asterisks (*$P < 0.05$).

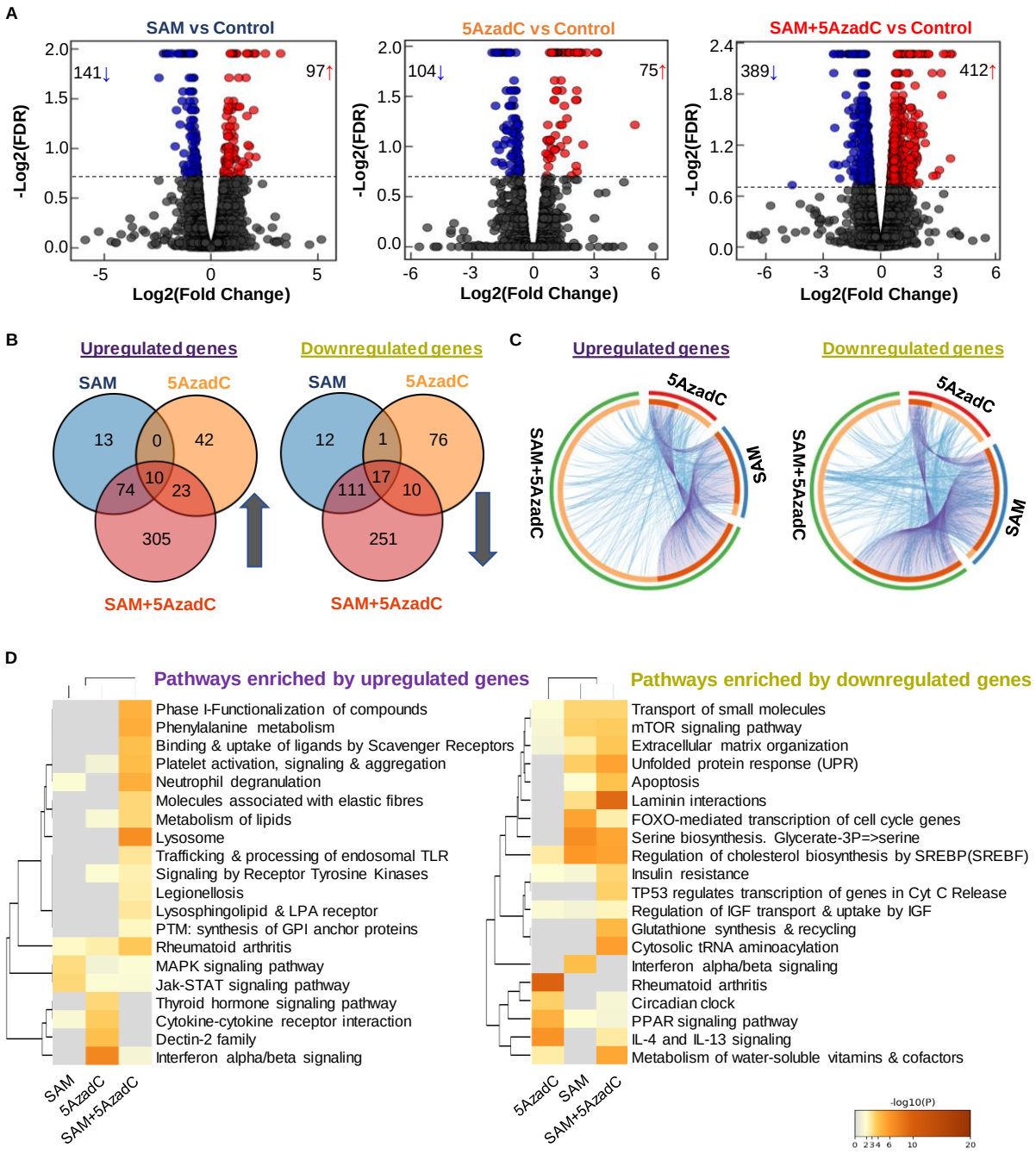

Figure 3: Transcriptome analysis of MDA-MB-231 cells.

(A) The volcano plot of the DEGs obtained from global transcriptome analyses in each treatment group relative to vehicle-treated control MDA-MB-231 cells are shown (n=3/group). **(B)** Venn diagrams representing the overlap of DEGs among different treatment groups. The upregulated and downregulated genes were analyzed and

represented separately. **(C)** The circos plot depicting the functional overlap between the up- and downregulated DEGs in each treatment group. On the arc, there is a spot for each of the genes showing significant down- or upregulation (for all three treatment groups). The darker orange indicates the genes common in multiple groups, while the lighter orange indicates the unique genes for a particular treatment. The purple (criss-crossed) lines represent the genes that are common in different groups, while the blue lines are given for the genes with similar functions. **(D)** Comparative heatmap of the pathways enriched by the up- and downregulated genes in different treatment groups, as determined by Metascape [41].

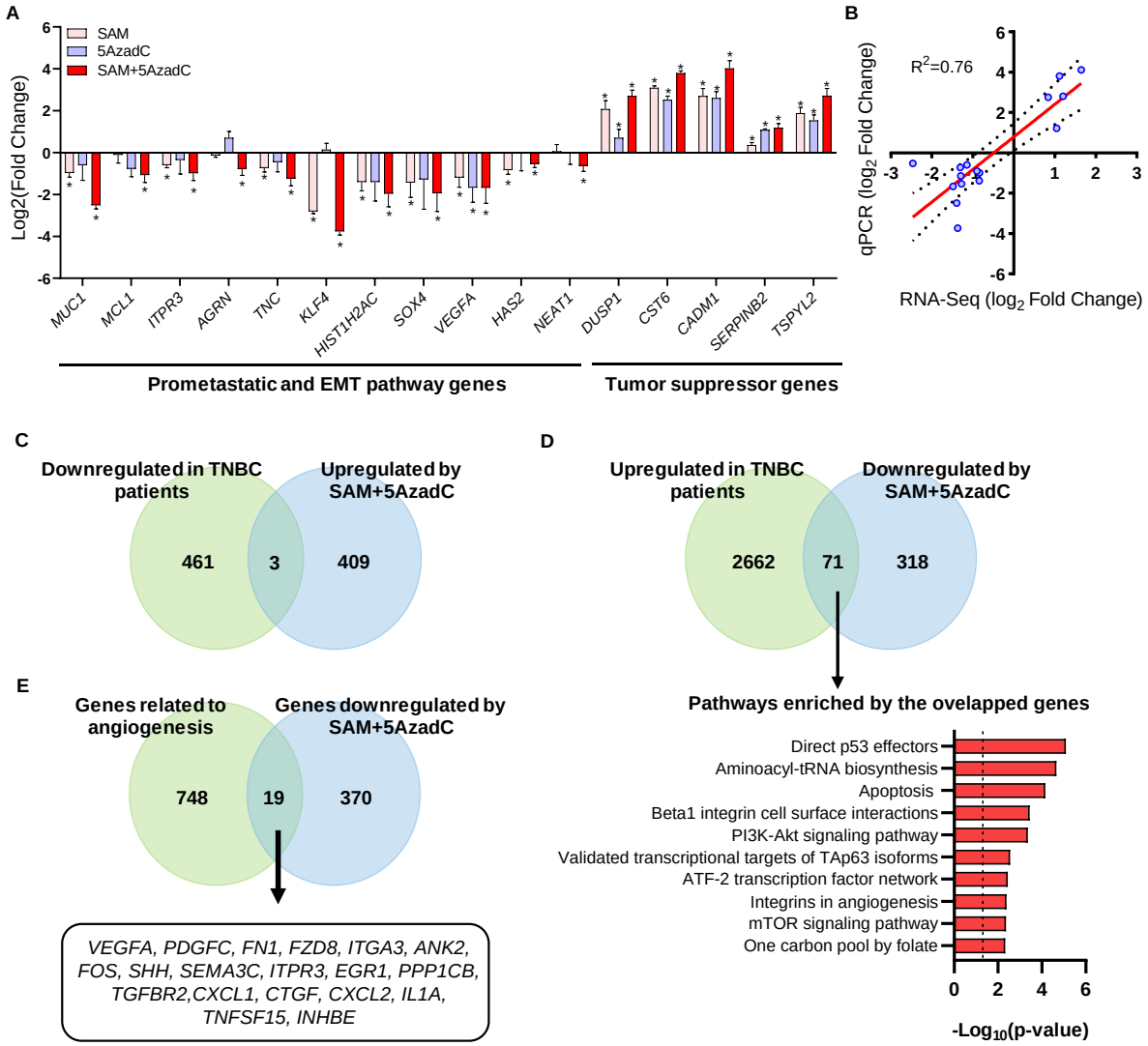

Figure 4: Validation of selected genes that showed significant differential expression following SAM+5AzadC combination treatment.

(A) qPCR validation of selected cancer-related genes obtained from RNA-Sequencing. Results are represented as the mean ± SEM. (*P < 0.05; n=3/group). **(B)** The correlation coefficient between RNA-Seq (in x-axis) and qPCR (in y-axis) data [presented as Log_2(Fold Change)] was performed using a Pearson test was found to be 0.75 with a p<0.001. **(C-D)** Comparison of the significantly up or downregulated genes upon SAM+5AzadC treatment with differentially expressed genes obtained from the transcriptome analyses of TNBC patients showed an overlap of 3 and 71 genes,

respectively. A pathway analysis [bottom panel of **(D)**] of 71 overlapped genes that were upregulated in TNBC but downregulated in the combination showed involvement of molecular signatures related to cancer growth, metastasis, and apoptosis. **(E)** A comparison of the significantly downregulated genes upon SAM+5AzadC treatment with the genes involved in angiogenesis (from the Metascape database) showed a significant overlap of 19 genes.

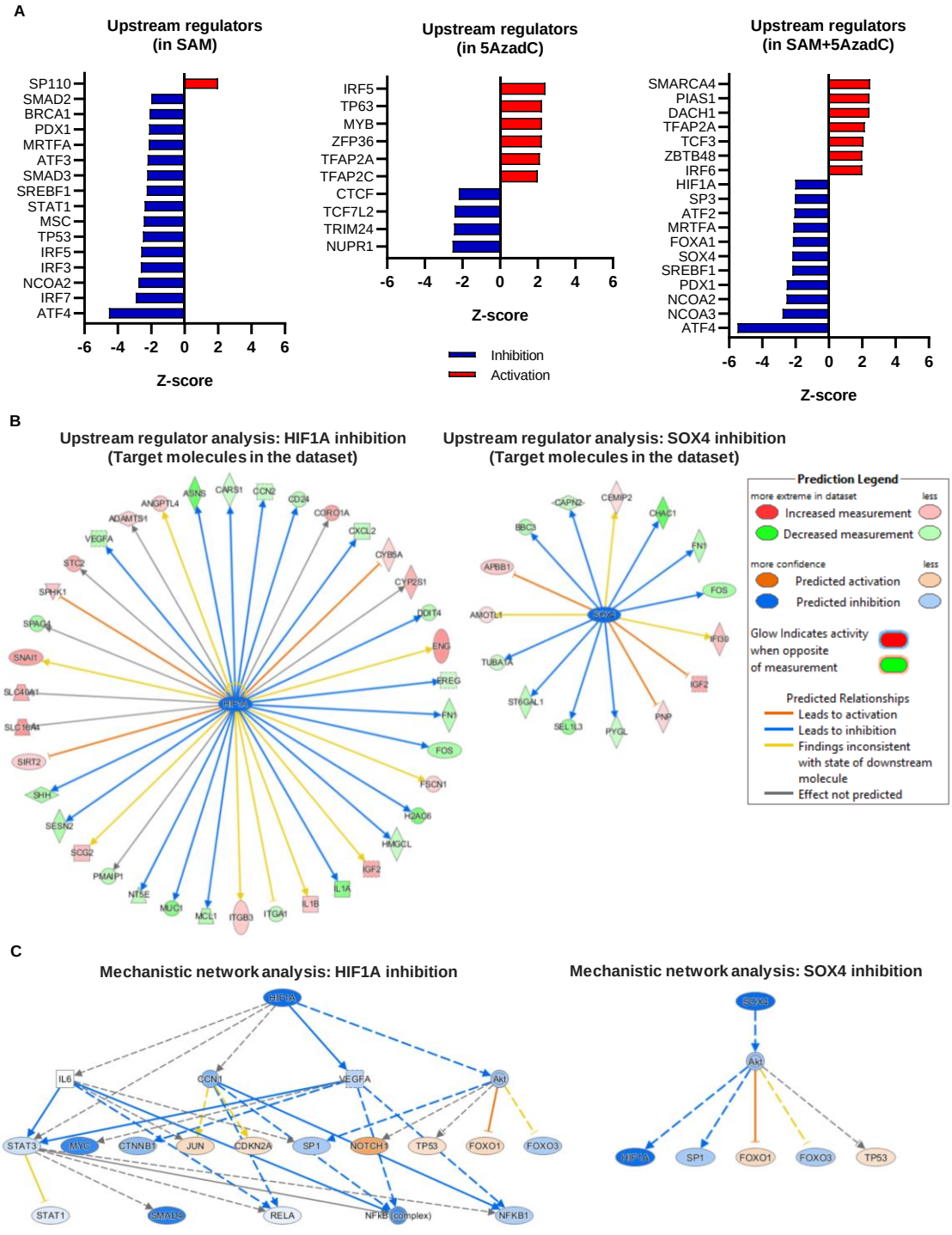

Figure 5: Upstream transcription regulator analyses.

(A) IPA tool predicted list of significantly activated and inhibited upstream transcription regulators in each treatment group are shown as bar graphs. A z-score greater than 2.0 defines significant activation of the node, whereas a z-score less than 2.0 defines inhibition. **(B)** HIF1A and SOX4 are among the several transcription regulators predicted to be inhibited by SAM+5AzadC treatment. Target molecules of HIF1A and SOX4 from the list of DEGs upon SAM+5AzadC treatment are shown. **(C)** Mechanistic pathway analyses of HIF1A and SOX4, according to the IPA knowledge base, show the network of molecular targets that are possibly affected by the combination treatment.

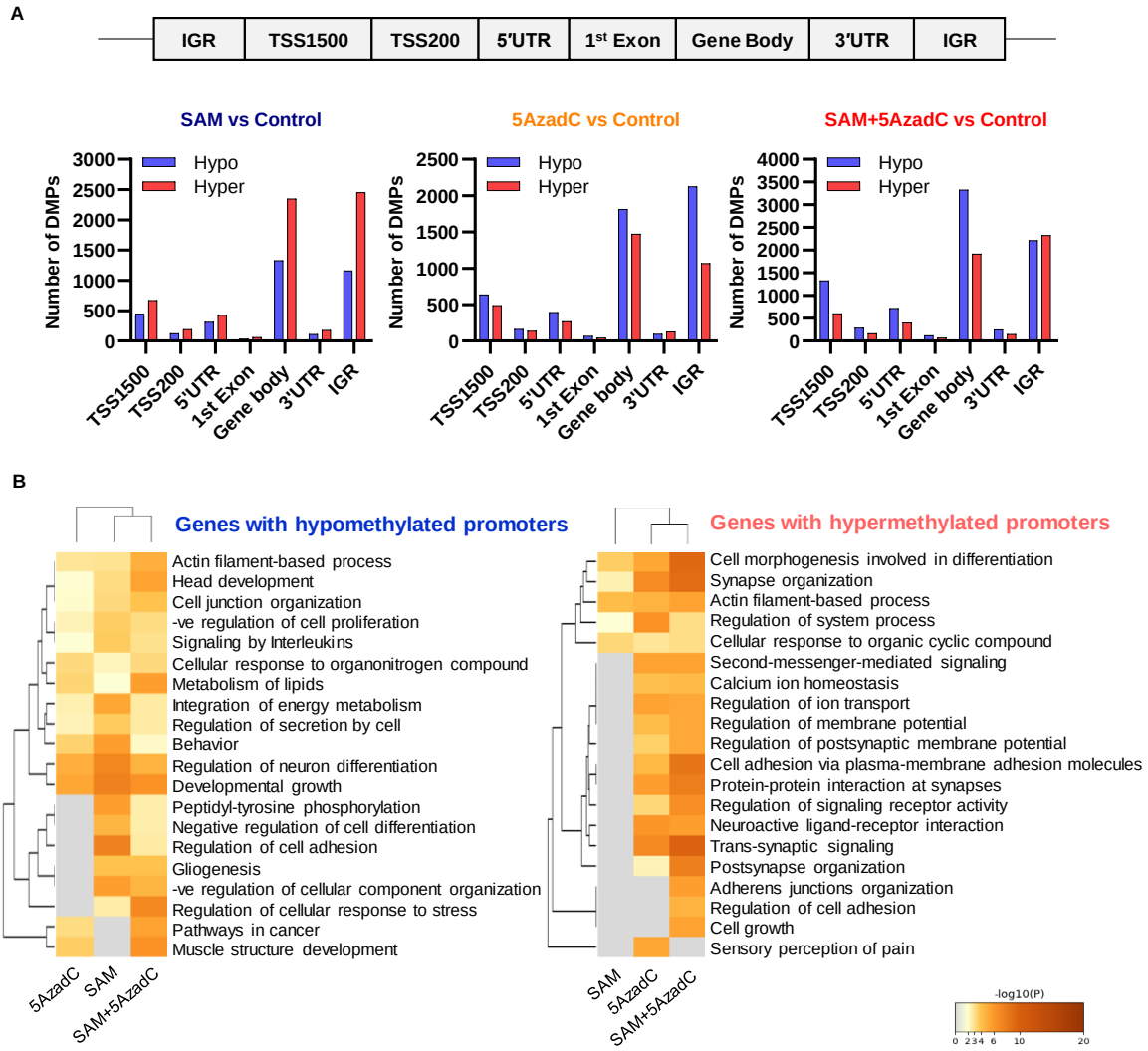

Figure 6: Methylome analyses of MDA-MB-231 cells.

(A) Genome-wide distribution of the differentially methylated CGs from each treatment (n=2/group). Here, UTR: Untranslated Region; IGR: Intergenic Region; TSS: Transcription Start Site. **(B)** Pathway enrichment analyses of the genes associated with differentially methylated probes near the promoter regions following treatments with SAM, 5AzadC, and SAM+5AzadC.

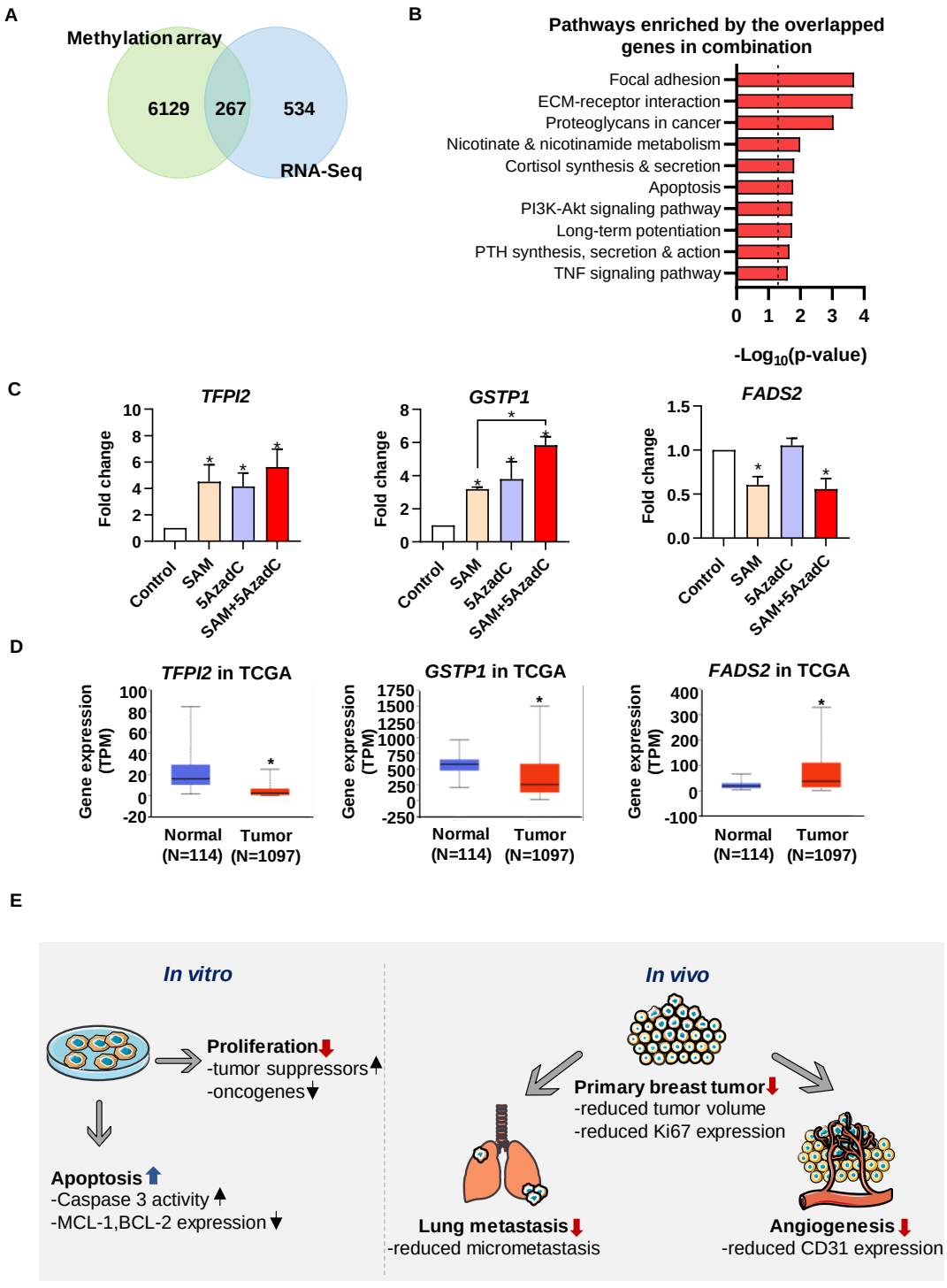

Figure 7: Integrative analyses of MDA-MB-231 methylome and transcriptome.

(A) Venn diagram depicting the overlap of genes that showed hypomethylation-mediated inactivation and hypermethylation-mediated activation upon the combination therapy treatment in genome-wide methylation and RNA-Seq datasets. **(B)** Pathways enriched by the overlapping genes from the methylation array and RNA-Seq. **(C)** qPCR validation of several overlapped genes (*TFPI2*, *GSTP1*, and *FADS2*) in response to the indicated treatments. Results are shown as the mean ± SEM. (*P < 0.05; n=3/group). **(D)** The expression of *TFPI2* and *GSTP1* genes are downregulated, while *FADS2* expression is upregulated in the TCGA transcriptome datasets of breast cancer patients. **(E)** Schematic summarization of the SAM+5AzadC mediated anti-cancer effects, according to the results of this study.

Supplementals for Chapter 3

Supplementary File 1

Supplementary Table S1: The primers used in this study are listed below [1-16]

Gene Name		**Sequences used for qPCR (5'→ 3')**
MUC1	For	CTGCTCCTCACAGTGCTTACAGTTG
	Rev	TGAACCGGGGCTGTGGCTGG
MCL1	For	CCAAGAAAGCTGCATCGAACCAT
	Rev	CAGCACATTCCTGATGCCACCT
DUSP1	For	GGCCCCGAGAACAGACAAA
	Rev	GTGCCCACTTCCATGACCAT
KLF4	For	GTGCCCCGAATAACAGCTCA
	Rev	TTCTCACCTGTGTGGGTTCG
SOX4	For	CCAAATCTTTTGGGGACTTTT
	Rev	CTGGCCCCTCAACTCCTC
ITPR3	For	TATGCAGTTTCGGGACCACC
	Rev	TGCCCTTGTACTCGTCACAC
AGRN	For	CCTGACCCTCAGCTGGCCCT
	Rev	AGATACCCAGGCAGGCGGCA
TSPYL2	For	AGGCACTGGAGGATATTCAG
	Rev	GAAGGGTCTTCGCATCTGGAT
TNC	For	AAGTGAACCTGTCTCAGGGTCATT
	Rev	GCTGTCACCAGGCCAGATG
CADM1	For	ATGGCGAGTGTAGTGCTGC
	Rev	GATCACTGTCACGTCTTTCGT
FADS2	For	ACAAGGATCCCGATGTGAAC
	Rev	TTCGTGCTGGTGATTGTAGG
TFPI2	For	GTCGATTCTGCTGCTTTTCC
	Rev	CAGCTCTGCGTGTACCTGTC
HIST1H2AC	For	GACGAGGAGCTCAACAAACTG
	Rev	ACCTGTCAAATCACTTGCCC
HAS2	For	TTATGGGCAGCCAATGTA
	Rev	ACTTGCTCCAACGGGTCT
CST6	For	CAGGGGCGCAGCAGGAGAAG
	Rev	GCCCACGGACCTGAAGTGCC
NEAT1	For	CCAGTTTTCCGAGAACCAAA
	Rev	ATGCTGATCTGCTGCGTATG
VEGF	For	CCTTGCTGCTGCTCTACCTCCAC
	Rev	CCATGAACTTCACCACTTCG
SERPINB2	For	GAAACGCACTTTCGTGGCAG
	Rev	ACAGCTGTGAACTTGGGCAG

GSTP1	For Rev	GAGGACCTCCGCTGCAAATA CAGCAGGGTCTCAAAAGGCT
GAPDH	For Rev	TGCACCACCAACTGCTTA AGAGGCAGGGATGATGTTC

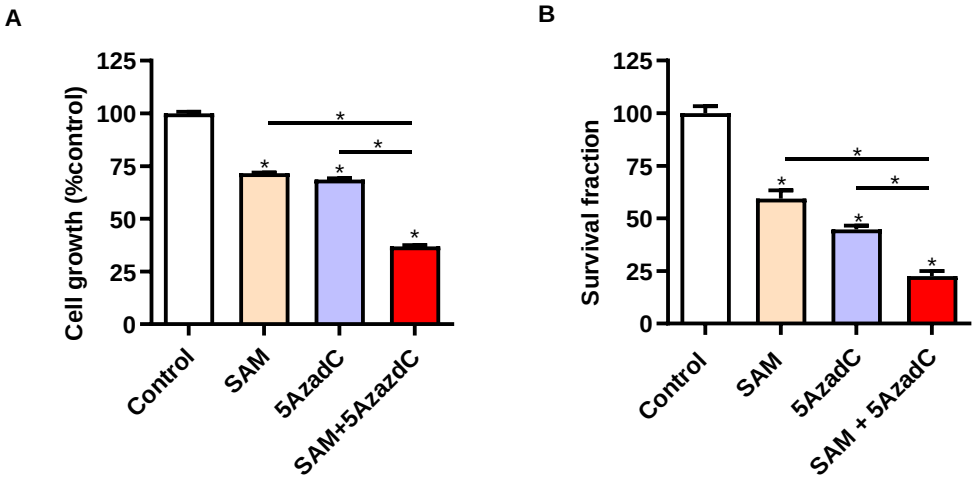

Supplementary Figure S1: Effect of SAM, 5AzadC, and their combination on PyMT-R221A breast cancer cell proliferation and colony formation *in vitro*. (A) Murine PyMT-R221A (luminal B subtype) seeded onto 6-well cell-culture grade plates were treated with vehicle only (as control), SAM (200.0 µM), 5AzadC (1.0 µM) and SAM+5AzadC every second day for a period of six days, and the cell proliferation at experimental endpoint was determined through direct cell counting using a Coulter counter. **(B)** At the end of the usual treatment regimen, $5x10^3$ cells from each group were plated in triplicates in each well of six-well plates containing soft agar for a colony assay. The growth medium was replenished every 2-3 days over the next couple of weeks, and the total number of colonies in each well were directly counted under a light microscope and plotted as a bar graph. Results are represented as the mean ± SEM of three independent experiments. Statistical analysis was done using ANOVA followed by *post hoc* Tukey's test, and significant differences are shown by asterisks (*$P < 0.05$).

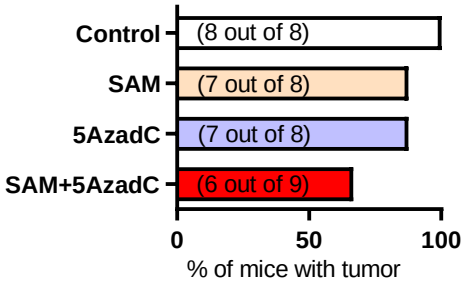

Supplementary Figure S2: Effect of SAM, 5AzadC, and their combination on tumor incidence in NOD-SCID mouse inoculated with MDA-MB-231 cells. While all animals in the control group developed mammary tumors, the percentage of mice with palpable tumors by the experimental endpoint at week 10 markedly decreased in the SAM+5AzadC combination-treated groups. Such an effect on reduced tumor incidence in the combination arm was better than either of the monotherapy treated arms.

Supplementary Table S2: The toxicity profile of the different therapeutic regiment used *in vivo* was measured through biochemical analyses from blood samples. The results are shown as mean ± SEM from three different mice per group. Here, BUN: Blood urea nitrogen; ALT: Alanine aminotransferase; CK: Creatinine kinase

Parameter	**Control**	**SAM**	**5AzadC**	**SAM+5AzadC**
Total protein (g/L)	39 ± 0.82	41 ± 0.94	41.67 ± 1.36	45 ± 0.47
Albumin (g/L)	20.67 ± 0.72	21 ± 0.82	22.67 ± 0.27	23 ± 0.47
Glucose (mmol/L)	15.11 ± 0.83	12.93 ± 0.96	15.33 ± 1.4	10.07 ± 0.54
BUN Urea (mmol/L)	6.93 ± 0.25	5.53 ± 0.19	5.7 ± 0.39	7.23 ± 1.08
Creatinine (µmol/L)	10.33 ± 0.27	9.67 ± 0.54	10 ± 0.47	12.33 ± 1.96
Total Bilirubin (µmol/L)	4.67 ± 0.54	3.67 ± 0.54	4.67 ± 0.27	4.67 ± 0.72
ALT (U/L)	35 ± 1.89	29.67 ± 1.19	31 ± 1.25	38.33 ± 3.95
CK (U/L)	306 ± 109.7	349 ± 128.55	450 ± 148.14	435.67 ± 150.18
Sodium (mmol/L)	156.67 ± 3.84	152.67 ± 2.23	152.33 ± 1.91	152.33 ± 0.72
Chloride (mmol/L)	115.33 ± 1.36	118 ± 1.7	116 ± 0.82	115.67 ±1.09

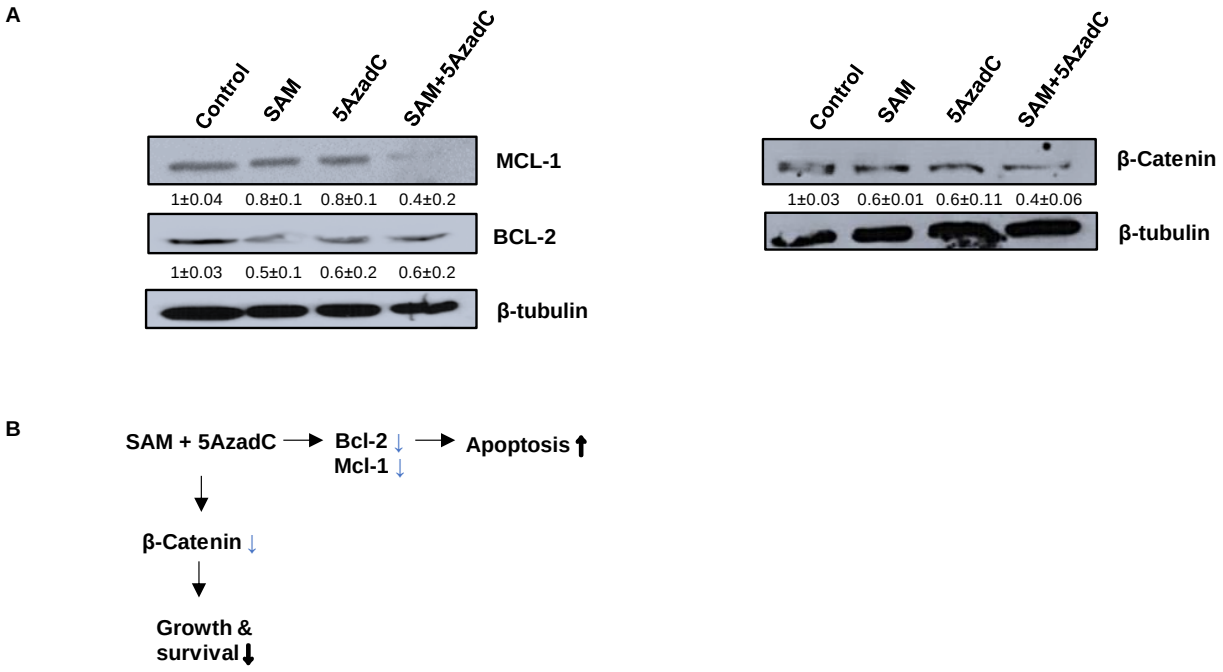

Supplementary Figure S3: Effect of SAM, 5AzadC, and their combination on pro-proliferative and anti-apoptotic factors. (A) Representative western blot of control, SAM, 5AzadC, and combination-treated MDA-MB-231 cells using antibodies against MCl-1, BCl-1, β-Catenin proteins. The β-tubulin expression was used as a loading control and normalization of the samples during band intensity measurement. The normalized densitometric value of the bands were measured by ImageJ (Fiji plugin) and shown as mean ± SEM of two independent experiments. **(B)** Schematic diagram of the functional pathways affected by the SAM+5AzadC combination.

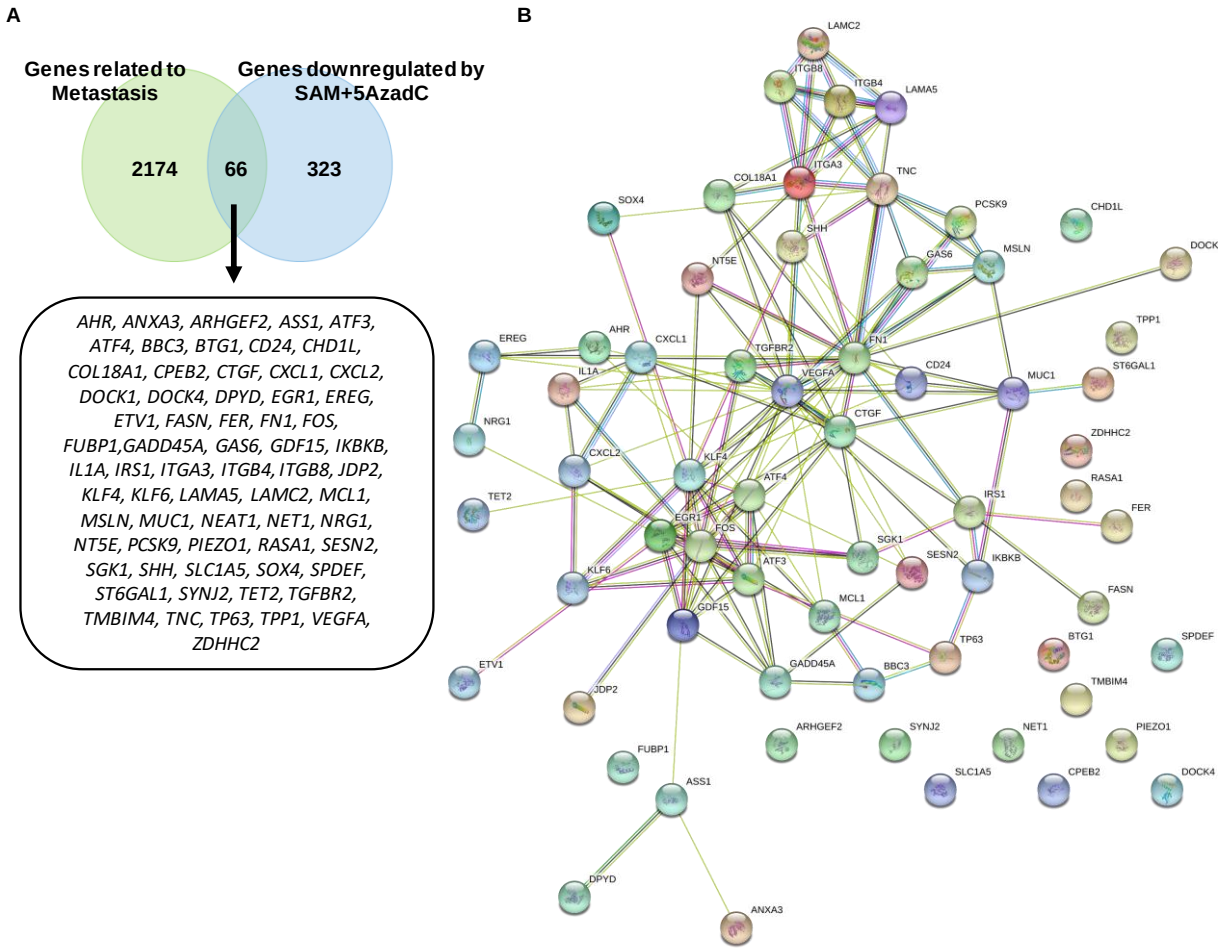

Supplementary Figure S4: (A) Comparison of the significantly downregulated genes upon SAM+5AzadC treatment with the list of metastatic genes obtained from the human cancer metastasis database showed a significant overlap of 66 genes. **(B)** A string network analysis was performed from the genes that showed overlap in **(A)**.

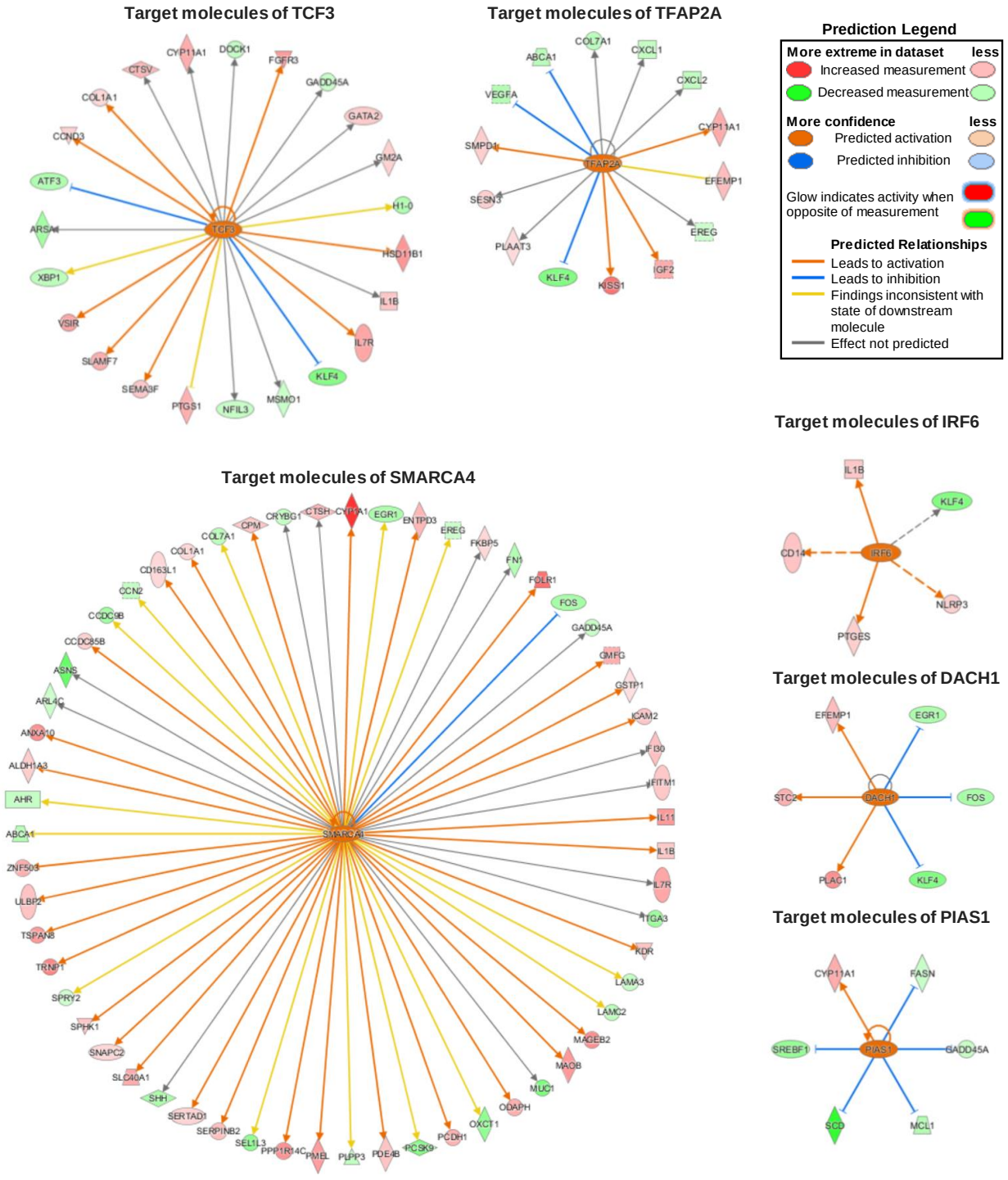

Supplementary Figure S5: Target molecules of the upstream transcription regulators that are significantly activated by SAM+5AzadC treatment according to the IPA tool.

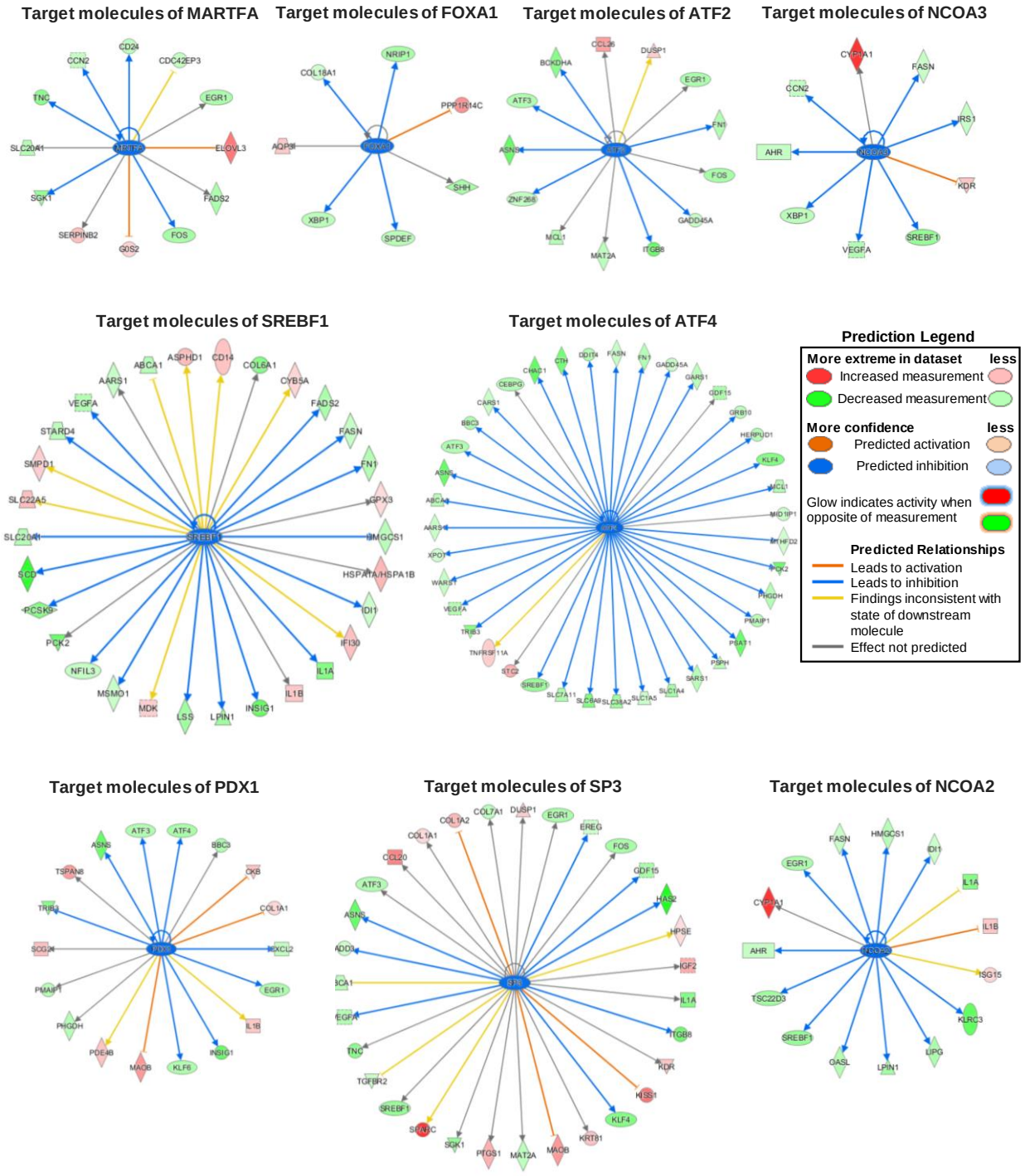

Supplementary Figure S6: Target molecules of several upstream transcription regulators that are significantly inhibited by SAM+5AzadC treatment according to the IPA tool.

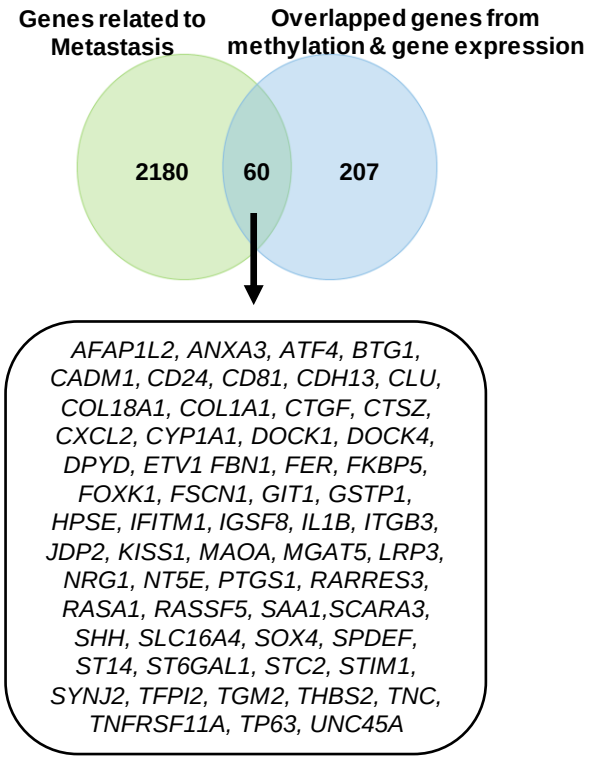

Supplementary Figure S7: Comparison of the 267 genes obtained from the integrative analysis of DNA methylation and RNA expression (in SAM+5AzadC group) with the list of metastatic genes obtained from the human cancer metastasis database showed a significant overlap of 60 genes.

Supplementary Table S3: List of overlapped genes that showed significant changes in the promoter methylation-mediated alteration of gene expression

Genes with promoter hypomethylation-mediated upregulation		Genes with promoter hypermethylation-mediated downregulation
TNFRSF11A	*LOC101927476*	*PHGDH*
PRSS35	*CYP1A1*	*NRIP1*
NIPAL3	*CTSZ*	*LZTFL1*
NINJ1	*LGMN*	*UFSP2*
AFAP1L2	*SCAND1*	*ACTR1B*
OSGIN1	*MAP1S*	*TRNT1*
TFPI2	*RARRES3*	*SEC31B*
SHROOM3	*KISS1*	*CALHM2*
VTN	*CAPN5*	*NAPRT*
LYPD6B	*FAM8A1*	*ANKRD29*
DDAH1	*MAP6D1*	*TMEM67*
SCG2	*MAP2K3*	*CAB39L*
CD81	*SLAMF7*	*SLC16A7*
CCDC106	*HS6ST1*	*SLC29A2*
GSTP1	*MFAP1*	*FADS2*
SECTM1	*MAGEB2*	
SLC16A4	*SH2D2A*	
SAA1	*LY6E*	
LPPR2	*ITM2C*	
SELO	*CHRNA1*	
SCARF2	*TPST2*	
CCND3	*ICAM2*	
EXTL3		

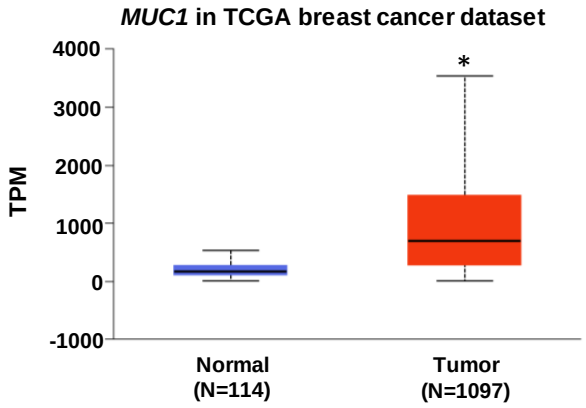

Supplementary Figure S8: The *MUC1* gene expression is significantly elevated in human breast tumor samples relative to the normal samples. Here, TPM: Transcript Per Million.

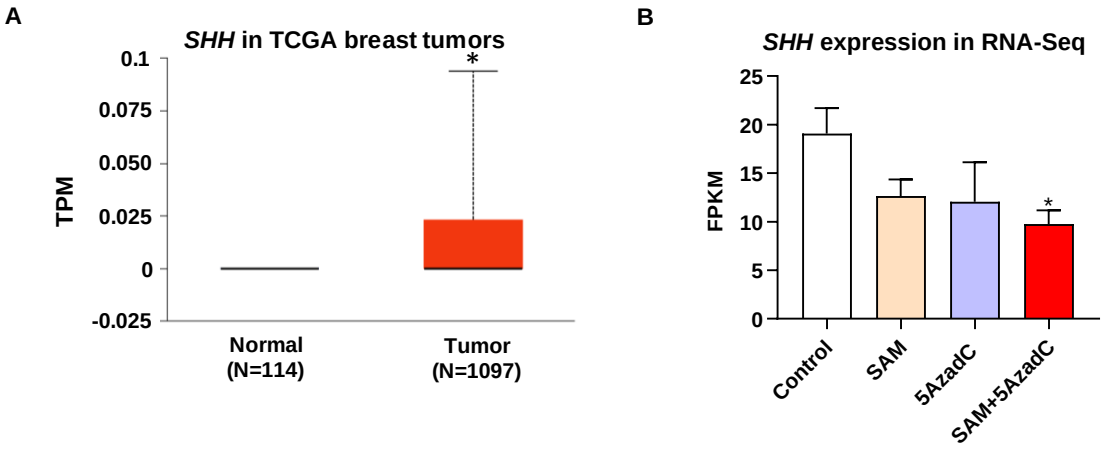

Supplementary Figure S9: The Sonic Hedgehog (*SHH*) gene expression. **(A)** The *SHH* gene expression is significantly elevated in human breast tumor samples relative to the normal samples according to the TCGA database. Here, TPM: transcript per million. **(B)** RNA-Sequencing from the current study revealed that the expression of *SHH* is significantly reduced in the combination setting. Here, FPKM refers to Fragments Per Kilobase of transcript per Million mapped reads.

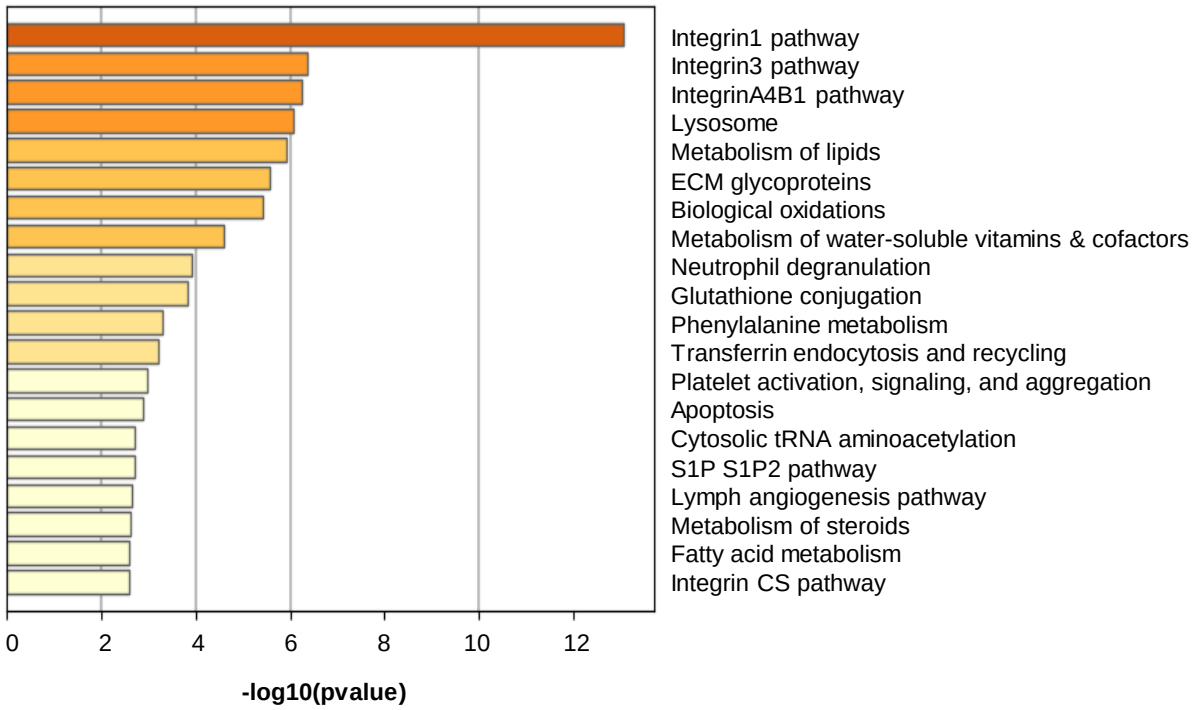

Supplementary Figure S10: Pathways regulated by RNA-Seq obtained unique DEGs in the SAM+5AzadC combination. Several pathways related to invasion and metastasis showed enrichment suggesting their possible regulation by the combination treatment.

Reference (for Supplementals presented in Chapter 3)

1. **Gholami O, Jeddi-Tehrani M, Iranshahi M, Zarnani AH, Ziai SA.** Mcl-1 is up regulated by prenylated coumarin, umbelliprenin in jurkat cells. *Iran J Pharm Res*. 2014; 13: 1387-92.
2. **Leyva-Illades D, Cherla RP, Lee MS, Tesh VL.** Regulation of cytokine and chemokine expression by the ribotoxic stress response elicited by Shiga toxin type 1 in human macrophage-like THP-1 cells. *Infect Immun*. 2012; 80: 2109-20.
3. **Riverso M, Montagnani V, Stecca B.** KLF4 is regulated by RAS/RAF/MEK/ERK signaling through E2F1 and promotes melanoma cell growth. *Oncogene*. 2017; 36: 3322-33.
4. **Tiwari N, Tiwari Vijay K, Waldmeier L, Balwierz Piotr J, Arnold P, Pachkov M, Meyer-Schaller N, Schübeler D, van Nimwegen E, Christofori G.** Sox4 Is a

Master Regulator of Epithelial-Mesenchymal Transition by Controlling Ezh2 Expression and Epigenetic Reprogramming. *Cancer Cell*. 2013; 23: 768-83.

5. **Sankar N, deTombe PP, Mignery GA.** Calcineurin-NFATc regulates type 2 inositol 1,4,5-trisphosphate receptor (InsP3R2) expression during cardiac remodeling. *J Biol Chem*. 2014; 289: 6188-98.
6. **Eldridge S, Nalesso G, Ismail H, Vicente-Greco K, Kabouridis P, Ramachandran M, Niemeier A, Herz J, Pitzalis C, Perretti M, Dell'Accio F.** Agrin mediates chondrocyte homeostasis and requires both LRP4 and α-dystroglycan to enhance cartilage formation in vitro and in vivo. *Annals of the Rheumatic Diseases*. 2016; 75: 1228-35.
7. **Magni M, Buscemi G, Maita L, Peng L, Chan SY, Montecucco A, Delia D, Zannini L.** TSPYL2 is a novel regulator of SIRT1 and p300 activity in response to DNA damage. *Cell Death & Differentiation*. 2019; 26: 918-31.
8. **Zeeuwen PLJM, de Jongh GJ, Rodijk-Olthuis D, Kamsteeg M, Verhoosel RM, van Rossum MM, Hiemstra PS, Schalkwijk J.** Genetically Programmed Differences in Epidermal Host Defense between Psoriasis and Atopic Dermatitis Patients. *PLOS ONE*. 2008; 3: e2301.
9. **Chen Y, Liu L, Guo Z, Wang Y, Yang Y, Liu X.** Lost expression of cell adhesion molecule 1 is associated with bladder cancer progression and recurrence and its overexpression inhibited tumor cell malignant behaviors. *Oncology letters*. 2019; 17: 2047-56.
10. **Samanta D, Park Y, Andrabi SA, Shelton LM, Gilkes DM, Semenza GL.** PHGDH Expression is Required for Mitochondrial Redox Homeostasis, Breast Cancer Stem Cell Maintenance and Lung Metastasis. *Cancer Research*. 2016: canres.0530.2016.
11. **Vauzour D, Tejera N, O'Neill C, Booz V, Jude B, Wolf IMA, Rigby N, Silvan JM, Curtis PJ, Cassidy A, de Pascual-Teresa S, Rimbach G, Minihane AM.** Anthocyanins do not influence long-chain n-3 fatty acid status: studies in cells, rodents and humans. *The Journal of Nutritional Biochemistry*. 2015; 26: 211-8.
12. **Valdes-Mora F, Song JZ, Statham AL, Strbenac D, Robinson MD, Nair SS, Patterson KI, Tremethick DJ, Stirzaker C, Clark SJ.** Acetylation of H2A.Z is a key epigenetic modification associated with gene deregulation and epigenetic remodeling in cancer. *Genome Res*. 2012; 22: 307-21.
13. **Mino K, Nishimura S, Ninomiya S, Tujii H, Matsumori Y, Tsuchida M, Hosoi M, Koseki K, Wada S, Hasegawa M, Sasaki R, Murakami-Yamaguchi Y, Narita H, Suzuki T, Miyata N, Mizukami T.** Regulation of tissue factor pathway inhibitor-2 (TFPI-2) expression by lysine-specific demethylase 1 and 2 (LSD1 and LSD2). *Bioscience, biotechnology, and biochemistry*. 2014; 78: 1010-7.
14. **Pirngruber J, Shchebet A, Schreiber L, Shema E, Minsky N, Chapman RD, Eick D, Aylon Y, Oren M, Johnsen SA.** CDK9 directs H2B monoubiquitination and controls replication-dependent histone mRNA 3'-end processing. *EMBO reports*. 2009; 10: 894-900.
15. **Chaika NV, Gebregiworgis T, Lewallen ME, Purohit V, Radhakrishnan P, Liu X, Zhang B, Mehla K, Brown RB, Caffrey T, Yu F, Johnson KR, Powers R,**

Hollingsworth MA, Singh PK. MUC1 mucin stabilizes and activates hypoxia-inducible factor 1 alpha to regulate metabolism in pancreatic cancer. *Proc Natl Acad Sci U S A*. 2012; 109: 13787-92.

16. **Mahmood N, Cheishvili D, Arakelian A, Tanvir I, Khan HA, Pépin A-S, Szyf M, Rabbani SA.** Methyl donor S-adenosylmethionine (SAM) supplementation attenuates breast cancer growth, invasion, and metastasis in vivo; therapeutic and chemopreventive applications. *Oncotarget*. 2018; 9: 5169.

Supplementary File 2

The differentially expressed genes from RNA-Seq datasets can be viewed by downloading the 'jcmm15642-sup-0002-AppendixS2.xlsx' file under supporting information from the following link:

https://onlinelibrary.wiley.com/doi/full/10.1111/jcmm.15642

Supplementary File 3

The differentially methylated CGs from Infinium Human MethylationEpic 850K BeadChip microarray datasets can be viewed by downloading the 'jcmm15642-sup-0003-AppendixS3.xlsx' file under supporting information from the following link:

https://onlinelibrary.wiley.com/doi/full/10.1111/jcmm.15642

Chapter Four: An enhanced chemopreventive effect of methyl donor S-adenosylmethionine in combination with 25-hydroxyvitamin D in blocking mammary tumor growth and metastasis

Preface

In Chapters 2 and 3, we have used MDA-MB-231 xenografts to study the anti-cancer effects of SAM-treatment alone or in combination with Decitabine. A major limitation of the xenograft model is the use of already transformed cell lines during implantation, which does not assess the potential effect of the therapeutic regimen on tumor emergence. Therefore, to understand whether SAM treatment has any role in delaying tumor emergence as monotherapy or in combination with a known chemopreventive agent 25(OH)D, we used the well-established transgenic MMTV-PyMT model of breast cancer. In addition, the effect of the monotherapy and combination treatment on breast tumor colonization to the bone was assessed using an intratibial model.

Herein, an author-generated version of the manuscript is presented. The manuscript related to this study was published in 'Bone Research' in 2020:

> "**Mahmood,N.,** Arakelian,A., Muller, W.J., Szyf,M. and Rabbani, S.A. (2020) An enhanced chemopreventive effect of methyl donor S-adenosylmethionine in combination with 25-hydroxyvitamin D in blocking mammary tumor growth and metastasis. Bone Res. 8:28."

Abstract

Therapeutic targeting of metastatic breast cancer still remains a challenge as the tumor cells are highly heterogenous and exploit multiple pathways for their growth and metastatic spread that cannot always be targeted by a single-agent monotherapy regimen. Therefore, a rational approach through simultaneous targeting of several pathways may provide a better anti-cancer therapeutic effect. We tested this hypothesis using a combination of two nutraceutical agents S-adenosylmethionine (SAM) and Vitamin D (Vit. D) prohormone [25-hydroxyvitamin D; '25(OH)D'] that are individually known to exert distinct changes in the expression of genes involved in tumor growth and metastasis. Our results show that both SAM and 25(OH)D monotherapy significantly reduced proliferation and clonogenic survival of a panel of breast cancer cell lines *in vitro* and inhibited tumor growth, lung metastasis, and breast tumor cell colonization to the skeleton *in vivo*. However, these effects were significantly more pronounced in the combination setting. RNA-Sequencing revealed that the transcriptomic footprint on key cancer-related signaling pathways is broader in the combination setting than any of the monotherapies. Furthermore, comparison of the differentially expressed genes from our transcriptome analyses with publicly available cancer-related dataset demonstrated that the combination treatment upregulates genes from immune-related pathways that are otherwise downregulated in bone metastasis *in vivo*. Since SAM and Vit. D are both approved nutraceuticals with known safety profiles, this combination treatment may serve as a novel strategy to reduce breast cancer-associated morbidity and mortality.

Introduction

Breast cancer is one of the most prevalent malignancies in women worldwide[1]. Despite the recent advances in the development of anti-cancer therapeutic agents, the overall survival rate for patients with metastatic breast cancer remains poor, which highlights the need for more innovative and rational therapeutic strategies[2]. Among the various nutraceutical agents tested for treatment of breast cancer, Vitamin D (Vit. D) showed significant promise as it decreases cell proliferation, angiogenesis, promotes cellular differentiation and apoptosis, and stimulates immune response[3]. However, the clinical and epidemiological evidence of the anticancer effects of Vit. D remains inconclusive[4,5]. The SUNSHINE clinical trial done on previously untreated advanced/metastatic colorectal cancer patients found that the group receiving a high dose of Vit. D, along with the standard of care chemotherapy, showed a significantly higher progression-free survival rate in comparison to the group receiving low dose Vit D. in combination with chemotherapy[6]. The results from the recently concluded VITAL (VITamin D and OmegA-3 TriaL) study showed no statistical correlation between Vit. D supplementation and reduced incidence of cancer compared with the placebo group over a median follow-up period of 5.3 years[7]. However, further analysis of the participants from the VITAL study who were taking Vit. D supplements for at least 2 years demonstrated a 25% reduction in cancer-related mortality. Taken together, these observations indicate the potential benefits of Vit. D supplementation alone and in combination with other well-characterized anti-cancer therapeutic agents.

Our recent studies have demonstrated that the universal methyl group donor S-adenosylmethionine (SAM) shows an antiproliferative and antimetastatic effect in the well-characterized MDA-MB-231 xenograft model of breast cancer[8]. SAM also reduces angiogenesis and promotes apoptosis of cancer cells[9,10]. Epigenome-wide studies in different malignancies have revealed that SAM treatment leads to hypermethylation-mediated inactivation of several key growth factors and prometastatic genes[11,12].

Since cancer growth and metastasis requires the activity of multiple pathways, we reasoned that effective anticancer treatment strategies need to focus on coordinate targeting of several pathways. We, therefore, tested whether the combined administration of two different nutraceutical agents SAM and Vit. D, which act on different pathways critical for cancer growth and metastasis, would exhibit an enhanced anticancer and antimetastatic effect over the monotherapy with either compound on its own.

Although various types of Vit. D metabolites have shown anticancer properties, the prohormone 25(OH)D has better circulating half-life ($t_{1/2} = 3$ weeks versus 4–6 h) and lesser tendency to induce hypercalcemia than the active 1,25$(OH)_2$D form[13]. Furthermore, a recent meta-analysis demonstrated an inverse relationship between the serum levels of 25(OH)D and mortality of breast cancer patients[14]. It has been shown that 25(OH)D can be converted to the active 1,25$(OH)_2$D form locally in normal and cancerous mammary tissues by 1α-hydroxylase (CYP27B1) enzyme[15]. Therefore, in the present study, the combined anti-cancer therapeutic potential of SAM and 25(OH)D was assessed *in vitro* using a panel of breast cancer cell lines. For *in vivo* studies, we used the well-established transgenic

MMTV-PyMT (mouse mammary tumor virus promoter-driven polyoma middle T oncoprotein) mouse model of breast cancer to monitor mammary tumor emergence, growth, and lung metastasis and a syngeneic model using PyMT-R221A cells to evaluate the effect on skeletal colonization by breast tumor cells[16]. Our results show that combination treatment significantly delays mammary tumor emergence, reduces tumor volume, and metastasis in comparison with either monotherapy without showing any adverse effects.

Results

Combination of SAM and 25(OH)D suppresses cell proliferation and clonogenic survival potential *in vitro*

Since cancer is a disease of uncontrolled cell proliferation and survival[17], a panel of human (ZR-75-1, MDA-MB-231) and murine (PyMT-R221A, E0771) breast cancer cell lines with different levels of endogenous Vit. D receptor expression (Supplementary File 1, Figure S1) was used to examine the possible growth inhibitory effects of SAM and 25(OH)D combination *in vitro*. Using a treatment protocol shown in Figure 1a, we found that single-agent treatment with SAM (200 μM) resulted in a significant reduction in cell proliferation as compared to the control cells treated with vehicle alone during the same period (Figure 1b). Treatment with 25(OH)D (100 nM) monotherapy also caused significant repression in the growth properties of PyMT-R221A, E0771, and ZR-75-1 cells, results which are consistent with previous reports[18,19]. Notably, the anti-cancer effects on the growth properties were more pronounced in the cells treated with the

combination of SAM and 25(OH)D (Figure 1b). Next, we calculated the coefficient of drug interaction (CDI) to characterize whether the nature of the interaction between the SAM and 25(OH)D are synergistic, additive, or antagonistic using the following equation: $CDI = AB/(A \times B)$[20,21]. The CDI value indicated that the combination of SAM and 25(OH)D shows an additive effect to moderately synergistic effect at the doses used in this study (Supplementary File 1, Figure S2). We also treated normal human breast epithelial cells (HBEC) with SAM, 25(OH)D, and SAM+25(OH)D combination and found no significant change in the viability of HBEC cells treated with different agents when compared to the vehicle-treated control cells, suggesting that the treatments are not toxic at the drug concentration used *in vitro* (Supplementary File 1, Figure S3).

Next, to further test the antiproliferative effect, we examined the impact of different treatments on the colony-forming ability of these cell lines using a clonogenic survival assay. Our data showed that the SAM + 25(OH)D combination decreases the colony-forming potential of all four cells compared with the vehicle-treated controls as well as those treated with either SAM or 25(OH)D alone (Figure 1c). Taken together, these results suggest that the combined use of SAM and 25(OH)D may serve as an effective strategy for breast cancer treatment.

Combination of SAM and 25(OH)D delays mammary tumor development and attenuates tumor growth and lung metastasis in transgenic MMTV-PyMT mice

To assess whether the combination treatment has any effect on mammary tumor emergence and volume, we used the well-characterized transgenic MMTV-PyMT mice (in

FVB background) that mimic the stepwise progression of breast cancer in humans[22]. Female MMTV-PyMT mice were randomized on day 28 after birth to four different treatment groups: vehicle-treated controls, SAM (160.0 mg/kg/day) via oral gavage, 25(OH)D (40.0 ng/kg/day) by intraperitoneal injection, and combination of SAM and 25(OH)D at the same concentrations (Figure 2a).

Control and experimental groups of animals were monitored for the appearance of both axillary (anterior) and inguinal (posterior) mammary tumors from day 35 after birth. We found that the vehicle-treated control mice spontaneously developed palpable mammary tumors at around 42 days of age while a substantial delay in tumor emergence was observed for all three treatment groups (Figure 2b). The median value for tumor emergence in the control group was day 45.5 after birth, which was delayed to day 49.5 and 52.5 in the 25(OH)D (log-rank $P = 0.05$) and SAM (log-rank $P = 0.006$) monotherapy treated groups, respectively (log-rank $P = 0.021$) (Figure 2b). A further delay in tumor appearance was observed in groups treated with SAM + 25(OH)D combination (log-rank $P = 0.003$), with a median of 56 days.

Next, the total mammary tumor volume (sum of individual axillary and inguinal tumor volumes for each of the animals as described in 'Materials and Methods') was measured for each animal from day 49 until sacrifice on day 77 (Figure 2c). Our data indicated a significant reduction in primary mammary tumor volumes in all three treatment groups (Figure 2c&d). However, these effects were more pronounced in the SAM + 25(OH)D treated animals suggesting enhanced therapeutic potential of the combination treatment compared with the single-agent monotherapies *in vivo.*

One of the known adversities of long-term administration of Vit. D is the possibility to develop hypercalcemia[23]. Therefore, at the time of sacrifice, serum from all animals was collected and levels of calcium and other biochemical parameters were examined. No significant difference in serum calcium or any other biochemical parameter was seen between control and experimental animals (Supplementary File 1, Table S1), suggesting that SAM and 25(OH)D had no adverse effects *in vivo* at these doses. In addition, no significant difference in the total body weight over time was observed in the animals from control and different treatment groups (Supplementary File 1, Figure S4).

Immunohistochemical assessment of formalin-fixed tumor tissues showed that the expression of ki67 proliferation marker was markedly decreased in all three treatment groups compared with the vehicle-treated controls, with the highest reduction in the SAM + 25(OH)D cohort (Figure 2e). This further validates the reduction of tumor volumes seen in the animals receiving combination therapy at the protein level.

Virgin female MMTV-PyMT mice spontaneously develop lung metastases that arise from the primary breast tumor by 10–12 weeks (70–84 days) of age[24], which allows assessing the antimetastatic potential of a treatment regimen. On day 77, animals from all four groups were sacrificed, and lung tissues were collected. The extent of visceral metastasis mediated by the breast tumor cells was assessed by evaluating the formalin-fixed paraffin-embedded sections of the entire lung tissue. We found that breast tumor cells invaded the lung in all four groups (Figure 2f, left panel). However, the area of lung metastases showed a significant decrease in the treatment groups compared with the vehicle-treated control animals, as determined by the measurement of the total area of

micrometastases in the lungs (Figure 2f, right panel). Moreover, the SAM + 25(OH)D combination-treated animals showed the lowest metastatic burden amongst the three treatment groups. These results suggest that SAM + 25(OH)D combination treatment cannot block the development of lung metastases but significantly reduces them.

The efficacy of a therapeutic molecule is dependent on its serum bioavailability for a reasonable period of time that will allow its absorption and subsequent distribution to the target tissues[8]. We, therefore, performed a time-course experiment to determine the duration of SAM bioavailability in the serum following oral administration using LC-MS/MS. We found that SAM reaches its peak 30 min after administration, and its level drops down to the baseline after 240 min suggesting possible uptake by different tissues (Supplementary File 1, Figure S5a). Next, we compared the SAM levels in the control and SAM-treated experimental MMTV-PyMT animals at sacrifice on week 11 and found a 3.6-fold increase in SAM concentration in the experimental group (Supplementary File 1, Figure S5b).

We then checked the serum bioavailability of the intraperitoneally injected 25(OH)D by LC-MS/MS and found a significant elevation of the metabolite in the treated animals compared with the controls (Supplementary File 1, Figure S6a). In addition, 25(OH)D injection elevated the levels of $1,25(OH)_2D$ and $24,25(OH)_2D$ in the serum of the experimental animals (Supplementary File1, Figure S6b, c). Taken together, these results suggest both SAM and 25(OH)D are bioavailable at the doses used in this study.

Combination of SAM+25(OH)D represses breast tumor cell growth in the skeleton in a syngeneic intratibial mouse model

We then assessed the effect of SAM + 25(OH)D in reducing the establishment of breast tumors in the skeleton using an immunocompetent syngeneic intratibial mouse model. The PyMT-R221A cells were utilized for intratibial implantation into female FVB mice as they were originally extracted from MMTV-PyMT mammary tumors[16], and also to keep a consistency of genetic background between the different *in vivo* models used in the study. Following a treatment strategy shown Figure 3a, animals from control and different treatment groups were treated daily from day 3 post tumor cell injection until sacrifice on day 14. Previous studies have demonstrated that by this time point, the cortical bone becomes compromised by these tumor cells, and they start to grow in the soft tissues in the surrounding area[25,26]. After sacrifice, tibias from all animals were collected, and H&E staining of the fixed paraffin-embedded bone tissue sections revealed that the percentage of animals that developed tumors was lower in the combination-treated group than that of control as well as the monotherapy treated groups (Figure 3b,c). In addition, the skeletal tumor area was the smallest in the combination arm relative to monotherapy treated animals (Figure 3d). Collectively, these observations suggest that the SAM + 25(OH)D combination treatment can reduce breast tumor growth in the skeleton, which is a major site where breast tumor cells migrate and establish to cause a secondary tumor in clinical settings.

Effect of the combination treatment on PyMT-R221A transcriptome

To characterize the molecular mechanisms underpinning the enhanced anticancer effect of the combination versus the effects of the monotherapy treatments with either SAM or 25(OH)D, we compared the drug-induced changes of PyMT-R221A transcriptome by RNA-Sequencing (RNA-Seq) of control (vehicle), 200 μM SAM, 100 nM 25(OH)D and SAM+25(OH)D treated samples. The differentially expressed genes (DEGs) between control and different treatment groups were delineated using DeSeq2 ($\log_2$ fold change > 0.5 and FDR < 0.05). A total of 387 (182 upregulated and 205 downregulated), 269 (141 upregulated and 128 downregulated), and 652 (306 upregulated and 346 downregulated) DEGs were detected in SAM versus control, 25(OH)D versus control, and SAM + 25(OH)D versus control groups, respectively (Figure 4a, Supplementary File 2). Hierarchical clustering of the top 50 DEGs in the three groups is shown separately in Supplementary File 1, Figure S7. The number of common and unique genes that are differentially up- and downregulated in different treatment groups illustrated by the Venn diagrams showed that the transcriptomic footprint of the combination therapy is broader than any of the single treatments (Figure 4b). Circos plots revealed the numerical and functional overlaps between the up- and downregulated genes from the different treatment groups (Figure 4c). The combination treatment provides unique functionality compared with the single-agent treatment as shown by the higher number of blue lines within the Circos plots of up- and downregulated genes in combination treatment compared with the single-drug treatment. Interestingly, SAM, 25(OH)D and SAM + 25(OH)D treatments commonly target 106 genes (43 upregulated and 63 downregulated) suggesting overlap in

molecular targets of these agents (Fig. 4b, Supplementary File 1, Figure S8). Importantly, the combination treatment was not just a summation of the two monotherapies, but it had its unique footprint which involved changed expression of 331 genes (162 upregulated and 169 downregulated) indicating the possible modulation of additional biological signaling pathways.

A comparative Gene ontology (GO) enrichment analyses using the DEGs from all three treatment groups revealed that the genes upregulated by SAM + 25(OH)D are involved in crucial biological processes like regulation of type I interferon production (GO: 0032479), defense response to virus (GO: 0051607), while significantly downregulated genes by the combination are involved in key cancer-related processes such as response to hypoxia (GO:001666), angiogenesis (GO:0001525), and others as listed in Figure 4d.

Validation of the DEGs from the top enriched signaling pathways affected by the combination treatment

To gain further insight into the functional pathways that were significantly affected by the SAM + 25(OH)D combination treatment, a pathway enrichment analysis was done using the Kyoto Encyclopedia of Genes and Genomes (KEGG) and Reactome databases (Figure 5a). We found that the top pathway significantly enriched by genes upregulated in response to the combination treatment is the 'interferon alpha/beta signaling' pathway (Figure 5a). On the other hand, the top signaling pathway enriched for genes downregulated by the combination treatment is the 'HIF-1 signaling pathway' (Figure 5a). Gene Set Enrichment Analysis (GSEA) further confirmed the enrichment of genes from

the interferon alpha/beta and HIF-1 signaling pathways upon combination treatment (Figure 5b). We also performed pathway analysis of the 106 common DEGs shared by SAM, 25(OH)D, and SAM + 25(OH)D combination treatment and found that the 'HIF-1 signaling pathway' is the top signaling pathway enriched by these genes (P= $3.42x10^{-07}$; Supplementary File 1, Figure S9). We then analyzed the 331 DEGs that are uniquely regulated by the SAM + 25(OH)D combination treatment and found a significant enrichment of the 'interferon alpha/beta signaling' pathway (P=$3.33x10^{-11}$; Supplementary File 1, Figure S10).

We next validated the RNA-Seq results on selected genes from the top upregulated (interferon alpha/beta signaling) and downregulated pathways (HIF-1 signaling pathway) using quantitative polymerase chain reaction (qPCR) analysis. Several crucial genes from the 'interferon alpha/beta signaling' pathways were significantly upregulated in the SAM + 25(OH)D combination-treated cells only but not by either of the monotherapies (Figure 5c). On the other hand, in comparison with the control group, a significant decrease in the expression of selected genes from the 'HIF-1 signaling pathway' were observed in the combination-treated group, a trend that is also shared by the monotherapy treatments with either SAM or 25(OH)D (Figure 5b). Similar results were also seen when tumoral RNA from control and treated animals (from Figure 2) were analyzed by qPCR (Supplementary File 1, Figure S11). We also measured the levels of *Vdr, Cyp27b1*, and *Cyp24a1* in control and treated PyMT-R221A cells and found their expression to be differentially regulated upon combination treatment relative to the control cells (Supplementary File 1, Figure S12).

Since Stat1 plays a key role in mediating the immune responses activated by the interferon signaling pathway through the transcriptional regulation of several interferon related genes including *Irf7, Isg15, Oas2, Gbp3*—all of which are upregulated by the SAM + 25(OH)D (Figure 5c), we next tested the hypothesis that upregulation of Stat1 in part mediates the enhanced anti-cancer effect seen by the combination treatment. For that, we compared the effect of Stat1 activator [2-(1,8-naphthyridin-2-yl)-Phenol; in short '2-NP'] and SAM + 25(OH)D treatment on PyMT-R221A cell proliferation. Treatment with either 2-NP or SAM + 25(OH)D both reduced tumor cell proliferation (Supplementary File 1, Figure S13a). Interestingly, a triple combination of 2-NP with SAM + 25(OH)D showed an additive effect in reducing proliferation (Supplementary File 1, Figure S13a). The expression of *Irf7*, a known transcriptional target of Stat1, was found to be elevated by either 2-NP or SAM + 25(OH)D treatment with a further elevation of its gene expression in the triple combination (Supplementary File 1, Figure S13b). Taken together, these results indicate the possible involvement of the interferon signaling pathways in mediating the anticancer effects shown by the SAM + 25(OH)D combination treatment.

Comparison of the DEGs upon combination treatment with publicly available breast cancer dataset

We compared the DEGs in response to SAM + 25(OH)D combination treatment from our study with genes that are differentially regulated in a publicly available dataset of mouse model of spontaneous bone metastasis determined by Affymetrix mouse 430 v2.0 gene expression arrays[27] (GSE37975). (GSE37975). Differentially expressed transcripts

from GSE37975 were analyzed using the GEO2R tool from the NCBI GEO website and a total of 6305 (2 833 upregulated and 3472 downregulated) differentially expressed unique genes were obtained in the skeletal metastasis (spine) samples compared with the controls (at FDR <0.05). We then overlapped 2833 upregulated and 3472 downregulated genes from GSE37975 with the 346 downregulated and 306 upregulated genes upon SAM + 25(OH)D treatment from the current study. Our analysis showed that 53 transcripts that are downregulated in metastatic bone tissues, according to GSE37975, significantly overlapped with genes upregulated by SAM + 25(OH)D treatment as compared with the vehicle-treated control PyMT-R221A cells (hypergeometric test, $P \leq 0.05$) (Figure 6a, Supplementary Figure S14). More interestingly, out of these 53 transcripts, 27 were uniquely upregulated by the SAM + 25(OH)D combination. On the other hand, the overlap of 42 transcripts (16 hits unique for combination only) that are upregulated in the mouse model of bone metastasis but downregulated by SAM + 25(OH)D combination was not statistically significant by hypergeometric test (Figure 6a, Supplementary Figure S15). Next, we focused on the 27 genes that are downregulated in bone metastasis but uniquely upregulated by the combination. Protein-protein interaction (PPI) network analysis revealed a significant enrichment (PPI enrichment $P < 1.0e\text{-}16$) with 'response to virus' and 'type I interferon signaling pathway' as the top two most significantly enriched GO-pathways within the network (Supplementary File 1, Figure S15).

Next, we overlapped the DEGs responding to SAM+25(OH)D treatment with the ortholog human breast cancer patient gene list obtained from the BioXpress and we found a list of 87 genes (36 are unique in combination only) that were upregulated in human

breast tumors but downregulated by the combination treatment while there were 59 genes that were downregulated in patients but are upregulated by the combination treatment (Supplementary File 1, Figure S16). However, the overlap of genes did not reach statistical significance by a hypergeometric test. Nevertheless, pathway analysis of the overlapped genes revealed differential regulation of several known cancer-related pathways like HIF-1 and HIF-2 transcription factor networks and β3 integrin cell surface interactions (Supplementary File 1, Figure S16).

Discussion

It is now clear that the cancer phenotype involves concurrent alterations in multiple gene pathways where both hypermethylation of tumor-suppressor genes and hypomethylation of the tumor-promoting genes occur[29,30,31]. We, therefore, combined the methylating agent SAM with another commonly used nutraceutical agent Vit. D, a compound acting via its nuclear receptor triggers epigenetic reprogramming as well as demethylation[32,33], so that both hypermethylation and hypomethylation meditated abnormalities of the cancer methylome can be targeted concurrently. We found that the combination treatment caused a significant delay in the time of forming spontaneous tumors in experimental transgenic mice as compared with vehicle-treated control MMTV-PyMT mice. In addition, the combination showed a markedly improved therapeutic effect in reducing tumor volumes compared with the controls as well as that of single-agent treatment. The combination also reduced the extent of the metastatic burden to the lung

tissue, which is the major site where the primary tumor cells metastasize in this well-established model[22].

Skeletal metastasis is one of the main complications associated with advanced breast cancer which leads to intractable bone pain, hypercalcemia, increased bone fragility, nerve compression resulting in high incidence of morbidity and mortality[34,35]. Collectively, these complications are called skeletal-related events and significantly hamper the quality of life of cancers patients. Despite its widespread prevalence, only a few therapeutic options are available for skeletal metastasis[36]. Moreover, most of the available therapeutic options are palliative and are directed towards relieving bone pain and reducing the destruction of bone tissue[36]. Therefore, there is an unmet need for novel therapeutic intervention decreasing the secondary tumor growth to the skeleton. Towards these goals, we used the PyMT-R221A intratibial model of breast cancer colonization to the bone to assess the anti-cancer potential of SAM + 25(OH)D and found that the combination treatment significantly reduced tumor growth in the tibial region.

The dosage used for *in vivo* 25(OH)D administration was similar to the one described previously[19]. However, instead of using an osmotic pump for 25(OH)D administration, we used intraperitoneal injection so that it can be clinically translatable to humans. This mode of delivery is advantageous as it avoids re-implantation of the osmotic pump every 4 weeks and assures a uniform delivery of 25(OH)D, which is not always possible to maintain via other means like a dietary supplementation. To test the efficacy of our treatment strategy, we measured the levels of 25(OH)D, 1,25$(OH)_2$D and 24,25$(OH)_2$D

in the serum of control and 25(OH)D injected animals and found elevated levels of these metabolites that suggested bioavailability of 25(OH)D (Supplementary File 1, Figure S6). Based on our previous studies and results from our preliminary studies in these models using different doses of SAM (data not shown), 160 mg/kg/day via oral gavage was found to be most effective which was used in the current study. Using this dose, we have observed an elevated SAM concentration in the serum of experimental animals treated with SAM compared with the control animals (Supplementary File 1, Figure S5b). SAM is available as an approved dietary supplement for depressive disorders. However, in at least two different clinical trials, treatment with SAM ironically showed some transient behavioral abnormalities in a small number of participant[37,38]. To assess whether SAM elicits any potential behavioral adversities at the dose used in this study, we conducted an open field test. However, we did not observe any behavioral abnormalities in the SAM-treated animals when compared with the vehicle-treated control animals (Supplementary File 1, Figure S17).

One of the major aspects of the current study was to assess and compare the transcriptomic changes induced by single agents and their combination to understand the molecular footprint of the combination treatment as a possible explanation for its anticancer activity. We, therefore, performed RNA-Sequencing of samples obtained from control and all three treatments and compared their expression profiles. We chose to analyze the transcriptome of mouse PyMT-R221A cells so that the anti-cancer effects seen *in vivo* can be directly linked to the molecular changes seen in the cancer cells *in vitro* since

these cells were initially isolated from the MMTV-PyMT tumor[39]. We found that the combination treatment has a much broader footprint than either the monotherapies alone, but it shared 106 genes (43 upregulated, 63 downregulated) with both SAM and 25(OH)D treated groups which account for 12.6% of the total DEGs in all three groups (Figure 3c). Pathway analysis revealed that the combination treatment downregulates genes involved in key cancer-related signaling pathways like the HIF-1 pathway, MAPK pathway while the top pathway enriched by the upregulates genes is the p53 signaling pathway. GO analysis revealed that treatment with SAM+25(OH)D might also boost the immune system through modulation of immune-related genes and might be considered for enhancement of other immunotherapy regimens. Analysis of publicly available murine breast cancer bone metastasis datasets revealed that interferon regulatory factor *Irf7*, whose expression is repressed during bone metastasis (GSE37975), is upregulated by the SAM+25(OH)D combination treatment. It has been shown that *Irf7* repression promotes bone metastasis through immune escape in a mouse model of breast cancer bone metastasis[27]. Moreover, overexpression of IRF7 inhibited prostate cancer cell-mediated bone metastasis in mice[40], suggesting a common role of the Irf7 axis in bone metastasis mediated by different types of malignancies.

Our molecular analysis of the effect of the combination therapy on the transcriptome shows that the combination regulates a new molecular landscape than just a sum of both monotherapies explaining the expanded anti-cancer activity of the combination. The combination of SAM + 25(OH)D targets important biological processes for cancer that would not be hit using either monotherapies (Figure 4d). The 331 genes

(162 upregulated, 169 downregulated) unique for the combination-treated groups target a wide array of pathways (Supplementary File 1, Figure S10), of which the most notable are the immune-related ones (for example, response to type I interferon). The upregulation of the immune-related genes upon the combination treatment might induce an anti-viral immune response against the cancer cells, which could not be possibly attained at the same extent by either of the monotherapies. Moreover, these immune-related genes not only elicit better antitumor effects[41] but also provide a better antimetastatic response in the bone microenvironment[27,40]. This might be a possible reason behind the enhanced antitumor and antimetastatic response seen in animals receiving SAM + 25(OH)D combination in both transgenic and intratibial models of breast cancer. However, further experimental evidence is needed to confirm the exact role of the immune system in mediating these anticancer effects. We also found that several noncoding RNAs are changed upon SAM + 25(OH)D combination treatment, of which the most notable is the downregulation of the known oncogenic long non-coding RNA called *Rmrp* (Supplementary File 1, Figure S18). This implies that the molecular changes mediated by the combination are not only limited to genes with coding potential, but those with no known peptides are also regulated by SAM + 25(OH)D, which warrants future in-depth investigation of the non-coding repertoire of the transcriptome. Moreover, SAM as a methylating agent may have a profound impact on chromatin accessibility through its ability to methylate DNA and histone proteins, which in turn might be responsible for many of the gene expression changes seen in the RNA-Seq experiment. Future studies investigating the PyMT methylome and cistrome using the recently described methyl-ATAC-sequencing[42], as well

as chromatin immunoprecipitation sequencing using antibodies against different histone modifications, may provide further mechanistic insights to the epigenomic changes induced by SAM treatment.

In summary, this study strongly demonstrates the anti-cancer therapeutic effect of SAM + 25(OH)D combination in breast cancer *in vitro* and *in vivo* (Figure 6c), that may be used separately or in parallel with the current first-line therapy to improve patient outcomes. What is particularly attractive about this combination [SAM + 25(OH)D] is that both of them have a long safety record that positions them well for long term use as chemopreventive and therapeutic agents to reduce cancer-associated morbidity and mortality.

Materials and Methods

Cell culture and treatments

Human MDA-MB-231 (*ATCC*® HTB- 26™) and ZR-75-1 (*ATCC*® CRL-1500™) cell lines were obtained from the American Type Culture Collection (ATCC; Manassas, Virginia). The mouse breast cancer PyMT-R221A and E0771 cell lines were kindly gifted by Dr. Conor C. Lynch (H. Lee Moffitt Cancer Center and Research Institute, Tampa, FL, USA) and Dr. Jean S. Marshall (Dalhousie University, Halifax, Nova Scotia, Canada) respectively. MDA-MB-231, PyMT-R221A, and E0771 cells were maintained in Dulbecco's modified Eagle's medium (DMEM) supplemented with 10% fetal bovine serum (FBS), 2 mM L-glutamine and 100 units/ml penicillin-streptomycin sulfate. The ZR-75-1 cells were supplemented with RPMI-1640 containing 10% FBS, 2 mM L-glutamine

and 100 units/ml penicillin-streptomycin sulfate. The human breast epithelial cells (HBEC) were obtained from Celprogen (Cat# 36056-01) and supplemented with manufacturer recommended human breast epithelial cell culture serum-free media (Cat# M36056-01).

Our recent studies have demonstrated that treatment with 200 μM SAM elicits anti-cancer effects in different cancer cells[8]. Therefore, we used this dose for *in vitro* studies with all four cell lines. A human-grade SAM (Life Science Laboratories, Lakewood, NJ, USA) was used for all *in vitro* and *in vivo* experiments. On the other hand, 100 nM 25(OH)D (Cayman chemical company, Cat#9000683) was used *in vitro* as previously shown by others[13,18].

Cell proliferation and viability assay

MDA-MB-231, ZR-75-1, E0771, and PyMT-R221A breast cancer cells were plated onto 6-well plates containing 10% FBS supplemented growth media. The next day the cells were serum-starved for 24 hours before treatment with 200 μM SAM, 100 nM 25(OH)D, a combination of SAM + 25(OH)D, and vehicle (ethanol) by direct addition to 5% charcoal-stripped FBS containing growth medium. Treatment was done every other day three times, and the culture media was replenished at the time of each treatment, as shown in Figure 1a. At the end of the treatment period, the cells were trypsinized and counted using a Coulter counter (Model ZF; Coulter Electronics, Hertfordshire, UK). To determine whether these treatments show any effect on the viability of normal breast epithelial cells, a trypan blue cell viability assay was done. Briefly, HBEC cells were treated using the same protocol; however, there was no serum starving step as the culture media was already

serum-free. At the end of the treatment period, the cells were trypsinized, washed with PBS, and then stained with 0.4% trypan blue (Sigma). The viable cells were counted directly using a light microscope.

Clonogenic survival assay

After the completion of the usual in vitro treatment regimen, 5 000 cells from control and each treatment group were plated onto each well of standard six-well plates supplemented with FBS containing regular growth medium. The media was replenished every 3–4 days, and after 10–14 days from initial plating, the media was removed. The cells were then fixed with methanol: acetic acid at 3:1 ratio for 20 min at room temperature. Afterward, the fixing solution was removed, and the fixed cells were incubated for 15 min with the staining solution containing 0.5% crystal violet. The cells were then washed with water, dried overnight, and the next day the colonies were counted under a light microscope. A nonoverlapping group of at least 50 cells was considered as one colony, as described before[8].

***In vivo* models**

All *in vivo* procedures were done in compliance with the McGill University Facility Animal Care Committee approved protocol. Two mouse models were used: MMTV-PyMT transgenic mice (FVB background) and syngeneic FVB mice (in which the PyMT-R221A cells were injected via intratibial route). Only the female animals were used for experiments, and the number of animals in one cage ranged between 2 and 5. All animals

were housed at a 12 h light–dark cycle and had access to water and standard food (Teklad rodent diet 2918 containing 0.4% methionine and 1.5 IU/g of Vitamin D3) *ad libitum.*

(a) MMTV-PyMT transgenic mice:

The MMTV-PyMT mice develop spontaneous mammary tumors at around week 5-6 weeks (Day 35-42) after birth and by week 10-12 (Day 70-84)[24]. Therefore, on week 4 (Day 28) after birth, the MMTV-PyMT mice were randomized and treated in four different groups: phosphate buffer saline (PBS) as the vehicle-treated controls, a group of animal receiving 160.0 mg/kg/day of SAM via oral gavage, a group receiving 40.0 ng/kg/day 25(OH)D by intraperitoneal injection (i.p.) injection, and at the last group receiving both SAM and 25(OH)D (n=8/group). The diameters of primary mammary tumors were measured at weekly intervals using a caliper, and tumor volumes from different animals were calculated using the following formula: $V= (length \times Width^2)/2$. At the experimental endpoint, the animals were sacrificed, and different tissues were collected for downstream analysis. Tumor growth inhibition (TGI) at sacrifice was determined using the following formula: $100*(1-T_t/T_0)$, where T_t and T_0 refer to the average volumes of tumors for a given treatment group and control respectively[43].

(b) Intratibial model for skeletal metastasis

Murine PyMT-R221A cells were implanted into the tibia of female syngeneic FVB mice to assess whether SAM, 25(OH)D, and SAM+25(OH)D treatment could reduce breast tumor cell growth in the skeleton. The PyMT-R221A cells were initially isolated from MMTV-PyMT (or MMTV-PyVT) tumors[16] and have been shown to form tumors

within two weeks when injected into the intratibial region[25,26]. Briefly, $2x10^5$ PyMT-R221A cells were injected into the tibial region of 4-6-week-old female FVB albino mice. On day three post tumor cell implantation, the mice were randomized into four different groups and treated daily with vehicle (PBS), 160.0 mg/kg/day of SAM via oral gavage, 40.0 ng/kg/day 25(OH)D by i.p. injection and a combination of SAM+25(OH)D until sacrifice on day 14 (n=9/group). Afterwards the tibias were collected, fixed using Periodate-Lysine-Paraformaldehyde (PLP) solution, and decalcified for further histological assessment. The decalcified tibias were then dehydrated and embedded in paraffin before Haemotoxylin and Eosin (H&E) staining at the Research Institute of the McGill University Health Centre (RI-MUHC) histopathology platform. Tumor area from the H&E stained bone sections was determined using the Image J (Fiji plugin) software.

Immunohistochemistry

Immunohistochemical assessment of the formalin-fixed mammary tumor tissues from control and different treatment groups was done using an antibody against Ki67 (Cat# M7240, Dako, Glostrup, Denmark). The Ki67 positive proliferating cells from randomly selected fields from each group was determined by an automated approach using 'ImmunoRatio'[44].

Measurement of serum levels of SAM, 25(OH)D, 1,25(OH)2D, and 24,25(OH)2D

For the time-course experiment of SAM bioavailability (Supplementary File 1, Figure S5a), animals were treated with SAM and blood was collected by cardiac puncture

at different time points (15, 30, 60, 120, and 240 min) after administration. We also collected blood from an animal just before administration and plotted it as the baseline ($t = 0$). The serum was collected from the supernatants after centrifugation. For the experimental animals (Supplementary File 1, Figure S5b), serum was collected from 11-week-old SAM-treated mice within an hour after SAM administration by gavage. For comparison, serum was collected from the 11-week-old animals from the control group. Afterward, the protein contents of the serum were removed by acetonitrile precipitation, and the remainder was injected into the AB SCIEX SelexION™ (Framingham, Massachusetts, USA) for LC/MS-MS separation at the Proteomics Core Facility of the RI-MUHC. The data obtained were analyzed using Analyst TF 1.7 software (SCIEX, Framingham, Massachusetts, USA).

Measurement of serum 25(OH)D, 1,25$(OH)_2$D, and 24,25$(OH)_2$D levels in control and 25(OH)D treated animals was done by LC/MS-MS at the Heartland Assays Inc. (Ames, IA, USA).

RNA extraction and quantitative real-time PCR (qPCR)

Total RNA was extracted using the AllPrep DNA/RNA Mini Kit (Qiagen; Cat# 80204) following the standard protocol provided by the manufacturer. The qPCR assay was performed following our previously described protocol[12]. The list of primers used in this study is shown in Supplementary File 1, Table S2 and S3. Gene expression changes between the control and different treatment groups were carried out as described previously[45].

RNA Sequencing and analysis pipeline

For RNA Sequencing, biological replicates from the vehicle (control), 200 μM SAM, 100 nM 25(OH)D, and SAM+25(OH)D-treated PyMT-R221A cells was used (n=3 for all except 25(OH)D where n=2). Sample quality control was performed using the Agilent 2100 Bioanalyzer. Qualifying samples were then prepped following the standard protocol for the NEBnext Ultra ii Stranded mRNA (New England Biolabs). Sequencing was performed on the Illumina NextSeq 500 with paired end 43bp × 43bp reads. The RNA-seq data were processed and interpreted with the Genialis visual informatics platform (https://www.genialis.com). An automated data analysis pipeline run in the Genilais platform consisted of the following: Sequence quality checks were performed on raw and trimmed reads with FastQC (http://www.bioinformatics.babraham.ac.uk/projects/fastqc). Trimmomatic was used to trim adapters and filter out poor quality reads[46]. Trimmed reads were then mapped to the mm10 reference genome using the HISAT2 aligner[47]. Gene expression levels were quantified with HTSeq-count[48], and differential gene expression analyses were performed with DESeq2[49]. Lowly-expressed genes, which have expression count summed over all samples below 10, were filtered out from the differential expression analysis input matrix.

Behavior test

The open field test was performed and analyzed as described before[8].

Statistical and bioinformatics analyses

Results are expressed as the mean ± standard error of the mean (SEM). Statistical significance was carried out by Student's *t*-test and ANOVA depending on the type of data. A *P* value of less than or equal to 0.05 was considered statistically significant. The statistical significance of the overlapping genes between different transcriptome-wide studies was determined by a hypergeometric test using RStudio, where the total number of genes was arbitrarily set at 25000 to avoid cross-platform gene expression discrepancies. The pathway enrichment and GO analysis from different gene lists was carried out by using ConsensusPathDB[50], Gene Set Enrichment Analyses (GSEA)[51], and Metascape[52]. Protein-protein interaction was analyzed by the STRING database (https://string-db.org/).

Authors' contributions

SAR and MS conceived the study and experimental design. NM and AA carried out the experimental procedures. All data analysis was carried out by NM and AA. WJM provided MMTV-PyMT breeding pair and advised regarding breeding. NM wrote the manuscript with SAR and MS. All authors read and approved the final manuscript.

Conflict of interests

MS is the founder of HKG Epitherapeutics and Montreal EpiTerapia. All other authors declare no competing financial interests.

Acknowledgement

This work was supported by grants from the Canadian Institutes for Health Research “MOP 130410” to S.A.R. and M.S. and “PJT-156225” to S.A.R. N.M is the recipient of Fonds de la recherche en santé du Québec (FRQS) Doctoral fellowship from the Government of Quebec, Canada.

References

1 Torre, L. A. *et al.* Global cancer statistics, 2012. *CA: a cancer journal for clinicians* **65**, 87-108 (2015).

2 Singletary, S. E. & Connolly, J. L. Breast cancer staging: working with the sixth edition of the AJCC Cancer Staging Manual. *CA: a cancer journal for clinicians* **56**, 37-47 (2006).

3 Deeb, K. K., Trump, D. L. & Johnson, C. S. Vitamin D signalling pathways in cancer: potential for anticancer therapeutics. *Nature reviews cancer* **7**, 684 (2007).

4 Davis, C. D. Vitamin D and cancer: current dilemmas and future research needs–. *The American journal of clinical nutrition* **88**, 565S-569S (2008).

5 Rohan, T. Epidemiological studies of vitamin D and breast cancer. *Nutrition reviews* **65**, S80-S83 (2007).

6 Ng, K. *et al.* SUNSHINE: Randomized double-blind phase II trial of vitamin D supplementation in patients with previously untreated metastatic colorectal cancer. *Journal of Clinical Oncology* **35**, 3506-3506, doi:10.1200/JCO.2017.35.15_suppl.3506 (2017).

7 Manson, J. E. *et al.* Vitamin D supplements and prevention of cancer and cardiovascular disease. *New England Journal of Medicine* **380**, 33-44 (2019).

8 Mahmood, N. *et al.* Methyl donor S-adenosylmethionine (SAM) supplementation attenuates breast cancer growth, invasion, and metastasis in vivo; therapeutic and chemopreventive applications. *Oncotarget* **9**, 5169-5183 (2018).

9 Şahin, M., Şahin, E., Gümüşlü, S., Erdoğan, A. & Gültekin, M. Inhibition of angiogenesis by S-adenosylmethionine. *Biochemical and biophysical research communications* **408**, 145-148 (2011).

10 Li, T. W. *et al.* S-Adenosylmethionine and methylthioadenosine inhibit cellular FLICE inhibitory protein expression and induce apoptosis in colon cancer cells. *Molecular pharmacology* (2009).

11 Shukeir, N. *et al.* Pharmacological methyl group donors block skeletal metastasis in vitro and in vivo. *British journal of pharmacology* **172**, 2769-2781 (2015).

12 Parashar, S. *et al.* S-adenosylmethionine blocks osteosarcoma cells proliferation and invasion in vitro and tumor metastasis in vivo: therapeutic and diagnostic clinical applications. *Cancer medicine* **4**, 732-744 (2015).
13 Rossdeutscher, L. *et al.* Chemoprevention activity of 25-hydroxyvitamin D in the MMTV-PyMT mouse model of breast cancer. *Cancer Prevention Research*, canprevres. 0110.2014 (2014).
14 Mohr, S. B., Gorham, E. D., Kim, J., Hofflich, H. & Garland, C. F. Meta-analysis of vitamin D sufficiency for improving survival of patients with breast cancer. *Anticancer research* **34**, 1163-1166 (2014).
15 Townsend, K. *et al.* Autocrine metabolism of vitamin D in normal and malignant breast tissue. *Clinical Cancer Research* **11**, 3579-3586 (2005).
16 Martin, M. D. *et al.* Effect of ablation or inhibition of stromal matrix metalloproteinase-9 on lung metastasis in a breast cancer model is dependent on genetic background. *Cancer Res* **68**, 6251-6259, doi:10.1158/0008-5472.can-08-0537 (2008).
17 Evan, G. I. & Vousden, K. H. Proliferation, cell cycle and apoptosis in cancer. *Nature* **411**, 342 (2001).
18 Li, J. *et al.* Tumoral vitamin D synthesis by CYP27B1 1-α-hydroxylase delays mammary tumor progression in the PyMT-MMTV mouse model and its action involves NF-κB modulation. *Endocrinology* **157**, 2204-2216 (2016).
19 Rossdeutscher, L. *et al.* Chemoprevention activity of 25-hydroxyvitamin D in the MMTV-PyMT mouse model of breast cancer. *Cancer Prevention Research* **8**, 120-128 (2015).
20 Prichard, M. N. & Shipman Jr, C. A three-dimensional model to analyze drug-drug interactions. (1990).
21 Soica, C. *et al.* The synergistic biologic activity of oleanolic and ursolic acids in complex with hydroxypropyl-γ-cyclodextrin. *Molecules* **19**, 4924-4940 (2014).
22 Lin, E. Y. *et al.* Progression to malignancy in the polyoma middle T oncoprotein mouse breast cancer model provides a reliable model for human diseases. *The American journal of pathology* **163**, 2113-2126 (2003).
23 Leyssens, C., Verlinden, L. & Verstuyf, A. Antineoplastic effects of 1, 25 (OH) 2D3 and its analogs in breast, prostate and colorectal cancer. *Endocrine-related cancer* **20**, R31-R47 (2013).
24 Shishido, S., Delahaye, A., Beck, A. & Nguyen, T. A. The MMTV-PyVT transgenic mouse as a multistage model for mammary carcinoma and the efficacy of antineoplastic treatment. *Journal of Cancer Therapy* **4**, 1187 (2013).
25 Tauro, M. *et al.* Bone-Seeking Matrix Metalloproteinase-2 Inhibitors Prevent Bone Metastatic Breast Cancer Growth. *Mol Cancer Ther* **16**, 494-505, doi:10.1158/1535-7163.mct-16-0315-t (2017).
26 Thiolloy, S. *et al.* An Osteoblast-Derived Proteinase Controls Tumor Cell Survival via TGF-beta Activation in the Bone Microenvironment. *PLOS ONE* **7**, e29862, doi:10.1371/journal.pone.0029862 (2012).
27 Bidwell, B. N. *et al.* Silencing of Irf7 pathways in breast cancer cells promotes bone metastasis through immune escape. *Nature Medicine* **18**, 1224 (2012).

28 Wan, Q. *et al.* BioXpress: an integrated RNA-seq-derived gene expression database for pan-cancer analysis. *Database* **2015** (2015).
29 Mahmood, N. & Rabbani, S. A. in *Human Cell Transformation* 179-196 (Springer, 2019).
30 Cheishvili, D., Boureau, L. & Szyf, M. DNA demethylation and invasive cancer: implications for therapeutics. *British journal of pharmacology* **172**, 2705-2715 (2015).
31 Mahmood, N. & Rabbani, S. A. DNA methylation and breast cancer: mechanistic and therapeutic applications. *Trends Cancer Res* **12**, 1-18 (2017).
32 Rawson, J. B. *et al.* Vitamin D intake is negatively associated with promoter methylation of the Wnt antagonist gene DKK1 in a large group of colorectal cancer patients. *Nutrition and cancer* **64**, 919-928 (2012).
33 Tapp, H. S. *et al.* Nutritional factors and gender influence age-related DNA methylation in the human rectal mucosa. *Aging cell* **12**, 148-155 (2013).
34 Coleman, R. E. & Rubens, R. D. The clinical course of bone metastases from breast cancer. *Br J Cancer* **55**, 61-66 (1987).
35 Coleman, R. E. Skeletal complications of malignancy. *Cancer: Interdisciplinary International Journal of the American Cancer Society* **80**, 1588-1594 (1997).
36 Singh, G. & Rabbani, S. A. *Bone metastasis*. New Jersey: Human Press Inc; (2005).
37 Carney, M., Chary, T., Bottiglieri, T. & Reynolds, E. The switch mechanism and the bipolar/unipolar dichotomy. *The British Journal of Psychiatry* **154**, 48-51 (1989).
38 Gören, J. L., Stoll, A. L., Damico, K. E., Sarmiento, I. A. & Cohen, B. M. Bioavailability and lack of toxicity of S-adenosyl-L-methionine (SAMe) in humans. *Pharmacotherapy: The Journal of Human Pharmacology and Drug Therapy* **24**, 1501-1507 (2004).
39 Martin, M. D. *et al.* Effect of ablation or inhibition of stromal matrix metalloproteinase-9 on lung metastasis in a breast cancer model is dependent on genetic background. *Cancer research* **68**, 6251-6259 (2008).
40 Zhao, Y. *et al.* Overexpression of Interferon Regulatory Factor 7 (IRF7) Reduces Bone Metastasis of Prostate Cancer Cells in Mice. *Oncology research* **25**, 511-522, doi:10.3727/096504016x14756226781802 (2017).
41 Chiappinelli, K. B. *et al.* Inhibiting DNA Methylation Causes an Interferon Response in Cancer via dsRNA Including Endogenous Retroviruses. *Cell* **162**, 974-986, doi:10.1016/j.cell.2015.07.011 (2015).
42 Spektor, R., Tippens, N. D., Mimoso, C. A. & Soloway, P. D. methyl-ATAC-seq measures DNA methylation at accessible chromatin. *Genome Research* **29**, 969-977 (2019).
43 Ghosh, S. *et al.* TSR-033, a Novel Therapeutic Antibody Targeting LAG-3, Enhances T-Cell Function and the Activity of PD-1 Blockade In Vitro and In Vivo. *Mol Cancer Ther* **18**, 632-641, doi:10.1158/1535-7163.mct-18-0836 (2019).
44 Tuominen, V. J., Ruotoistenmäki, S., Viitanen, A., Jumppanen, M. & Isola, J. ImmunoRatio: a publicly available web application for quantitative image analysis

of estrogen receptor (ER), progesterone receptor (PR), and Ki-67. *Breast cancer research : BCR* **12**, R56-R56, doi:10.1186/bcr2615 (2010).

45 Cheishvili, D. *et al.* Synergistic effects of combined DNA methyltransferase inhibition and MBD2 depletion on breast cancer cells; MBD2 depletion blocks 5-aza-2′-deoxycytidine-triggered invasiveness. *Carcinogenesis* **35**, 2436-2446 (2014).

46 Bolger, A. M., Lohse, M. & Usadel, B. Trimmomatic: a flexible trimmer for Illumina sequence data. *Bioinformatics* **30**, 2114-2120 (2014).

47 Kim, D., Langmead, B. & Salzberg, S. L. HISAT: a fast spliced aligner with low memory requirements. *Nature methods* **12**, 357 (2015).

48 Anders, S., Pyl, P. T. & Huber, W. HTSeq—a Python framework to work with high-throughput sequencing data. *Bioinformatics* **31**, 166-169 (2015).

49 Love, M. I., Huber, W. & Anders, S. Moderated estimation of fold change and dispersion for RNA-seq data with DESeq2. *Genome biology* **15**, 550 (2014).

50 Kamburov, A., Stelzl, U., Lehrach, H. & Herwig, R. The ConsensusPathDB interaction database: 2013 update. *Nucleic acids research* **41**, D793-D800 (2013).

51 Subramanian, A. *et al.* Gene set enrichment analysis: A knowledge-based approach for interpreting genome-wide expression profiles. *Proceedings of the National Academy of Sciences* **102**, 15545-15550, doi:10.1073/pnas.0506580102 (2005).

52 Tripathi, S. *et al.* Meta-and orthogonal integration of influenza "OMICs" data defines a role for UBR4 in virus budding. *Cell host & microbe* **18**, 723-735 (2015).

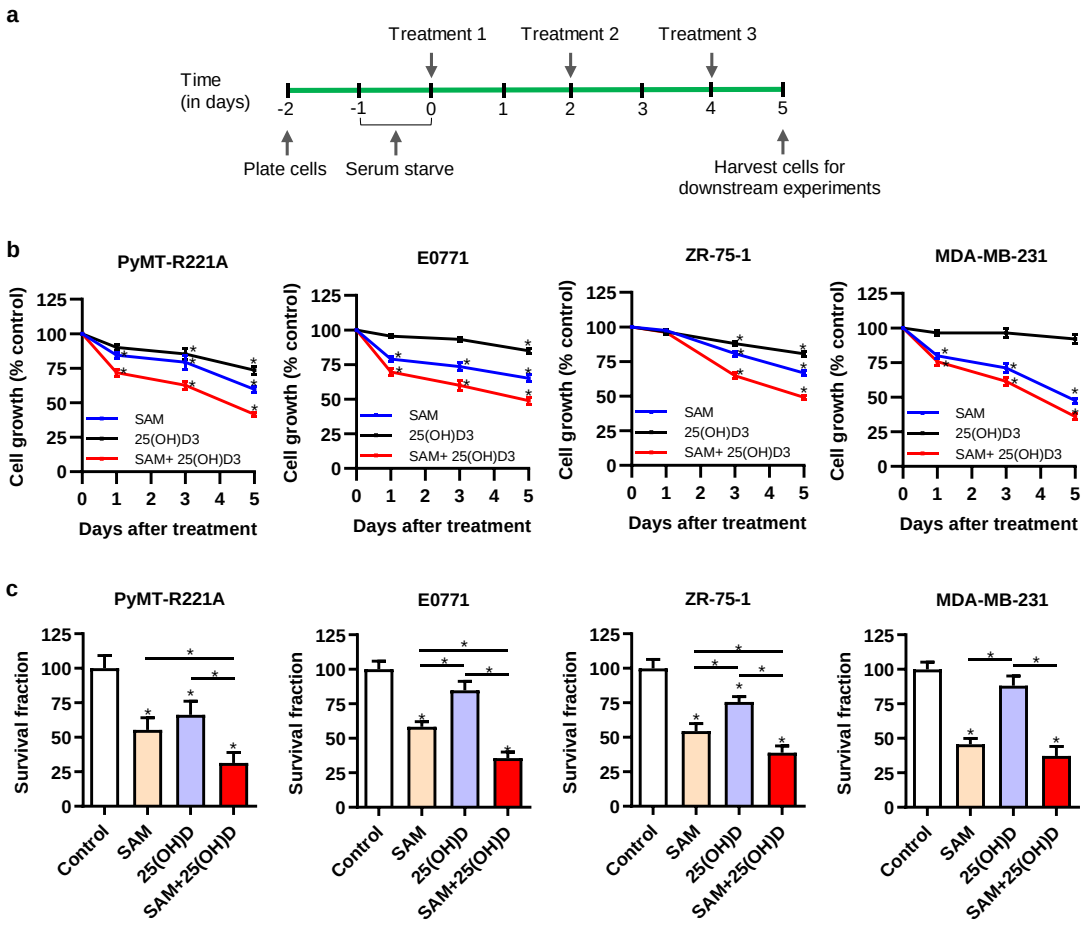

Figure 1: Effect of SAM, 25(OH)D, and their combination *in vitro*.

a Schematic of the in vitro treatment protocol. **b** Human (ZR-75-1, MDA-MB-231) and murine (PyMT-R221A, E0771) breast cancer cells were treated with vehicle alone control, SAM (200 µM) or 25(OH)D (100 nM) alone and SAM+25(OH)D every other day; and cell number was determined using Coulter counter on days 1,3, and 5 post-treatment. Results are shown as the mean ± SEM from at least five independent experiments. Significant differences from the control groups in each cell lines were determined using ANOVA followed by post hoc Tukey's test and are represented by asterisks. **c** Following treatment, $5x10^3$ cells from the control and different treatment groups were subjected to clonogenic survival assay. The culture media was refreshed every 3-4 days for a period of about two weeks, the cells were stained with crystal violet, and the total number of colonies was counted under the microscope. Results are shown as the mean ± SEM of at least five independent experiments. Significant differences were determined using ANOVA followed by post hoc Tukey's test and are represented by asterisks.

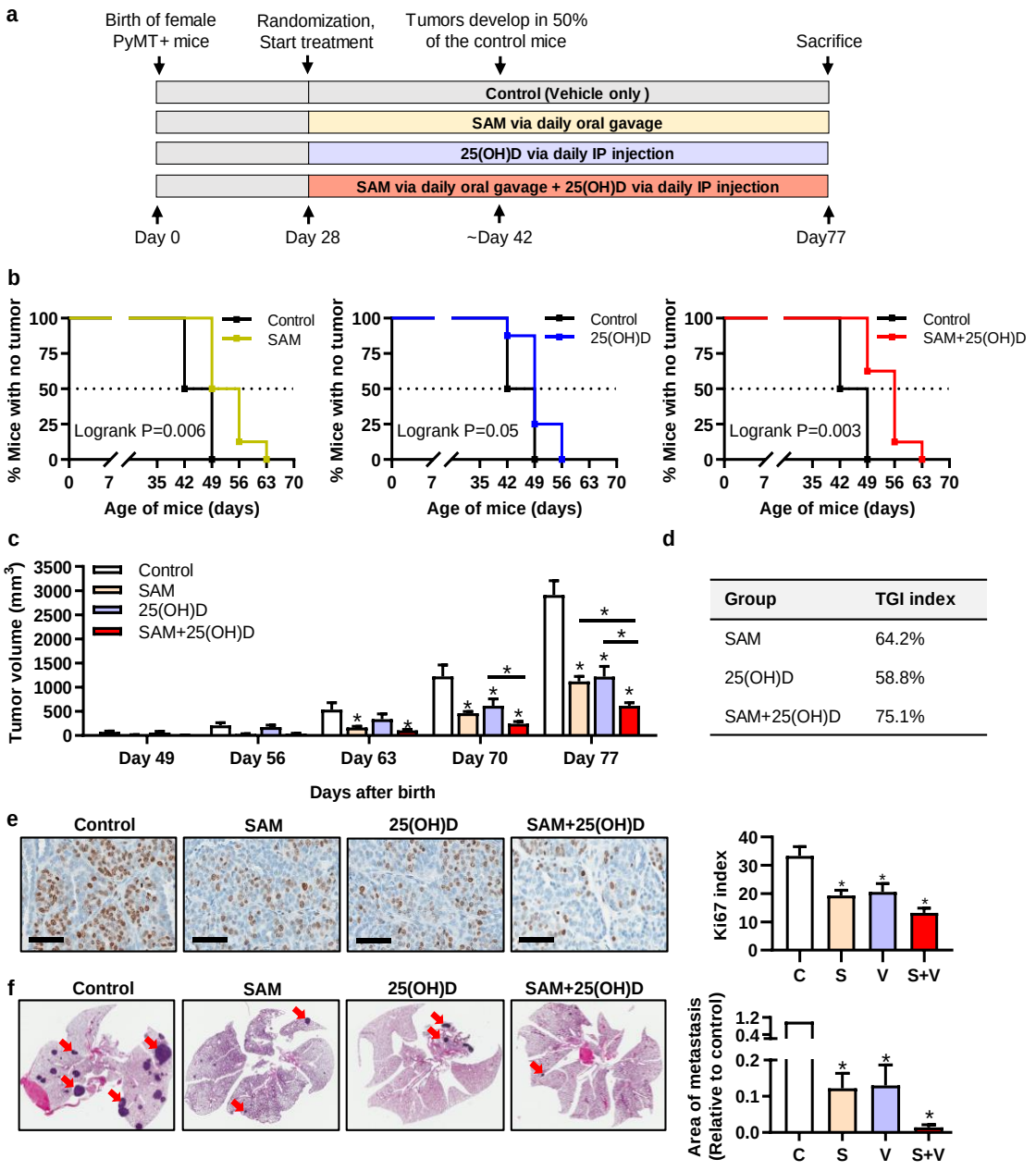

Figure 2: Effect of SAM, 25(OH)D, and their combination on mammary tumor emergence, growth, and lung metastasis in MMTV-PyMT transgenic female mice.

a Schematic representation of treatment protocol for the transgenic MMTV-PyMT mice. Briefly, female MMTV-PyMT mice were treated with vehicle alone as control, SAM (160 mg/kg/day) by daily oral gavage, 25(OH)D (40 ng/kg/day) by daily intraperitoneal (i.p) injection, and SAM+25(OH)D in combination from day 28 (week 4) after birth until the

experimental endpoint at day 77 (week 11) when the animals were all sacrificed (n=8 animals/group) and different tissues were collected for downstream experiments. **b** Kaplan-Meier curve showing the percentage of mice no tumor in control and different treatment groups, separately (n=8 animals/group). **c** Tumor volumes were measured at weekly intervals using calipers and are shown as a bar graph. Results are shown as the mean ± SEM of eight animals per group. Significant differences were determined using ANOVA followed by post hoc Tukey's test and are represented by asterisks. **d** Tumor growth inhibition (TGI) index at sacrifice was calculated using the formula described in 'Materials and Methods' and represented in a tabular format. **e** The formalin-fixed histologic sections of the mammary tumors from control and different treatment groups were probed with the antibody for ki67 proliferation marker, and representative images of the ki67 positive cells (brown color staining) is shown for different groups [scale bar size =60 μm]. The percentage of ki67 positive cells was determined and plotted as bar graphs (n=4 animals/group). **f** For the evaluation of lung metastasis, formalin-fixed histologic sections of the whole lung tissue sections from control and treated animals were stained with Haemotoxylin and Eosin (H&E) (left panel), and the relative area of metastases was quantified using the Fiji plugin (ImageJ) (right panel). The metastatic sites on the lung show darker staining patterns, as indicated by red arrowheads. Results are shown as mean ± SEM (n=4/group). The metastatic area in the control group was set to 1 for the statistical analysis for the bar graph. Here, C=control; S= SAM; V= 25(OH)D; S+V=SAM+25(OH)D treated group.

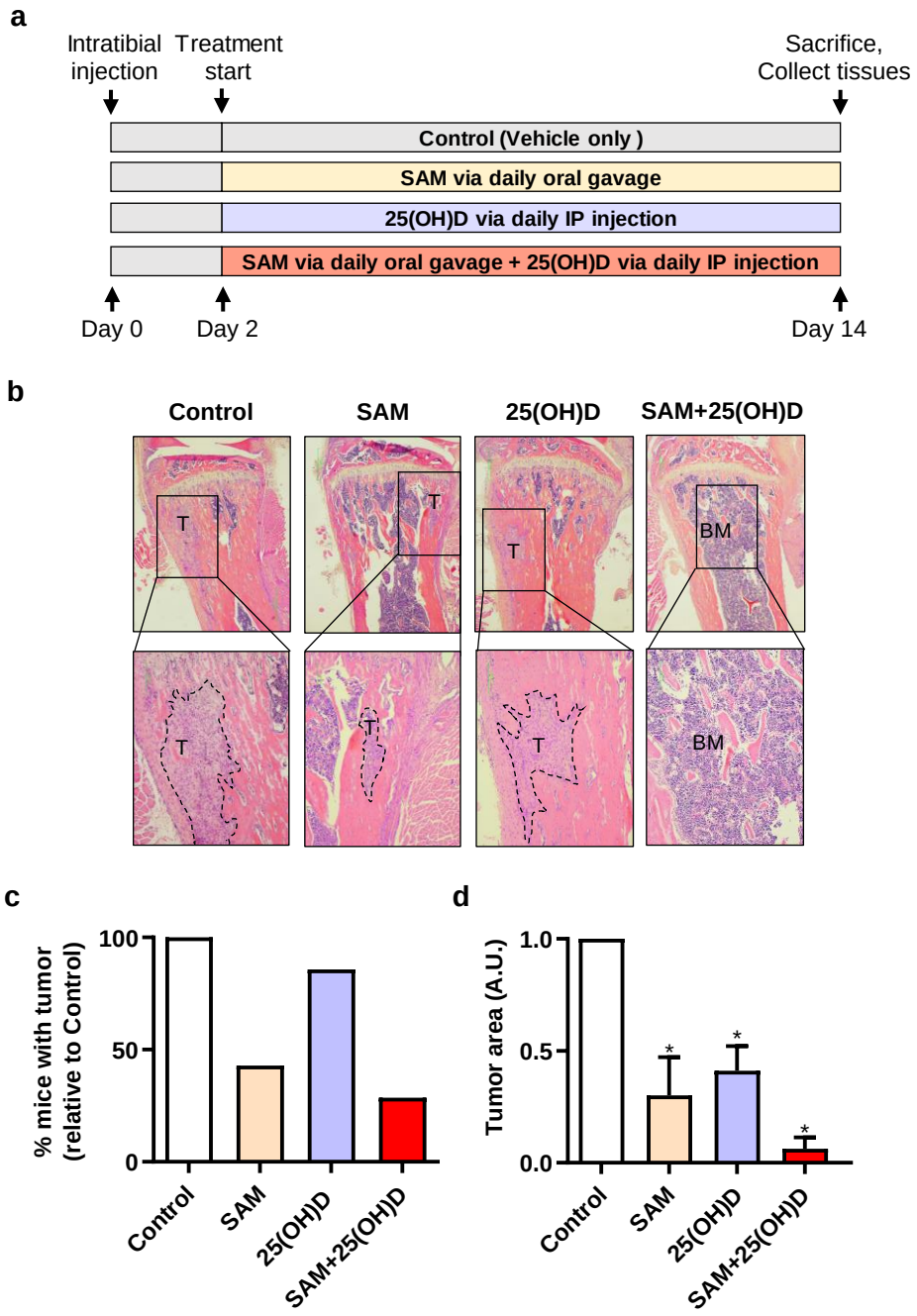

Figure 3: Effect of SAM, 25(OH)D, and their combination on breast cancer cell colonization to the bone in an intratibial model.

a Schematic representation of treatment protocol used for treating female mice (FVB background) injected with PyMT-R221A cells and then treated with vehicle alone as control, SAM (160.0 mg/kg/day) by daily oral gavage, 25(OH)D (40.0 ng/kg/day) by intraperitoneal (i.p) injection, and SAM+25(OH)D in combination from day 2 until day 14

when the mice were sacrificed (n=9 animals/group). The tibias were collected from all animals and fixed for further histologic studies. **b** Representative low (40X; upper panel) and high (100X; lower panel) magnificaion images of the formalin-fixed histologic sections of the decalcified tibias from control and treated animals stained with Haemotoxylin and Eosin (H&E), where the tumors are marked a 'T' and bone marrow as 'BM'. **c** Bar graph representing the percentage of mice that developed skeletal tumors in each group relative to the control group. **d** The relative area of tumor growth was quantified using the Fiji plugin (ImageJ), and the results are shown as mean ± SEM (n=9/group). Significant differences were determined using ANOVA followed by post hoc Tukey's test and are represented by asterisks.

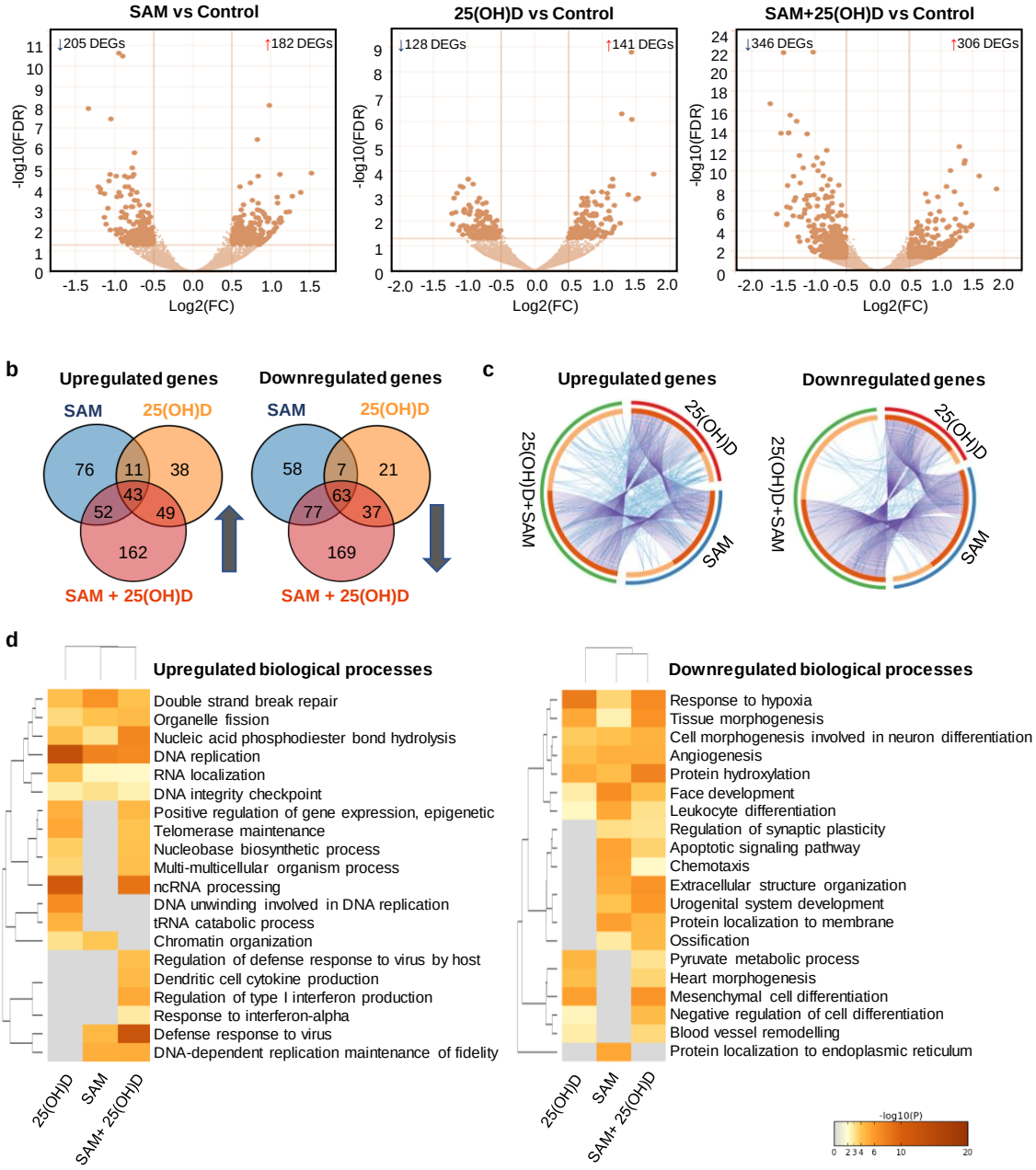

Figure 4: Transcriptome analysis of PyMT-R221A cells.

Murine PyMT-R221A cells were treated with vehicle (control), 200 μM SAM, 100 nM 25(OH)D and a combination of SAM and 25(OH)D every other day for three times (on days 0, 2, 4) using the *in vitro* treatment protocol described in Figure 1a. At the end of the experiment, RNA extracted from control and different treatment groups were subjected to RNA-Sequencing. **a** The volcano plots of the significantly differentially expressed genes

are shown (log10(FDR) versus log2FC). **b** Venn diagrams representing the frequency of common and unique genes among different treatment groups. **c** Circos plot further representing the commonality and uniqueness of the functionalities of the up- and downregulated genes from each group. Each gene from the up or downregulated gene lists has a spot on the arc. The dark orange color represents genes that are present in multiple treatment groups, and the light orange color shows genes that are unique for a treatment. In addition, the purple lines indicate the common genes that are found in different treatment groups, and the blue lines represent genes that are different but have similar functions. **d** Comparative heatmap of the Gene Ontology (GO) enrichment for biological processes for the different treatment groups, as determined by Metascape[52].

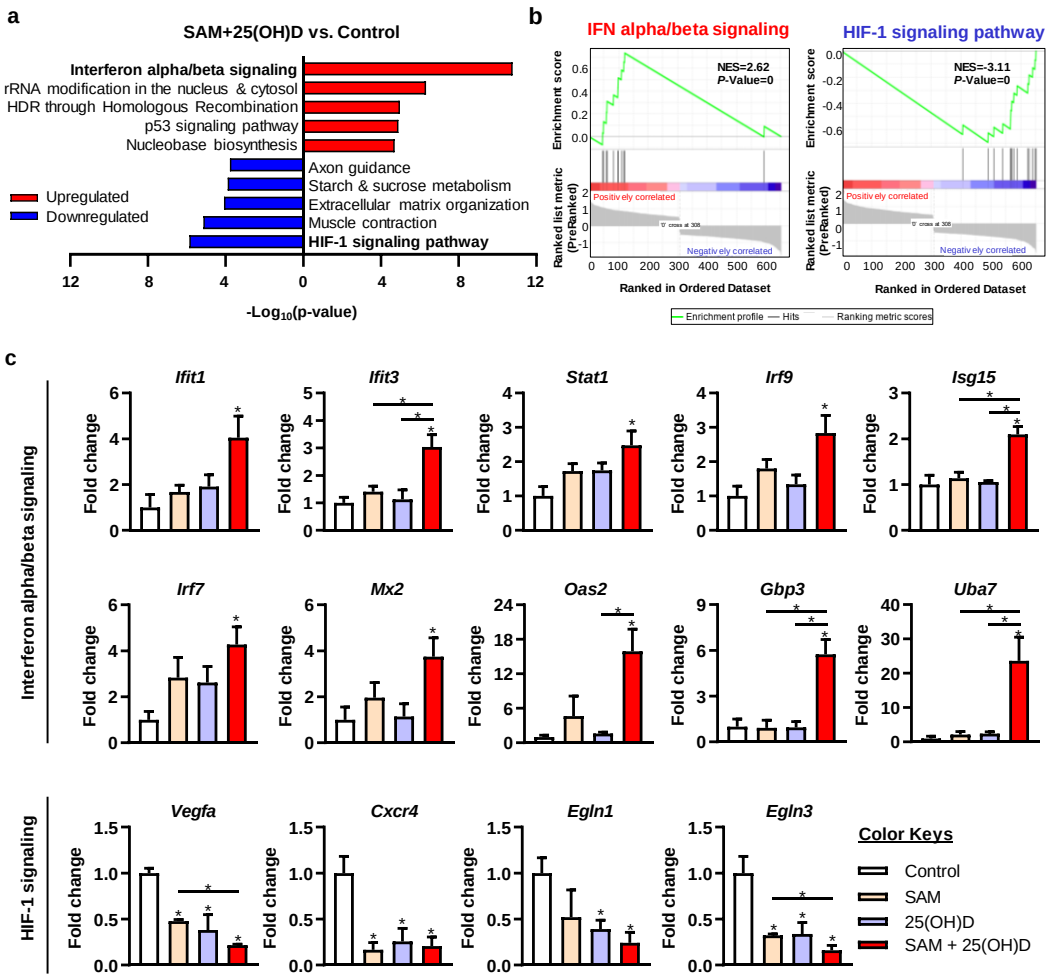

Figure 5: Functional validation of the genes identified by RNA-Sequencing.

a Pathway analysis of the up and downregulated DEGs from the SAM+25(OH)D combination-treated group was done by using the KEGG and Reactome databases. Top 5 up- and downregulated pathways are shown as bar graphs. **b** GSEA analyses further showed the enrichment of the genes from 'interferon alpha/beta signaling' and 'HIF-1 signaling pathway'. **c** RNA obtained from the control and treated PyMT-R221A cells was subjected to qPCR to validate the expression of selected genes from the 'interferon alpha/beta signaling' and 'HIF-1 signaling pathway'. Results are shown as mean ± SEM of samples obtained from at least three different experiments per group. Significant differences are represented by asterisks.

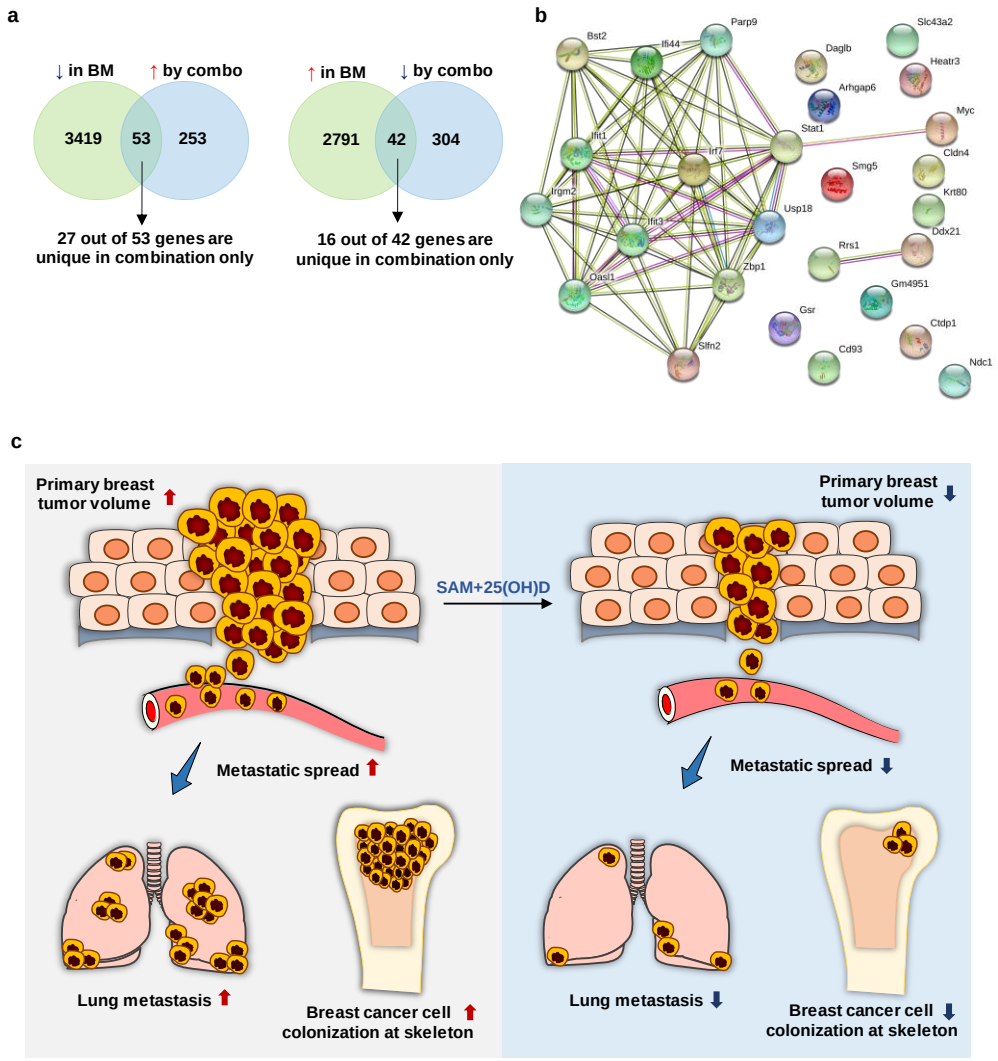

Figure 6: Comparison of DEGs in response to SAM + 25(OH)D with the DEGs in murine bone metastasis dataset.

a Venn diagram of the up and downregulated genes following combination treatment with SAM+25(OH)D that overlapped with differentially expressed genes in a murine model of breast cancer bone metastasis in GSE37975. Here, BM: Bone metastasis **b** Molecular interaction networks of the encoded proteins from the 27 uniquely upregulated genes in the combination treatment are determined by the STRING database. **c** Summary of the anti-cancer effects mediated by SAM+25(OH)D in vitro and in vivo. The combination treatment causes a significant reduction in cell proliferation and colony formation in a battery of breast cancer cell lines in vitro and reduces primary mammary tumor volume, visceral and skeletal metastasis in vivo. These anti-cancer effects were mediated through the differential

regulation of key cancer and immune-related pathways, as shown by the transcriptome analysis.

Supplementals for Chapter 4

Supplementary File 1

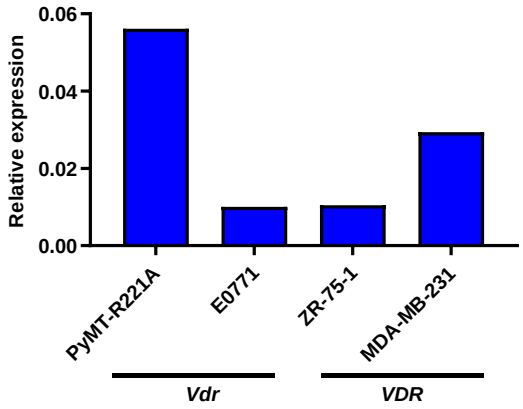

Figure S1: Expression of the gene encoding for vitamin D receptor in different human and murine breast cancer cell lines. RNA obtained from PyMT-R221A, E0771, ZR-75-1, and MDA-MB-231 cells were subjected to qPCR using mouse (*Vdr*) and human (*VDR*) specific primers to determine the basal levels of vitamin D receptor expression. The expression values were normalized using *Gapdh/GAPDH* as an internal loading control and expressed as a bar graph.

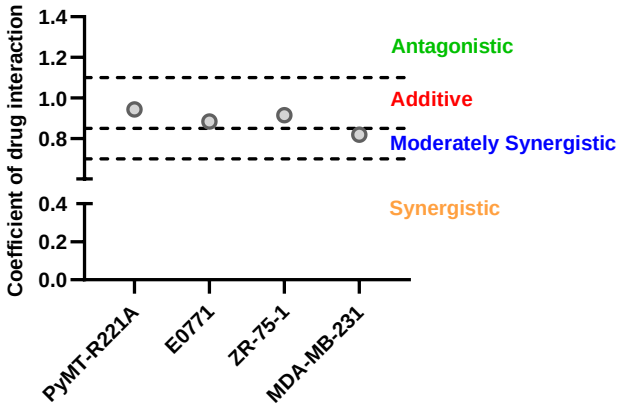

Figure S2: The coefficient of drug interaction (CDI) between SAM and 25(OH)D combination in different cell lines. The CDI values for each of the cell lines were calculated using the following equation, CDI = AB/(A × B). Here, AB: relative cell growth of the combination compared to control; A or B: relative cell growth of the single agent treated groups compared to the control. CDI < 0.7 indicates strong synergistic; CDI between 0.7 to 0.9 indicates moderately synergistic; CDI between 0.9 to 1.1 indicates additive and CDI > 1.1 indicates an antagonistic effect.

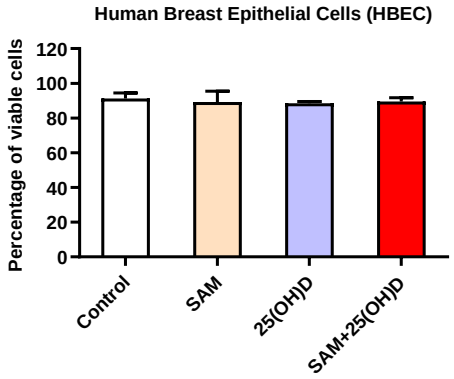

Figure S3: Effect on the viability of human breast epithelial cells (HBEC). HBEC cells were plated at the same density and treated with vehicle only control, 200 μM SAM, 100 nM 25(OH)D, and a combination of SAM+25(OH)D. At the end of the experiment, the cells were trypsinized, stained with trypan blue, and the total number of viable cells in each group was counted under a light microscope. Results are shown as the mean ± SEM (n=4). No significant difference was observed in the percentage of viable cells compared to the total number of cells in each group during the time of harvest, which indicated that the doses of the different anti-cancer agents used in this study are not toxic to the viability of the normal breast epithelial cells.

Table S1: Analyses of different biochemical parameters in the serum. The results are shown as mean ± SEM from three different mice in each group.

Parameter	Control	SAM	25(OH)D	SAM+25(OH)D
Calcium (mmol/L)	2.26 ± 0.05	2.26 ± 0.6	2.35 ± 0.02	2.40 ± 0.12
Total protein (g/L)	39.67 ± 1.36	42.33 ± 1.19	42.67 ± 0.27	44.67 ± 0.72
Albumin (g/L)	20.67 ± 0.54	22.33 ± 0.72	22.33 ± 0.27	21.67 ± 1.29
Albumin/Globulin ratio	1.1 ± 0.00	1.1 ± 0.00	1.1 ± 0.04	1.1 ± 0.04
Glucose (mmol/L)	16.1 ± 1.15	15.8 ± 0.49	15.5 ± 1.26	16.36 ± 0.66
BUN Urea (mmol/L)	9.23 ± 0.12	7.93 ± 0.48	7.23 ± 0.72	6.8 ± 0.23
Creatinine (µmol/L)	11 ± 0.81	10 ± 1.41	12.67 ± 0.54	11.33 ± 1.51
Total Bilirubin (µmol/L)	8.33 ± 1.09	9.33 ± 1.9	10.67 ± 0.98	8.67 ± 0.27
ALT (U/L)	56.6 7 ± 5.52	56.33 ± 3.95	41.67 ± 0.27	48.67 ± 3.81
Alkaline phosphatase (U/L)	71.5 ± 3.75	80.67 ± 13.37	76.67 ± 6.6	64.67 ± 4.65
Cholesterol (mmol/L)	2.82 ± 0.14	3.0 ± 0.11	2.79 ± 0.07	2.7 ± 0.18
Sodium (mmol/L)	143 ± 3.77	145.33 ± 3.81	152 ± 3.29	145.67 ± 6.36
Potassium (mmol/L)	4.16 ± 0.36	5.17 ± 0.14	4.8 ± 0.21	4.07 ± 0.22
Chloride (mmol/L)	110.67 ± 1.19	114 ± 2.05	118.67 ± 2.22	116.33 ± 4.72
Phosphorus (mmol/L)	2.79 ± 0.35	2.35 ± 0.03	2.64 ± 0.24	2.92 ± 0.13
Magnesium (mmol/L)	1.06 ± 0.03	1.0 ± 0.05	1.11 ± 0.06	1.05 ± 0.05

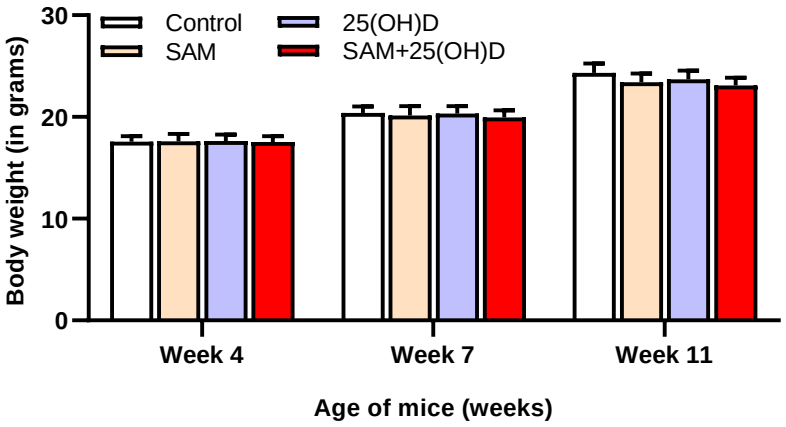

Figure S4: Total bodyweight of the transgenic MMTV-PyMT animals. The control and treated MMTV-PyMT animals are weighed at different time intervals from the beginning of the treatment regimen on week 4 after birth until sacrifice on week 11. No significant difference was observed in the total bodyweight of the animals from different treatment arms.

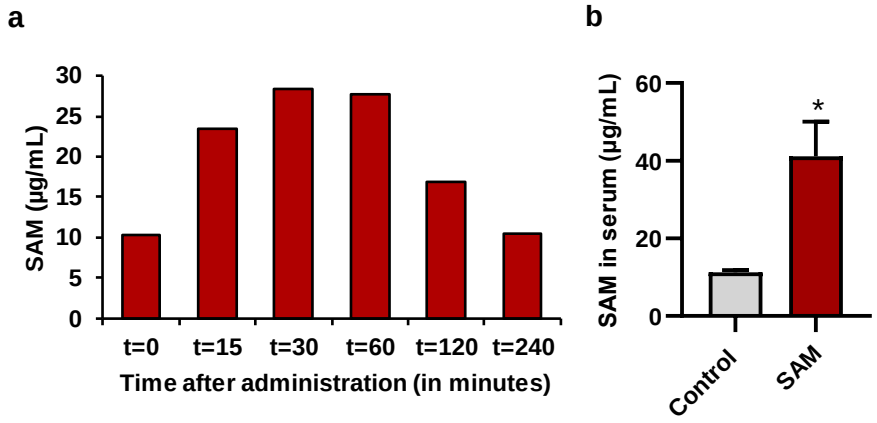

Figure S5: SAM bioavailability in the serum. a The SAM level in the serum of control and SAM-treated animals was assessed at different time points following oral gavage. Each bar represents the concentration obtained from the LC-MS/MS peak intensity for SAM at a specific time-point. Here, t=0 represents the baseline value of SAM just before treatment. The highest peak of SAM bioavailability in the serum was found between 30 to 60 minutes after administration, and the level comes down to the baseline at around 240 minutes after administration. **b** The serum from control (n=3) and SAM-treated (n=5) experimental animals were collected, and LC-MS/MS was done to determine the levels of SAM. Results are shown as the mean ± SEM. Significant differences were determined using a student's *t*-test and are represented by asterisks.

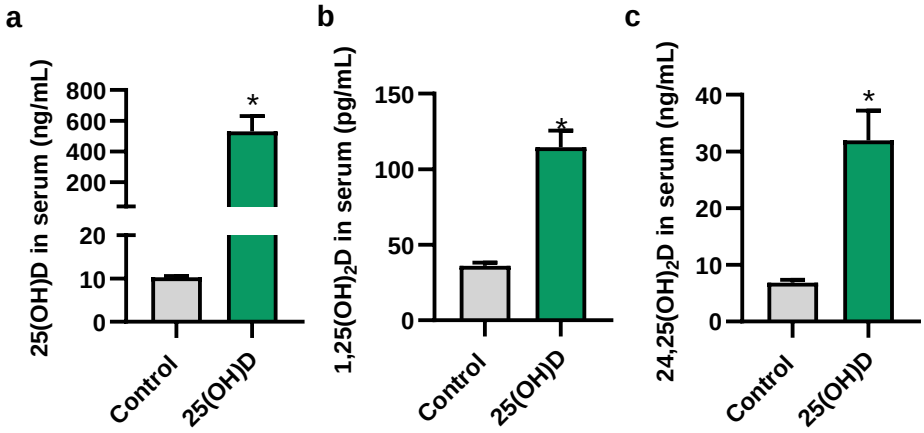

Figure S6: Serum levels of 25(OH)D,1,25(OH)$_2$D, and 24,25(OH)$_2$D. LC-MS/MS assays were done from the serum obtained from control (n=3) and 25(OH)D-treated (n=5) experimental animals to determine the levels of 25(OH)D (**a**), 1,25(OH)$_2$D (**b**) and 24,25(OH)$_2$D (**c**). Results are shown as the mean ± SEM. Significant differences were determined using a student's *t*-test and are represented by asterisks.

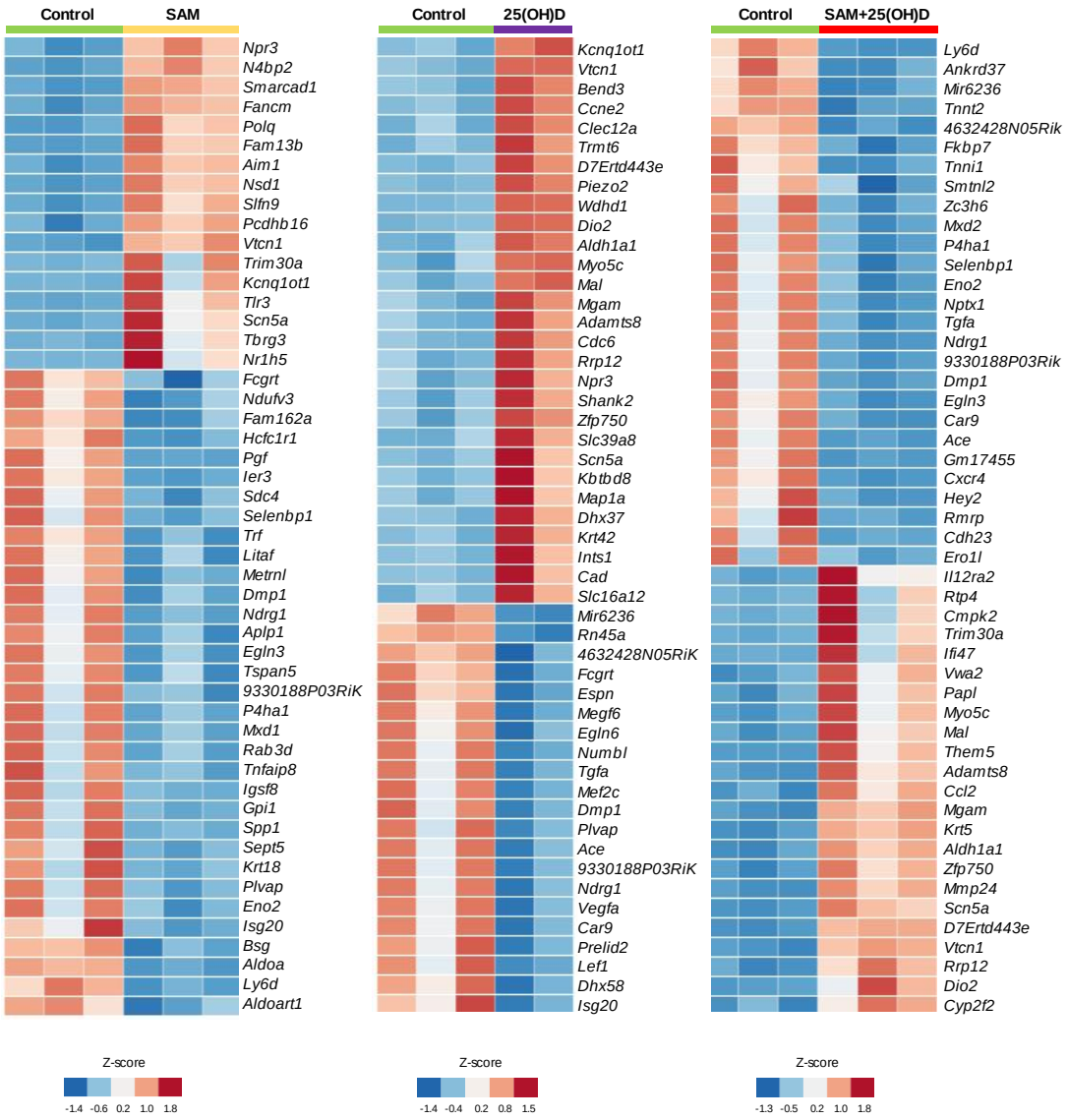

Figure S7: Heatmap of the top 50 significantly DEGs in each of the three treatment groups (log_2 fold change>0.5 and FDR<0.05).

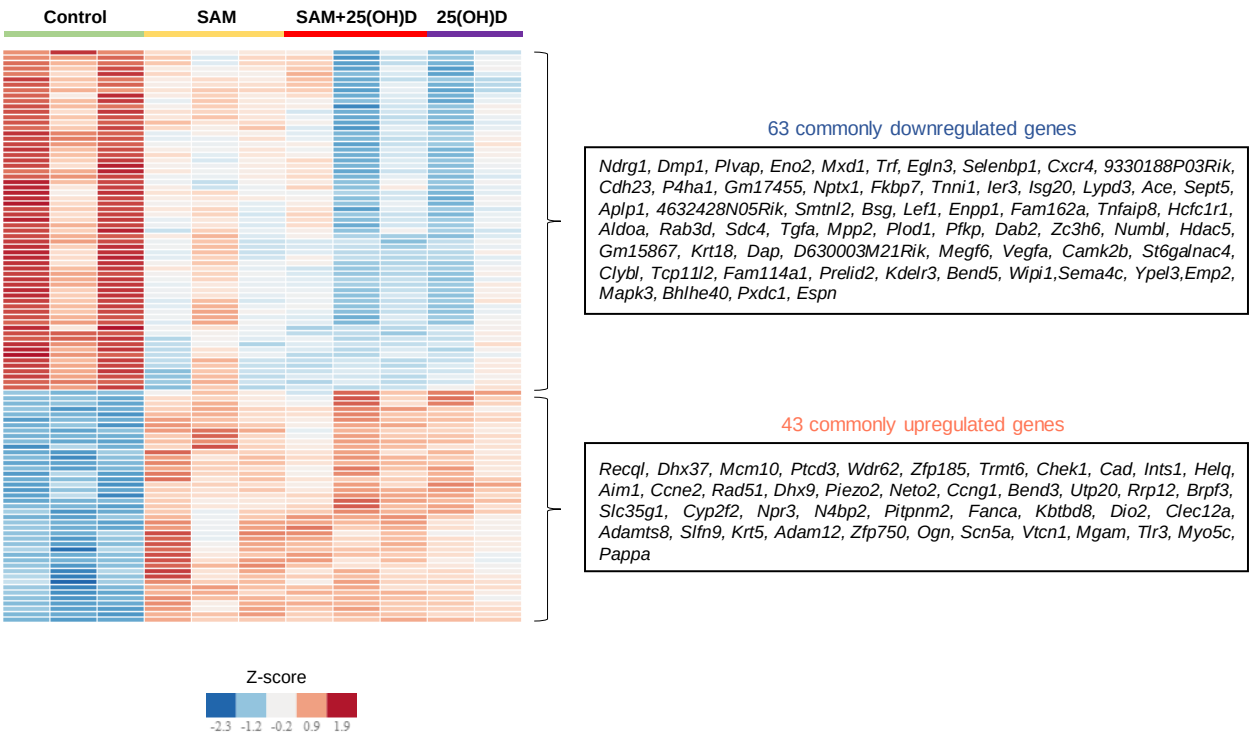

Figure S8: Heatmap of 106 common DEGs in each of the three treatment groups (log_2 fold change>0.5 and FDR<0.05). The lists of the commonly up and downregulated genes are shown within the boxes on the right.

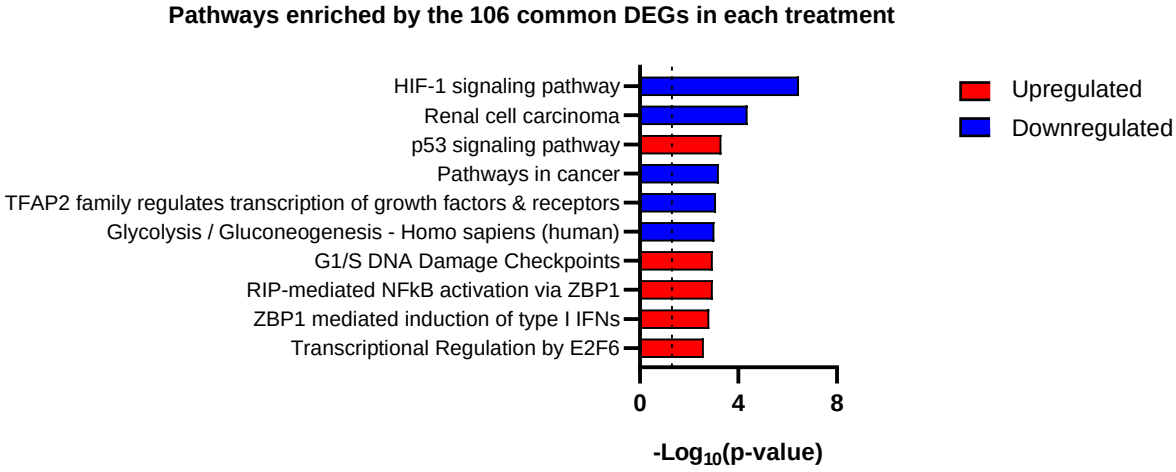

Figure S9: Enriched pathways affected by the genes that are commonly up and downregulated by all three treatment groups relative to the control PyMT-R221A cells. The pathways enriched with up and downregulated genes are shown in 'red' and 'blue', respectively. Top five up and top 5 downregulated pathways are shown together as a bar graph. The 'HIF-1 signaling pathway', which is enriched with the downregulated genes from all three treatment groups, showed the highest statistical significance (*P*= $3.42x10^{-07}$).

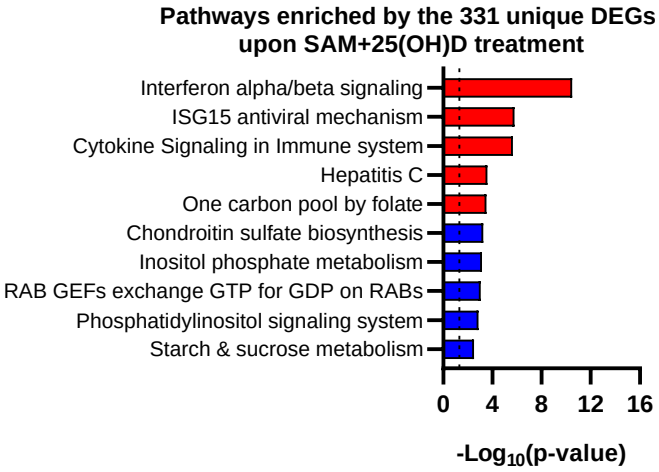

Figure S10: Enriched pathways and biological affected by the genes that are uniquely up and downregulated by SAM+25(OH)D treatment relative to the control PyMT-R221A cells. The pathways enriched with up and downregulated genes are shown in 'red' and 'blue', respectively. Top five up and top 5 downregulated pathways are shown together as a bar graph. An enrichment of several immune-related signaling pathways is seen when the analysis was done using the genes that are uniquely upregulated by SAM+25(OH)D. Interferon alpha/beta signaling pathway showed the highest statistical significance (*P*=$3.33x10^{-11}$).

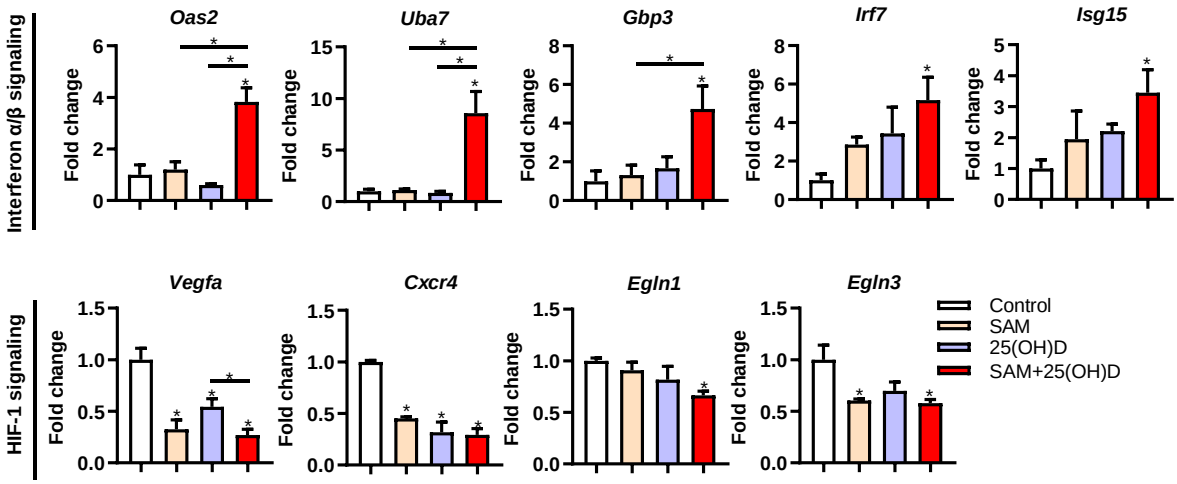

Figure S11: qPCR from RNA obtained from primary tumors. Briefly, total RNA obtained from the primary tumors of control and treated animals (from Figure 2) were subjected to qPCR to validate the expression of selected genes from the 'interferon alpha/beta signaling' and 'HIF-1 signaling pathway'. Results are shown as mean ± SEM of RNA obtained from at least three animals per group. Significant differences are denoted by an asterisk.

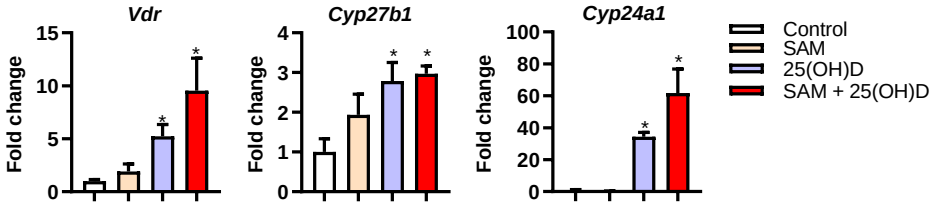

Figure S12: Expression of *Vdr*, *Cyp27b1*, and *Cyp24a1* in PyMT-R221A cells. Briefly, total RNA obtained from the control and treated PyMT-R221A cells were subjected to qPCR to validate the expression of *Vdr*, *Cyp27b1*, and *Cyp24a1*. Results are shown as mean ± SEM of RNA obtained from at least three different experiments. Significant differences are denoted by an asterisk.

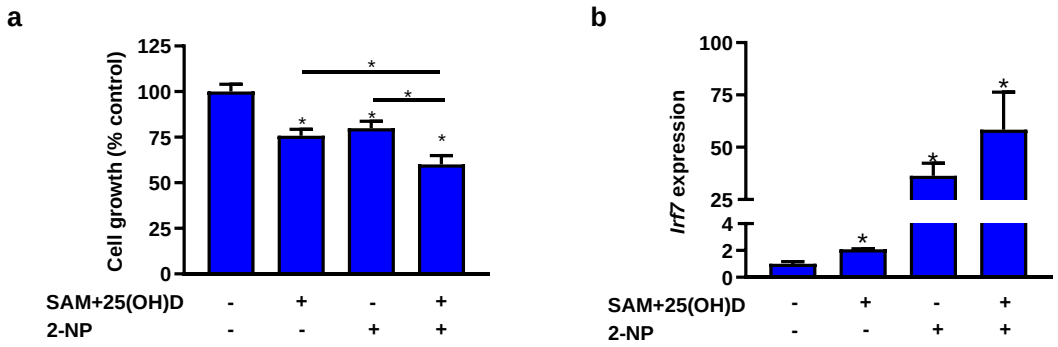

Figure S13: Effect of Stat1 activator on proliferation. **a** The PyMT-R221A cells were plated on 24 well plates and treated with vehicle control or SAM+25(OH)D for 24 hours. On the other hand, 25μM 2-(1,8-naphthyridin-2-yl)-Phenol (2-NP) [Sigma] was added directly into the media for 5 hours; the media was then removed and replenished with either regular culture media (for 2-NP monotherapy group) or media with SAM+25(OH)D for triple therapy treated group for 19 hours. At the end of 24 hours, cells were trypsinized and counted directed using a Coulter counter. Statistical analysis was done using ANOVA followed by *post hoc* Tukey's test from the data obtained from three independent experiments. **b** Total RNA obtained from the four different groups was subjected to qPCR to validate the increased expression of *Irf7*, which is a downstream target of the Stat1 transcription factor. A significant increase in the expression of *Irf7* was observed in all three treatment groups with the highest expression in the triple therapy group. It should be noted the cells were treated once for a period of 24 hours for this experiment in contrast to the other *in vitro* experiments during this study, where the cells were treated three times every second day. Hence, the level of *Irf7* increase upon SAM+25(OH)D treatment is less in Figure S13b compared to Figure 5c. Results are shown as mean ± SEM of RNA obtained from three experiments. Significant differences are denoted by an asterisk.

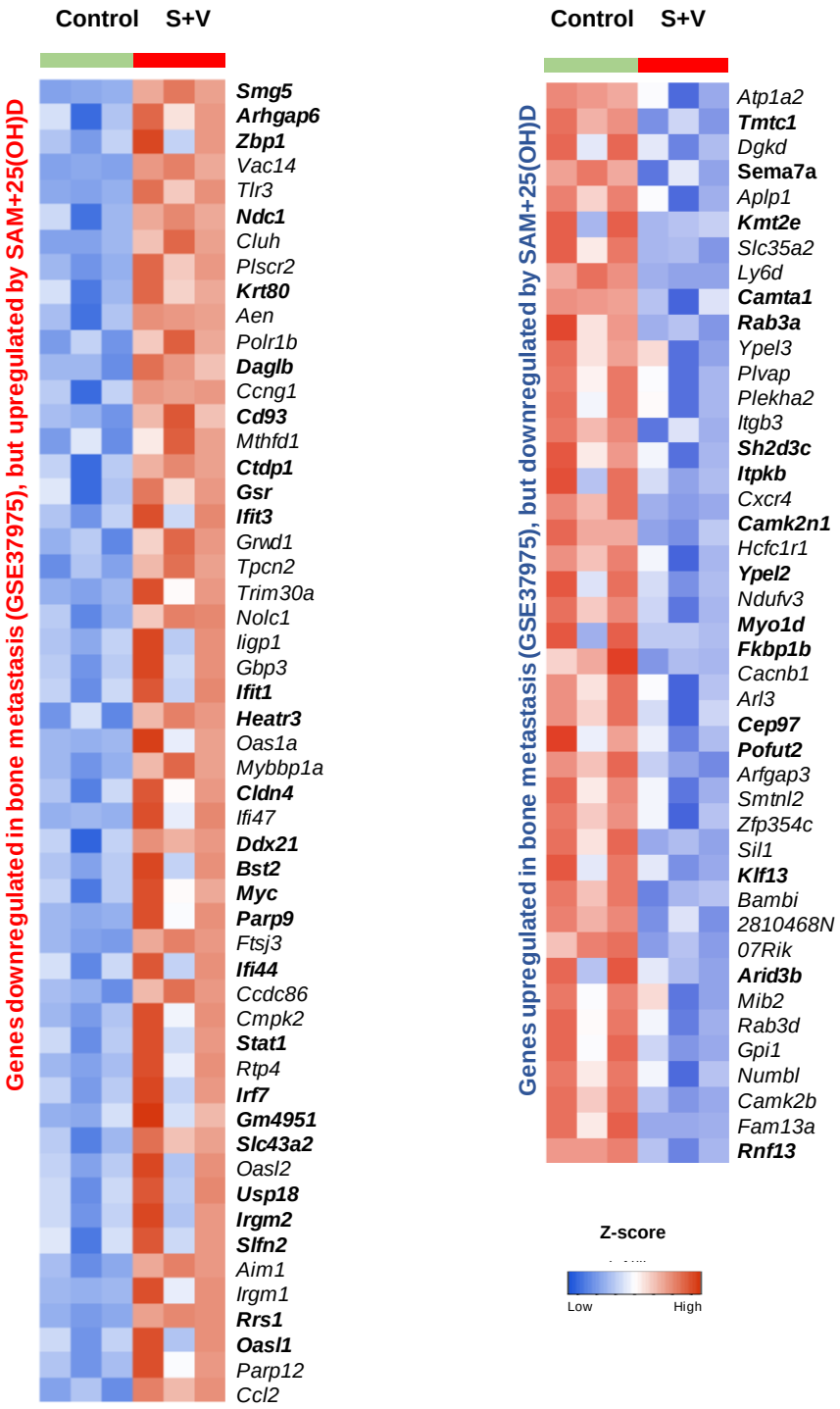

Figure S14: Heatmap of the significantly 53 upregulated and 42 downregulated genes following combination treatment with SAM+25(OH)D [denoted by 'S+V' in the figure], which are also differentially expressed in GSE76772 in the opposite direction. Moreover, 27 out of the 53 upregulated and 16 out of the 42 downregulated genes are significantly differentially regulated by the combination treatment only according to the cut-off set during RNA-Seq analysis. The genes unique in combination treatment only are shown by bold letters in the heatmap.

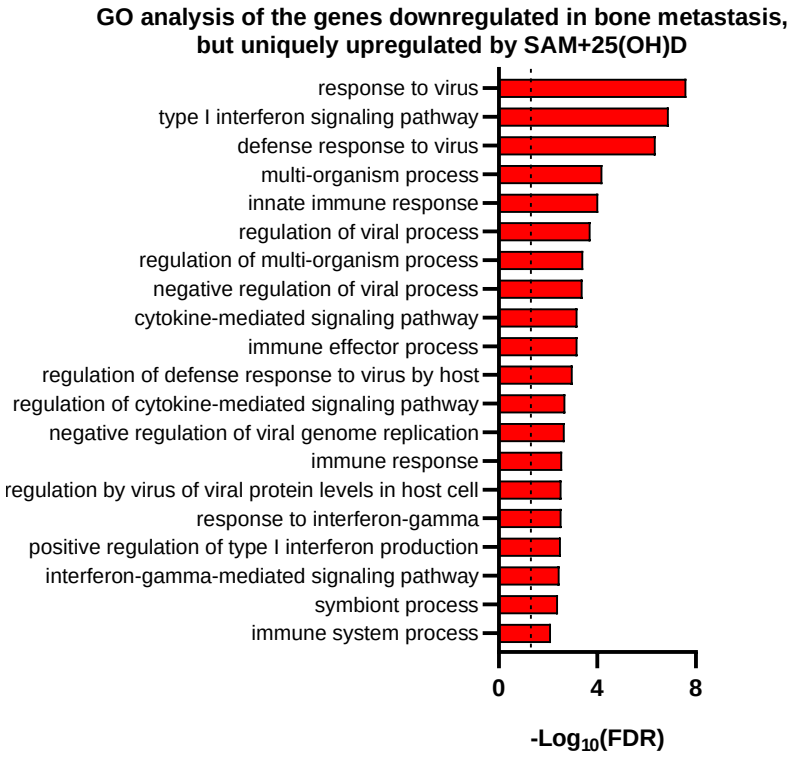

Figure S15: GO analysis of the 27 uniquely upregulated genes by SAM+25(OH)D that are downregulated in the bone metastasis dataset (GSE76772). The top 20 significant hits are shown as a bar graph where a significant enrichment of immune-related signaling pathways is seen.

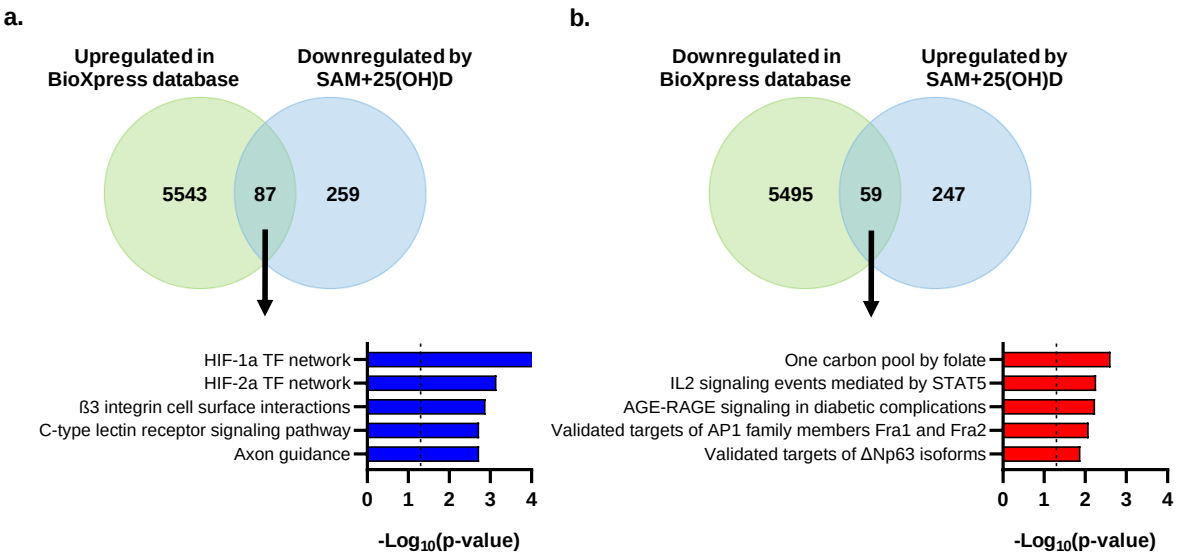

Figure S16: Comparison of DEGs in response to SAM + 25(OH)D with human breast cancer genes. **a** Venn diagram of the downregulated genes following combination treatment with SAM+25(OH)D showed an overlap of 87 genes that are upregulated in the human breast tumors in the BioXpress database. Pathway analysis of these genes is shown in the bar graph below (in blue). Out of these 87 overlapped genes, 36 are uniquely regulated by the combination only. **b** Venn diagram of the upregulated genes following combination treatment with SAM+25(OH)D showed an overlap of 59 genes that are downregulated in the human breast tumors in the BioXpress database. Pathway analysis of these genes is shown in the bar graph below (in red). Out of these 59 overlapped genes, 31 are uniquely regulated by the combination.

a

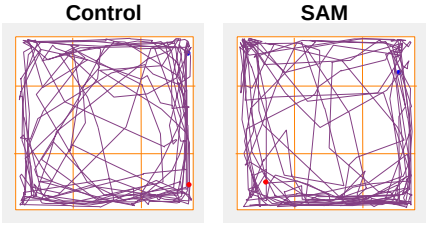

b

Open field test parameters	Control	SAM-treated	*P*-value
Total distance travelled (m)	29.7 ± 1.3	30.3 ± 1.9	0.83
Average speed (m/s)	0.1 ± 0.003	0.1 ± 0.006	0.74
Number of entries to the center zone	10.7 ± 0.9	10.6 ± 0.9	0.92
Time in the center zone (s)	7.5 ± 0.9	6.9 ± 0.9	0.65
Distance travelled in the center (m)	1.6 ± 0.1	1.6 ± 0.2	0.78

Figure S17: Assessment of animal behavior upon SAM-treatment. a Representative track plots from the video recordings of control and SAM-treated animals generated by using ANY-maze software are shown in the right panel. **b** Different parameters determined from the open field test of control and SAM-treated mice are provided in a tabular format. Results are shown as mean ± SEM (n=7). No significant alterations in animal behavior were observed upon SAM-treatment.

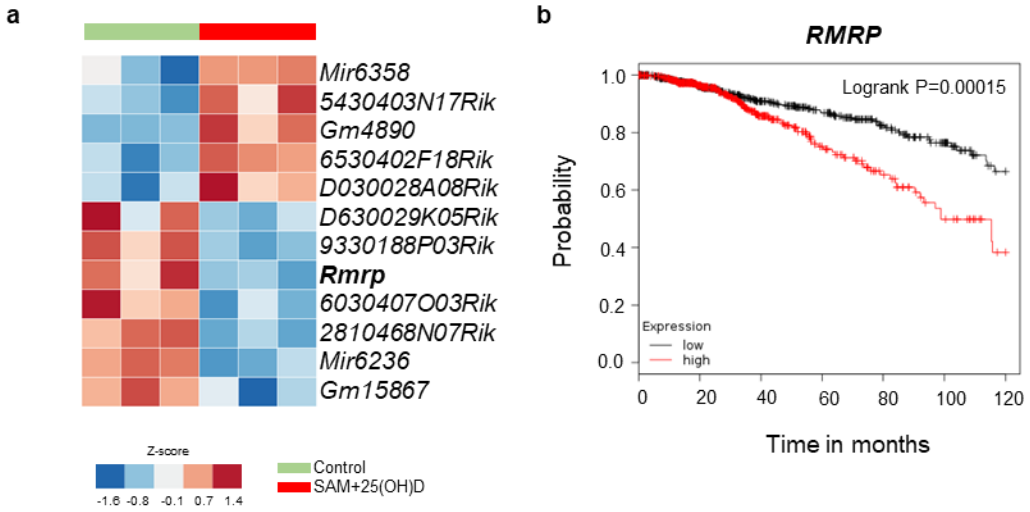

Figure S18: Differentially regulated non-coding RNAs upon SAM+25(OH)D combination treatment. a Heatmap of the significantly differentially expressed non-coding RNAs in SAM+25(OH)D combination relative to control cells. The expression of *Rmrp*, a known long non-coding RNA with oncogenic function, is downregulated by the combination treatment. **b** Kaplan-Meier survival plot from RNA-Seq data of 1089 breast cancer patients reveals that higher expression of the human *RMRP* gene is associated with poor overall survival.

Table S2: The mouse specific primers used in this study are listed below[1-9]

Gene Name		Sequences used for qPCR (5'→ 3')
Vegfa	For	CCACGTCAGAGAGCAACATCA
	Rev	TCATTCTCTCTATGTGCTGGCTTT
Cxcr4	For	TCCTCCTGACTATACCTGACTTCATCT
	Rev	CCTGTCATCCCCCTGACTGAT
Egln1	For	GCCCAGTTTGCTGACATTGAAC
	Rev	CCCTCACACCTTTCTCACCTGTTAG
Egln3	For	AGGCAATGGTGGCTTGCTATC
	Rev	GCGTCCCAATTCTTATTCAGGT
Irf7	For	GCCAGGAGCAAGACCGTGTT
	Rev	TGCCCCACCACTGCCTGTA
Uba7	For	GAGTTATACTCCAGGCAGCT
	Rev	CACTGAGCAGCCAAGTCAG
Gbp3	For	ACATGGCCAAATGAAGACACA
	Rev	TGAAAACCCACTTGTGCGTT
Oas2	For	GAAGGATGGCGAGTTCTCTACC
	Rev	GTGCTTGACCAGGCGGATG
Ifit1	For	CAGAAGCACACATTGAAGAA
	Rev	TGTAAGTAGCCAGAGGAAGG
Ifit3	For	CTGAAGGGGAGCGATTGATT
	Rev	AACGGCACATGACCAAAGAGTAGA
Isg15	For	TGACGCAGACTGTAGACACG
	Rev	TGGGGCTTTAGGCCATACTC
Mx2	For	CCAGTTCCTCTCAGTCCCAAGATT
	Rev	TACTGGATGATCAAGGGAACGTGG
Irf9	For	ACAACTGAGGCCACCATTAGAGA
	Rev	CACCACTCGGCCACCATAG
Stat1	For	GAACGCGCTCTGCTCAA
	Rev	TGCGAATAATATCTGGGAAAGTAA
Vdr	For	GATGCCCACCACAAGACCTA
	Rev	CGGTTCCATCATGTCCAGTG
Cyp24a1	For	AAGAGATTCGGGCTCCTTCA
	Rev	GCAGGGCTTGACTGATTTGA
Cyp27b1	For	GCATCACTTAACCCACTTCC
	Rev	CGGGAAAGCTCATAGAGTG
Gapdh	For	AGACGGCCGCATCTTCTTGT
	Rev	ACTGCAAATGGCAGCCCTGG

Table S3: The human specific primers used in this study are listed below

Gene Name		Sequences used for qPCR (5'→ 3')
VDR	For	CTCAAACGCTGTGTGGACAT
	Rev	ACTGTCCTTCAAGGCCTCCT
GAPDH	For	TGCACCACCAACTGCTTA
	Rev	AGAGGCAGGGATGATGTTC

References (for Supplementals of Chapter 4)

1 Olenchock, B. A. *et al.* EGLN1 Inhibition and Rerouting of alpha-Ketoglutarate Suffice for Remote Ischemic Protection. *Cell* **164**, 884-895, doi:10.1016/j.cell.2016.02.006 (2016).

2 Westernströer, B. *et al.* Profiling of Cxcl12 receptors, Cxcr4 and Cxcr7 in murine testis development and a spermatogenic depletion model indicates a role for Cxcr7 in controlling Cxcl12 activity. *PloS one* **9**, e112598-e112598, doi:10.1371/journal.pone.0112598 (2014).

3 Bordignon, J. *et al.* Expression profile of interferon stimulated genes in central nervous system of mice infected with dengue virus Type-1. *Virology* **377**, 319-329, doi:https://doi.org/10.1016/j.virol.2008.04.033 (2008).

4 Dong, H.-J. *et al.* The Wnt/β-catenin signaling/Id2 cascade mediates the effects of hypoxia on the hierarchy of colorectal-cancer stem cells. *Scientific Reports* **6**, 22966,

5 Zhao, W. *et al.* Cellular Intrinsic Mechanism Affecting the Outcome of AML Treated with Ara-C in a Syngeneic Mouse Model. *PLOS ONE* **9**, e109198, doi:10.1371/journal.pone.0109198 (2014).

6 Goo, Y. H., Son, S. H., Yechoor Vijay, K. & Paul, A. Transcriptional Profiling of Foam Cells Reveals Induction of Guanylate-Binding Proteins Following Western Diet Acceleration of Atherosclerosis in the Absence of Global Changes in Inflammation. *Journal of the American Heart Association* **5**, e002663, doi:10.1161/JAHA.115.002663.

7 del Fresno, C. *et al.* Interferon-beta production via Dectin-1-Syk-IRF5 signaling in dendritic cells is crucial for immunity to C. albicans. *Immunity* **38**, 1176-1186, doi:10.1016/j.immuni.2013.05.010 (2013).

8 White, C. L., Kessler, P. M., Dickerman, B. K., Ozato, K. & Sen, G. C. Interferon Regulatory Factor 8 (IRF8) Impairs Induction of Interferon Induced with Tetratricopeptide Repeat Motif (IFIT) Gene Family Members. *J Biol Chem* **291**, 13535-13545, doi:10.1074/jbc.M115.705467 (2016).

9 Nacionales, D. C. *et al.* Type I Interferon Production by Tertiary Lymphoid Tissue Developing in Response to 2,6,10,14-Tetramethyl-Pentadecane (Pristane). *The American Journal of Pathology* **168**, 1227-1240, doi:https://doi.org/10.2353/ajpath.2006.050125 (2006).

Supplementary File 2

The differentially expressed genes from RNA-Seq datasets can be viewed by downloading the ‘Supplementary File 2’ from the following link:

https://www.nature.com/articles/s41413-020-0103-6

Chapter Five: Methyl-CpG binding domain protein 2 plays a causal role in breast cancer growth and metastasis

Preface

Previous studies have demonstrated that SAM can repress the expression of *Mbd2* by direct methylation at the promoter and thereby inhibit the Mbd2-mediated DNA demethylation. Mbd2 expression is also upregulated in breast cancer patients. Therefore, targeting Mbd2 has been of great interest to our lab. Through gene knockdown based *in vitro* studies as well as implantation of *Mbd2* depleted cells into immunocompromised animals, it has been shown that Mbd2 can suppress tumor cell proliferation and invasion. One of the major limitations of these studies is that the cell lines are already transformed, and as a result, they can only address the functional significance of Mbd2 after the tumor is formed. To determine whether Mbd2 can also play a causal role in breast tumor growth and metastasis, we generated transgenic MMTV-PyMT animals with *Mbd2* depletion and assessed mammary tumor emergence, growth, and lung metastasis. An author-generated version of the manuscript is presented in this chapter. The manuscript is now in preparation for submission, and so there is no requirement of copyright licensing.

Abstract

Methyl-CpG-binding domain protein 2 (Mbd2), a reader of DNA-methylation, has been implicated in the progression of several types of malignancies, including breast cancer. To test whether Mbd2 plays a causal role in mammary tumor growth and metastasis, we depleted its gene expression in the transgenic MMTV-PyMT model ('PyMT' in short) of breast cancer by cross-breeding with *Mbd2* knockouts to generate heterozygous (PyMT;*Mbd2*$^{+/-}$) and homozygous (PyMT;*Mbd2*$^{-/-}$) animals. We found that *Mbd2* depletion caused a gene dose-dependent delay in mammary tumor formation, reduced primary tumor burden, and lung metastasis at the experimental endpoint. In addition, animals from the PyMT;*Mbd2*$^{-/-}$ group survived significantly longer compared to the wildtype (PyMT;*Mbd2*$^{+/+}$) and PyMT;*Mbd2*$^{+/-}$ arms. Transcriptomic and proteomic analyses of the primary tumors obtained from PyMT;*Mbd2*$^{+/+}$ and PyMT;*Mbd2*$^{-/-}$ groups revealed that *Mbd2* depletion alters several key determinants of the molecular signaling networks related to tumorigenesis and metastasis, which thereby demonstrate that Mbd2 is regulating transcriptional programs critical for breast cancer. Furthermore, a small molecule inhibitor (KCC-07) targeting the Mbd2 pathway markedly decreased proliferation and colony formation *in vitro* and reduced mammary tumor growth *in vivo*. To our knowledge, this is the first study demonstrating a causal role for a DNA-methylation reader in breast cancer. Results from this study will provide the rationale for further development of first-in-class targeted epigenetic therapies against Mbd2 to inhibit the progression of breast and other common cancers.

Introduction

DNA methylation is an evolutionarily ancient epigenetic process that, through the modulation of chromatin structure, regulates gene expression in a context-dependent manner (Greenberg and Bourc'his, 2019; Mahmood and Rabbani, 2019). The chemically reversible process of DNA methylation is mediated by a family of "writer" enzymes known as DNA methyltransferases (DNMTs) that catalyze the addition of methyl-moieties to the appropriate bases on the genome (Mahmood and Rabbani, 2017). A family of evolutionarily conserved "reader" proteins known as methyl-binding proteins (MBPs) then recognize, interpret, and relay the information from these methylation marks into different gene regulatory functionalities (Mahmood and Rabbani, 2019).

Aberrant DNA methylation is recognized as a paradigmatic hallmark of human cancer (Esteller, 2003), which led to its identification as an attractive therapeutic target. The first-generation epigenetic drugs developed to target the methylome are DNMT inhibitors (Vidaza and Decitabine) that showed robust clinical utilities against several hematological malignancies (Silverman et al., 2002). At the molecular level, through non-specific global demethylation, the DNMT inhibitors not only relieve the transcriptional repression of critical tumor-suppressors (Jones et al., 2016) but also cause transcriptional activation of several known prometastatic genes (Ateeq et al., 2008). Moreover, these drugs are highly toxic, less bioavailable, and showed a modest anti-cancer response in case of solid tumors (Cheishvili et al., 2015), which opens up novel avenues to selectively target the MBPs as an alternative approach to reverse the DNA-methylation mediated epigenetic abnormalities in cancer.

Among the different MBPs, methyl-CpG-binding domain protein 2 (MBD2) is positioned as a suitable anti-cancer drug target since its expression is deregulated in several human malignancies (Mahmood and Rabbani, 2019) and shows a relatively higher affinity to bind to the methylated DNA near the promoters of various known tumor suppressor genes to cause their transcriptional repression (Fraga et al., 2003). Moreover, genetic knockout (KO) of the *Mbd2* gene in mice produced viable off-springs, which suggests that the gene is not required for maintaining standard physiological functions (Hendrich et al., 2001) and, thus, could be used for targeted epigenetic therapies. Indeed, genetic depletion of *Mbd2* has been shown to protect mice from developing intestinal (Sansom et al., 2003) and lymphoid malignancies (Zhou et al., 2018). MBD2 also plays an important role in immune regulation by upregulating the expression of forkhead box P3 (*Foxp3*), which is the marker for regulatory T cells (Treg) (Wang et al., 2013b). Other studies have shown that the immunosuppressive Treg cells infiltrate into the tumors to promote immune evasion and pro-tumorigenic microenvironment and are associated with poor cancer prognosis in patients (Facciabene et al., 2012; Magnuson et al., 2018).

The role of MBD2 in breast cancer progression thus far has been studied through gene knockdown *in vitro* and subsequent implantation into xenograft models where *Mbd2* depletion has shown potent anti-cancer effects through inhibition and hypermethylation of prometastatic genes (Cheishvili et al., 2014b; Mian et al., 2011). However, these models lack functional immune systems and are not capable of fully reflecting the exact role of MBD2 during the highly complex multistep progression of human breast tumors. To dissect the role of MBD2 in a mouse model with a relatively faithful representation of

breast tumor progression, we used a transgenic MMTV-PyMT (mouse mammary tumor virus-polyoma middle tumor-antigen) model where the spontaneous and pregnancy-independent expression of PyMT oncoprotein results in the synchronous appearance of multifocal breast tumors that metastasize predominantly to the lung (Fantozzi and Christofori, 2006; Guy et al., 1992). Although the PyMT oncoprotein is not present in human breast tumors, the step-wise progression of the murine mammary tumor from benign premalignant stage to a highly malignant invasive stage as well as the activation of downstream molecular signaling pathways resemble that of human breast cancer progression (Lin et al., 2003). This positions the PyMT model as an attractive system to assess the oncogenic function of a particular gene during malignant transformation of breast tissues in a whole organism (Fluck and Schaffhausen, 2009).

Herein, using a gene-knockout based molecular genetics approach, we demonstrate that a reduction in the ability to read and interpret epigenetic modification due to the depletion of the *Mbd2* gene significantly decreases mammary tumor burden and metastasis in the transgenic PyMT model of breast cancer.

Results

Mbd2 KO attenuates primary breast tumor growth and metastases in MMTV-PyMT

We first interrogated the publicly available proteomics datasets from the Clinical Proteomic Tumor Analysis Consortium (CPTAC) to check the expression of MBD2 and found that its expression to be significantly upregulated in different subtypes of human breast tumors compared to their normal counterpart (Figure 1A). Interestingly, mouse Mbd2 protein expression is also upregulated in mammary fat pads and primary tumors obtained from PyMT animals compared with the fat pad of wildtype C57BL/6 animals, suggesting that Mbd2 upregulation by the *PyMT* gene precedes malignant transformation (Figure 1B). This is consistent with the hypothesis that Mbd2 is mediating some of the oncogenic effects of PyMT.

Next, to test whether *Mbd2* plays a causal role in tumorigenesis, we generated female PyMT;$Mbd2^{+/-}$ (heterozygous KO) and PyMT;$Mbd2^{-/-}$ (homozygous KO) mice in C57BL/6 background using a cross-breeding strategy, and compared their tumor growth kinetics with PyMT;$Mbd2^{+/+}$ (denoted as wildtype hereafter) animals from week 11 after birth until sacrifice (Figure 1C). As shown by the Kaplan-Meier curve in Figure 1D, animals from the wildtype group started to develop palpable tumors at around week 11 (day 77) after birth. By week 14 (day 98) of age, all animals from the wildtype group had developed primary tumors [wildtype tumor incidence: 77–98 days; 50% mice with palpable tumor, T_{50}=84 days] (Figure 1D). The onset of palpable tumor was not significantly different in the case of the animals from the heterozygous KO group, where primary mammary tumors started to emerge at around the same time as control, i.e., around week

11 after birth. By week 15 (day 105) of age, 100% of the animals in the heterozygous KO group showed palpable mammary tumors [heterozygous KO group tumor incidence: 77–105 days; T_{50}=84 days]. In the homozygous KO group, tumors started to emerge from week 12 (day 84), and all the animals developed palpable tumors by week 16 (day 112) of age [homozygous KO tumor incidence: 84–112 days; T_{50}=91 days]. The onset of the palpable tumor was significantly delayed in the homozygous KO group compared to the wildtype arm (log rank *P*=0.002), suggesting the possible involvement of *Mbd2* in mammary tumor onset in this model.

Next, we compared the tumor growth kinetics of the animals from the three groups by measuring the primary tumor volumes at weekly intervals from the time the animals had started to develop measurable tumors until they were sacrificed. The experimental endpoint was set at week 20 after birth when most of the wildtype animals reached the humane endpoint. We found that the tumor growth over time was significantly reduced in a gene dose-dependent manner (Figure 1E), an observation consistent with similar results shown in the case of intestinal tumorigenesis (Sansom et al., 2003). We then measured the total weight of the extirpated tumors of the animals sacrificed either before or at week 20 after birth and found a significant reduction in tumor weight in the heterozygous and homozygous KO groups in comparison with the wildtype animals (Figure 1F). To test whether *Mbd2* plays a role in prolonging the survival of the mammary tumor-affected mice, we kept several animals from each group beyond the experimental endpoint at week 20 and found that the animals from the homozygous KO group reached the tumor volume

requiring humane sacrifice significantly later than animals from wildtype and heterozygous KO groups (Figure 1G).

We then evaluated the formalin-fixed mammary tumor tissues from each group with an antibody for the Ki67 cell proliferation marker and found a significant decrease of Ki67 positive cells in the homozygous KO group (Figure 1H). Next, using the RNA from flash-frozen lung tissues collected at around week 20, we checked for the expression of several known cancer genes (*Fabp7, Has3, Wnt1, Ccdn1, Bcl2*) that were previously shown to be regulated either directly through MBD2 or its downstream signaling pathways, and found a significant decrease in their expression in the homozygous KO tumors compared to the tumors from the wildtype animals (Figure 1I).

The female PyMT animals develop pulmonary metastases, which allowed us to examine the role of Mbd2 in metastatic dissemination of primary breast tumor cells into distant secondary organs, a condition that is common in clinical settings in breast cancer patients. For that, we used the formalin-fixed lung tissue sections collected at sacrifice (at around week 20 after birth) and stained them with Hematoxylin and Eosin (H&E) to assess the breast tumor colonization in the lung. We found a significant decrease in the number of micrometastases in the lungs collected from the homozygous KO group compared to the wildtype animals (Figure 1J). However, we did not observe any statistically significant difference in micrometastasis between the heterozygous KO and wildtype groups.

Taken together, these results demonstrate that the genetic ablation of the *Mbd2* gene significantly attenuates the ability of the MMTV-PyMT animals to grow spontaneous mammary tumors with a significant reduction in pulmonary metastasis.

Mbd2 depletion affects the several crucial players of PyMT-mediated oncogenic signaling pathways

PyMT is a membrane-associated oncoprotein that does not have any kinase activity of its own (Fluck and Schaffhausen, 2009). However, when it interacts with receptor tyrosine kinases (RTKs) [for example, c-Src, p85 subunit of phosphoinositide 3-kinase (PI3K)], the resultant protein complex gains constitutive tyrosine kinase activities required for activation of downstream signaling pathways to promote cellular transformation, growth, and survival (Guy et al., 1992). To examine whether the *Mbd2* depletion directly impairs the downstream effectors of PyMT-mediated oncogenic signaling, we first checked the levels of activated c-Src, PI3K, and AKT in proteins extracted from wildtype and *Mbd2* KO tumors. We found a substantial decrease in the total c-Src levels in *Mbd2* KO tumors that, in turn, caused a reduction in p-c-Src (Y416) levels required for the oncogenic transformation function of the PyMT-c-Src complex (Cartwright et al., 1986) (Figure 2A). Previous studies have shown that PyMT oncoprotein also complexes with the p85 subunit of PI3K to mediate transformation (Cheng et al., 2009; Cohen et al., 1990). When we checked the phosphorylation status of PI3K (at Y458), a significant decrease in activated PI3K was observed in *Mbd2* KO tumors (Figure 2A). In addition, a significant impairment in the activation of AKT (at S473), which is downstream to the PI3K signaling pathway, was observed in *Mbd2* KO tumors compared to their wildtype counterparts (Figure 2A-B).

Since AKT is known to activate IκB kinase (IKK) activity through phosphorylation and thereby activate the downstream NF-κB signaling cascade (Bai et al., 2009), we next checked and found that the phosphorylation of IKK and the levels of activated NF-κB (p65

subunit) were both decreased in the *Mbd2* KO tumors compared to the wildtype tumors (Figure 2A-B). Furthermore, several known target genes of NF-κB transcription factor like *Plau* (also known as *uPA*), *Mmp2*, *Mmp9*, *Has2*, and *Muc1* were downregulated in the RNA extracted from *Mbd2* KO tumors (Figure 2C). Taken together, these data suggest that *Mbd2* depletion impairs the ability of the PyMT oncoprotein to stimulate the oncogenic PI3K/Akt/NF-κB axis.

Transcriptome and proteome analyses reveal decrease in EMT markers in *Mbd2* KO tumors

We then investigated the transcriptomic changes triggered by the genetic depletion of *Mbd2* by RNA-Seq of primary tumors obtained from wildtype and *Mbd2* KO animals (n=3 samples/group). We found that, in comparison to the wildtype arm, the primary tumors from the *Mbd2* KO group caused a significant change in the expression of 453 genes ($|\log2(\text{Fold Change})| > 1$, $P<0.05$). The expression changes occurred in both directions, i.e., 121 genes were upregulated, and 332 genes were downregulated in the *Mbd2* KO tumors (Figure 3A). Using the Ingenuity Pathway Analysis (IPA) tool (Kramer et al., 2014), we found that some of the notable 'molecular and cellular functions' enriched with differentially expressed genes (DEGs) in *Mbd2* KO tumors include cellular movement, cell-cell signaling & interaction, cellular assembly & organization, molecular transport, cell death & survival, and cellular growth & proliferation (Supplementary Figure S1A). IPA analyses also identified that the top two 'disease and disorders' pathways significantly enriched with DEGs in *Mbd2* KO tumors include 'cancer' and 'organismal

injury and abnormalities' (Supplementary Figure S1B). We then subjected the entire list of DEGs to pathway analyses using the Pathway Interaction Database (PID) and found a statistically significant enrichment of the genes in integrin signaling, syndecan-4 mediated signaling, adherens junction stability and disassembly pathways (Figure 3B). Interestingly, most of these pathways are related to cancer progression, especially during the epithelial-to-mesenchymal transition (EMT). Therefore, we next overlapped the complete repertoire of EMT-related genes obtained from the publicly available dbEMT database with the genes downregulated in *Mbd2* KO tumors and found a significant intersection of 35 genes (hypergeometric test, $p<0.05$, Figure 3C). A heatmap of the differentially expressed EMT genes in *Mbd2* KO tumors is shown in Figure 3D. To validate the results from the RNA-Seq experiment, we performed a quantitative polymerase chain reaction (qPCR) analysis of several crucial EMT genes (*Sparc*, *Spp1,* and *Cdh2*) and found a concordant decrease in their expression in the *Mbd2* KO tumors (Figure 3E). Importantly, *Sparc, Spp1,* and *Cdh2* are all upregulated in the human breast cancer tumors from the TCGA (The Cancer Genome Atlas) database (Figure 3F), suggesting the clinical relevance of MBD2 regulated genes in breast cancer. We also performed qPCR validation of several known tumor suppressor genes (*Brca1*, *Dusp5*) that were upregulated upon *Mbd2* gene KO (Supplementary Figure S1C).

Next, we employed the IPA upstream regulator analysis (URA) for the identification of potential transcription factors, cytokines, growth factors, or any chemical entities that could regulate the gene expression changes seen in our transcriptome datasets (Figure 3G). Interestingly, the top upstream regulators that were predicted to be

downregulated include TGFB1, SRF, CTNNB1, and JUN, all of which are known to be involved in the EMT pathway. In addition, we employed an alternative approach for predicting the upstream transcription factors of the DEGs identified in *Mbd2* KO tumors by searching the ChIP Enrichment Analysis (ChEA) database (Lachmann et al., 2010). This analysis identified 57 transcription factors that include several EMT-related transcription factors like MTF2, SOX2, SOX9, JUN, and others listed in Supplementary Figure S1D.

Next, we performed a uHPLC/MS-MS to assess the proteomic differences between the mammary tumors extracted from wildtype and *Mbd2* homozygous KO animals. A total of 2231 proteins were identified. To gain insights into the biological processes affected by the deletion of the *Mbd2* gene, we focused on the changes in the abundance of proteins between the two groups as a measure of differential protein expression. This approach identified 215 proteins with differential abundance, of which 158 were upregulated and 57 were downregulated in the KO samples compared to the wildtype counterparts (Figure 3H). Protein-protein interaction meta-analyses of the 215 proteins revealed their involvement in biological processes like metabolism of RNA, telomerase RNA localization, cytoplasmic translation initiation (Figure 3I). Since our transcriptome analyses revealed the downregulation of several key cancer-related genes in homozygous KO tumors, we then focused on the downregulated proteins. Pathway analysis of the downregulated proteins in *Mbd2* KO tumors revealed their involvement in osteopontin-mediated signaling, N-cadherin signaling, TGFBR pathways, all of which are involved in the EMT (Figure 3J). We next validated the downregulation of Osteopontin (encoded by *Spp1* gene) and N-

cadherin (encoded by *Cdh2* gene) in protein level (Figure 3K) that also showed similar patterns of downregulation in the transcript levels (Figure 3E). We also overlapped the list of differentially expressed proteins and RNAs obtained from our proteomics and transcriptomics studies and found an overlap of 10 entities, all of which showed concordant changes in their expression patterns in *Mbd2* KO tumors (Supplementary Figure 1E-F). Taken together, these observations indicate the possible involvement of Mbd2 in modulating different components of EMT during breast tumor progression in this model.

Mbd2 modulates the oncogenic Pvt1-Myc axis

Emerging evidence suggests that pervasive transcription of genes beyond the protein-coding boundaries of the genome plays a role in the regulation of gene expression as well as the pathogenesis of the disease (Birney et al., 2007; Djebali et al., 2012; Zhang et al., 2019). Therefore, we next focused on deciphering the long non-coding RNAs (lncRNAs) that are differentially expressed upon homozygous deletion of the *Mbd2* gene using our RNA-Seq data and found that 60 lncRNAs are differentially expressed in *Mbd2* KO tumors compared to their wildtype counterparts (Supplementary Figure S2A). Gene ontology (GO) analyses of the lncRNAs revealed their involvement in a wide range of biological processes related to RNA processing and transcriptional regulation (Supplementary Figure S2B). Since a vast majority of the lncRNAs are still uncharacterized in the context of cancer, we focused on the lncRNAs either with known biological function(s) or known human orthologs in the TCGA breast cancer patient dataset. A curated list of 16 lncRNAs that fulfilled these criteria is shown as a heatmap in

Figure 4A. We further validated the expression of several lncRNAs [X-inactive specific transcript (*Xist*), chaperonin containing Tcp1 and subunit 6a (*Cct6a*), and plasmacytoma variant translocation 1 (*Pvt1*)] by qPCR (Figure 4B), where the expression change showed concordance with the RNA-Seq results. The expression of the corresponding orthologous genes in human breast cancer patients from the TCGA database showed that *XIST* expression is significantly downregulated, while *CCT6A* and *PVT1* expressions are significantly upregulated (Figure 4C). Moreover, the *PVT1* and *MYC* genes are coexpressed in the human breast cancer when we performed a Pearson correlation analysis using data obtained from 4307 patients (Figure 4D). Similar to their human counterpart, these two genes are also located in close proximity on chromosome 15 of the mouse genome (Figure 4E). We, therefore, checked whether *Myc* is differentially regulated upon *Mbd2* depletion and found significant repression of its expression both in the transcript and protein levels in PyMT;$Mbd2^{-/-}$ tumors compared to PyMT;$Mbd2^{+/+}$ (Figure 4F-G). These results suggest the possible role of Mbd2 in modulating the oncogenic Pvt1-Myc axis in cancer.

Small molecule inhibitor of Mbd2 pathway (KCC-07) represses tumor cell proliferation *in vitro* and *in vivo*

We next assessed whether pharmacological inhibition of Mbd2 binding to methylated DNA using KCC-07, a recently described small molecule inhibitor (Zhu et al., 2018), could suppress breast tumor cell proliferation. Towards this goal, we performed dose-response and time-course experiments where a panel of human and murine breast

cancer cells (PyMT-R221A, E0771, Hs578T) expressing the gene encoding for MBD2 reader protein were incubated with increasing concentrations of KCC-07 ranged between 1 to 10 μM and cell proliferation was measured by direct cell counting after days 1, 2, and 3 post-treatment. In all three cell lines tested, our data showed a significant reduction in cell proliferation in a dose- and time-dependent manner (Figure 5A). Since 10 μM KCC-07 treatment for 3 days produced an approximately 50% reduction in cell proliferation in these cell lines, we used this dose and incubation time for clonogenic survival assay and found that KCC-07 treatment markedly reduced clonogenic survival of all the cell lines (Figure 5B).

We then assessed whether KCC-07 would inhibit breast cancer growth in a syngeneic model of breast cancer where 5×10^5 PyMT-R221A cells were injected into 6-8-week-old female FVB albino mice. Three days post tumor cell inoculation, the animals were randomized and treated with 100mg/kg KCC-07 as depicted in Figure 5C. Our results show that treatment with KCC-07 caused a significant reduction in mammary tumor growth in the animals from the treatment arm compared to the DMSO-treated control arm, which is consistent with the results from a previous study done using medulloblastoma xenografts(Zhu et al., 2018) (Figure 5D). In addition, analyses of different biochemical measurements (Kidney and liver function test, measurement of electrolytes and minerals) did not show any discernible difference between the two groups except a downregulation of ALT level upon KCC-07 treatment (Supplementary Table S1).

Discussion

In this study, we genetically depleted *Mbd2* in the well-characterized transgenic MMTV-PyMT mouse model that recapitulates the stepwise progression of tumors from localized to metastatic variant and share similar pathology and biomarkers found in patients with metastatic breast cancer (Lin et al., 2003). Since the gene is depleted preconception, gene loss certainly precedes tumor initiation, and thus this study design provides definitive conclusions on the causal role of *Mbd2* in breast cancer.

Our data demonstrate that the PyMT oncogene driven spontaneous mammary tumor formation is delayed upon homozygous depletion of the *Mbd2* gene (Figure 1D). *Mbd2* might not be involved in tumor initiation as tumors are delayed but nevertheless appear in the KO animals, but it is required for tumor growth since tumor growth is significantly delayed by *Mbd2* deficiency (Figure 1E). The late appearance of tumors in $Mbd2^{-/-}$ mice might be a consequence of slowing down tumor growth, and therefore tumors reach detection size later. This conclusion is further supported by the significant decrease of Ki67 positive cells in the homozygous KO group suggesting reduced proliferation of the KO cancer cells (Figure 1H). Moreover, we found that even at a haploinsufficiency state where one of the allele is not present, the heterozygous PyMT;$Mbd2^{+/-}$ group is still able to cause a significant reduction in primary breast tumor burden, further implicating the role of *Mbd2* in tumor growth.

In addition to tumor growth, lung metastasis is significantly reduced upon the genetic ablation of the *Mbd2* gene (Figure 1J). This is consistent with previous results implicating *Mbd2* in breast cancer metastasis (Cheishvili et al., 2014a; Pakneshan et al.,

2004); our results provide evidence that *Mbd2* plays a causal role in breast cancer metastasis. These results indicate a multifaceted role of Mbd2 during mammary tumor progression.

Mbd2 is upregulated by PyMT, and upregulation of Mbd2 precedes tumor formation consistent with the idea that Mbd2 is mediating the effects of PyMT on cellular pathways that precipitate uncontrolled growth and metastasis; *Mbd2* depletion blocks activation of these pathways. PyMT activates a panel of downstream oncogenic signaling pathways (for example, Src, PI3K/Akt) that are involved in tumor cell proliferation, survival, inhibition of apoptosis, and promotion of metastasis (Fluck and Schaffhausen, 2009). Our analyses of the proteins obtained from the primary tumors revealed that *Mbd2* deletion represses the activation of the PI3K/Akt axis (Figure 2), which has been previously shown to be essential for mammary tumorigenesis (Webster et al., 1998). Furthermore, *Mbd2* depletion interferes with the oncogenic NF-κB signaling pathway, which results in the repression of critical cancer-related downstream targets of NF-κB like *Plau, Mmp2, Mmp3* and several others. These targets are also involved in breast cancer invasion and metastasis. It is unclear how Mbd2 alters signaling cascades since it seems to affect phosphorylation. This is intriguing since Mbd2 is a well-established regulator of gene expression. Is it possible that Mbd2 has an additional role in signaling? Alternatively, it might regulate signaling cascade through the regulation of genes that control the signaling events described in our study. This question needs to be addressed in future studies.

Transcriptome analyses provide insights into the global gene expression changes mediated by *Mbd2* KO. Although Mbd2 is generally believed to be a suppressor of gene

activity through recruitment of the nucleosome remodeling and deacetylase (NuRD) complex and histone deacetylase to methylated promoters (Zhang et al., 1999) and a previous study in an isogenic model of breast cancer transformation showed that the majority of genes whose expression changes following *Mbd2* knockdown are upregulated (Devailly et al., 2015), we show here that the majority of genes are silenced rather than activated by *Mbd2* depletion. Many of these genes play an active role in cancer growth and metastasis. Thus, Mbd2 serves as an activator of several cancer genes in our model. However, although the silencing activity of Mbd2 has been emphasized in past studies, several studies have shown that Mbd2 is involved in gene activation as well. For example, Baubec *et al*., show that Mbd2 plays a bimodal role in embryonal stem cells and that Mbd2 binds to methylated regions in the genome which are enriched with repressive marks as well as to active unmethylated regulatory regions that are enriched with DNAse hypersensitive sites and activating chromatin marks (Baubec et al., 2013). Several studies have shown that Mbd2 activates promoters and induces hypomethylation (Alvarado et al., 2013; Angrisano et al., 2006; Detich et al., 2002; Ego et al., 2005; Fujita et al., 2003; Shukeir et al., 2006; Stefanska et al., 2013; Wang et al., 2013a; Weaver et al., 2014). Relevant to our studies, we have previously shown that depletion of *Mbd2* leads to silencing and hypermethylation of prometastatic genes in breast cancer cells (Cheishvili et al., 2014a; Pakneshan et al., 2004). Mbd2 is most probably targeted by different factors to either activate or silence gene expression. It was proposed that the NuRD complex targets Mbd2 to active unmethylated regions in embryonal stem cells (Baubec et al., 2013). Stefanska et al. has shown that Mbd2 activates and triggers hypomethylation of cancer-

promoting genes in liver cancer (Stefanska et al., 2011) and that the transcription factor CCAAT/enhancer-binding protein alpha (CEBPA) recruits Mbd2 to its targets to trigger transcription onset (Stefanska et al., 2013). Mbd2 is recruited to the *Foxp3* gene in regulatory T cells, which results in loss of methylation possibly through the recruitment of Tet2 (Wang et al., 2013a). Thus, our data is consistent with previous data suggesting that Mbd2 plays a role in the activation of several cancer-related gene pathways, most probably through recruitment to specific genomic regions by transcription factors that are activated by triggers of cancer such as PyMT. Further studies are required to test this hypothesis. Our transcriptome analysis supports a bimodal role for Mbd2 in breast cancer, both activating genes that promote and silencing genes that suppress cancer. Importantly, our RNA-Seq results indicated that several key EMT pathway-related gene signatures encoding for mesenchymal markers like N-Cadherin, Osteopontin were significantly downregulated by Mbd2. EMT is a highly dynamic biologic process that directs the epithelial cells within a particular tissue to go through multiple biochemical changes rendering their transformation to more invasive mesenchymal cells (Roche, 2018). Therefore, a decrease in the expression of the mesenchymal marker reduces the metastatic spread of primary tumors. Proteomic analysis of the lysates obtained from wildtype and *Mbd2* KO tumors further indicated and confirmed that the top pathways enriched by the differentially downregulated proteins in *Mbd2* KO tumors are Osteopontin, N-cadherin and TGFR mediated signaling events- all of which involved in EMT (Figure 3J).

It is estimated that around 75% of the human genome can undergo active transcription; however, only 2% transcripts can be further translated into proteins (Djebali

et al., 2012; Zhang et al., 2019). This implies that a huge portion of the transcriptome does not have any known coding potential but undergo pervasive transcription (Birney et al., 2007), and many of these non-coding RNAs play an important role in gene regulation and disease pathology (Zhang et al., 2019). Such pervasive transcription is also observed in other mammals, including mouse (Clark et al., 2011). Among the various types of non-coding RNAs, the lncRNAs have gained much attention in the past few years. When we analyzed the differentially expressed lncRNA in *Mbd2* depleted PyMT tumors, we found that the expression of 60 lncRNAs are significantly altered. We found that *Pvt1*, an evolutionarily conserved lncRNA with well-established oncogenic function (Onagoruwa et al., 2020), is downregulated in the PyMT*;Mbd2*$^{-/-}$ tumors (Figure 3B). The *Pvt1* and *Myc* genes are adjacently localized in the mouse (chromosome 15) and human (chromosome 8) genomes and are frequently seen to be overexpressed together in many cancer-types (Onagoruwa et al., 2020). It has been shown that *Pvt1* provides stability to Myc protein from undergoing proteasomal degradation through the blockade of GSK3-β mediated Myc phosphorylation at Thr-58 residue (Tseng et al., 2014). Moreover, the *PVT1* promoter contains two E-box regions where Myc can bind and subsequently promote *PVT1* transcription (Onagoruwa et al., 2020). This positive feedback loop between *Myc* and *Pvt1* expression synergizes to promote tumorigenesis (Jin et al., 2019), all of which are reversed in transgenic MMTV-PyMT mice upon the depletion of *Mbd2*. Since there is a high degree of conservation in the synteny between coding and non-coding genes across species (Ulitsky et al., 2011), we speculate a similar regulation in the human counterpart.

It has been shown that the depletion of *Xist* lncRNA promotes EMT through the downregulation of E-cadherin and upregulation of Vimentin in breast cancer (Xing et al., 2018). Our data shows that *Mbd2* depletion upregulates *Xist* expression with the downregulation of Vimentin (from proteomics analyses), which might contribute to the reversal of the mesenchymal state. Taken together, the results from the proteomics and transcriptomics studies showed congruence with the anti-tumorigenic and anti-metastatic phenotype mediated by the *Mbd2* depletion *in vivo.* Mbd2 coordinately activates and suppresses gene expression leading to tumor growth and metastasis. Although the PyMT model used in this study share similar molecular signatures found in the human luminal B subtype of breast cancer (Fluck and Schaffhausen, 2009), the broader incidence of elevated Mbd2 expression in the publicly available human breast tumor dataset (Figure 1A) indicate a similar regulation by the Mbd2 protein in the case of other breast cancer subtypes as well.

Our data show that Mbd2 bimodally regulates a broad panel of tumor-suppressing genes that block cancer and activating genes that promote tumor growth and metastasis, positioning it as a candidate target for breast cancer therapeutics. To assess the feasibility of using a therapeutic agent targeting the Mbd2 pathway, we used a small molecule inhibitor called KCC-07 and found a significant decrease in breast tumor cell growth *in vitro* and *in vivo.* The dose and bioavailability of the KCC-07 have been previously established in the case of highly aggressive medulloblastoma tumors (Zhu et al., 2018), and our data in breast tumors further confirm the anti-cancer potential of the drug. During this study, another group reported the discovery of two lead compounds targeting MBD2 to reduce metastasis *in vivo* (Kim et al., 2019), which further confirms that Mbd2 is a

druggable target. However, further research is warranted to compare the anti-breast cancer therapeutic activity of different Mbd2 inhibitors in preclinical and clinical settings as well as long term adverse effects.

To our knowledge, this is the first report describing the multifaceted function of an epigenetic reader during mammary tumor progression and metastasis. Since *Mbd2* depleted animals are viable and fecund, it would be similarly interesting to test whether targeting Mbd2 and/or its methylated DNA binding ability would produce a similar anti-cancer effect in patients with breast cancer to reduce cancer-associated morbidity and mortality. It will also open a novel avenue for the use of targeted epigenetic therapies against methylation abnormalities in cancer as single-agent monotherapy or in combination with standard of care treatment regimens.

Materials and Methods

Mouse strains and genotyping

The embryo straws for the *Mbd2* heterozygous KO mice ($Mbd2^{+/-}$) in the C57BL/6 background were a kind gift by Dr. Brian Hendrich (Department of Biochemistry, University of Cambridge). The embryos were first recovered from the straws at the Transgenic Core Facility, Rosalind and Morris Goodman Cancer Research Centre, McGill University, and then they were implanted into two female foster mice to generate the heterozygous KOs ($Mbd2^{+/-}$). Afterwards, the animals were bred and maintained at the Animal Resource Division of the Research Institute of the McGill University Health

Center. The breeder pair of male heterozygous MMTV-PyMT (in C57BL/6 background) carrying a single copy of the PyMT transgene and noncarrier wildtype C57BL/6 female were purchased from The Jackson Laboratory (Bar Harbor, ME, USA) and they were crossed to generate MMTV-PyMT (also denoted as PyMT) mice that are wildtype for the *Mbd2* gene. The male PyMT mice were then crossed with female $Mbd2^{+/-}$ mice to generate the PyMT;$Mbd2^{+/-}$ (heterozygous KO for *Mbd2*) littermates. Next, male PyMT;$Mbd2^{+/-}$ and female $Mbd2^{+/-}$ mice were crossed to generate female PyMT;$Mbd2^{+/+}$, PyMT;$Mbd2^{+/-}$, and PyMT;$Mbd2^{-/-}$ (homozygous KO for *Mbd2*) for assessing tumors. All animals were heterozygous for the PyMT transgene.

For genotyping, DNA was extracted from the tails snips obtained from the mice followed by polymerase chain reaction (PCR) using primers for the detection of specific alleles. The PyMT allele was detected using the following primers: GGAAGCAAGTACTTCACAAGGG (forward) and GGAAGTCACTAGGAGCAGGG (reverse). The *Mbd2* mice were genotyped using a combination of three primers: TTGTGAGCTGTTGGCATTGT, GTCAACAGCATTTCCCAGGT, and TGTCCTCCAGTCTCCTCCAC. The wildtype *Mbd2* mice showed a single band with a size of 377 bp; the homozygous KOs amplified a single 250 bp product while the heterozygous showed bands for both 377 and 250 bp products when the PCR amplified products were run on an agarose gel.

Once the animals start to develop palpable mammary tumors spontaneously, the size of the tumors were measured at weekly intervals using a Vernier caliper and the tumor

volume was calculated by the following formula: $V= (length \times Width^2)/2$, as described by us before (Mahmood et al., 2020a).

Cell culture

For PyMT-R221A and E0771 cells, Dulbecco's modified Eagle's medium (DMEM) (Wisent, Saint-Jean-Baptiste QC, Canada; Cat# 319-015-CL) complemented with 10% fetal bovine serum (FBS) (Wisent; Cat# 085450), and antibiotic-antimycotic solution (Wisent; Cat#450-115-EL) was used as the growth medium. For Hs578T, the conditions were the same as the other two cell lines, except an additional 1.25 mg/mL insulin was supplemented to the cell culture medium.

Cell proliferation and colony assay

PyMT-R221A, E0771, and Hs578T cells were treated with different doses of KCC-07, and the number of cells was counted 1, 2, and 3 days post-treatment using a Coulter counter (Model ZF; Coulter Electronics, Hertfordshire, UK).

For colony assay, cells were treated for three days with either vehicle (DMSO as control) or 10µM KCC-07 for three days, trypsinized, and $5x10^3$ cells were plated onto six-well plates. Replenishment of the media was done every 2-3 days, and after 14 days from the time of plating, the cells were fixed, stained with 0.5% crystal violet, and colonies were counted directly under the microscope, as described before (Mahmood et al., 2020b).

RNA extraction and quantitative polymerase chain reaction (qPCR)

RNA extraction was done from frozen tissues and cell lines. The processing of frozen primary tumors and lung tissues had an extra step where they were first homogenized under cryogenic conditions using pre-chilled mortar and pestle before RNA isolation. Total RNA was extracted using the AllPrep DNA/RNA Mini Kit (Cat# 80204, Qiagen, Hilden, Germany). The RNA concentration was measured using BioDrop, and 2 µg of total RNA from each sample was used for reverse transcription-polymerase chain reaction (RT-PCR) with random hexamer primers (Invitrogen, Waltham, MA, USA; Cat#58875). SYBR® Green (Applied Biosystems, Cat#A25742) based quantitative PCR (qPCR) assay was performed using an ABI StepOnePlus™ (Applied Biosystems) machine. The changes in gene expression between the control and different treatment groups were determined using the $2^{-\Delta\Delta C}$T method as described by Livak and Schmittgen (Livak and Schmittgen, 2001).

RNA-Seq and analysis pipeline

RNA extracted from the mammary tumors of PyMT;*Mbd2*$^{+/+}$ and PyMT;*Mbd2*$^{-/-}$ animals were subjected to RNA-Sequencing (n=3/group). First, the integrity of the RNA was checked and confirmed with an Agilent 2100 Bioanalyzer, and then ribosomal RNA was removed from the samples by the Ribo-Zero kit (Illumina, San Diego, CA, United States). The sequencing library was prepared following the standard protocol for TruSeq Stranded Total RNA Sample Prep Kit (Illumina), and paired-ended [2x150 bp] sequencing was performed on NovaSeq 6000 sequencing system (Illumina). Once the sequencing run

was completed, the adaptor sequences, low quality and undetermined bases were removed, and the quality of the reads was verified by FastQC (http://www.bioinformatics.babraham.ac.uk/projects/fastqc/). The de-multiplexed reads were then mapped to the reference genome of *Mus musculus* (Version: v90) using Bowtie2 (Langmead and Salzberg, 2012) and HISAT2 (Kim et al., 2015) aligners. Assembly of the mapped sequencing reads, and differential expression of the transcripts were estimated using StringTie (Pertea et al., 2015) and edgeR (Robinson et al., 2010). The known long non-coding RNAs (lncRNA) were identified based on sequence similarities. To identify the novel lncRNAs, we first filtered out the transcripts having an overlap with known mRNAs, known lncRNAs, and transcripts shorter than 200 bp. Then Coding Potential Calculator (CPC) (Kong et al., 2007) and Coding-Non-Coding-Index (CNCI) (Sun et al., 2013) tools were used for predicting the transcripts having coding potential. The transcripts having CPC score <-1 and CNCI score <0 were then filtered out, and the remaining transcripts were considered as novel lncRNAs. The known and novel lncRNAs were then combined together and used for downstream analyses. For both mRNAs and lncRNAs, the transcripts passing the following two criteria: (1) $\log_2$ (fold change) greater than 1 or $\log_2$ (fold change) less than -1, and (2) *P*-value < 0.05 (parametric F-test comparing nested linear models) were considered as differentially expressed. Pathway analyses were performed by using ConsensusPathDB (Kamburov et al., 2013).

Immunoblotting

Immunoblotting was performed from snap-frozen mouse primary tumor tissues and cell lines. Like the RNA extraction procedure, frozen tumors' processing had an extra homogenization step under cryogenic conditions. We used a radioimmunoprecipitation assay (RIPA) buffer supplemented with a mixture of appropriate protease and phosphatase inhibitors to prepare cell lysates. Following quantification, an equal amount of proteins was electrophoresed on 8 to 15% sodium dodecyl sulfate-polyacrylamide gels prepared in-house and transferred to polyvinylidene difluoride (PVDF) (Bio-Rad, Hercules, CA, USA; Cat# 1620177) membrane at 4°C. The membrane was soaked into 5% milk in Tris-buffered saline (TBS) to block non-specific antibody binding. Then appropriate primary and secondary antibodies were used, and an enhanced chemiluminescence detection kit (Amersham, GE Healthcare Life Sciences, Cat# RPN2232) was used for the visualization of different proteins by a ChemiDoc MP Imaging System (Bio-Rad Laboratories, Inc., Hercules, CA, United States).

Proteomics analyses of the tumor samples

Cell lysates obtained from the homogenized mammary tumors of PyMT;*Mbd2*$^{+/+}$ and PyMT;*Mbd2*$^{-/-}$ animals were subjected to proteomic profiling using an Ultra performance liquid chromatography-tandem mass spectrometer (uHPLC/MS-MS) at the RI-MUHC proteomics core (n=3/group). For the identification of peptides and proteins, Scaffold (version 4.9) was used (Searle, 2010). The cut-off probability for peptide identification was set at 90% minimum. For the identification of proteins, the threshold

was set at 95.0% minimum and at least two peptides minimum. For identification of protein with differential abundance in the two groups, a P-value cut-off of less than or equal to 0.05 was considered statistically significant.

Lung isolation and analyses of metastasis

For the analyses of metastasis, whole lung tissues were first collected at the time of sacrifice, fixed in formalin for 3-4 days at room temperature, and then stored in 70% ethanol at 4 °C until they were embedded in paraffin. The deparaffinized lung tissue slides were then stained with H&E and scanned using Leica Aperio AT Turbo digital pathology scanner (Leica Microsystems, Wetzlar, Germany) at the RI-MUHC Histopathology platform.

Ki67 staining

The formalin-fixed mammary tumor tissues were stained with a monoclonal antibody against Ki67 (Dako, Cat# M7240), and the number of ki67 positive cells was determined from the photomicrographs of five randomly selected fields for each sample by 'ImmunoRatio' (Tuominen et al., 2010).

Mammary fat pad implantation of tumor cells

For this experiment, $5x10^5$ PyMT-R221A cells were implanted into the fourth mammary fat pad of 6-8-week-old female syngeneic FVB mice. Three days post-implantation, the animals were randomized and treated with either vehicle (DMSO) or

100.0 mg/kg of KCC-07 via intraperitoneal injection (i.p.) 3 days/week for 3 weeks. The doses used for KCC-07 were the same as previously described (Zhu et al., 2018). The tumor volumes were measured at weekly intervals from week one until sacrifice on week 3 post-tumor cell implantation.

Statistical analyses

Results in different graphical representations are shown as the mean ± standard error of the mean (SEM) unless mentioned otherwise. Depending on the number of groups during analyses, a student's *t*-test or ANOVA was done to measure statistical significance. A *P-value* of less than or equal to 0.05 was considered statistical significance.

References

Alvarado, S., Wyglinski, J., Suderman, M., Andrews, S.A., and Szyf, M. (2013). Methylated DNA binding domain protein 2 (MBD2) coordinately silences gene expression through activation of the microRNA hsa-mir-496 promoter in breast cancer cell line. PLoS One *8*, e74009.

Angrisano, T., Lembo, F., Pero, R., Natale, F., Fusco, A., Avvedimento, V.E., Bruni, C.B., and Chiariotti, L. (2006). TACC3 mediates the association of MBD2 with histone acetyltransferases and relieves transcriptional repression of methylated promoters. Nucleic Acids Res *34*, 364-372.

Ateeq, B., Unterberger, A., Szyf, M., and Rabbani, S.A. (2008). Pharmacological inhibition of DNA methylation induces proinvasive and prometastatic genes in vitro and in vivo. Neoplasia (New York, NY) *10*, 266-278.

Bai, D., Ueno, L., and Vogt, P.K. (2009). Akt-mediated regulation of NFκB and the essentialness of NFκB for the oncogenicity of PI3K and Akt. International journal of cancer *125*, 2863-2870.

Baubec, T., Ivanek, R., Lienert, F., and Schubeler, D. (2013). Methylation-Dependent and -Independent Genomic Targeting Principles of the MBD Protein Family. Cell *153*, 480-492.

Birney, E., Stamatoyannopoulos, J.A., Dutta, A., Guigo, R., Gingeras, T.R., Margulies, E.H., Weng, Z., Snyder, M., Dermitzakis, E.T., Thurman, R.E., *et al.* (2007).

Identification and analysis of functional elements in 1% of the human genome by the ENCODE pilot project. Nature *447*, 799-816.

Cartwright, C., Kaplan, P., Cooper, J., Hunter, T., and Eckhart, W. (1986). Altered sites of tyrosine phosphorylation in pp60c-src associated with polyomavirus middle tumor antigen. Molecular and cellular biology *6*, 1562-1570.

Cheishvili, D., Boureau, L., and Szyf, M. (2015). DNA demethylation and invasive cancer: implications for therapeutics. British journal of pharmacology *172*, 2705-2715.

Cheishvili, D., Chik, F., Li, C.C., Bhattacharya, B., Suderman, M., Arakelian, A., Hallett, M., Rabbani, S.A., and Szyf, M. (2014a). Synergistic effects of combined DNA methyltransferase inhibition and MBD2 depletion on breast cancer cells; MBD2 depletion blocks 5-aza-2'-deoxycytidine-triggered invasiveness. Carcinogenesis *35*, 2436-2446.

Cheishvili, D., Chik, F., Li, C.C., Bhattacharya, B., Suderman, M., Arakelian, A., Hallett, M., Rabbani, S.A., and Szyf, M. (2014b). Synergistic effects of combined DNA methyltransferase inhibition and MBD2 depletion on breast cancer cells; MBD2 depletion blocks 5-aza-2′-deoxycytidine-triggered invasiveness. Carcinogenesis *35*, 2436-2446.

Cheng, J., DeCaprio, J.A., Fluck, M.M., and Schaffhausen, B.S. (2009). Cellular transformation by simian virus 40 and murine polyoma virus T antigens. Paper presented at: Seminars in cancer biology (Elsevier).

Clark, M.B., Amaral, P.P., Schlesinger, F.J., Dinger, M.E., Taft, R.J., Rinn, J.L., Ponting, C.P., Stadler, P.F., Morris, K.V., Morillon, A., *et al.* (2011). The reality of pervasive transcription. PLoS Biol *9*, e1000625-e1001102.

Cohen, B., Liu, Y., Druker, B., Roberts, T.M., and Schaffhausen, B.S. (1990). Characterization of pp85, a target of oncogenes and growth factor receptors. Molecular and cellular biology *10*, 2909-2915.

Detich, N., Theberge, J., and Szyf, M. (2002). Promoter-specific activation and demethylation by MBD2/demethylase. J Biol Chem *277*, 35791-35794.

Devailly, G., Grandin, M., Perriaud, L., Mathot, P., Delcros, J.G., Bidet, Y., Morel, A.P., Bignon, J.Y., Puisieux, A., Mehlen, P., *et al.* (2015). Dynamics of MBD2 deposition across methylated DNA regions during malignant transformation of human mammary epithelial cells. Nucleic Acids Res.

Djebali, S., Davis, C.A., Merkel, A., Dobin, A., Lassmann, T., Mortazavi, A., Tanzer, A., Lagarde, J., Lin, W., Schlesinger, F., *et al.* (2012). Landscape of transcription in human cells. Nature *489*, 101-108.

Ego, T., Tanaka, Y., and Shimotohno, K. (2005). Interaction of HTLV-1 Tax and methyl-CpG-binding domain 2 positively regulates the gene expression from the hypermethylated LTR. Oncogene *24*, 1914-1923.

Esteller, M. (2003). Cancer epigenetics: DNA methylation and chromatin alterations in human cancer. In New Trends in Cancer for the 21St Century (Springer), pp. 39-49.

Facciabene, A., Motz, G.T., and Coukos, G. (2012). T-regulatory cells: key players in tumor immune escape and angiogenesis. Cancer research *72*, 2162-2171.

Fantozzi, A., and Christofori, G. (2006). Mouse models of breast cancer metastasis. Breast Cancer Research *8*, 212.

Fluck, M.M., and Schaffhausen, B.S. (2009). Lessons in signaling and tumorigenesis from polyomavirus middle T antigen. Microbiol Mol Biol Rev *73*, 542-563.

Fraga, M.F., Ballestar, E., Montoya, G., Taysavang, P., Wade, P.A., and Esteller, M. (2003). The affinity of different MBD proteins for a specific methylated locus depends on their intrinsic binding properties. Nucleic acids research *31*, 1765-1774.

Fujita, H., Fujii, R., Aratani, S., Amano, T., Fukamizu, A., and Nakajima, T. (2003). Antithetic effects of MBD2a on gene regulation. Mol Cell Biol *23*, 2645-2657.

Greenberg, M.V., and Bourc'his, D. (2019). The diverse roles of DNA methylation in mammalian development and disease. Nature reviews Molecular cell biology, 1-18.

Guy, C.T., Cardiff, R., and Muller, W.J. (1992). Induction of mammary tumors by expression of polyomavirus middle T oncogene: a transgenic mouse model for metastatic disease. Molecular and cellular biology *12*, 954-961.

Hendrich, B., Guy, J., Ramsahoye, B., Wilson, V.A., and Bird, A. (2001). Closely related proteins MBD2 and MBD3 play distinctive but interacting roles in mouse development. Genes & development *15*, 710-723.

Jin, K., Wang, S., Zhang, Y., Xia, M., Mo, Y., Li, X., Li, G., Zeng, Z., Xiong, W., and He, Y. (2019). Long non-coding RNA PVT1 interacts with MYC and its downstream molecules to synergistically promote tumorigenesis. Cell Mol Life Sci *76*, 4275-4289.

Jones, P.A., Issa, J.-P.J., and Baylin, S. (2016). Targeting the cancer epigenome for therapy. Nature Reviews Genetics *17*, 630.

Kamburov, A., Stelzl, U., Lehrach, H., and Herwig, R. (2013). The ConsensusPathDB interaction database: 2013 update. Nucleic acids research *41*, D793-D800.

Kim, D., Langmead, B., and Salzberg, S.L. (2015). HISAT: a fast spliced aligner with low memory requirements. Nature methods *12*, 357-360.

Kim, M.Y., Na, I., Kim, J.S., Son, S.H., Choi, S., Lee, S.E., Kim, J.-H., Jang, K., Alterovitz, G., and Chen, Y. (2019). Rational discovery of antimetastatic agents targeting the intrinsically disordered region of MBD2. Science advances *5*, eaav9810.

Kong, L., Zhang, Y., Ye, Z.-Q., Liu, X.-Q., Zhao, S.-Q., Wei, L., and Gao, G. (2007). CPC: assess the protein-coding potential of transcripts using sequence features and support vector machine. Nucleic acids research *35*, W345-W349.

Kramer, A., Green, J., Pollard, J., Jr., and Tugendreich, S. (2014). Causal analysis approaches in Ingenuity Pathway Analysis. Bioinformatics *30*, 523-530.

Lachmann, A., Xu, H., Krishnan, J., Berger, S.I., Mazloom, A.R., and Ma'ayan, A. (2010). ChEA: transcription factor regulation inferred from integrating genome-wide ChIP-X experiments. Bioinformatics *26*, 2438-2444.

Langmead, B., and Salzberg, S.L. (2012). Fast gapped-read alignment with Bowtie 2. Nature methods *9*, 357.

Lin, E.Y., Jones, J.G., Li, P., Zhu, L., Whitney, K.D., Muller, W.J., and Pollard, J.W. (2003). Progression to malignancy in the polyoma middle T oncoprotein mouse breast cancer model provides a reliable model for human diseases. The American journal of pathology *163*, 2113-2126.

Livak, K.J., and Schmittgen, T.D. (2001). Analysis of relative gene expression data using real-time quantitative PCR and the 2(-Delta Delta C(T)) Method. Methods (San Diego, Calif) *25*, 402-408.

Magnuson, A.M., Kiner, E., Ergun, A., Park, J.S., Asinovski, N., Ortiz-Lopez, A., Kilcoyne, A., Paoluzzi-Tomada, E., Weissleder, R., and Mathis, D. (2018). Identification and validation of a tumor-infiltrating Treg transcriptional signature conserved across species and tumor types. Proceedings of the National Academy of Sciences *115*, E10672-E10681.

Mahmood, N., Arakelian, A., Khan, H.A., Tanvir, I., Mazar, A.P., and Rabbani, S.A. (2020a). uPAR antibody (huATN-658) and Zometa reduce breast cancer growth and skeletal lesions. Bone Research *8*, 1-12.

Mahmood, N., Arakelian, A., Muller, W.J., Szyf, M., and Rabbani, S.A. (2020b). An enhanced chemopreventive effect of methyl donor S-adenosylmethionine in combination with 25-hydroxyvitamin D in blocking mammary tumor growth and metastasis. Bone Research *8*, 28.

Mahmood, N., and Rabbani, S.A. (2017). DNA methylation and breast cancer: mechanistic and therapeutic applications. Trends Cancer Res *12*, 1-18.

Mahmood, N., and Rabbani, S.A. (2019). DNA methylation readers and cancer: mechanistic and therapeutic applications. Frontiers in oncology *9*, 489.

Mian, O.Y., Wang, S.Z., Zu Zhu, S., Gnanapragasam, M.N., Graham, L., Bear, H.D., and Ginder, G.D. (2011). Methyl-binding domain protein 2–dependent proliferation and survival of breast cancer cells. Molecular Cancer Research *9*, 1152-1162.

Onagoruwa, O., Pal, G., Ochu, C., and Ogunwobi, O. (2020). Oncogenic Role of PVT1 and Therapeutic Implications. Front. Oncol *10*, 17.

Pakneshan, P., Szyf, M., Farias-Eisner, R., and Rabbani, S.A. (2004). Reversal of the hypomethylation status of urokinase (uPA) promoter blocks breast cancer growth and metastasis. J Biol Chem *279*, 31735-31744.

Pertea, M., Pertea, G.M., Antonescu, C.M., Chang, T.-C., Mendell, J.T., and Salzberg, S.L. (2015). StringTie enables improved reconstruction of a transcriptome from RNA-seq reads. Nature biotechnology *33*, 290-295.

Robinson, M.D., McCarthy, D.J., and Smyth, G.K. (2010). edgeR: a Bioconductor package for differential expression analysis of digital gene expression data. Bioinformatics *26*, 139-140.

Roche, J. (2018). The epithelial-to-mesenchymal transition in cancer (Multidisciplinary Digital Publishing Institute).

Sansom, O.J., Berger, J., Bishop, S.M., Hendrich, B., Bird, A., and Clarke, A.R. (2003). Deficiency of Mbd2 suppresses intestinal tumorigenesis. Nature genetics *34*, 145-147.

Searle, B.C. (2010). Scaffold: a bioinformatic tool for validating MS/MS-based proteomic studies. Proteomics *10*, 1265-1269.

Shukeir, N., Pakneshan, P., Chen, G., Szyf, M., and Rabbani, S.A. (2006). Alteration of the Methylation Status of Tumor-Promoting Genes Decreases Prostate Cancer Cell Invasiveness and Tumorigenesis In vitro and In vivo. Cancer Res *66*, 9202-9210.

Silverman, L.R., Demakos, E.P., Peterson, B.L., Kornblith, A.B., Holland, J.C., Odchimar-Reissig, R., Stone, R.M., Nelson, D., Powell, B.L., and DeCastro, C.M. (2002). Randomized controlled trial of azacitidine in patients with the myelodysplastic syndrome: a study of the cancer and leukemia group B. Journal of Clinical oncology *20*, 2429-2440.

Stefanska, B., Huang, J., Bhattacharyya, B., Suderman, M., Hallett, M., Han, Z.G., and Szyf, M. (2011). Definition of the landscape of promoter DNA hypomethylation in liver cancer. Cancer Res. *71*:5891-903

Stefanska, B., Suderman, M., Machnes, Z., Bhattacharyya, B., Hallett, M., and Szyf, M. (2013). Transcription onset of genes critical in liver carcinogenesis is epigenetically regulated by methylated DNA-binding protein MBD2. Carcinogenesis *34*, 2738-2749.

Sun, L., Luo, H., Bu, D., Zhao, G., Yu, K., Zhang, C., Liu, Y., Chen, R., and Zhao, Y. (2013). Utilizing sequence intrinsic composition to classify protein-coding and long non-coding transcripts. Nucleic acids research *41*, e166-e166.

Tseng, Y.Y., Moriarity, B.S., Gong, W., Akiyama, R., Tiwari, A., Kawakami, H., Ronning, P., Reuland, B., Guenther, K., Beadnell, T.C., *et al.* (2014). PVT1 dependence in cancer with MYC copy-number increase. Nature *512*, 82-86.

Tuominen, V.J., Ruotoistenmäki, S., Viitanen, A., Jumppanen, M., and Isola, J. (2010). ImmunoRatio: a publicly available web application for quantitative image analysis of estrogen receptor (ER), progesterone receptor (PR), and Ki-67. Breast cancer research : BCR *12*, R56-R56.

Ulitsky, I., Shkumatava, A., Jan, C.H., Sive, H., and Bartel, D.P. (2011). Conserved function of lincRNAs in vertebrate embryonic development despite rapid sequence evolution. Cell *147*, 1537-1550.

Wang, L., Liu, Y., Han, R., Beier, U.H., Thomas, R.M., Wells, A.D., and Hancock, W.W. (2013a). Mbd2 promotes foxp3 demethylation and T-regulatory-cell function. Mol Cell Biol *33*, 4106-4115.

Wang, L., Liu, Y., Han, R., Beier, U.H., Thomas, R.M., Wells, A.D., and Hancock, W.W. (2013b). Mbd2 promotes foxp3 demethylation and T-regulatory-cell function. Molecular and cellular biology *33*, 4106-4115.

Weaver, I.C., Hellstrom, I.C., Brown, S.E., Andrews, S.D., Dymov, S., Diorio, J., Zhang, T.Y., Szyf, M., and Meaney, M.J. (2014). The methylated-DNA binding protein MBD2 enhances NGFI-A (egr-1)-mediated transcriptional activation of the glucocorticoid receptor. Philos Trans R Soc Lond B Biol Sci *369*.

Webster, M.A., Hutchinson, J.N., Rauh, M.J., Muthuswamy, S.K., Anton, M., Tortorice, C.G., Cardiff, R.D., Graham, F.L., Hassell, J.A., and Muller, W.J. (1998). Requirement for both Shc and phosphatidylinositol 3′ kinase signaling pathways in polyomavirus middle T-mediated mammary tumorigenesis. Molecular and Cellular Biology *18*, 2344-2359.

Xing, F., Liu, Y., Wu, S.Y., Wu, K., Sharma, S., Mo, Y.Y., Feng, J., Sanders, S., Jin, G., Singh, R., *et al.* (2018). Loss of XIST in Breast Cancer Activates MSN-c-Met and Reprograms Microglia via Exosomal miRNA to Promote Brain Metastasis. Cancer Res *78*, 4316-4330.

Zhang, T., Hu, H., Yan, G., Wu, T., Liu, S., Chen, W., Ning, Y., and Lu, Z. (2019). Long Non-Coding RNA and Breast Cancer. Technol Cancer Res Treat *18*, 1533033819843889-1533033819843889.

Zhang, Y., Ng, H.H., Erdjument-Bromage, H., Tempst, P., Bird, A., and Reinberg, D. (1999). Analysis of the NuRD subunits reveals a histone deacetylase core complex and a connection with DNA methylation. Genes Dev *13*, 1924-1935.

Zhou, M., Zhou, K., Cheng, L., Chen, X., Wang, J., Wang, X.-M., Zhang, Y., Yu, Q., Zhang, S., and Wang, D. (2018). MBD2 ablation impairs lymphopoiesis and impedes progression and maintenance of T-ALL. Cancer research *78*, 1632-1642.

Zhu, D., Osuka, S., Zhang, Z., Reichert, Z.R., Yang, L., Kanemura, Y., Jiang, Y., You, S., Zhang, H., and Devi, N.S. (2018). BAI1 suppresses medulloblastoma formation by protecting p53 from Mdm2-mediated degradation. Cancer cell *33*, 1004-1016. e1005.

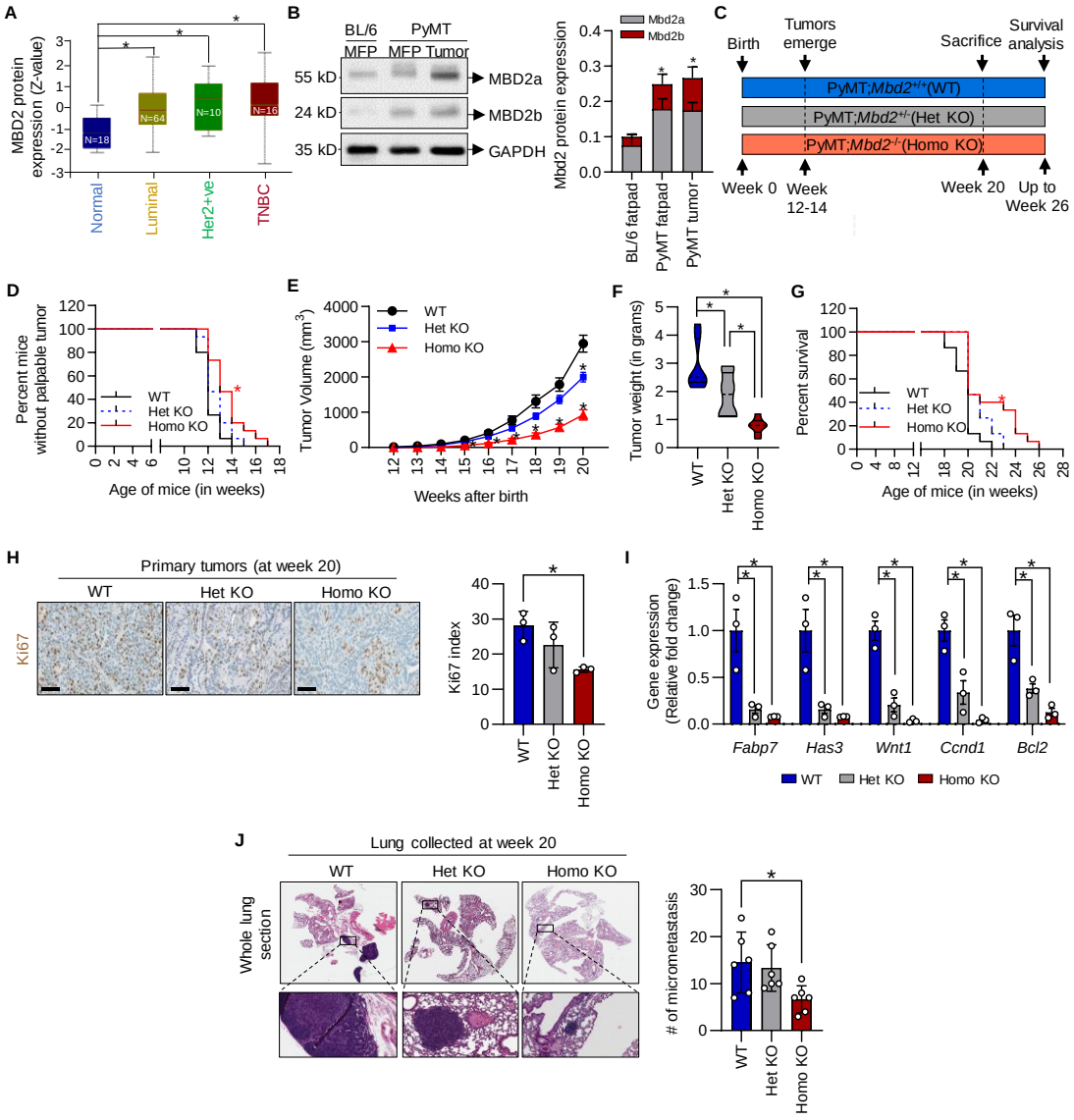

Figure 1: MBD2 is upregulated in breast tumors, and knockout of the *Mbd2* gene affects tumor and progression in transgenic PyMT mice.

(A) MBD2 protein levels in normal subjects and different subtypes of breast cancer according to the CPTAC database. **(B)** Immunoblot of the mouse Mbd2 protein from lysates obtained from the mammary fat pad of 11-week-old female C57BL/6 (lane 1) and PyMT mice (lane 2), and mammary tumors 20-week-old PyMT mice (lane 3). GAPDH was used as a loading control. The right panel shows normalized densitometric quantification of the total Mbd2 signals (n=3 animals/group). **(C)** Schematic representation of the endpoints of this study. **(D)** A Kaplan-Meier curve showing tumor emergence in the three groups. **(E)** Tumor volumes were measured at weekly intervals until sacrifice (n=15

animals/group). **(F)** Violin plot showing the distribution of tumor weight in each group measured at week 20. At least eight animals in each group were sacrificed at this point in addition to the ones that researched to a level requiring humane sacrifice. The rest of the animals were used for Kaplan-Meier survival analysis in **(G)** until they required humane sacrifice. **(H)** Immunohistochemical staining of the primary tumors from each group of animals with an antibody against Ki67 proliferation marker (left panel). The percentage of Ki67 positive tumor cells was determined from five high-power fields for each sample and plotted as a bar graph in the right panel (n=3 animals/group). **(I)** qPCR of several known cancer-related genes using RNA extracted from primary tumors (n=3 animals/group). **(J)** H&E staining of formalin-fixed lung tissues obtained at experimental endpoint at week 20. The number of micrometastases were counted and plotted as a bar graph (n=6 animals/group). Results are represented as the mean ± SEM, and statistically significant differences were determined using ANOVA followed by post hoc Tukey's test. $P < 0.05$.

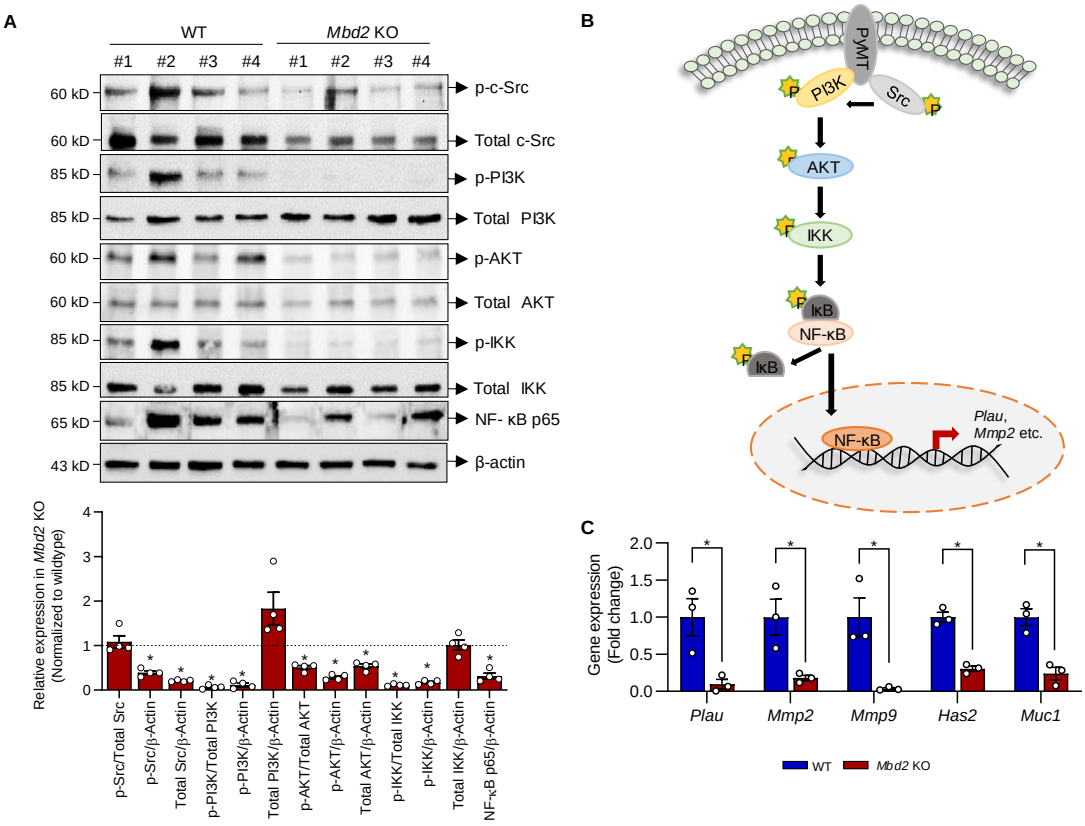

Figure 2: *Mbd2* depletion interferes with the PyMT-dependent activation of the PI3K/Akt/NF-κB axis.

(A) Immunoblots from whole tumor lysates obtained from four distinct animals/group (upper panel). Densitometric quantification of the bands for each protein was determined and plotted as mean ± SEM (n=4 tumors/group) (lower panel). **(B)** Schematic diagram of PyMT-mediated oncogenic signaling pathways downregulated by Mbd2 depletion. **(C)** qPCR of several NF-κB regulated genes (n=3/group). Statistical significance was determined using the student's *t*-test. **P* < 0.05.

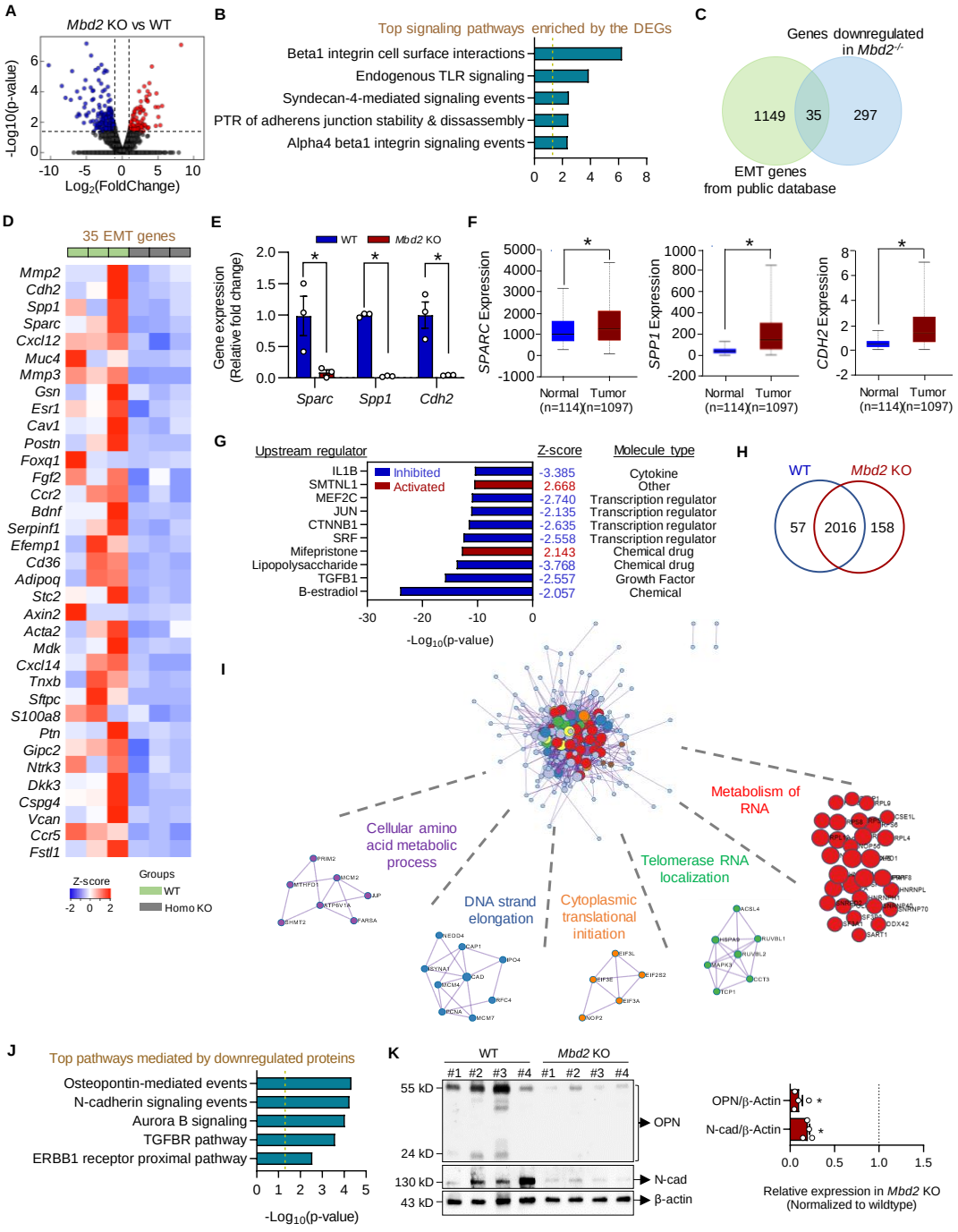

Figure 3: Transcriptomic and proteomic analyses of wildtype and *Mbd2* KO tumors.

(A) RNA extracted from mammary tumors of control and knockout mouse were subjected to RNA-Sequencing (n=3 samples/group). A volcano plot showing the DEGs (332

downregulated and 121 upregulated) in the Mbd2 KO vs. wildtype groups. **(B)** Pathway enrichment analysis (PID database) of the DEGs in *Mbd2* KO tumors. **(C)** Venn diagram of the 332 downregulated genes in *Mbd2* KO tumors with the complete repertoire of genes from the epithelial–mesenchymal transition (EMT) database showed an overlap of 35 genes that are presented in the heatmap in **(D)**. **(E)** qPCR validation of the selected EMT-related genes (*Sparc, Spp1, Cdh2*) obtained from RNA-Seq was done using tumoral RNA from at least three animals/group. **(F)** The gene expression pattern of the human orthologs of the qPCR validated genes in normal and breast tumors according to the TCGA database. **(G)** Top ten upstream regulators of the DEGs obtained from RNA-Seq as predicted by IPA upstream regulator analyses tool. **(H)** Venn diagram of the common and unique protein hits in wildtype and *Mbd2* KO animals according to the proteomics analyses. **(I)** Protein-protein interaction network of the obtained hits from wildtype and *Mbd2* KO animals. **(J)** Pathway enrichment analysis (PID database) of the significantly downregulated proteins in *Mbd2* KO tumors. **(K)** Analysis of Osteopontin and N-Cadherin proteins in the immunoblots of whole tumor lysates. The right panel shows the densitometric quantification of the immunoblots plotted as mean ± SEM (n=4 tumors/group). Statistical significance was determined using the student's *t*-test. $*P < 0.05$.

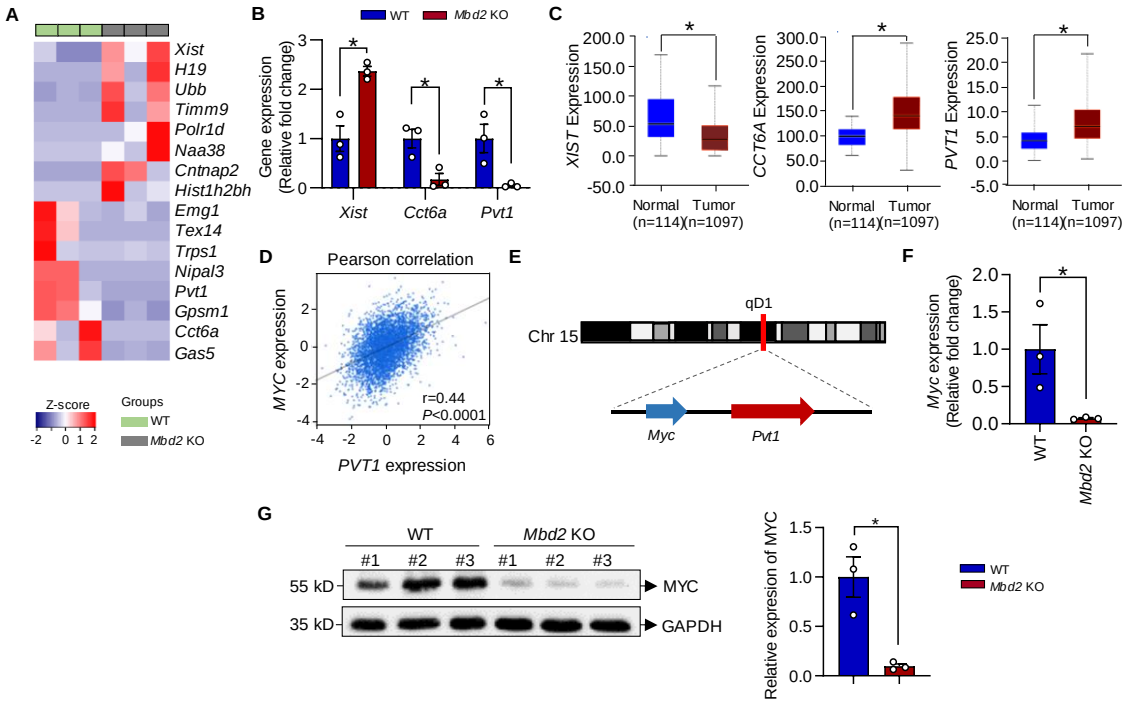

Figure 4: Analyses of differentially expressed lncRNAs in *Mbd2* KO tumors.

(A) Heatmap of differentially expressed lncRNAs in *Mbd2* KO tumors with known biological function(s) or known human orthologs in the TCGA breast cancer patient dataset. **(B)** qPCR validation of the selected lncRNAs (*Xist*, *Cct6a*, *Pvt1*) obtained from RNA-Seq was done using tumoral RNA from at least three animals/group. **(C)** The gene expression pattern of the human orthologs of the qPCR validated genes in normal and breast tumors according to the TCGA database. **(D)** Pearson correlation between human *PVT1* and *MYC* genes using data obtained from 4307 patients in TCGA, GSE81538, and GSE96058. **(E)** Schematic of the chromosomal location of *Myc* and *Pvt1* genes revealing proximity of the genes on the mouse genome (not drawn to scale). **(F-G)** RNA and protein levels of Myc is significantly altered in *Mbd2* KO tumors relative to wildtype counterparts. Results are shown as mean ± SEM (n=3 tumors/group). Statistical significance was determined using the student's *t*-test. **P* < 0.05.

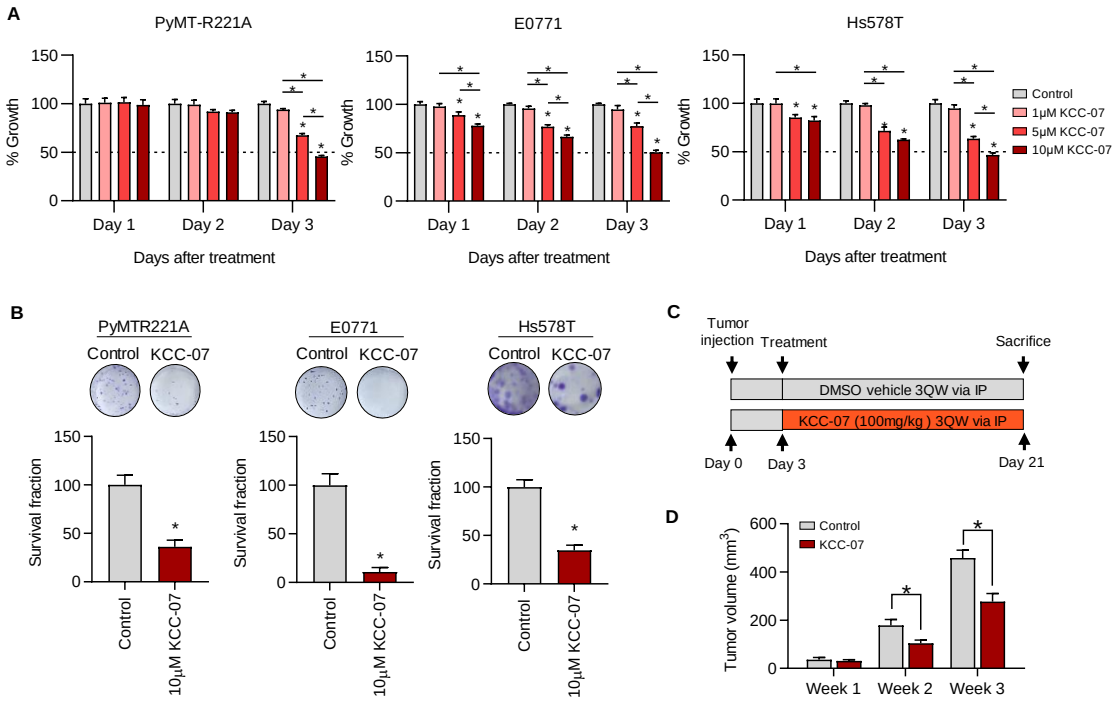

Figure 5: Effect of pharmacological inhibition of Mbd2 pathway using a small molecule inhibitor KCC07.

(A) Mouse PyMT-R221A, E0771, and human Hs578T breast cancer cells were treated with different doses of MBD2 pathway inhibitor (KCC07) for three days, and cell number of determined by a Coulter Counter (n=3). **(B)** The number of colonies in vehicle-treated control and 10.0 μM KCC07 cells were counted under a microscope and represented as survival fraction (n=3). **(C)** Schematic representation of treatment protocol in PyMT-R221A syngeneic mice. Three days post-implantation of the PyMT-R221A cells via the orthotopic route, the animals were randomized, and intraperitoneal injection with either DMSO-vehicle or 100mg/kg/ mice KCC-07 was administered three times per week until sacrifice. **(D)** Tumor volume was measured at weekly intervals and plotted as mean ± SEM (n=7 animals/group). Statistical significance was determined using the student's *t*-test. **P* < 0.05.

Supplementals for Chapter 5

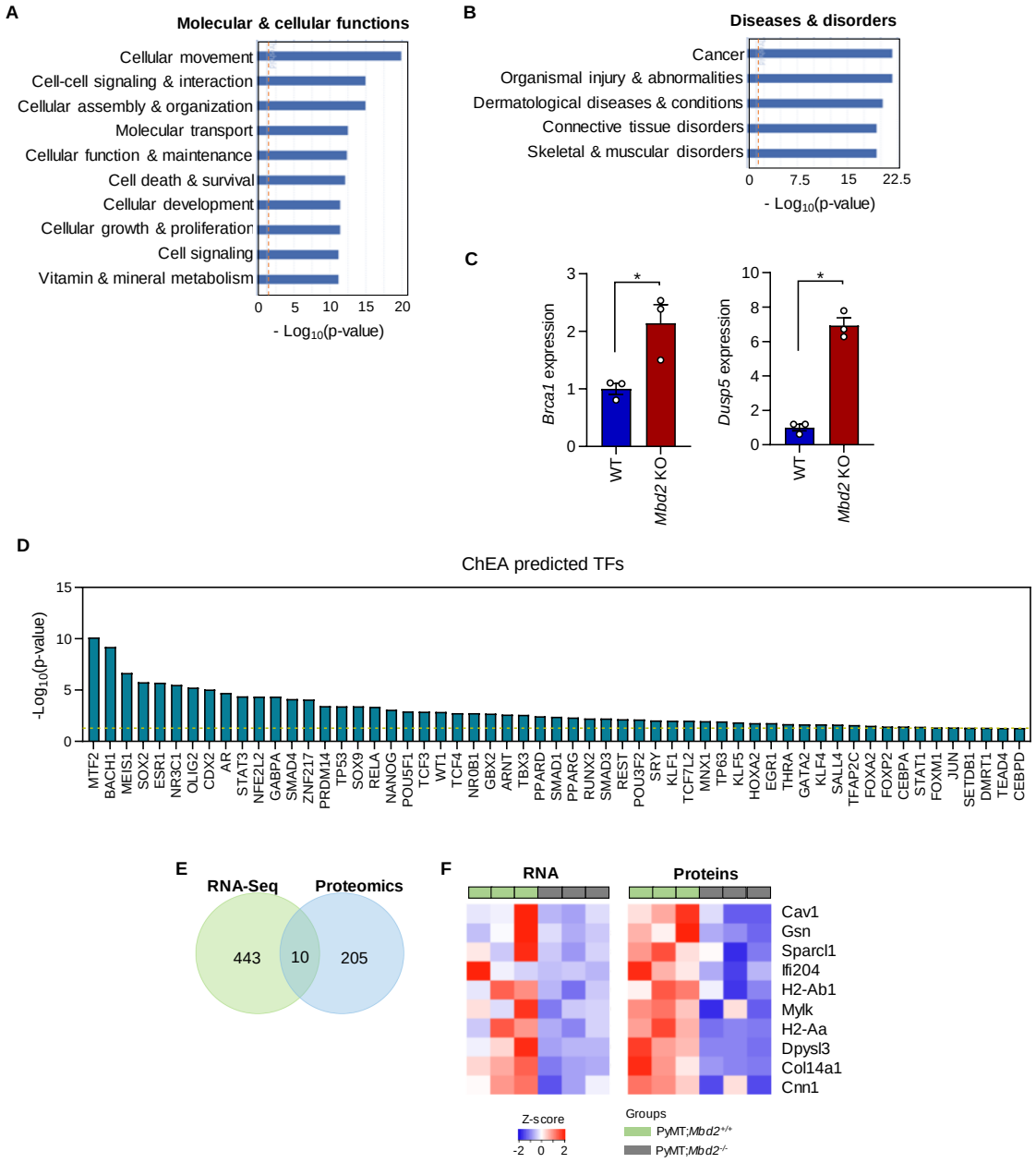

Supplementary Figure S1: Transcriptomic and proteomic analyses. IPA predicted **(A)** Top ten 'molecular and cellular functions' and **(B)** top five 'diseases and disorders' altered by the DEGs in Mbd2 KO tumors. **(C)** qPCR validation of the selected tumor suppressor genes (*Brca1*, *Dusp5*) obtained from RNA-Seq. **(D)** ChEA predicted upstream transcription factors for the DEGs identified in *Mbd2* KO tumors. **(E)** Venn diagram showing the overlap of 10 genes between RNA-Seq and proteomics analyses. **(F)** Heatmap showing the overlapped genes showed concordant downregulation.

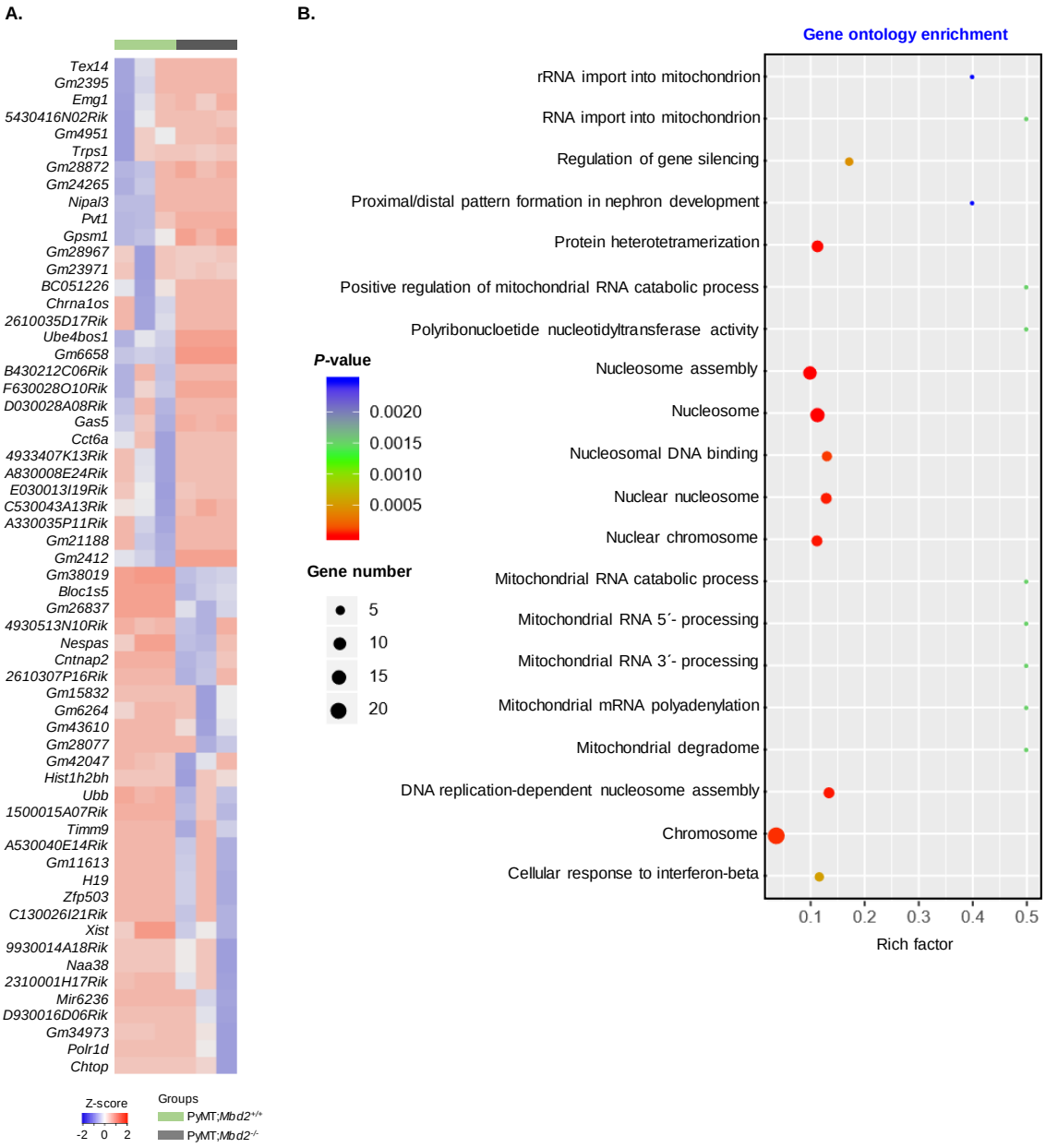

Supplementary Figure S2: *Mbd2* regulated lncRNAs. (A) Heatmap of the 60 differentially regulated lncRNAs in Mbd2 KO tumors. **(B)** Gene ontology (GO) enrichment analyses using the list of differentially regulated lncRNAs.

Supplementary Table S1: Biochemical analyses of the serum from DMSO and KCC-07 treated animals (n=3/group).

Parameter	**Reference Value**	**DMSO-treated mice**	**KCC-treated mice**	***P*-value**
Total protein (g/L)	36-66	43 ± 0.47	41.33 ± 0.72	0.19
Albumin (g/L)	25-48	22.33 ± 0.27	21.33 ± 0.27	0.1
Albumin/Globulin ratio		1.1 ± 0	1.03 ± 0.02	0.12
Glucose (mmol/L)	5.0-10.7	17.47 ± 0.98	15.93 ± 0.62	0.34
BUN Urea (mmol/L)	6.4-10.4	8.0 ± 0.26	9.33 ± 0.83	0.28
Total Bilirubin (µmol/L)	2-15	5.37 ± 0.14	4.83 ± 0.35	0.31
ALT (U/L)	28-132	27.7 ± 0.17	21.70 ± 0.27	0.003
AST (U/L)	59-247	107 ± 3.68	97.67 ± 3.06	0.19
CK (U/L)	68-1070	318 ± 87.58	222.33 ± 16.13	0.43
Cholesterol (mmol/L)	0.93-2.48	2.88 ± 0.12	2.7 ± 0.09	0.39
Sodium (mmol/L)	124-174	140.67 ± 0.27	142 ± 0.47	0.12
Potassium (mmol/L)	4.6-8.0	4.06 ± 0.07	4.26 ± 0.07	0.18
Chloride (mmol/L)	92-120	111 ± 0.82	112 ± 0	0.37
Calcium (mmol/L)	1.47-2.35	2.28 ± 0.00	2.27 ± 0.01	0.6
Phosphorus (mmol/L)	1.97-3.26	1.74 ± 0.01	1.91 ± 0.23	0.61
Magnesium (mmol/L)	0.33-1.60	1.15 ± 0.01	1.19 ± 0.05	0.59

*ALT: Alanine aminotransferase; AST: Aspartate aminotransferase; CK: Creatinine kinase

Chapter Six: General discussion, conclusion, and future direction

Abnormal DNA methylation is the first described epigenetic alteration in cancer (Feinberg and Vogelstein, 1983). Due to the technological constraints, the earlier studies mainly focused on site-specific methylation changes near the gene promoters. It was shown that the promoters of several known tumor suppressor genes are hypermethylated in cancer, resulting in their transcriptional repression (Esteller et al., 1999; Yoshiura et al., 1995). Using gene-knockout based studies, it was shown that genetic depletion of the DNA methylation writer (DNMT) protects animals from developing tumors (Laird et al., 1995). As a result, the research paradigm in epigenetic-based therapies mainly focused on targeting DNA hypermethylation in the 1990s and early 2000s (MacLeod and Szyf, 1995; Miki et al., 2001; Ramchandani et al., 1997), and two DNMT inhibitors targeting hypermethylation are already approved for the treatment of several hematological cancers.

Our lab has previously shown that the DNMT inhibitors also induce the expression of prometastatic genes along with the tumor suppressor genes (Ateeq et al., 2008). This may lead to the increased ability of the tumor cells to metastasize to distant organs, which is the most morbid aspect of cancer. Recent advances in high-throughput sequencing technologies revealed that both hypermethylation and hypomethylation mediated epigenetic abnormalities are present in cancer (Cheishvili et al., 2015). Therefore, targeting one arm of the methylation abnormality is not always sufficient to achieve a potent anti-tumor response. Moreover, the patterns of methylation abnormalities are cancer subtype dependent. For example, an integrative analysis of DNA methylation and gene expression in the TCGA breast cancer dataset revealed that the group with most hypomethylation overlapped with the highly aggressive basal-like TNBC gene expression patterns

(Network, 2012). Therefore, a rational strategy is needed to target the methylation abnormalities in cancer to achieve and maintain a balance between DNA hyper- and hypomethylation.

This thesis was aimed at examining the effectiveness of different types of anti-cancer agents targeting the methylome. In line with that, we first tested the preclinical therapeutic potential of SAM in reversing the hypomethylated state in TNBCs using well-established *in vitro* and *in vivo* models. Results from these studies provided the first-ever evidence for the potential anti-cancer effects of SAM in reducing breast tumor growth and metastasis *in vivo.*

We also assessed the global gene expression changes of the MDA-MB-231 transcriptome upon SAM-treatment by Affymetrix microarray (Chapter 2) and RNA-Seq (Chapter 3). Regardless of the platform used for analyses, we have consistently found a significant repression of genes involved in metastasis, angiogenesis, and EMT in the SAM-treated group. Several crucial prometastatic genes that are always downregulated upon SAM treatment include *uPA, MUC1, SOX4,* etc. More importantly, SAM treatment did not downregulate the expression of known tumor suppressor genes. We found that several tumor suppressor genes like *DUSP1, TFPI2, SERPINB2* (encoding for PAI-2) were upregulated upon SAM-treatment. Since PAI-2 is a known inhibitor of *uPA* (Thorsen et al., 1988), these results further confirmed our previous observation that the anti-cancer effects of SAM are mediated through the modulation of the uPA-uPAR axis which could be potentially used as response-predicting biomarkers in future clinical trials.

The RNA-Seq experiments related to the administration of SAM (Chapters 3 and 4) were done using an average sequencing depth of 20 million reads per sample with read lengths of 43bps (paired-end), which is enough for differential gene expression calling but not enough to analyze the differential alternative splicing (AS) events that are seen in many types of cancer including breast tumors. Since the cost of sequencing is plummeting with time and more powerful algorithms to precisely analyze the AS events are becoming available, future RNA-Seq experiments with read lengths greater than 100 bp and sequencing depth beyond 50 million reads per sample would provide a more detailed picture of the splicing changes mediated by SAM.

To analyze the methylation changes induced by SAM-treatment, we performed both site-specific and genome-wide methylation assays. Our results demonstrated that SAM-treatment indeed caused more hypermethylation near the gene promoters (Figure 6, Chapter 3). Intriguingly, SAM also caused hypomethylation near the promoters of many genes. Similar bidirectional methylation changes were seen in the genome-wide methylation studies done in control and SAM-treated liver cancer cells (Wang et al., 2017). One possible explanation behind such observation might be an indirect effect of SAM, where it modulates the expression of downstream gene(s) involved in hypomethylation. However, further studies are warranted to understand how a methylating agent like SAM also causes hypomethylation.

Pathway enrichment analyses of the genes with differentially methylated CGs upon SAM-treatment revealed their involvement in negative regulation of cell proliferation and differentiation, regulation of cell adhesion etc. (Figure 6, Chapter 3). We also found that

SAM-mediated DNA methylation changes are not always congruent with the gene expression changes, as demonstrated by the pyrosequencing and qPCR experiments in Chapter 2. There are several possible explanations behind this observation. SAM is a pleiotropic agent that can also act as a methyl donor for other biological substrates than DNA. It is known that SAM can also methylate RNA, protein, and lipids (Chiang et al., 1996). SAM is the methyl donor for histone methyltransferases and thereby affects the methylation status of histone proteins (Serefidou et al., 2019). These methylated histones are then recognized by the chromatin readers and thereby attract the recruitment of other factors of the chromatin remodeling complex to cause transcriptional activation or repression of genes in a context-dependent manner. Whether the chromatin would be accessible or repressed depends on the sites and degrees of histone methylation (Greer and Shi, 2012). Therefore, in-depth studies are needed in future to decipher the role of SAM on the methylation of the known active and repressive histone marks in the context of breast tumors. In addition, genome-wide changes in chromatin accessibilities need to be measured by Assay for Transposase-Accessible Chromatin using sequencing (ATAC-Seq). This will help to explain, in part, the transcriptomic changes seen upon SAM-treatment. Alternatively, SAM may also change the RNA methylation landscape of breast tumors. Emerging evidence indicates the involvement of RNA methylation, particularly at N^6-methyladenosine (m^6A), during tumor progression and metastasis (Chen et al., 2019). Therefore, it will be equally interesting to check the effects of SAM on RNA methylation writers, readers, and eraser proteins and integrate those observations with the transcriptomic changes induced upon SAM-treatment. Another important aspect that is still

not fully explored is the role of SAM on the metabolome. Recent evidence suggests that there is a crosstalk between the epigenetic and metabolomic processes that drives multiple steps of tumor progression and metastasis (Wong et al., 2017). Since SAM itself is a product of one-carbon metabolism and have distinct epigenetic functions, it will be interesting to assess the metabolomic changes in breast tumors upon SAM-treatment in the future.

One of the major advantages of using SAM as an anti-cancer agent is its long safety records when used in humans for depression and other disorders. More than 100 clinical trials have already been conducted using SAM for indications other than cancer (Sharma et al., 2017). At present, at least two clinical trials intended to test the anti-cancer therapeutic potential of SAM against liver cancer are at the initial stages of patient recruitment. Based on the promising anti-cancer effects of SAM in preclinical settings, as shown in Chapter 2, our group is currently assessing the feasibility and logistics of testing the efficacy of SAM administration for patients with breast cancer in phase 1 clinical trials.

Since there are intratumor and intertumor heterogeneity in breast cancer cells where the tumor cells are at different stages of aggressiveness and show differential DNA methylation patterns, we next tested whether concurrent treatment with demethylating (Decitabine/5AzadC) and methylating (SAM) agents would suppress breast tumor growth and metastasis *in vivo* (Chapter 3). Our results show that the SAM+5AzazdC combination treatment enhanced the anti-cancer effect in reducing breast tumor growth and lung metastasis compared to the monotherapy arms (Figure 2, Chapter 3). Furthermore, RNA-Seq based transcriptome analyses revealed that the combinatorial treatment with SAM and

5AzadC does not nullify the molecular effects of each other, suggesting their potential use in clinical settings to target the heterogeneous population of breast tumor cells. Taken together, the results from Chapter 2 and 3 demonstrated the anti-cancer therapeutic potential of SAM alone or in combination with an approved chemotherapeutic agent like 5AzadC.

There is a growing consensus that the control of neoplastic growth should focus on both prevention and treatment (Noguchi et al., 1996). Approaches to prevent breast cancer has been attempted for decades with the earlier strategies involving prophylactic mastectomy for which little to no agreement exists at present (Noguchi et al., 1996). The advancement in our understanding of the molecular events during cancer progression paved the way for 'chemoprevention' where one or more drugs or nutraceutical agents are used to control or prevent the occurrence of cancer (Wattenberg, 1985). An often-desirable characteristic of an ideal chemopreventive agent is to show therapeutic efficacy at doses that elicit little or no toxicity (Steward and Brown, 2013). In line with that, we next assessed whether SAM alone or in combination with a known chemopreventive agent Vitamin D prohormone [25(OH)D] would prevent or delay the occurrence of breast tumor in transgenic MMTV-PyMT model (Chapter 4). Our results showed that combination treatment markedly delayed the appearance of palpable breast tumors, reduced tumor growth and lung metastasis compared to the control and monotherapy arms. Transcriptome analyses revealed the combination treatment significantly downregulated several key components of the HIF-1 signaling pathway like *Egln1*, *Egln3*, *Cxcr4*, *Vegfa*, and others. More importantly, the SAM+25(OH)D combination upregulated the genes from interferon-

alpha/beta signaling that are crucial for mediating anti-tumor response as well as boosting the immune response. Emerging evidence suggests that epigenetic agents can prime the immune system and thereby enhance the anti-cancer therapeutic potential of immune checkpoint inhibitors (Dunn and Rao, 2017; Turpin and Vatner, 2019). It will be interesting to see if SAM alone or in combination with 25(OH)D would be able to sufficiently prime the immune system to maximize the effects of immune checkpoint inhibitors in reducing breast tumor growth and progression.

To gain further mechanistic insights into the SAM-mediated molecular events, we next aimed to target a downstream molecular effector of SAM. Our previous studies have demonstrated that SAM treatment inhibits DNA demethylation by increasing the DNMT activity and inhibiting the Mbd2 mediated demethylation (Detich et al., 2003; Pakneshan et al., 2004). Mbd2 is classically known to link DNA methylation to chromatin remodeling through the recruitment of the corepressor complex to the methylated regions of the genome (Le Guezennec et al., 2006). Moreover, Mbd2 has been suggested to be involved in promoting breast cancer growth and metastasis, however past studies were performed in cancer cell lines and xenografts in mice and used either antisense or siRNA knockdown approaches (Cheishvili et al., 2014; Mian et al., 2011). Since these methodologies are highly confounded, the main question that remained to be answered is whether Mbd2 plays a causal role in breast cancer. The previous studies could only address the role of Mbd2 once the cancer has evolved but could not capture its role during the multistep process of malignant transformation and early stages of cancer. Therefore, in Chapter 5, we show that genetic depletion of *Mbd2* in a well-established transgenic mouse model of breast cancer

caused a significant delay in mammary tumor emergence, reduced tumor burden and lung metastasis, and prolonged the survival rate. Transcriptomic and proteomic analyses of the primary tumors obtained from wildtype and *Mbd2* depleted tumors demonstrated that several key molecular determinants of the EMT pathway (for example, osteopontin, N-cadherin) were downregulated in *Mbd2*$^{-/-}$ tumors. *Mbd2* depletion interfered with the PyMT mediated stimulation of the PI3K/Akt/NF-κB axis and thereby reduced the expression *uPA, Mmp2,* and other prometastatic genes. Moreover, administration of a small molecule inhibitor targeting the Mbd2 pathway significantly reduced breast tumor growth *in vivo.* These results may open new avenues for the development of targeted epigenetic therapies to block the aberrant expression of DNA methylation readers in breast cancer.

The global burden of cancer is expanding, and therefore, there is an urgent need for novel, cost-effective anti-cancer therapeutic strategies. In this regard, the idea of drug repurposing is becoming very popular in the recent times (Pushpakom et al., 2019). This not only reduces the time associated with the development and evaluation of new therapeutic agents but also allows their availability at a much-reduced cost. Our approach is particularly attractive as it demonstrates that a widely used nutraceutical agent SAM can be used alone or in combination with a clinically approved chemotherapeutic drug like decitabine or chemopreventive agent like Vitamin D prohormone would provide a sustained anti-cancer effect which can be translated in clinical settings at a much faster timeframe and reduced cost to reduce the morbidity and mortality associated with breast and other common cancers.

REFERENCES (Chapters 1 and 6)

Adorján, P., Distler, J., Lipscher, E., Model, F., Müller, J., Pelet, C., Braun, A., Florl, A.R., Gütig, D., and Grabs, G. (2002). Tumour class prediction and discovery by microarray-based DNA methylation analysis. Nucleic acids research *30*, e21-e21.

Aguilera, O., Peña, C., García, J.M., Larriba, M.J., Ordóñez-Morán, P., Navarro, D., Barbáchano, A., López de Silanes, I., Ballestar, E., and Fraga, M.F. (2007). The Wnt antagonist DICKKOPF-1 gene is induced by 1α, 25-dihydroxyvitamin D 3 associated to the differentiation of human colon cancer cells. Carcinogenesis *28*, 1877-1884.

Alhosin, M., León-González, A.J., Dandache, I., Lelay, A., Rashid, S.K., Kevers, C., Pincemail, J., Fornecker, L.-M., Mauvieux, L., and Herbrecht, R. (2015). Bilberry extract (Antho 50) selectively induces redox-sensitive caspase 3-related apoptosis in chronic lymphocytic leukemia cells by targeting the Bcl-2/Bad pathway. Scientific reports *5*, 8996.

Almeida, A., Kokalj-Vokac, N., Lefrancois, D., Viegas-Pequignot, E., Jeanpierre, M., Dutrillaux, B., and Malfoy, B. (1993). Hypomethylation of classical satellite DNA and chromosome instability in lymphoblastoid cell lines. Human genetics *91*, 538-546.

Angrisano, T., Lembo, F., Pero, R., Natale, F., Fusco, A., Avvedimento, V.E., Bruni, C.B., and Chiariotti, L. (2006). TACC3 mediates the association of MBD2 with histone acetyltransferases and relieves transcriptional repression of methylated promoters. Nucleic acids research *34*, 364-372.

Arima, Y., Hirota, T., Bronner, C., Mousli, M., Fujiwara, T., Niwa, S.i., Ishikawa, H., and Saya, H. (2004). Down-regulation of nuclear protein ICBP90 by p53/p21Cip1/WAF1-dependent DNA-damage checkpoint signals contributes to cell cycle arrest at G1/S transition. Genes to Cells *9*, 131-142.

Ateeq, B., Unterberger, A., Szyf, M., and Rabbani, S.A. (2008). Pharmacological inhibition of DNA methylation induces proinvasive and prometastatic genes in vitro and in vivo. Neoplasia *10*, 266-278.

Avery, O.T., MacLeod, C.M., and McCarty, M. (1944). Studies on the chemical nature of the substance inducing transformation of pneumococcal types induction of transformation by a desoxyribonucleic acid fraction isolated from pneumococcus type III. The Journal of experimental medicine *79*, 137-158.

Bakker, J., Lin, X., and Nelson, W.G. (2002). Methyl-CpG binding domain protein 2 represses transcription from hypermethylated π-class glutathione S-transferase gene promoters in hepatocellular carcinoma cells. Journal of Biological Chemistry *277*, 22573-22580.

Bannister, A.J., and Kouzarides, T. (2005). Reversing histone methylation. Nature *436*, 1103.

Barkan, D., Green, J.E., and Chambers, A.F. (2010). Extracellular matrix: a gatekeeper in the transition from dormancy to metastatic growth. European journal of cancer *46*, 1181-1188.

Baubec, T., Ivánek, R., Lienert, F., and Schübeler, D. (2013). Methylation-dependent and-independent genomic targeting principles of the MBD protein family. Cell *153*, 480-492.

Berger, N.A. (2016). Epigenetics, Energy Balance, and Cancer, Vol 11 (Springer).

Bestor, T.H. (2000). The DNA methyltransferases of mammals. Human molecular genetics *9*, 2395-2402.

Bhattacharya, S.K., Ramchandani, S., Cervoni, N., and Szyf, M. (1999). A mammalian protein with specific demethylase activity for mCpG DNA. nature *397*, 579.

Billard, L.-M., Magdinier, F., Lenoir, G.M., Frappart, L., and Dante, R. (2002). MeCP2 and MBD2 expression during normal and pathological growth of the human mammary gland. Oncogene *21*, 2704.

Bird, A. (2002). DNA methylation patterns and epigenetic memory. Genes & development *16*, 6-21.

Boeke, J., Ammerpohl, O., Kegel, S., Moehren, U., and Renkawitz, R. (2000). The minimal repression domain of MBD2b overlaps with the methyl-CpG-binding domain and binds directly to Sin3A. Journal of Biological Chemistry *275*, 34963-34967.

Bottiglieri, T. (2002). S-Adenosyl-L-methionine (SAMe): from the bench to the bedside—molecular basis of a pleiotrophic molecule. The American journal of clinical nutrition *76*, 1151S-1157S.

Cadieux, B., Ching, T.-T., VandenBerg, S.R., and Costello, J.F. (2006). Genome-wide hypomethylation in human glioblastomas associated with specific copy number alteration, methylenetetrahydrofolate reductase allele status, and increased proliferation. Cancer research *66*, 8469-8476.

Cai, Y., Geutjes, E.-J., De Lint, K., Roepman, P., Bruurs, L., Yu, L., Wang, W., Van Blijswijk, J., Mohammad, H., and De Rink, I. (2014). The NuRD complex cooperates with DNMTs to maintain silencing of key colorectal tumor suppressor genes. Oncogene *33*, 2157.

Calvisi, D.F., Pinna, F., Meloni, F., Ladu, S., Pellegrino, R., Sini, M., Daino, L., Simile, M.M., De Miglio, M.R., and Virdis, P. (2008a). Dual-specificity phosphatase 1 ubiquitination in extracellular signal-regulated kinase–mediated control of growth in human hepatocellular carcinoma. Cancer research *68*, 4192-4200.

Calvisi, D.F., Pinna, F., Pellegrino, R., Sanna, V., Sini, M., Daino, L., Simile, M.M., De Miglio, M.R., Frau, M., and Tomasi, M.L. (2008b). Ras-driven proliferation and apoptosis signaling during rat liver carcinogenesis is under genetic control. International journal of cancer *123*, 2057-2064.

Cameron, E.E., Bachman, K.E., Myöhänen, S., Herman, J.G., and Baylin, S.B. (1999). Synergy of demethylation and histone deacetylase inhibition in the re-expression of genes silenced in cancer. Nature genetics *21*, 103-107.

Campbell, P.M., Bovenzi, V., and Szyf, M. (2004). Methylated DNA-binding protein 2 antisense inhibitors suppress tumourigenesis of human cancer cell lines in vitro and in vivo. Carcinogenesis *25*, 499-507.

Cantoni, G. (1951). Methylation of nicotinamide with a soluble enzyme system from rat liver. J Biol Chem *189*, 203-216.

Cave, D.D., Desiderio, V., Mosca, L., Ilisso, C.P., Mele, L., Caraglia, M., Cacciapuoti, G., and Porcelli, M. (2018). S-Adenosylmethionine-mediated apoptosis is potentiated by autophagy inhibition induced by chloroquine in human breast cancer cells. Journal of cellular physiology *233*, 1370-1383.

Cervoni, N., and Szyf, M. (2001). Demethylase activity is directed by histone acetylation. Journal of Biological Chemistry *276*, 40778-40787.

Chatagnon, A., Bougel, S., Perriaud, L., Lachuer, J., Benhattar, J., and Dante, R. (2008). Specific association between the methyl-CpG-binding domain protein 2 and the hypermethylated region of the human telomerase reverse transcriptase promoter in cancer cells. Carcinogenesis *30*, 28-34.

Cheishvili, D., Boureau, L., and Szyf, M. (2015). DNA demethylation and invasive cancer: implications for therapeutics. British journal of pharmacology *172*, 2705-2715.

Chen, H., Li, S., Liu, J., Diwan, B.A., Barrett, J.C., and Waalkes, M.P. (2004). Chronic inorganic arsenic exposure induces hepatic global and individual gene hypomethylation: implications for arsenic hepatocarcinogenesis. Carcinogenesis *25*, 1779-1786.

Chen, R.Z., Pettersson, U., Beard, C., Jackson-Grusby, L., and Jaenisch, R. (1998). DNA hypomethylation leads to elevated mutation rates. Nature *395*, 89.

Cheng, C.K., Chow, L.W., Loo, W.T., Chan, T.K., and Chan, V. (2005). The cell cycle checkpoint gene Rad9 is a novel oncogene activated by 11q13 amplification and DNA methylation in breast cancer. Cancer research *65*, 8646-8654.

Chik, F., Machnes, Z., and Szyf, M. (2013). Synergistic anti-breast cancer effect of a combined treatment with the methyl donor S-adenosyl methionine and the DNA methylation inhibitor 5-aza-2′-deoxycytidine. Carcinogenesis *35*, 138-144.

Civitelli, R., Kim, Y.S., Gunsten, S.L., Fujimori, A., Huskey, M., Avioli, L.V., and HRUSKA, K.A. (1990). Nongenomic activation of the calcium message system by vitamin D metabolites in osteoblast-like cells. Endocrinology *127*, 2253-2262.

Compere, S.J., and Palmiter, R.D. (1981). DNA methylation controls the inducibility of the mouse metallothionein-I gene in lymphoid cells. Cell *25*, 233-240.

Conway, K.E., McConnell, B.B., Bowring, C.E., Donald, C.D., Warren, S.T., and Vertino, P.M. (2000). TMS1, a novel proapoptotic caspase recruitment domain protein, is a target of methylation-induced gene silencing in human breast cancers. Cancer Research *60*, 6236-6242.

Cornejo, K.M., Kandil, D., Khan, A., and Cosar, E.F. (2014). Theranostic and molecular classification of breast cancer. Archives of Pathology and Laboratory Medicine *138*, 44-56.

Cortázar, D., Kunz, C., Selfridge, J., Lettieri, T., Saito, Y., MacDougall, E., Wirz, A., Schuermann, D., Jacobs, A.L., and Siegrist, F. (2011). Embryonic lethal phenotype reveals a function of TDG in maintaining epigenetic stability. Nature *470*, 419-423.

Cortellino, S., Xu, J., Sannai, M., Moore, R., Caretti, E., Cigliano, A., Le Coz, M., Devarajan, K., Wessels, A., and Soprano, D. (2011). Thymine DNA glycosylase is essential for active DNA demethylation by linked deamination-base excision repair. Cell *146*, 67-79.

Cronin, M., Sangli, C., Liu, M.-L., Pho, M., Dutta, D., Nguyen, A., Jeong, J., Wu, J., Langone, K.C., and Watson, D. (2007). Analytical validation of the Oncotype DX genomic diagnostic test for recurrence prognosis and therapeutic response prediction in node-negative, estrogen receptor–positive breast cancer. Clinical chemistry *53*, 1084-1091.

Cuzick, J., Dowsett, M., Pineda, S., Wale, C., Salter, J., Quinn, E., Zabaglo, L., Mallon, E., Green, A.R., and Ellis, I.O. (2011). Prognostic value of a combined estrogen receptor, progesterone receptor, Ki-67, and human epidermal growth factor receptor 2 immunohistochemical score and comparison with the Genomic Health recurrence score in early breast cancer. Journal of Clinical Oncology *29*, 4273-4278.

Dammann, R., Schagdarsurengin, U., Strunnikova, M., Rastetter, M., Seidel, C., Liu, L., Tommasi, S., and Pfeifer, G. (2003). Epigenetic inactivation of the Ras-association domain family 1 (RASSF1A) gene and its function in human carcinogenesis.

Dammann, R., Yang, G., and Pfeifer, G.P. (2001). Hypermethylation of the cpG island of Ras association domain family 1A (RASSF1A), a putative tumor suppressor gene from the 3p21. 3 locus, occurs in a large percentage of human breast cancers. Cancer research *61*, 3105-3109.

Deeb, K.K., Trump, D.L., and Johnson, C.S. (2007). Vitamin D signalling pathways in cancer: potential for anticancer therapeutics. Nature reviews cancer *7*, 684-700.

Delle Cave, D., Ilisso, C., Mosca, L., Pagano, M., Martino, E., Porcelli, M., and Cacciapuoti, G. (2017). The Anticancer Effects of S-Adenosylmethionine on Breast Cancer Cells. JSM CHEMISTRY *5*, 1049-1056.

DeLuca, H.F. (1988). The vitamin D story: a collaborative effort of basic science and clinical medicine 1. The FASEB Journal *2*, 224-236.

Derissen, E.J., Beijnen, J.H., and Schellens, J.H. (2013). Concise drug review: azacitidine and decitabine. The oncologist *18*, 619-624.

DeSantis, C.E., Fedewa, S.A., Goding Sauer, A., Kramer, J.L., Smith, R.A., and Jemal, A. (2016). Breast cancer statistics, 2015: Convergence of incidence rates between black and white women. CA: a cancer journal for clinicians *66*, 31-42.

Doig, C.L., Singh, P.K., Dhiman, V.K., Thorne, J.L., Battaglia, S., Sobolewski, M., Maguire, O., O'Neill, L.P., Turner, B.M., and McCabe, C.J. (2013). Recruitment of NCOR1 to VDR target genes is enhanced in prostate cancer cells and associates with altered DNA methylation patterns. Carcinogenesis *34*, 248-256.

Du, Q., Luu, P.-L., Stirzaker, C., and Clark, S.J. (2015). Methyl-CpG-binding domain proteins: readers of the epigenome. Epigenomics *7*, 1051-1073.

Eden, A., Gaudet, F., Waghmare, A., and Jaenisch, R. (2003). Chromosomal instability and tumors promoted by DNA hypomethylation. Science *300*, 455-455.

Ehrlich, M. (2003). The ICF syndrome, a DNA methyltransferase 3B deficiency and immunodeficiency disease. Clinical immunology *109*, 17-28.

Ehrlich, M. (2009). DNA hypomethylation in cancer cells. Epigenomics *1*, 239-259.

Elangovan, S., Pathania, R., Ramachandran, S., Ananth, S., Padia, R.N., Srinivas, S.R., Babu, E., Hawthorn, L., Schoenlein, P.V., and Boettger, T. (2013). Molecular

mechanism of SLC5A8 inactivation in breast cancer. Molecular and cellular biology *33*, 3920-3935.

Esteller, M., Corn, P.G., Baylin, S.B., and Herman, J.G. (2001). A gene hypermethylation profile of human cancer. Cancer research *61*, 3225-3229.

Esteller, M., Hamilton, S.R., Burger, P.C., Baylin, S.B., and Herman, J.G. (1999). Inactivation of the DNA repair gene O6-methylguanine-DNA methyltransferase by promoter hypermethylation is a common event in primary human neoplasia. Cancer research *59*, 793-797.

Esteller, M., and Herman, J.G. (2004). Generating mutations but providing chemosensitivity: the role of O6-methylguanine DNA methyltransferase in human cancer. Oncogene *23*, 1-8.

Esteller, M., Silva, J.M., Dominguez, G., Bonilla, F., Matias-Guiu, X., Lerma, E., Bussaglia, E., Prat, J., Harkes, I.C., and Repasky, E.A. (2000). Promoter hypermethylation and BRCA1 inactivation in sporadic breast and ovarian tumors. Journal of the National Cancer Institute *92*, 564-569.

Fackler, M.J., McVeigh, M., Evron, E., Garrett, E., Mehrotra, J., Polyak, K., Sukumar, S., and Argani, P. (2003). DNA methylation of RASSF1A, HIN-1, RAR-β, Cyclin D2 and Twist in in situ and invasive lobular breast carcinoma. International journal of cancer *107*, 970-975.

Feinberg, A.P., and Tycko, B. (2004). The history of cancer epigenetics. Nature Reviews Cancer *4*, 143.

Feinberg, A.P., and Vogelstein, B. (1983a). Hypomethylation distinguishes genes of some human cancers from their normal counterparts. Nature *301*, 89.

Feinberg, A.P., and Vogelstein, B. (1983b). Hypomethylation of ras oncogenes in primary human cancers. Biochemical and biophysical research communications *111*, 47-54.

Feng, Q., Cao, R., Xia, L., Erdjument-Bromage, H., Tempst, P., and Zhang, Y. (2002). Identification and functional characterization of the p66/p68 components of the MeCP1 complex. Molecular and cellular biology *22*, 536-546.

Feng, Q., and Zhang, Y. (2001). The MeCP1 complex represses transcription through preferential binding, remodeling, and deacetylating methylated nucleosomes. Genes & development *15*, 827-832.

Feo, F., Garcea, R., Pascale, R., Pirisi, L., Daino, L., and Donaera, A. (1987). The variations of S-adenosyl-L-methionine content modulate hepatocyte growth during phenobarbital promotion of diethylnitrosamine-induced rat liver carcinogenesis. Toxicologic pathology *15*, 109-114.

Ferguson, A.T., Lapidus, R.G., Baylin, S.B., and Davidson, N.E. (1995). Demethylation of the estrogen receptor gene in estrogen receptor-negative breast cancer cells can reactivate estrogen receptor gene expression. Cancer research *55*, 2279-2283.

Fetahu, I.S., Höbaus, J., and Kállay, E. (2014). Vitamin D and the epigenome. Frontiers in physiology *5*, 164.

Filipits, M., Rudas, M., Jakesz, R., Dubsky, P., Fitzal, F., Singer, C.F., Dietze, O., Greil, R., Jelen, A., and Sevelda, P. (2011). A new molecular predictor of distant recurrence

in ER-positive, HER2-negative breast cancer adds independent information to conventional clinical risk factors. Clinical Cancer Research *17*, 6012-6020.

Finkelstein, J.D. (1990). Methionine metabolism in mammals. The Journal of nutritional biochemistry *1*, 228-237.

Flatau, E., Gonzales, F., Michalowsky, L., and Jones, P. (1984). DNA methylation in 5-aza-2'-deoxycytidine-resistant variants of C3H 10T1/2 C18 cells. Molecular and cellular biology *4*, 2098-2102.

Fraga, M.F., Ballestar, E., Villar-Garea, A., Boix-Chornet, M., Espada, J., Schotta, G., Bonaldi, T., Haydon, C., Ropero, S., and Petrie, K. (2005). Loss of acetylation at Lys16 and trimethylation at Lys20 of histone H4 is a common hallmark of human cancer. Nature genetics *37*, 391.

Frau, M., Feo, F., and Pascale, R.M. (2013). Pleiotropic effects of methionine adenosyltransferases deregulation as determinants of liver cancer progression and prognosis. Journal of hepatology *59*, 830-841.

Fujii, H., Biel, M.A., Zhou, W., Weitzman, S.A., Baylin, S.B., and Gabrielson, E. (1998). Methylation of the HIC-1 candidate tumor suppressor gene in human breast cancer. Oncogene *16*.

Gama-Sosa, M.A., Slagel, V.A., Trewyn, R.W., Oxenhandler, R., Kuo, K.C., Gehrke, C.W., and Ehrlich, M. (1983). The 5-methylcytosine content of DNA from human tumors. Nucleic acids research *11*, 6883-6894.

Ganesan, A. (2016). Multitarget Drugs: an Epigenetic Epiphany. ChemMedChem.

Gao, L., Bellantuono, I., Elsasser, A., Marley, S.B., Gordon, M.Y., Goldman, J.M., and Stauss, H.J. (2000). Selective elimination of leukemic CD34(+) progenitor cells by cytotoxic T lymphocytes specific for WT1. Blood *95*, 2198-2203.

Gardiner-Garden, M., and Frommer, M. (1987). CpG islands in vertebrate genomes. Journal of molecular biology *196*, 261-282.

Gaudet, F., Hodgson, J.G., Eden, A., Jackson-Grusby, L., Dausman, J., Gray, J.W., Leonhardt, H., and Jaenisch, R. (2003). Induction of tumors in mice by genomic hypomethylation. Science *300*, 489-492.

Gaudet, M.M., Campan, M., Figueroa, J.D., Yang, X.R., Lissowska, J., Peplonska, B., Brinton, L.A., Rimm, D.L., Laird, P.W., and Garcia-Closas, M. (2009). DNA hypermethylation of ESR1 and PGR in breast cancer: pathologic and epidemiologic associations. Cancer Epidemiology Biomarkers & Prevention *18*, 3036-3043.

Giovannucci, E. (2004). Alcohol, one-carbon metabolism, and colorectal cancer: recent insights from molecular studies. The Journal of nutrition *134*, 2475S-2481S.

Gnanapragasam, M.N., Scarsdale, J.N., Amaya, M.L., Webb, H.D., Desai, M.A., Walavalkar, N.M., Wang, S.Z., Zu Zhu, S., Ginder, G.D., and Williams, D.C. (2011). p66α–MBD2 coiled-coil interaction and recruitment of Mi-2 are critical for globin gene silencing by the MBD2–NuRD complex. Proceedings of the National Academy of Sciences *108*, 7487-7492.

Goldberg, B., Urnovitz, H.B., and Stricker, R.B. (2000). Beyond danger: unmethylated CpG dinucleotides and the immunopathogenesis of disease. Immunology letters *73*, 13-18.

Greer, E.L., Blanco, M.A., Gu, L., Sendinc, E., Liu, J., Aristizábal-Corrales, D., Hsu, C.-H., Aravind, L., He, C., and Shi, Y. (2015). DNA methylation on N 6-adenine in C. elegans. Cell *161*, 868-878.

Gupta, A., Godwin, A.K., Vanderveer, L., Lu, A., and Liu, J. (2003). Hypomethylation of the synuclein γ gene CpG island promotes its aberrant expression in breast carcinoma and ovarian carcinoma. Cancer research *63*, 664-673.

Gyorffy, B., Bottai, G., Fleischer, T., Munkácsy, G., Budczies, J., and Paladini, L. (2016). Aberrant DNA methylation impacts gene expression and prognosis in breast cancer subtypes. Int J Cancer *138*, 87-97.

Habets, G., Van der Kammen, R., Scholtes, E., and Collard, J. (1990). Induction of invasive and metastatic potential in mouse T-lymphoma cells (BW5147) by treatment with 5-azacytidine. Clinical & experimental metastasis *8*, 567-577.

Ham, M.-S., Lee, J.-K., and Kim, K.-C. (2013). S-adenosyl methionine specifically protects the anticancer effect of 5-FU via DNMTs expression in human A549 lung cancer cells. Molecular and clinical oncology *1*, 373-378.

Hendrich, B., Abbott, C., McQueen, H., Chambers, D., Cross, S., and Bird, A. (1999). Genomic structure and chromosomal mapping of the murine and human Mbd1, Mbd2, Mbd3, and Mbd4 genes. Mammalian Genome *10*, 906-912.

Hendrich, B., and Bird, A. (1998). Identification and characterization of a family of mammalian methyl CpG-binding proteins. Genetics Research *72*, 59-72.

Hendrich, B., Guy, J., Ramsahoye, B., Wilson, V.A., and Bird, A. (2001). Closely related proteins MBD2 and MBD3 play distinctive but interacting roles in mouse development. Genes & development *15*, 710-723.

Hendrich, B., and Tweedie, S. (2003). The methyl-CpG binding domain and the evolving role of DNA methylation in animals. TRENDS in Genetics *19*, 269-277.

Herman, J.G., Umar, A., Polyak, K., Graff, J.R., Ahuja, N., Issa, J.-P.J., Markowitz, S., Willson, J.K., Hamilton, S.R., and Kinzler, K.W. (1998). Incidence and functional consequences of hMLH1 promoter hypermethylation in colorectal carcinoma. Proceedings of the National Academy of Sciences *95*, 6870-6875.

Hermann, A., Goyal, R., and Jeltsch, A. (2004). The Dnmt1 DNA-(cytosine-C5)-methyltransferase methylates DNA processively with high preference for hemimethylated target sites. Journal of Biological Chemistry *279*, 48350-48359.

Hinshelwood, R.A., and Clark, S.J. (2008). Breast cancer epigenetics: normal human mammary epithelial cells as a model system. Journal of molecular medicine *86*, 1315-1328.

Hoffman, R.M. (1984). Altered methionine metabolism, DNA methylation and oncogene expression in carcinogenesis: a review and synthesis. Biochimica et Biophysica Acta (BBA)-Reviews on Cancer *738*, 49-87.

Hoffmann, M.J., and Schulz, W.A. (2005). Causes and consequences of DNA hypomethylation in human cancer. Biochemistry and Cell Biology *83*, 296-321.

Holick, M.F. (1995). Noncalcemic actions of 1, 25-dihydroxyvitamin D3 and clinical applications. Bone *17*, S107-S111.

Holik, A.Z., Young, M., Krzystyniak, J., Williams, G.T., Metzger, D., Shorning, B.Y., and Clarke, A.R. (2014). Brg1 loss attenuates aberrant wnt-signalling and prevents wnt-dependent tumourigenesis in the murine small intestine. PLoS genetics *10*, e1004453.

Holliday, R., and Pugh, J. (1975). DNA modification mechanisms and gene activity during development. Science *187*, 226-232.

Hori, M., Iwasaki, M., Yoshimi, F., Asato, Y., and Ibaraki, M. (1999). Hypermethylation of the estrogen receptor alpha gene is not related to lack of receptor protein in human breast cancer. Breast Cancer *6*, 79-86.

Hotchkiss, R.D. (1948). The quantitative separation of purines, pyrimidines, and nucleosides by paper chromatography. Journal of Biological Chemistry *175*, 315-332.

Huang, Y., Nayak, S., Jankowitz, R., Davidson, N.E., and Oesterreich, S. (2011). Epigenetics in breast cancer: what's new? Breast Cancer Research *13*, 1.

Hudson, N.O., and Buck-Koehntop, B.A. (2018). Zinc Finger Readers of Methylated DNA. Molecules *23*, 2555.

Hussain, Z., Khan, M., Shahid, M., and Almajhdi, F. (2013). S-adenosylmethionine, a methyl donor, up regulates tissue inhibitor of metalloproteinase-2 in colorectal cancer. Genet Mol Res *12*, 1106-1118.

Iacobuzio-Donahue, C.A., Maitra, A., Olsen, M., Lowe, A.W., Van Heek, N.T., Rosty, C., Walter, K., Sato, N., Parker, A., and Ashfaq, R. (2003). Exploration of global gene expression patterns in pancreatic adenocarcinoma using cDNA microarrays. The American journal of pathology *162*, 1151-1162.

Ilisso, C.P., Castellano, M., Zappavigna, S., Lombardi, A., Vitale, G., Dicitore, A., Cacciapuoti, G., Caraglia, M., and Porcelli, M. (2015). The methyl donor S-adenosylmethionine potentiates doxorubicin effects on apoptosis of hormone-dependent breast cancer cell lines. Endocrine *50*, 212-222.

Ilisso, C.P., Sapio, L., Delle Cave, D., Illiano, M., Spina, A., Cacciapuoti, G., Naviglio, S., and Porcelli, M. (2016). S-Adenosylmethionine Affects ERK1/2 and Stat3 Pathways and Induces Apotosis in Osteosarcoma Cells. Journal of cellular physiology *231*, 428-435.

Jackson-Grusby, L., Beard, C., Possemato, R., Tudor, M., Fambrough, D., Csankovszki, G., Dausman, J., Lee, P., Wilson, C., and Lander, E. (2001). Loss of genomic methylation causes p53-dependent apoptosis and epigenetic deregulation. Nature genetics *27*, 31.

James, S.J., Pogribny, I.P., Pogribna, M., Miller, B.J., Jernigan, S., and Melnyk, S. (2003). Mechanisms of DNA damage, DNA hypomethylation, and tumor progression in the folate/methyl-deficient rat model of hepatocarcinogenesis. The Journal of nutrition *133*, 3740S-3747S.

Jeltsch, A. (2002). Beyond Watson and Crick: DNA methylation and molecular enzymology of DNA methyltransferases. Chembiochem *3*, 274-293.

Jin, Z., Tamura, G., Tsuchiya, T., Sakata, K., Kashiwaba, M., Osakabe, M., and Motoyama, T. (2001). Adenomatous polyposis coli (APC) gene promoter hypermethylation in primary breast cancers. British journal of cancer *85*, 69.

Jones, P.A., and Taylor, S.M. (1980). Cellular differentiation, cytidine analogs and DNA methylation. Cell *20*, 85-93.

Jones, P.A., and Taylor, S.M. (1981). Hemimethylated duplex DNAs prepared from 5-azacytidine-treated cells. Nucleic acids research *9*, 2933-2947.

Jovanovic, J., Rønneberg, J.A., Tost, J., and Kristensen, V. (2010). The epigenetics of breast cancer. Molecular oncology *4*, 242-254.

Kamalakaran, S., Varadan, V., Russnes, H.E.G., Levy, D., Kendall, J., Janevski, A., Riggs, M., Banerjee, N., Synnestvedt, M., and Schlichting, E. (2011). DNA methylation patterns in luminal breast cancers differ from non-luminal subtypes and can identify relapse risk independent of other clinical variables. Molecular oncology *5*, 77-92.

Kantarjian, H., Oki, Y., Garcia-Manero, G., Huang, X., O'Brien, S., Cortes, J., Faderl, S., Bueso-Ramos, C., Ravandi, F., and Estrov, Z. (2007). Results of a randomized study of 3 schedules of low-dose decitabine in higher-risk myelodysplastic syndrome and chronic myelomonocytic leukemia. Blood *109*, 52-57.

Karlic, H., and Varga, F. (2011). Impact of vitamin D metabolism on clinical epigenetics. Clinical epigenetics *2*, 55-61.

Karpf, A.R., and Matsui, S.-i. (2005). Genetic disruption of cytosine DNA methyltransferase enzymes induces chromosomal instability in human cancer cells. Cancer research *65*, 8635-8639.

Kim, S.J., Kang, H.-S., Chang, H.L., Jung, Y.C., Sim, H.-B., Lee, K.S., Ro, J., and Lee, E.S. (2008). Promoter hypomethylation of the N-acetyltransferase 1 gene in breast cancer. Oncology reports *19*, 663-668.

Kim, Y.I. (2000). Methylenetetrahydrofolate reductase polymorphisms, folate, and cancer risk: a paradigm of gene-nutrient interactions in carcinogenesis. Nutrition reviews *58*, 205-209.

Kimmel-Jehan, C., Darwish, H.M., Strugnell, S.A., Jehan, F., Wiefling, B., and DeLuca, H.F. (1999). DNA bending is induced by binding of vitamin D receptor-retinoid X receptor heterodimers to vitamin D response elements. Journal of cellular biochemistry *74*, 220-228.

Klutstein, M., Nejman, D., Greenfield, R., and Cedar, H. (2016). DNA Methylation in Cancer and Aging. Cancer research.

Kohli, R.M., and Zhang, Y. (2013). TET enzymes, TDG and the dynamics of DNA demethylation. Nature *502*, 472.

Kongsbak, M., Levring, T., Geisler, C., and von Essen, M. (2013). The Vitamin D Receptor and T Cell Function. Frontiers in immunology *4*.

Koturbash, I., Pogribny, I., and Kovalchuk, O. (2005). Stable loss of global DNA methylation in the radiation-target tissue—A possible mechanism contributing to radiation carcinogenesis? Biochemical and biophysical research communications *337*, 526-533.

Krifa, M., Alhosin, M., Muller, C.D., Gies, J.-P., Chekir-Ghedira, L., Ghedira, K., Mély, Y., Bronner, C., and Mousli, M. (2013). Limoniastrum guyonianum aqueous gall extract induces apoptosis in human cervical cancer cells involving p16 INK4A re-expression related to UHRF1 and DNMT1 down-regulation. Journal of Experimental & Clinical Cancer Research *32*, 30.

Lapidus, R.G., Ferguson, A.T., Ottaviano, Y.L., Parl, F.F., Smith, H.S., Weitzman, S.A., Baylin, S.B., Issa, J., and Davidson, N.E. (1996). Methylation of estrogen and

progesterone receptor gene 5'CpG islands correlates with lack of estrogen and progesterone receptor gene expression in breast tumors. Clinical Cancer Research *2*, 805-810.

Lee, Y.M., Lee, J.Y., Kim, M.J., Bae, H.I., Park, J.Y., Kim, S.G., and Kim, D.S. (2006). Hypomethylation of the protein gene product 9.5 promoter region in gallbladder cancer and its relationship with clinicopathological features. Cancer science *97*, 1205-1210.

Lewis, J.D., Meehan, R.R., Henzel, W.J., Maurer-Fogy, I., Jeppesen, P., Klein, F., and Bird, A. (1992). Purification, sequence, and cellular localization of a novel chromosomal protein that binds to methylated DNA. Cell *69*, 905-914.

Li, E. (2002). Chromatin modification and epigenetic reprogramming in mammalian development. Nature Reviews Genetics *3*, 662.

Li, E., Bestor, T.H., and Jaenisch, R. (1992). Targeted mutation of the DNA methyltransferase gene results in embryonic lethality. Cell *69*, 915-926.

Li, L., Olin, E., Buskirk, H., and Reineke, L. (1970). Cytotoxicity and mode of action of 5-azacytidine on L1210 leukemia. Cancer research *30*, 2760-2769.

Li, Q., Ahuja, N., Burger, P.C., and Issa, J.-P.J. (1999). Methylation and silencing of the Thrombospondin-1 promoter in human cancer. Oncogene *18*, 3284-3289.

Li, T.W., Yang, H., Peng, H., Xia, M., Mato, J.M., and Lu, S.C. (2011). Effects of S-adenosylmethionine and methylthioadenosine on inflammation-induced colon cancer in mice. Carcinogenesis *33*, 427-435.

Liang, X., Xu, Y., Xu, K., Liu, J., and Qian, X. (2010). B1, a novel amonafide analogue, overcomes the resistance conferred by Bcl-2 in human promyelocytic leukemia HL60 cells. Molecular Cancer Research *8*, 1619-1632.

Lin, X., and Nelson, W.G. (2003). Methyl-CpG-binding domain protein-2 mediates transcriptional repression associated with hypermethylated GSTP1 CpG islands in MCF-7 breast cancer cells. Cancer research *63*, 498-504.

Lister, R., Pelizzola, M., Dowen, R.H., Hawkins, R.D., Hon, G., Tonti-Filippini, J., Nery, J.R., Lee, L., Ye, Z., and Ngo, Q.-M. (2009). Human DNA methylomes at base resolution show widespread epigenomic differences. nature *462*, 315.

Liu, C., Ou, T., Wu, C., Li, R., Lin, Y., Lin, C., Tsai, W., Liu, H., and Yen, J. (2011). Global DNA methylation, DNMT1, and MBD2 in patients with systemic lupus erythematosus. Lupus *20*, 131-136.

Liu, H., Liu, W., Wu, Y., Zhou, Y., Xue, R., Luo, C., Wang, L., Zhao, W., Jiang, J.-D., and Liu, J. (2005). Loss of epigenetic control of synuclein-γ gene as a molecular indicator of metastasis in a wide range of human cancers. Cancer research *65*, 7635-7643.

Lopes, N., Carvalho, J., Duraes, C., Sousa, B., Gomes, M., Costa, J.L., Oliveira, C., Paredes, J., and Schmitt, F. (2012). 1Alpha, 25-dihydroxyvitamin D3 induces de novo E-cadherin expression in triple-negative breast cancer cells by CDH1-promoter demethylation. Anticancer research *32*, 249-257.

Lotsari, J.E., Gylling, A., Abdel-Rahman, W.M., Nieminen, T.T., Aittomäki, K., Friman, M., Pitkänen, R., Aarnio, M., Järvinen, H.J., and Mecklin, J.-P. (2012). Breast carcinoma and Lynch syndrome: molecular analysis of tumors arising in mutation carriers, non-carriers, and sporadic cases. Breast Cancer Research *14*, 1.

Lu, S.C. (2000). S-adenosylmethionine. The international journal of biochemistry & cell biology *32*, 391-395.

Lu, S.C., and Mato, J.M. (2005). Role of methionine adenosyltransferase and S-adenosylmethionine in alcohol-associated liver cancer. Alcohol *35*, 227-234.

Lu, Y., Loh, Y.-H., Li, H., Cesana, M., Ficarro, Scott B., Parikh, Jignesh R., Salomonis, N., Toh, C.-Xu D., Andreadis, Stelios T., Luckey, C.J., *et al.* (2014). Alternative Splicing of MBD2 Supports Self-Renewal in Human Pluripotent Stem Cells. Cell Stem Cell *15*, 92-101.

Lübbert, M., Suciu, S., Baila, L., Rüter, B.H., Platzbecker, U., Giagounidis, A., Selleslag, D., Labar, B., Germing, U., and Salih, H.R. (2011). Low-dose decitabine versus best supportive care in elderly patients with intermediate-or high-risk myelodysplastic syndrome (MDS) ineligible for intensive chemotherapy: final results of the randomized phase III study of the European Organisation for Research and Treatment of Cancer Leukemia Group and the German MDS Study Group. Journal of Clinical Oncology, JCO. 2010.2030. 9245.

Luo, J., Li, Y.-N., Wang, F., Zhang, W.-M., and Geng, X. (2010). S-adenosylmethionine inhibits the growth of cancer cells by reversing the hypomethylation status of c-myc and H-ras in human gastric cancer and colon cancer. International journal of biological sciences *6*, 784.

Macnab, J., Adams, R., Rinaldi, A., Orr, A., and Clark, L. (1988). Hypomethylation of host cell DNA synthesized after infection or transformation of cells by herpes simplex virus. Molecular and cellular biology *8*, 1443-1448.

Magdinier, F., and Wolffe, A.P. (2001). Selective association of the methyl-CpG binding protein MBD2 with the silent p14/p16 locus in human neoplasia. Proceedings of the National Academy of Sciences *98*, 4990-4995.

Mahmood, N., Cheishvili, D., Arakelian, A., Tanvir, I., Ahmed, H., Khan, A.-S.P., Szyf, M., and Rabbani, S.A. (2018a). Methyl donor S-adenosylmethionine (SAM) supplementation attenuates breast cancer growth, invasion, and metastasis in vivo; therapeutic and chemopreventive applications. Oncotarget *9*, 5169-5183.

Mahmood, N., Mihalcioiu, C., and Rabbani, S.A. (2018b). Multifaceted Role of the Urokinase-Type Plasminogen Activator (uPA) and Its Receptor (uPAR): Diagnostic, Prognostic, and Therapeutic Applications. Frontiers in Oncology *8*.

Mahmood, N., and Rabbani, S.A. (2017). DNA methylation and breast cancer: Mechanistic and therapeutic applications. Trends Cancer Res *12*, 1-18.

Mahmood, N., and Rabbani, S.A. (2019a). DNA methylation readers and cancer: mechanistic and therapeutic applications. Frontiers in oncology *9*, 489.

Mahmood, N., and Rabbani, S.A. (2019b). Targeting DNA Hypomethylation in Malignancy by Epigenetic Therapies. Advances in experimental medicine and biology *1164*, 179-196.

Mariani, C.J., Madzo, J., Moen, E.L., Yesilkanal, A., and Godley, L.A. (2013). Alterations of 5-hydroxymethylcytosine in human cancers. Cancers *5*, 786-814.

Meehan, R.R., Lewis, J.D., McKay, S., Kleiner, E.L., and Bird, A.P. (1989). Identification of a mammalian protein that binds specifically to DNA containing methylated CpGs. Cell *58*, 499-507.

Mehlen, P., and Puisieux, A. (2006). Metastasis: a question of life or death. Nature reviews cancer *6*, 449.

Mian, O.Y., Wang, S.Z., Zu Zhu, S., Gnanapragasam, M.N., Graham, L., Bear, H.D., and Ginder, G.D. (2011). Methyl-Binding Domain Protein 2–Dependent Proliferation and Survival of Breast Cancer Cells. Molecular Cancer Research.

Mirza, S., Sharma, G., Parshad, R., Gupta, S.D., Pandya, P., and Ralhan, R. (2013). Expression of DNA methyltransferases in breast cancer patients and to analyze the effect of natural compounds on DNA methyltransferases and associated proteins. J Breast Cancer *16*, 23-31.

Miyamoto, K., Fukutomi, T., Akashi-Tanaka, S., Hasegawa, T., Asahara, T., Sugimura, T., and Ushijima, T. (2005). Identification of 20 genes aberrantly methylated in human breast cancers. International journal of cancer *116*, 407-414.

Momparler, R., Rossi, M., Bouchard, J., Vaccaro, C., Momparler, L., and Bartolucci, S. (1984). Kinetic interaction of 5-AZA-2'-deoxycytidine-5'-monophosphate and its 5'-triphosphate with deoxycytidylate deaminase. Molecular pharmacology *25*, 436-440.

Moore, L.D., Le, T., and Fan, G. (2013). DNA methylation and its basic function. Neuropsychopharmacology *38*, 23.

Müller, H., Fiegl, H., Goebel, G., Hubalek, M., Widschwendter, A., Müller-Holzner, E., Marth, C., and Widschwendter, M. (2003). MeCP2 and MBD2 expression in human neoplastic and non-neoplastic breast tissue and its association with oestrogen receptor status. British journal of cancer *89*, 1934.

Nakagawa, T., Kanai, Y., Ushijima, S., Kitamura, T., Kakizoe, T., and Hirohashi, S. (2005). DNA hypomethylation on pericentromeric satellite regions significantly correlates with loss of heterozygosity on chromosome 9 in urothelial carcinomas. The Journal of urology *173*, 243-246.

Nan, X., Meehan, R.R., and Bird, A. (1993). Dissection of the methyl-CpG binding domain from the chromosomal protein MeCP2. Nucleic Acids Res *21*, 4886-4892.

Nan, X., Ng, H.-H., Johnson, C.A., Laherty, C.D., Turner, B.M., Eisenman, R.N., and Bird, A. (1998). Transcriptional repression by the methyl-CpG-binding protein MeCP2 involves a histone deacetylase complex. Nature *393*, 386.

Neuhausen, A., Florl, A.R., Grimm, M.-O., and Schulz, W.A. (2006). DNA methylation alterations in urothelial carcinoma. Cancer biology & therapy *5*, 993-1001.

Ng, H.-H., Zhang, Y., Hendrich, B., Johnson, C.A., Turner, B.M., Erdjument-Bromage, H., Tempst, P., Reinberg, D., and Bird, A. (1999). MBD2 is a transcriptional repressor belonging to the MeCP1 histone deacetylase complex. Nature genetics *23*, 58.

Nishigaki, M., Aoyagi, K., Danjoh, I., Fukaya, M., Yanagihara, K., Sakamoto, H., Yoshida, T., and Sasaki, H. (2005). Discovery of aberrant expression of R-RAS by cancer-linked DNA hypomethylation in gastric cancer using microarrays. Cancer research *65*, 2115-2124.

Ogishima, T., Shiina, H., Breault, J.E., Tabatabai, L., Bassett, W.W., Enokida, H., Li, L.-C., Kawakami, T., Urakami, S., and Ribeiro-Filho, L.A. (2005). Increased heparanase expression is caused by promoter hypomethylation and up-regulation of

transcriptional factor early growth response-1 in human prostate cancer. Clinical cancer research *11*, 1028-1036.

Ohminami, H., Yasukawa, M., and Fujita, S. (2000). HLA class I-restricted lysis of leukemia cells by a CD8(+) cytotoxic T-lymphocyte clone specific for WT1 peptide. Blood *95*, 286-293.

Ohno, S., Okuyama, R., Aruga, A., Sugiyama, H., and Yamamoto, M. (2012). Phase I trial of Wilms' Tumor 1 (WT1) peptide vaccine with GM-CSF or CpG in patients with solid malignancy. Anticancer Res *32*, 2263-2269.

Oji, Y., Inoue, M., Takeda, Y., Hosen, N., Shintani, Y., Kawakami, M., Harada, T., Murakami, Y., Iwai, M., Fukuda, M., *et al.* (2018). WT1 peptide-based immunotherapy for advanced thymic epithelial malignancies. International Journal of Cancer *142*, 2375-2382.

Oka, Y., Tsuboi, A., Nakata, J., Nishida, S., Hosen, N., Kumanogoh, A., Oji, Y., and Sugiyama, H. (2017). Wilms' Tumor Gene 1 (WT1) Peptide Vaccine Therapy for Hematological Malignancies: From CTL Epitope Identification to Recent Progress in Clinical Studies Including a Cure-Oriented Strategy. Oncology Research and Treatment *40*, 682-690.

Okano, M., Bell, D.W., Haber, D.A., and Li, E. (1999). DNA methyltransferases Dnmt3a and Dnmt3b are essential for de novo methylation and mammalian development. Cell *99*, 247-257.

Okano, M., Xie, S., and Li, E. (1998). Cloning and characterization of a family of novel mammalian DNA (cytosine-5) methyltransferases [letter]. Nat Genet *19*, 219-220.

Olsson, L., and Forchhammer, J. (1984). Induction of the metastatic phenotype in a mouse tumor model by 5-azacytidine, and characterization of an antigen associated with metastatic activity. Proceedings of the National Academy of Sciences *81*, 3389-3393.

Ottaviano, Y.L., Issa, J.-P., Parl, F.F., Smith, H.S., Baylin, S.B., and Davidson, N.E. (1994). Methylation of the estrogen receptor gene CpG island marks loss of estrogen receptor expression in human breast cancer cells. Cancer Research *54*, 2552-2555.

Pakneshan, P., Szyf, M., Farias-Eisner, R., and Rabbani, S.A. (2004a). Reversal of the hypomethylation status of urokinase (uPA) promoter blocks breast cancer growth and metastasis. Journal of Biological Chemistry *279*, 31735-31744.

Pakneshan, P., Têtu, B., and Rabbani, S.A. (2004b). Demethylation of urokinase promoter as a prognostic marker in patients with breast carcinoma. Clinical Cancer Research *10*, 3035-3041.

Pandey, M., Shukla, S., and Gupta, S. (2010). Promoter demethylation and chromatin remodeling by green tea polyphenols leads to re-expression of GSTP1 in human prostate cancer cells. International Journal of Cancer *126*, 2520-2533.

Parashar, S., Cheishvili, D., Arakelian, A., Hussain, Z., Tanvir, I., Khan, H.A., Szyf, M., and Rabbani, S.A. (2015). S-adenosylmethionine blocks osteosarcoma cells proliferation and invasion in vitro and tumor metastasis in vivo: therapeutic and diagnostic clinical applications. Cancer medicine *4*, 732-744.

Parashar, S., Cheishvili, D., Mahmood, N., Arakelian, A., Tanvir, I., Khan, H.A., Kremer, R., Mihalcioiu, C., Szyf, M., and Rabbani, S.A. (2018). DNA methylation signatures of breast cancer in peripheral T-cells. BMC cancer *18*, 574.

Paredes, J., Albergaria, A., Oliveira, J.T., Jerónimo, C., Milanezi, F., and Schmitt, F.C. (2005). P-cadherin overexpression is an indicator of clinical outcome in invasive breast carcinomas and is associated with CDH3 promoter hypomethylation. Clinical cancer research *11*, 5869-5877.

Parrella, P., Poeta, M.L., Gallo, A.P., Prencipe, M., Scintu, M., Apicella, A., Rossiello, R., Liguoro, G., Seripa, D., and Gravina, C. (2004). Nonrandom distribution of aberrant promoter methylation of cancer-related genes in sporadic breast tumors. Clinical Cancer Research *10*, 5349-5354.

Peinado, M.A. (2011). Hypomethylation of DNA. In Encyclopedia of Cancer, M. Schwab, ed. (Berlin, Heidelberg: Springer Berlin Heidelberg), pp. 1791-1792.

Peters, A.H., O'Carroll, D., Scherthan, H., Mechtler, K., Sauer, S., Schöfer, C., Weipoltshammer, K., Pagani, M., Lachner, M., and Kohlmaier, A. (2001). Loss of the Suv39h histone methyltransferases impairs mammalian heterochromatin and genome stability. Cell *107*, 323-337.

Phesse, T.J., Parry, L., Reed, K.R., Ewan, K.B., Dale, T.C., Sansom, O.J., and Clarke, A.R. (2008). Deficiency of Mbd2 attenuates Wnt signaling. Molecular and cellular biology *28*, 6094-6103.

Pogribny, I.P., Ross, S.A., Wise, C., Pogribna, M., Jones, E.A., Tryndyak, V.P., James, S.J., Dragan, Y.P., and Poirier, L.A. (2006). Irreversible global DNA hypomethylation as a key step in hepatocarcinogenesis induced by dietary methyl deficiency. Mutation Research/Fundamental and Molecular Mechanisms of Mutagenesis *593*, 80-87.

Prokhortchouk, A., Hendrich, B., Jørgensen, H., Ruzov, A., Wilm, M., Georgiev, G., Bird, A., and Prokhortchouk, E. (2001). The p120 catenin partner Kaiso is a DNA methylation-dependent transcriptional repressor. Genes & development *15*, 1613-1618.

Prokhortchouk, A., Sansom, O., Selfridge, J., Caballero, I.M., Salozhin, S., Aithozhina, D., Cerchietti, L., Meng, F.G., Augenlicht, L.H., and Mariadason, J.M. (2006). Kaiso-deficient mice show resistance to intestinal cancer. Molecular and cellular biology *26*, 199-208.

Pulukuri, S., and Rao, J.S. (2006). CpG island promoter methylation and silencing of 14-3-3σ gene expression in LNCaP and Tramp-C1 prostate cancer cell lines is associated with methyl-CpG-binding protein MBD2. Oncogene *25*, 4559.

Pulukuri, S.M.K., Estes, N., Patel, J., and Rao, J.S. (2007). Demethylation-linked activation of urokinase plasminogen activator is involved in progression of prostate cancer. Cancer research *67*, 930-939.

Raman, V., Martensen, S.A., Reisman, D., Evron, E., Odenwald, W.F., Jaffee, E., Marks, J., and Sukumar, S. (2000). Compromised HOXA5 function can limit p53 expression in human breast tumours. Nature *405*, 974-978.

Ramchandani, S., Bhattacharya, S.K., Cervoni, N., and Szyf, M. (1999). DNA methylation is a reversible biological signal. Proceedings of the National Academy of Sciences *96*, 6107-6112.

Rawson, J.B., Sun, Z., Dicks, E., Daftary, D., Parfrey, P.S., Green, R.C., Gallinger, S., McLaughlin, J.R., Wang, P.P., and Knight, J.A. (2012). Vitamin D intake is negatively

associated with promoter methylation of the Wnt antagonist gene DKK1 in a large group of colorectal cancer patients. Nutrition and cancer *64*, 919-928.

Rius, M., Stresemann, C., Keller, D., Brom, M., Schirrmacher, E., Keppler, D., and Lyko, F. (2009). Human concentrative nucleoside transporter 1-mediated uptake of 5-azacytidine enhances DNA demethylation. Molecular cancer therapeutics *8*, 225-231.

Rivenbark, A.G., Jones, W.D., and Coleman, W.B. (2006). DNA methylation-dependent silencing of CST6 in human breast cancer cell lines. Laboratory investigation *86*, 1233-1242.

Roje, S. (2006). S-Adenosyl-L-methionine: beyond the universal methyl group donor. Phytochemistry *67*, 1686-1698.

Roman-Gomez, J., Jimenez-Velasco, A., Agirre, X., Castillejo, J.A., Navarro, G., San Jose-Eneriz, E., Garate, L., Cordeu, L., Cervantes, F., and Prosper, F. (2007). Epigenetic regulation of human cancer/testis antigen gene, HAGE, in chronic myeloid leukemia. Haematologica *92*, 153-162.

Roman-Gomez, J., Jimenez-Velasco, A., Agirre, X., Cervantes, F., Sanchez, J., Garate, L., Barrios, M., Castillejo, J.A., Navarro, G., and Colomer, D. (2005). Promoter hypomethylation of the LINE-1 retrotransposable elements activates sense/antisense transcription and marks the progression of chronic myeloid leukemia. Oncogene *24*, 7213.

Sadikovic, B., and Rodenhiser, D.I. (2006). Benzopyrene exposure disrupts DNA methylation and growth dynamics in breast cancer cells. Toxicology and applied pharmacology *216*, 458-468.

Şahin, M., Şahin, E., Gümüşlü, S., Erdoğan, A., and Gültekin, M. (2011). Inhibition of angiogenesis by S-adenosylmethionine. Biochemical and biophysical research communications *408*, 145-148.

Sánchez-Romero, M.A., Cota, I., and Casadesús, J. (2015). DNA methylation in bacteria: from the methyl group to the methylome. Current opinion in microbiology *25*, 9-16.

Sansom, O.J., Berger, J., Bishop, S.M., Hendrich, B., Bird, A., and Clarke, A.R. (2003). Deficiency of Mbd2 suppresses intestinal tumorigenesis. Nature genetics *34*, 145.

Sato, N., Fukushima, N., Matsubayashi, H., and Goggins, M. (2004). Identification of maspin and S100P as novel hypomethylation targets in pancreatic cancer using global gene expression profiling. Oncogene *23*, 1531.

Sato, N., Maehara, N., Su, G.H., and Goggins, M. (2003). Effects of 5-aza-2′-deoxycytidine on matrix metalloproteinase expression and pancreatic cancer cell invasiveness. Journal of the National Cancer Institute *95*, 327-330.

Saxonov, S., Berg, P., and Brutlag, D.L. (2006). A genome-wide analysis of CpG dinucleotides in the human genome distinguishes two distinct classes of promoters. Proceedings of the National Academy of Sciences *103*, 1412-1417.

Schmidt, T., Leha, A., and Salinas-Riester, G. (2016). Treatment of prostate cancer cells with S-adenosylmethionine leads to genome-wide alterations in transcription profiles. Gene *595*, 161-167.

Schulz, W.A., Elo, J.P., Florl, A.R., Pennanen, S., Santourlidis, S., Engers, R., Buchardt, M., Seifert, H.H., and Visakorpi, T. (2002). Genomewide DNA hypomethylation

is associated with alterations on chromosome 8 in prostate carcinoma. Genes, Chromosomes and Cancer *35*, 58-65.

Scott, E.C., Gardner, E.J., Masood, A., Chuang, N.T., Vertino, P.M., and Devine, S.E. (2016). A hot L1 retrotransposon evades somatic repression and initiates human colorectal cancer. Genome research.

Shapiro, C.L., and Recht, A. (2001). Side effects of adjuvant treatment of breast cancer. New England Journal of Medicine *344*, 1997-2008.

Sharif, T., Alhosin, M., Auger, C., Minker, C., Kim, J.-H., Etienne-Selloum, N., Bories, P., Gronemeyer, H., Lobstein, A., and Bronner, C. (2012). Aronia melanocarpa juice induces a redox-sensitive p73-related caspase 3-dependent apoptosis in human leukemia cells. PloS one *7*, e32526.

Sharif, T., Auger, C., Alhosin, M., Ebel, C., Achour, M., Étienne-Selloum, N., Fuhrmann, G., Bronner, C., and Schini-Kerth, V.B. (2010). Red wine polyphenols cause growth inhibition and apoptosis in acute lymphoblastic leukaemia cells by inducing a redox-sensitive up-regulation of p73 and down-regulation of UHRF1. European journal of cancer *46*, 983-994.

Sheng, W., Qian, Y., Wang, H., Ma, X., Zhang, P., Chen, L., Ma, D., and Huang, G. (2013). Association between mRNA levels of DNMT1, DNMT3A, DNMT3B, MBD2 and LINE-1 methylation status in infants with tetralogy of Fallot. International journal of molecular medicine *32*, 694-702.

Shitara, K., and Nishikawa, H. (2018). Regulatory T cells: a potential target in cancer immunotherapy. Ann N Y Acad Sci *1417*, 104-115.

Shukeir, N., Pakneshan, P., Chen, G., Szyf, M., and Rabbani, S.A. (2006). Alteration of the methylation status of tumor-promoting genes decreases prostate cancer cell invasiveness and tumorigenesis in vitro and in vivo. Cancer research *66*, 9202-9210.

Shukeir, N., Stefanska, B., Parashar, S., Chik, F., Arakelian, A., Szyf, M., and Rabbani, S.A. (2015). Pharmacological methyl group donors block skeletal metastasis in vitro and in vivo. British journal of pharmacology *172*, 2769-2781.

Silverman, L.R., Demakos, E.P., Peterson, B.L., Kornblith, A.B., Holland, J.C., Odchimar-Reissig, R., Stone, R.M., Nelson, D., Powell, B.L., and DeCastro, C.M. (2002). Randomized controlled trial of azacitidine in patients with the myelodysplastic syndrome: a study of the cancer and leukemia group B. Journal of Clinical oncology *20*, 2429-2440.

Smith, Z.D., and Meissner, A. (2013). DNA methylation: roles in mammalian development. Nature Reviews Genetics *14*, 204.

Soojin, V.Y. (2012). Birds do it, bees do it, worms and ciliates do it too: DNA methylation from unexpected corners of the tree of life. Genome biology *13*, 1.

Šorm, F., Piskala, A., Čihák, A., and Veselý, J. (1964). 5-Azacytidine, a new, highly effective cancerostatic. Cellular and Molecular Life Sciences *20*, 202-203.

Spitzwieser, M., Holzweber, E., Pfeiler, G., Hacker, S., and Cichna-Markl, M. (2015). Applicability of HIN-1, MGMT and RASSF1A promoter methylation as biomarkers for detecting field cancerization in breast cancer. Breast Cancer Research *17*, 125.

Stefanska, B., Huang, J., Bhattacharyya, B., Suderman, M., Hallett, M., Han, Z.-G., and Szyf, M. (2011). Definition of the landscape of promoter DNA hypomethylation in liver cancer. Cancer research, 71,5891-903.

Stefansson, O.A., Moran, S., Gomez, A., Sayols, S., Arribas-Jorba, C., Sandoval, J., Hilmarsdottir, H., Olafsdottir, E., Tryggvadottir, L., and Jonasson, J.G. (2015). A DNA methylation-based definition of biologically distinct breast cancer subtypes. Molecular oncology *9*, 555-568.

Stirzaker, C., Song, J., Ng, W., Du, Q., Armstrong, N., Locke, W., Statham, A., French, H., Pidsley, R., and Valdes-Mora, F. (2017). Methyl-CpG-binding protein MBD2 plays a key role in maintenance and spread of DNA methylation at CpG islands and shores in cancer. Oncogene *36*, 1328-1338.

Stone, A., Cowley, M.J., Valdes-Mora, F., McCloy, R.A., Sergio, C.M., Gallego-Ortega, D., Caldon, C.E., Ormandy, C.J., Biankin, A.V., and Gee, J.M. (2013). BCL-2 hypermethylation is a potential biomarker of sensitivity to antimitotic chemotherapy in endocrine-resistant breast cancer. Molecular cancer therapeutics *12*, 1874-1885.

Stresemann, C., and Lyko, F. (2008). Modes of action of the DNA methyltransferase inhibitors azacytidine and decitabine. International journal of cancer *123*, 8-13.

Suzuki, H., Toyota, M., Caraway, H., Gabrielson, E., Ohmura, T., Fujikane, T., Nishikawa, N., Sogabe, Y., Nojima, M., and Sonoda, T. (2008). Frequent epigenetic inactivation of Wnt antagonist genes in breast cancer. British journal of cancer *98*, 1147-1156.

Suzuki, M.M., and Bird, A. (2008). DNA methylation landscapes: provocative insights from epigenomics. Nature Reviews Genetics *9*, 465.

Szyf, M. (1994). DNA methylation properties: consequences for pharmacology. Trends Pharmacol Sci *15*, 233-238.

Szyf, M. (2009). Epigenetics, DNA methylation, and chromatin modifying drugs. Annual review of pharmacology and toxicology *49*, 243-263.

Szyf, M., Pakneshan, P., and Rabbani, S.A. (2004). DNA methylation and breast cancer. Biochemical pharmacology *68*, 1187-1197.

Tahiliani, M., Koh, K.P., Shen, Y., Pastor, W.A., Bandukwala, H., Brudno, Y., Agarwal, S., Iyer, L.M., Liu, D.R., and Aravind, L. (2009). Conversion of 5-methylcytosine to 5-hydroxymethylcytosine in mammalian DNA by MLL partner TET1. Science *324*, 930-935.

Tangkijvanich, P., Hourpai, N., Rattanatanyong, P., Wisedopas, N., Mahachai, V., and Mutirangura, A. (2007). Serum LINE-1 hypomethylation as a potential prognostic marker for hepatocellular carcinoma. Clinica chimica acta *379*, 127-133.

Tapp, H.S., Commane, D.M., Bradburn, D.M., Arasaradnam, R., Mathers, J.C., Johnson, I.T., and Belshaw, N.J. (2013). Nutritional factors and gender influence age-related DNA methylation in the human rectal mucosa. Aging cell *12*, 148-155.

Tate, P.H., and Bird, A.P. (1993). Effects of DNA methylation on DNA-binding proteins and gene expression. Current opinion in genetics & development *3*, 226-231.

Teschendorff, A.E., Menon, U., Gentry-Maharaj, A., Ramus, S.J., Gayther, S.A., Apostolidou, S., Jones, A., Lechner, M., Beck, S., and Jacobs, I.J. (2009). An epigenetic signature in peripheral blood predicts active ovarian cancer. PloS one *4*, e8274.

Thakur, S., Feng, X., Shi, Z.Q., Ganapathy, A., Mishra, M.K., Atadja, P., Morris, D., and Riabowol, K. (2012). ING1 and 5-azacytidine act synergistically to block breast cancer cell growth. PloS one *7*, e43671.

Tomasi, M.L., Cossu, C., Spissu, Y., Floris, A., Ryoo, M., Iglesias-Ara, A., Wang, Q., Pandol, S.J., Bhowmick, N.A., and Seki, E. (2017). S-adenosylmethionine and methylthioadenosine inhibit cancer metastasis by targeting microRNA 34a/b-methionine adenosyltransferase 2A/2B axis. Oncotarget *8*, 78851.

Tomasi, M.L., Ramani, K., Lopitz-Otsoa, F., Rodríguez, M.S., Li, T.W., Ko, K., Yang, H., Bardag-Gorce, F., Iglesias-Ara, A., and Feo, F. (2010). S-adenosylmethionine regulates dual-specificity mitogen-activated protein kinase phosphatase expression in mouse and human hepatocytes. Hepatology *51*, 2152-2161.

Toussaint, J., Sieuwerts, A.M., Haibe-Kains, B., Desmedt, C., Rouas, G., Harris, A.L., Larsimont, D., Piccart, M., Foekens, J.A., and Durbecq, V. (2009). Improvement of the clinical applicability of the Genomic Grade Index through a qRT-PCR test performed on frozen and formalin-fixed paraffin-embedded tissues. BMC genomics *10*, 1.

Toyooka, K.O., Toyooka, S., Virmani, A.K., Sathyanarayana, U.G., Euhus, D.M., Gilcrease, M., Minna, J.D., and Gazdar, A.F. (2001). Loss of expression and aberrant methylation of the CDH13 (H-cadherin) gene in breast and lung carcinomas. Cancer research *61*, 4556-4560.

Tserga, A., Michalopoulos, N.V., Levidou, G., Korkolopoulou, P., Zografos, G., Patsouris, E., and Saetta, A.A. (2012). Association of aberrant DNA methylation with clinicopathological features in breast cancer. Oncology reports *27*, 1630.

Tsuboi, A., Hashimoto, N., Fujiki, F., Morimoto, S., Kagawa, N., Nakajima, H., Hosen, N., Nishida, S., Nakata, J., Morita, S., *et al.* (2019). A phase I clinical study of a cocktail vaccine of Wilms' tumor 1 (WT1) HLA class I and II peptides for recurrent malignant glioma. Cancer Immunology, Immunotherapy *68*, 331-340.

Tubio, J.M., Li, Y., Ju, Y.S., Martincorena, I., Cooke, S.L., Tojo, M., Gundem, G., Pipinikas, C.P., Zamora, J., and Raine, K. (2014). Extensive transduction of nonrepetitive DNA mediated by L1 retrotransposition in cancer genomes. Science *345*, 1251343.

Vanoirbeek, E., Eelen, G., Verlinden, L., Carmeliet, G., Mathieu, C., Bouillon, R., O'Connor, R., Xiao, G., and Verstuyf, A. (2014). PDLIM2 expression is driven by vitamin D and is involved in the pro-adhesion, and anti-migration and-invasion activity of vitamin D. Oncogene *33*, 1904-1911.

Veselý, J., and Čihák, A. (1978). 5-Azacytidine: mechanism of action and biological effects in mammalian cells. Pharmacology & Therapeutics Part A: Chemotherapy, Toxicology and Metabolic Inhibitors *2*, 813-840.

Vilain, A., Bernardino, J., Gerbault-Seureau, M., Vogt, N., Niveleau, A., Lefrancois, D., Malfoy, B., and Dutrillaux, B. (2000). DNA methylation and chromosome instability in lymphoblastoid cell lines. Cytogenetic and Genome Research *90*, 93-101.

Vo, Q.N., Kim, W.-J., Cvitanovic, L., Boudreau, D.A., Ginzinger, D.G., and Brown, K.D. (2004). The ATM gene is a target for epigenetic silencing in locally advanced breast cancer. Oncogene *23*, 9432-9437.

Von hoff, D.D., Slavik, M., and Muggia, F.M. (1976). 5-Azacytidine: a new anticancer drug with effectiveness in acute myelogenous leukemia. Annals of internal Medicine *85*, 237-245.

Wajed, S.A., Laird, P.W., and DeMeester, T.R. (2001). DNA methylation: an alternative pathway to cancer. Annals of surgery *234*, 10-20.

Walter, A., Etienne-Selloum, N., Brasse, D., Khallouf, H., Bronner, C., Rio, M.-C., Beretz, A., and Schini-Kerth, V.B. (2010). Intake of grape-derived polyphenols reduces C26 tumor growth by inhibiting angiogenesis and inducing apoptosis. The FASEB Journal *24*, 3360-3369.

Wang, L., Liu, Y., Han, R., Beier, U.H., Thomas, R., Wells, A.D., and Hancock, W.W. (2013). Mbd2 promotes Foxp3 demethylation and T-regulatory cell function. Molecular and cellular biology, MCB. 00144-00113.

Wang, Y., Sun, Z., and Szyf, M. (2017). S-adenosyl-methionine (SAM) alters the transcriptome and methylome and specifically blocks growth and invasiveness of liver cancer cells. Oncotarget *8*, 111866.

Weaver, I.C., Hellstrom, I.C., Brown, S.E., Andrews, S.D., Dymov, S., Diorio, J., Zhang, T.-Y., Szyf, M., and Meaney, M.J. (2014). The methylated-DNA binding protein MBD2 enhances NGFI-A (egr-1)-mediated transcriptional activation of the glucocorticoid receptor. Phil Trans R Soc B *369*, 20130513.

Weigel, M.T., and Dowsett, M. (2010). Current and emerging biomarkers in breast cancer: prognosis and prediction. Endocrine-related cancer *17*, R245-R262.

Weigel, R.J. (1993). Transcriptional control of estrogen receptor in estrogen receptor-negative breast carcinoma. Cancer research *53*, 3472-3474.

Weiss, A., Metter, G., Nealon, T., Keanan, J., Ramirez, G., Swaiminathan, A., Fletcher, W., Moss, S., and Manthei, R. (1976). Phase II study of 5-azacytidine in solid tumors. Cancer treatment reports *61*, 55-58.

Weiss, A., Stambaugh, J., Mastrangelo, M., Laucius, J., and Bellet, R. (1972). Phase I study of 5-azacytidine (NSC-102816). Cancer chemotherapy reports Part 1 *56*, 413-419.

Widschwendter, M., Berger, J., Hermann, M., Müller, H.M., Amberger, A., Zeschnigk, M., Widschwendter, A., Abendstein, B., Zeimet, A.G., and Daxenbichler, G. (2000). Methylation and silencing of the retinoic acid receptor-β2 gene in breast cancer. Journal of the National Cancer Institute *92*, 826-832.

Widschwendter, M., Jiang, G., Woods, C., Müller, H.M., Fiegl, H., Goebel, G., Marth, C., Müller-Holzner, E., Zeimet, A.G., and Laird, P.W. (2004). DNA hypomethylation and ovarian cancer biology. Cancer research *64*, 4472-4480.

Wilson, A.S., Power, B.E., and Molloy, P.L. (2007). DNA hypomethylation and human diseases. Biochimica et Biophysica Acta (BBA)-Reviews on Cancer *1775*, 138-162.

Wong, N., Lam, W.-C., Bo-San Lai, P., Pang, E., Lau, W.-Y., and Johnson, P.J. (2001). Hypomethylation of chromosome 1 heterochromatin DNA correlates with q-arm

copy gain in human hepatocellular carcinoma. The American journal of pathology *159*, 465-471.

Wood, K.H., Johnson, B.S., Welsh, S.A., Lee, J.Y., Cui, Y., Krizman, E., Brodkin, E.S., Blendy, J.A., Robinson, M.B., and Bartolomei, M.S. (2016). Tagging methyl-CpG-binding domain proteins reveals different spatiotemporal expression and supports distinct functions. Epigenomics *8*, 455-473.

Wood, K.H., and Zhou, Z. (2016). Emerging molecular and biological functions of MBD2, a reader of DNA methylation. Frontiers in genetics *7*, 93.

Xie, Z.-H., Huang, Y.-N., Chen, Z.-X., Riggs, A.D., Ding, J.-P., Gowher, H., Jeltsch, A., Sasaki, H., Hata, K., and Xu, G.-L. (2006). Mutations in DNA methyltransferase DNMT3B in ICF syndrome affect its regulation by DNMT3L. Human molecular genetics *15*, 1375-1385.

Yamada, Y., Jackson-Grusby, L., Linhart, H., Meissner, A., Eden, A., Lin, H., and Jaenisch, R. (2005). Opposing effects of DNA hypomethylation on intestinal and liver carcinogenesis. Proceedings of the National Academy of Sciences *102*, 13580-13585.

Yao, Y., and Dai, W. (2014). Genomic instability and cancer. Journal of carcinogenesis & mutagenesis *5*.

Ye, L., Li, X., Kong, X., Wang, W., Bi, Y., Hu, L., Cui, B., Li, X., and Ning, G. (2005). Hypomethylation in the promoter region of POMC gene correlates with ectopic overexpression in thymic carcinoids. Journal of endocrinology *185*, 337-343.

Yuan, Y., Mendez, R., Sahin, A., and Le Dai, J. (2001). Hypermethylation leads to silencing of the SYK gene in human breast cancer. Cancer research *61*, 5558-5561.

Zhang, J., and Zheng, Y.G. (2015). SAM/SAH analogs as versatile tools for SAM-dependent methyltransferases. ACS chemical biology *11*, 583-597.

Zhang, Y., Ng, H.-H., Erdjument-Bromage, H., Tempst, P., Bird, A., and Reinberg, D. (1999). Analysis of the NuRD subunits reveals a histone deacetylase core complex and a connection with DNA methylation. Genes & development *13*, 1924-1935.

Zhang, Y., Petropoulos, S., Liu, J., Cheishvili, D., Zhou, R., Dymov, S., Li, K., Li, N., and Szyf, M. (2018). The signature of liver cancer in immune cells DNA methylation. Clinical epigenetics *10*, 8.

Zhao, Y., Li, J., Guo, M., Feng, B., and Zhang, J. (2010). Inhibitory effect of S-adenosylmethionine on the growth of human gastric cancer cells in vivo and in vitro. Chin J Cancer *29*, 752-760.

Zhu, D., Osuka, S., Zhang, Z., Reichert, Z.R., Yang, L., Kanemura, Y., Jiang, Y., You, S., Zhang, H., Devi, N.S., *et al.* (2018). BAI1 Suppresses Medulloblastoma Formation by Protecting p53 from Mdm2-Mediated Degradation. Cancer Cell *33*, 1004-1016.e1005.

Zhu, H., Wang, X., Shi, H., Su, S., Harshfield, G.A., Gutin, B., Snieder, H., and Dong, Y. (2013). A genome-wide methylation study of severe vitamin D deficiency in African American adolescents. The Journal of pediatrics *162*, 1004-1009. e1001.

APPENDICES

Copyright license for Chapter 1

This chapter contains excerpts from two review articles and one book chapter. The copyright permissions for all three are given below:

Email consent for using excerpts from the review article Copyright license for 'DNA methylation and breast cancer: Mechanistic and therapeutic applications' by Niaz Mahmood and Shafaat A. Rabbani published in Trends in Cancer Research, Vol. 12, 1 – 18. [Review]

0 July 2020
Ref. No. RT/CNR/135
Dear Niaz Mahmood,
Thanks for the mail. We understand that you would like to re-use material from the below stated article you published in our journal 'Trends in Cancer Research':
'Niaz Mahmood and Shafaat A. Rabbani, 2017, DNA methylation and breast cancer: Mechanistic and therapeutic applications,
Trends in Cancer Research, Vol. 12, 1 – 18'.
We grant you permission to re-use the figures and text from the above-mentioned article in your PhD thesis.
This permission is subject to the usual requirement of acknowledgment being made to our journal within the text as the source of original publication. The acknowledgement may please be cited along the following lines by clearly stating the source:
Reproduced from, 'Niaz Mahmood and Shafaat A. Rabbani, 2017, DNA methylation and breast cancer: Mechanistic and therapeutic applications, Trends in Cancer Research, Vol. 12, 1 – 18'.
If any part of the material to be used has appeared in our publication with credit or acknowledgement to another source, permission must also be sought from that source. If
such permission is not obtained then that material may not be included in your publication.
At this point, we would like to wish you all the best with your thesis work.
Sivaprasad S.
Research Trends (P) Ltd.

Email consent for using excerpts from the review article Copyright license for 'Targeting DNA Hypomethylation in Malignancy by Epigenetic Therapies' by Niaz Mahmood and Shafaat A. Rabbani published in Adv Exp Med Biol. 1164:179-196. [Book Chapter]

This part was originally published as a Book Chapter, and so we got permissions through emails from two Editors (Dr. Richard Kremer and Dr. Johng Rhim) of this book, which are attached below:

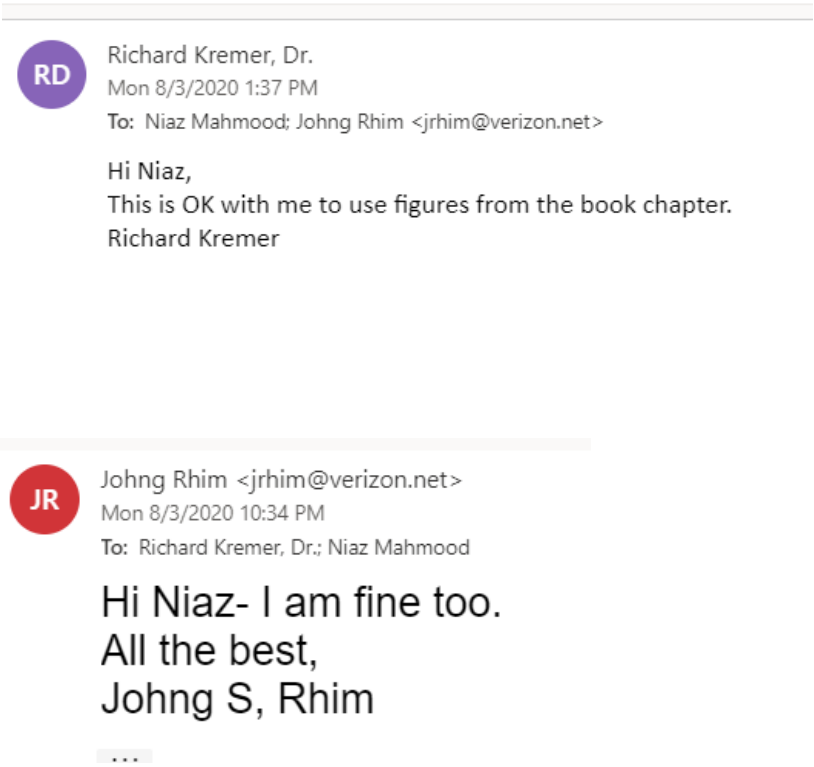

RD

Richard Kremer, Dr.
Mon 8/3/2020 1:37 PM
To: Niaz Mahmood; Johng Rhim <jrhim@verizon.net>

Hi Niaz,
This is OK with me to use figures from the book chapter.
Richard Kremer

JR

Johng Rhim <jrhim@verizon.net>
Mon 8/3/2020 10:34 PM
To: Richard Kremer, Dr.; Niaz Mahmood

Hi Niaz- I am fine too.
All the best,
Johng S, Rhim

...

Copyright license for 'DNA methylation readers and breast cancer: mechanistic and therapeutic applications' by Niaz Mahmood and Shafaat A. Rabbani published in Front Oncol. 9: 489. [Review]

This article was published under open access Creative Commons Attribution License, which allows use in the thesis with proper acknowledgement. The publisher does not give formal permission as it can be used under Creative Commons Attribution License. No extra permission is required for use in thesis.

Copyright consents for Chapter 2

This research article was published in 'Oncotarget' under open access Creative Commons Attribution License, which allows use in the thesis with proper acknowledgement. However, we also got the Editor and the publisher's consents through email, which are provided below:

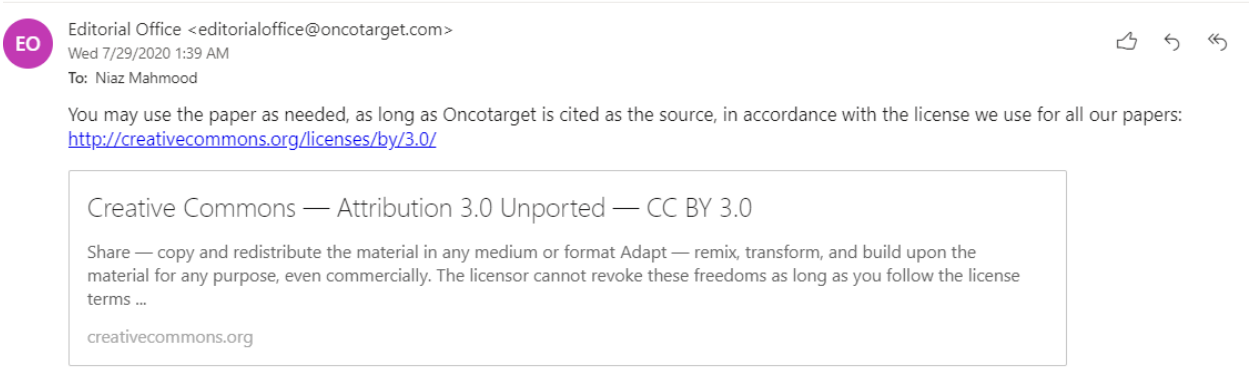

Copyright consents for Chapter 3

This research article was published in the 'Journal of Cellular and Molecular Medicine' under open access Creative Commons Attribution License, which allows use in the thesis with proper acknowledgement. However, we also got the Editor and the publisher's consents through email, which are provided below:

Email 1

Dear Niaz,

OK with me. I cc our Wiley Editorial Office for validation.

Your sincerely,

Prof. Stefan N. Constantinescu, MD, PhD, EiC JCMM

Email 2

Dear both,

Articles in JCMM are published as open access articles under the terms of the Creative Commons Attribution License, which permits use, distribution and reproduction in any medium, provided the original work is properly cited. So basically it's fine as long as you state that the work was published in JCMM.

Best wishes,

Vanessa Moir
Associate Managing Editor, Content Review
Research Content Management

Copyright consents for Chapter 4

This research article was published in ‘Bone Research’ under open access CC BY license (Creative Commons Attribution 4.0 International Licence), which allows use in the thesis with proper acknowledgement. However, we also got the Editor’s consent through email, which is provided below:

> Dear Niaz Mahmood,
>
> Of course, you can use it. For the articles in Bone Research, they are published under a CC BY licence (Creative Commons Attribution 4.0 International Licence). It allows for maximum dissemination and re-use of open access materials: users are free to share (copy, distribute and transmit) and remix (adapt) the contribution including for commercial purposes, providing they attribute the contribution in the manner specified by the author or licensor (read the full legal code). The copyright of the article entitled "An enhanced chemopreventive effect of methyl donor S-adenosylmethionine in combination with 25-hydroxyvitamin D in blocking mammary tumor growth and metastasis" is belonged to the authors, so you have the right to decide to use it or not.
> Hope this will help.
> Best Regards,
>
> Hui Yang
> Editor